Performance Evaluation and Spectral Efficiency Improvements for Wireless Networks With Interference

by

Kasun Thilina Hemachandra

A thesis submitted in partial fulfillment of the requirements for the degree of

Doctor of Philosophy

in

Communications

Department of Electrical and Computer Engineering

University of Alberta

Abstract

The demand for high data rate wireless services has grown tremendously. The demand is expected to grow further at an increased pace. The scarcity of the usable radio frequency spectrum is a major bottleneck to cater to the growing demand for high data rate wireless services. Current cellular wireless networks rely on deploying small cells as a possible solution to cater to the growing demand. However, this practice has resulted in severe co-channel interference (CCI) levels in cellular networks.

The first phase of this thesis investigates the impact of CCI on relay networks and distributed antenna systems, which are included in recent wireless standards such as long-term evolution advanced (LTE-A). The analytical results derived for system performance metrics, such as the outage probability and the ergodic rate, are used to obtain valuable insights for system design. The second stage of this thesis research proposes interference reduction schemes for wireless relay networks operating in the presence of CCI and analytically investigates the performance of each scheme. The analytical results are used to obtain crucial design insights such as the feedback rate and position of the relay nodes.

Another approach to compensate for the spectrum scarcity is through improving the spectral efficiency (SE) of the wireless networks. As a step towards increasing SE, recently, there has been research efforts to implement full-duplex (FD) wireless communications. The main challenge in FD is the interference on the reception by its own transmission. Recent advances in self-interference reduction schemes have made FD communications feasible for short range communications. This thesis develops a theoretical framework to study the average data rate of FD communications for short range communications using device-to-device networks.

Preface

The research included in this thesis was conducted under the supervision of, and in collaboration with Dr. Norman C. Beaulieu, Dr. Nandana Rajatheva and Dr. Matti Latva-aho. The findings of the research are published as co-authored articles in The Institute of Electrical and Electronics Engineers (IEEE) journals and conference proceedings.

Chapter 3 of this thesis is published as:

K. T. Hemachandra and N. C. Beaulieu, "Outage analysis of opportunistic scheduling in dual-hop multiuser relay networks in the presence of interference," *IEEE Trans. Commun.*, vol. 61, no. 5, pp. 1786–1796, May 2013.

Chapter 4 of this thesis is published as:

K. T. Hemachandra and N. C. Beaulieu, "A moment matching technique to estimate the achievable ergodic rate for limited feedback distributed antenna systems in the presence of out-of-cell interference," *IEEE Commun. Lett.*, vol. 17, no. 7, pp. 1360–1363, July 2013.

Chapter 5 of this thesis is published as:

K. T. Hemachandra and N. C. Beaulieu, "Relay coordination schemes for two-hop networks: Two-cell case," *IEEE Trans. Commun.*, vol. 63, no. 4, pp. 1178–1190, Apr. 2015

Chapter 6 of this thesis is published as:

K. T. Hemachandra and N. C. Beaulieu, "Shared relay networks with linear receivers at the relay: Two-cell case," *IEEE Trans. Commun.*, vol. 62, no. 4, pp. 1230–1239, Apr. 2014.

Chapter 7 of this thesis is published as:

K. T. Hemachandra, N. Rajatheva, and M. Latva-aho, "Sum-rate analysis for

full-duplex underlay device-to-device networks," in Proc. *IEEE Wireless Commun. and Networking Conf. (WCNC)*, Apr. 2014, pp. 514–519.

Dedicated to my family...

Acknowledgements

First and foremost, I extend my sincere gratitude to my research supervisor Dr. Norman C. Beaulieu. His expertise, continuous advice, guidance, feedback and encouragement have been a crucial component in making this thesis a success.

I greatly appreciate my supervisor Dr. Ying Y. Tsui for his continuous support and guidance towards successful completion of my thesis. His tremendous experience in research and graduate supervision helped me in great deal during my Ph.D. program.

I would like to express my deep gratitude to my Ph.D. supervisory and examining committee members for their invaluable feedback.

I am extremely thankful to Dr. Matti Latva-aho and Dr. Nandana Rajatheva at the Centre for Wireless Communications, University of Oulu, Finland for providing me with a visiting researcher opportunity at their research facility. This visit and subsequent collaborations were extremely beneficial for my research in full-duplex networks.

I gratefully acknowledge the financial support from the Alberta Innovates Technology Futures graduate student scholarship. I am also thankful to the Department of Electrical and Computer Engineering, the Graduate Student Association and the Faculty of Graduate Studies and Research for their financial support during my Ph.D. program.

I am also thankful to all the past and present colleagues at the *i*CORE Wireless Communications Laboratory (*i*WCL) and the Department of Electrical and Computer Engineering for their friendship, valuable support and continuous encouragement.

My heartfelt gratitude goes to my loving wife Ranusha and my beloved parents, sister and brother who have always been an inspiration for me to reach higher goals.

Their unconditional love and support was the major force that kept me moving forward during my stay at the University of Alberta.

Finally, I thank everyone else who supported me in both academic and non-academic endeavors during my stay in Canada and the University of Alberta.

Table of Contents

List of Tables

List of Figures

List of Abbreviations

Abbreviation	Description
3GPP	3rd-Generation Partnership Project
4G	fourth generation
5G	fifth generation
AF	amplify-and-forward
AWGN	additive white Gaussian noise
BER	bit error rate
BS	base station
BT	blanket transmission
CBF	coordinated beamforming
CCI	co-channel interference
CDF	cumulative distribution function
CDI	channel direction information
CoMP	coordinated multi-point transmission/reception
CR	cognitive radio
CSI	channel-state information
CU	cellular user
D2D	device-to-device
DAS	distributed antenna system
DAU	distributed antenna unit
DF	decode-and-forward
e2e	end-to-end
FCC	Federal Communications Commission
FD	full-duplex
FDD	frequency division duplexing
HD	half-duplex

Abbreviation	Description
ICI	inter-cell interference
i.i.d.	independent and identically distributed
JP	joint processing
LTE	Long Term Evolution
METIS	Mobile and Wireless Communications Enablers for the Twenty-Twenty Information Society project
MIMO	multiple-input multiple-output
MISO	multiple-input single-output
MMSE	minimum mean-square error
mmW	millimeter-wave
MRC	maximal ratio combining
MRN	multiuser relay network
MRT	maximal ratio transmission
MS	mobile station
NLOS	non line-of-sight
OC	optimal combining
PDF	probability density function
PS	power save
PU	primary user
QoS	quality-of-service
RF	radio frequency
RRU	remote radio unit
RS	relay station
RV	random variable
RVQ	random vector quantization
Rx	receiver
SC	selection combining
SE	spectral efficiency
SI	self-interference
SIMO	single-input multiple-output
SINR	signal-to-interference plus noise ratio
SIR	signal-to-interference ratio
SISO	single-input single-output

Abbreviation	Description
SNR	signal-to-noise ratio
SRN	shared relay networks
STC	space-time code
SU	secondary user
TAS	transmit antenna selection
TDD	time division duplexing
TV	television
TWRN	two-way relay network
Tx	transmitter
ZF	zero forcing

List of Symbols

- Basic arithmetic, set, and calculus symbols have standard form.

Elementary & Special Functions

Notation	Definition
$\beta(\cdot,\cdot)$	beta function
$\Gamma(\cdot)$	Euler gamma function
$\Gamma(k,\theta)$	gamma distribution with parameters k and θ
$\gamma(\cdot,\cdot)$	lower incomplete gamma function
$\boldsymbol{Q}(\cdot,\cdot)$	upper incomplete gamma function
${}_2F_1(\cdot;\cdot;\cdot)$	Gaussian hypergeometric function
$\mathcal{I}_\nu(\cdot)$	modified Bessel function of the first kind of order ν
$\mathcal{K}_\nu(\cdot)$	modified Bessel function of the second kind of order ν
$\ln(\cdot)$	natural logarithm
$\log_2(\cdot)$	logarithm to base 2
$\mathcal{W}_{a,b}(\cdot)$	Whittaker function
$\boldsymbol{K}(\cdot)$	complete elliptic integral of the second kind
$\boldsymbol{E}_1(\cdot)$	exponential integral function of order 1
$\mathrm{Ei}(\cdot)$	exponential integral function
$\psi_0(\cdot)$	psi function

Probability & Statistics

Let X be a random variable, and $\mathcal{D}$ be an arbitrary event.

Notation	Definition
$\mathbb{E}\{\cdot\}$	expectation
$f_X(\cdot)$	probability density function (PDF) of X
$f_{X\|Y}(\cdot)$	PDF of X given Y
$F_X(\cdot)$	cumulative distribution function (CDF) of X
$\Pr[\mathcal{D}]$	probability of $\mathcal{D}$

$X \sim \mathcal{CN}(\cdot, \cdot)$	circularly symmetric complex Gaussian (CSCG) random variable X
$X \sim \mathcal{N}(\cdot, \cdot)$	Gaussian random variable X
$\mathbb{V}\text{ar}\{\cdot\}$	variance

Miscellaneous

Notation	**Definition**
$\lvert\mathbf{a}\rvert$	absolute value of **a**
$k!$	factorial of k
$\binom{n}{k}$	binomial coefficient n choose k
$\arg\min_i (a_i)$	index i corresponding to the smallest a_i
$\lim_{x \to a} f(x)$	the limit of function $f(x)$ as x tends to a
$\max(a_1, a_2)$	maximum of scalars a_1 and a_2
$\max(a_1, \ldots, a_n)$	maximum of all scalars a_i for relevant i; also $\max_i (a_i)$
$\min(a_1, a_2)$	minimum of scalars a_1 and a_2
$\min(a_1, \ldots, a_n)$	minimum of all scalars a_i for relevant i; also $\min_i (a_i)$
$\mathcal{O}(x^{-n})$	the remainder in a series of a function of x with the exponent of x smaller than n
$\Pi_X^{\perp}$	projection onto the orthogonal complement of the column space of X
$\boldsymbol{I}_N$	identity matrix of size $N \times N$

Chapter 1

Introduction

1.1 Wireless Communications

Nikola Tesla and Guglielmo Marconi envisioned a wirelessly connected world in the late 1800s. More than 120 years later, it is now possible to say that their vision has become a reality. Wireless technologies have revolutionized the way humans interact with other humans and machines. During the last three decades, the popularity of wireless communications grew exponentially. The invention of low cost computers, mobile phones, smartphones, tablet computers and wearable devices catalyzed this growth. Furthermore, new paradigms of the internet such as social networking and e-commerce have also contributed to this growth. According to latest surveys [1], the number of cellular phones has exceeded the population of the earth and there will be 1.4 devices per person by the year 2018. Therefore, it is safe to claim that wireless technologies have become a vital component of human life.

A decade ago, mobile wireless communications were primarily used for voice communications. However, current advancements of wireless technologies have overtaken the role played by wireline systems to provide broadband data communication services such as on demand video, video conferencing, media sharing and video surveillance. Surveys show that the amount of data transferred through mobile wireless techniques have grown in multiple orders of magnitude during the past decade. This demand is expected to grow further in the future and it is expected that by the year 2018, the total data transferred through mobile wireless devices will exceed 15 Exabytes per month [1].

1.2 Fundamental Challenges and Solutions

The wireless channel is a challenging environment to be used for reliable communications. Apart from additive thermal noise, a designer of a mobile wireless system has to overcome two fundamental performance degrading factors inherent in wireless communications, namely fading (small-scale and large-scale) and interference.

Small-scale fading occurs as a result of multipath propagation of radio waves and the relative motion between a transmitter and a receiver. Due to the natural and man-made objectives located between a transmitter and a receiver, the transmitted radio waves will reach the receiver via reflections, diffraction and scattering. The composite received signal at the receiver will be a combination of waves arriving from different paths with different amplitudes and delays. This property is known as multipath propagation [2]. The relative motion between the transmitter and receiver introduces Doppler shifts to waves arriving from different paths. Due to the time delays and frequency shifts, the phases of the arriving waves are varied and they result in constructive or destructive superposition of the multipath components at the receiver, causing rapid random fluctuations in the received composite signal strength [3]. Large-scale fading is caused by path-loss and shadowing. Path-loss refers to the attenuation of radio signal power with the distance. Shadowing refers to the drop in received signal power due to a large obstruction such as a building in the main path between the transmitter and receiver.

The radio frequency (RF) spectrum is the most valuable resource for wireless communications. Different parts of the spectrum are allocated to different wireless services. The spectrum chunks in the region 800 MHz to 3 GHz are allocated for cellular wireless networks. These bands demonstrate superior propagation characteristics desirable for mobile communications. Therefore, this portion of the RF spectrum is extremely crowded and acquiring a vacant band for new services has become nearly impossible. Therefore, the use of these bands must be carefully managed and heavily regulated.

In order to increase the number of simultaneous users served using the available RF spectrum, the concept of frequency reuse is practiced in current mobile wireless

systems. Spectrum chunks allocated to a particular network operator are allocated to a cell cluster. A cell cluster consists of multiple cells. Each cell contains a base station (BS) and multiple mobile stations (MSs). In order to provide network coverage to a larger geographical area, a cell cluster is repeated multiple times. The cells which use same frequency band are known as co-channel cells and the interference between them is referred to as co-channel interference (CCI). The boundary of a cell cluster is shown in Fig. 1.1. Cluster size is a key factor which determines the CCI level in a cellular mobile network. A larger cluster size will result in a higher reuse distance, thus a lower CCI level. However, the bandwidth available per cell is reduced. Since the achievable data rate is directly proportional to the bandwidth, this will affect the achievable throughput of the network. A smaller cluster size will provide more bandwidth per cell. However, the CCI level is higher due to the smaller reuse distance. The broadband nature of the user service demands, it is not

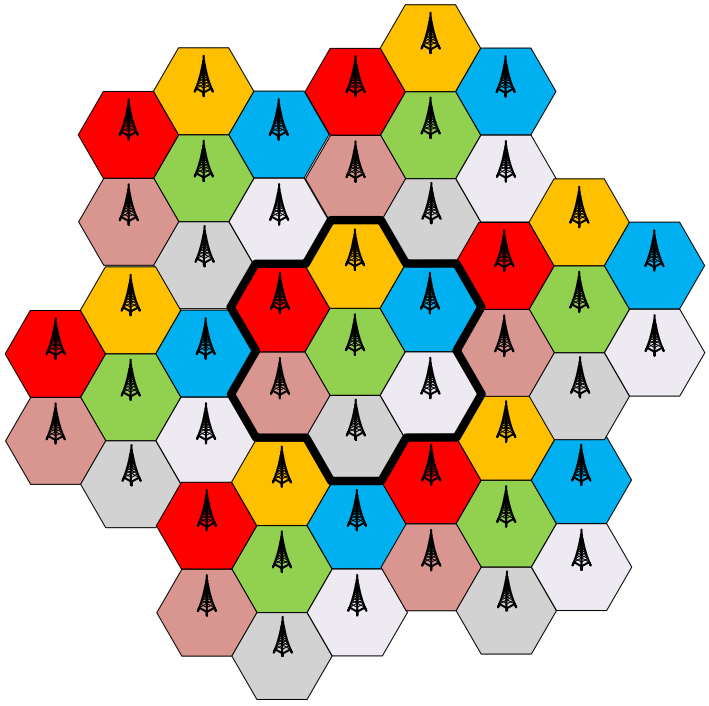

Figure 1.1: A frequency reuse pattern with 7-cell clusters.

desirable to have cells with low bandwidth. Therefore, the operators use smaller cluster sizes with smaller cells to cater to the user demand in densely populated areas. In such scenarios, the achievable performance is limited by the CCI level of the

network. Therefore, CCI reduction techniques without compromising the available bandwidth are required to provide broadband services with an acceptable quality of service.

Several new techniques have been proposed and studied as possible solutions for the challenges described above.

1.2.1 Multiple antenna systems

It has been identified that implementing multiple antennas at the transmitter and at the receiver results in significant increase in data rates (spatial multiplexing gain) and improve the reliability (diversity gain) of wireless communications. These systems are generally known as multiple-input-multiple-output (MIMO) systems. There exists a rich collection of literature evaluating the benefits and performance limits of MIMO systems. Seminal work on performance of MIMO systems can be found in [4–6]. MIMO has been identified as a transmission technique in IEEE 802.11n, long term evolution (LTE) and LTE-Advanced (LTE-A).

If the antenna elements are placed such that the fading channels between the transmit antennas and the receiver antennas are independent, the channel coefficient matrix becomes full rank with higher probability. Then, the channel matrix can be decomposed by signal processing at the transmitter and the receiver such that multiple independent data streams can be sent from the transmitter [6]. The maximum number of independent data streams that can be transmitted by a MIMO system is known as the spatial multiplexing gain of the system.

Multiple antennas can be used to obtain a diversity gain by sending multiple copies of the same signal through different antenna elements such that the probability of all the copies of the signal are at a deep fade is minimized [7]. In order to obtain full benefits of MIMO systems, it is generally required that both the transmitter and the receiver have information of the channel coefficient matrix. This information is known as channel state information (CSI). The obtained CSI can be used to perform signal processing at the transmitter and at the receiver in multiple ways, namely transmit precoding, receiver beamforming [8], and transmit antenna selection [9, 10].

1.2.2 Relay communications

Relay communication was introduced as a technique to overcome the effects of shadowing and to extend the coverage of a wireless network without using large transmit powers. The basic relay communication system model consist of a source node (S) which has data to be transmitted to a destination node (D) with the assistance of an intermediate node known as the relay node (R). The two fundamental relay protocols are amplify-and-forward (AF) and decode-and-forward (DF). In AF relaying (also known as non-regenerative relaying) the relay node applies a linear transformation on the received signal and forwards the transformed signal towards the destination. On the other hand, DF relay nodes decode the data symbols in the received signal and re-encode the decoded data symbols before retransmitting. Seminal work on relay protocols is contained in [11–13].

AF relay has lower complexity than DF relay and also imposes lower processing delay at the relay. The key limitation of AF relaying is the noise amplification at the relay. A DF relay is useful only when the $S - R$ link is reliable. Furthermore, a DF relay may use more power and has higher hardware complexity since it has to act as a complete radio transceiver. When the $S - R$ link is reliable, DF relays provide higher data throughput than AF relays. Another advantage of DF relays is that they can be integrated into an existing wireless system with minimal changes to the network hardware architecture. Therefore, both AF and DF relays have their pros and cons, thus both types of relays have attracted research interest over the past 15 years. Relay techniques are included as transmission technologies in latest standards such as IEEE 802.16m [14] and LTE-A [15], to provide better coverage and higher throughput.

1.2.3 Distributed antenna systems

In a conventional MIMO system, multiple antenna elements are located in a single location. In a distributed antenna system (DAS), the antenna elements are geographically distributed and each antenna element is connected to a central unit via a wired connection, fiber optic cable or a dedicated radio link. DASs can be distinguished

from conventional repeater systems since in DASs, each antenna element can transmit different data stream whereas repeater systems merely repeat the signal from central unit. DASs were primarily introduced to remove the coverage dead spots in indoor wireless networks [16]. From the network architecture point-of-view, DASs can be used to reduce the number of BSs in a particular service area. Furthermore, DASs have other advantages such as lower transmit powers, higher SINR for distant users, and reducing interference to other cells [17].

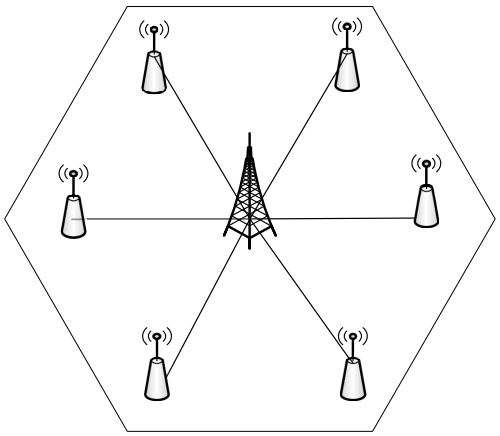

Figure 1.2: A DAS system with 6 remote radio units.

Widely used transmission techniques for DASs include blanket transmission (BT) and antenna selection. In BT scheme, all the distributed antenna elements participate in transmission either by sending same signals or different signals. Therefore, the blanket transmission scheme generates a macroscopic multiple antenna system. In antenna selection scheme, only a single antenna element or the central unit performs the transmission [17]. This scheme tries to exploit macroscopic selection diversity and reduce interference to other cells by reducing the number of transmitters.

1.2.4 Shared relay networks

Shared relay networks were introduced as a low complexity solution for interference coordination in multi-cell wireless networks [18]. In a shared relay network (SRN), a single relay node is placed at the intersection of multiple adjacent cells and shared among the BSs of these cells. The relay is generally equipped with

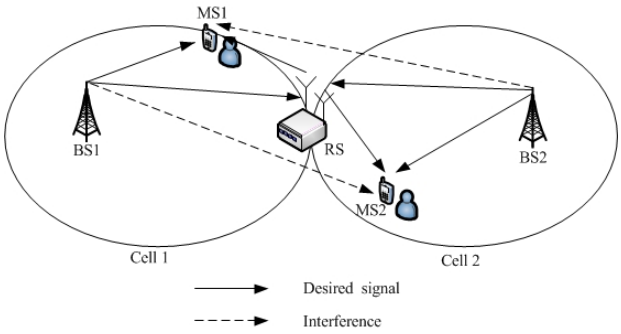

Figure 1.3: A shared relay network model.

multiple antennas. The relay uses reception techniques for the MIMO multiple access channel to separate signals from multiple interfering BSs and use transmission techniques of MIMO broadcast channel to transmit interference free signals for MSs in multiple cells. In this way, CCI can be effectively nulled without coordination among multiple cells. However, the complexity of the relay node will be increased.

1.2.5 Interference coordination

Interference coordination techniques attempt to reduce the CCI levels using signal processing techniques. The concept was first introduced in [19], promising tremendous improvements in SE at the cost of increased network infrastructure complexity. The basic idea was to coordinate the transmissions of interfering transmitters such that the interference received at the MSs are effectively null. Based on the availability of user data symbols, interference coordination techniques are categorized into two broad categories [20].

- ***Joint processing (JP)***: When a MS is located close to the cell edge, it is able to receive signals from multiple base stations. In present systems, the MS will connect to the BS with the strongest signal while the signals received from the other BSs are considered as CCI. JP schemes attempt to use the signals from neighboring BSs to improve the performance of cell edge users. Two types of JP schemes can be identified. In joint transmission scheme, multiple BSs share the user data and transmit to cell edge users collaboratively, creating a

super BS. In dynamic point selection schemes, user data is shared between multiple BSs and only a single BS is dynamically selected to transmit in a particular time-frequency resource block, to improve the performance of a particular cell edge user. Both these schemes require exchanging user data between the BSs through backhaul links.

- ***Coordinated scheduling and beamforming (CS/CB)***: In contrast to JP schemes, in CS/CB schemes, user data for a particular user is available only at a single BS. Each User is served by only one BS while the other BSs align their transmissions such that the interference received at that particular MS is zero or below a predetermined threshold. To implement CB/CS, the MSs should estimate and feedback the CSI of the channels from interfering BSs. Then the coordinating BSs exchange the CSI and compute and select their beamforming vectors/matrices such that their transmissions lie in a space orthogonal to the interference channels of other users.

Interference coordination schemes have received a significant research interest during the past 5 years and it has been recognized as a key feature in LTE-A standard.

1.2.6 Use of new spectrum bands

An obvious solution to spectrum scarcity in the extremely crowded bands below 3 GHz will be to design the future wireless systems such that they operate in different frequency bands where plenty of bandwidth is available for new services. However, finding an alternative frequency band suitable for mobile communications appears to be a great challenge. This is evident from the fact that even though many aspects of mobile communications changed since its inception while the carrier frequencies did not change significantly. Recently, there have been significant interest in the millimeter-wave (mmW) bands (frequencies between 30 and 300 GHz) as a possible alternative band for mobile wireless communications. The bandwidth available in mmW bands is 200 times greater than the bands currently used for mobile communications. Furthermore, the small wavelength of mmW carriers

will allow system designers to implement large number of miniaturized antennas in a single device, taking advantages of massive MIMO technologies [21]. Despite the highly lucrative benefits available in mmW bands, the use of mmW bands for mobile wireless communications remains largely unexplored. Initial field trials have demonstrated undesirable characteristics for long range NLOS communications [21]. However, it is expected that mmW communications will play a major role in future wireless communications and it has been identified as a possible fifth-generation (5G) wireless technique.

1.3 Increasing the Spectral Efficiency

Another possible way to address the spectrum scarcity is through improving the SE of the wireless communications. Sending more bits per second per unit bandwidth will essentially reduce the amount of bandwidth required for high data rate services. Since 1990s MIMO was identified as a promising technique to improve the SE of wireless networks. In LTE-A, it is predicted that using 8×8 MIMO will achieve a peak SE of 30 bits/s/Hz.

1.3.1 Massive MIMO

Massive MIMO is a disruptive technology which scales up MIMO by orders of magnitude compared to current standards [22, 23]. Massive MIMO systems are expected to simultaneously serve several tens of users with several hundreds of antenna elements. With this approach, massive MIMO systems aim to reap the benefits of conventional multi-user MIMO (MU-MIMO) systems in a much larger scale. Aggressive spatial multiplexing employed in massive MIMO enables tremendous capacity improvements. Furthermore, with large number of antennas, the RF energy can be focused with sharp beams in to smaller regions and creating lower interference levels. Since several tens of users can be served simultaneously using the same time-frequency resources, the spectral efficiency of massive MIMO systems can be more than 10 times larger than the conventional MIMO systems. Since massive MIMO systems can be fed using low-cost, low-power amplifiers, the de-

vice costs can be lowered. Other benefits of massive MIMO include the robustness to interference and jamming, and reduced latency in the air interface.

Even though massive MIMO has shown a great potential as a prime enabler for future broadband services, there are some issues that need to be addressed prior to standardization. Massive MIMO systems rely on good enough channel knowledge for both the uplink and the downlink at the BS. However, estimating the downlink CSI could be problematic since the user devices have to estimate and feedback the CSI to the BS. This may not be feasible for practical implementation. Therefore, massive MIMO systems are normally operated in the time division duplex (TDD), relying on the uplink-downlink channel reciprocity.

Compared to conventional MIMO systems, massive MIMO systems performance is severely affected by pilot contamination. When pilot sequences are reused at interfering cells, the estimated channel will be a linear combination of the desired channel and the interference channels with the same pilot sequence. Beamforming based on contaminated CSI will direct interference and this residual interference level grows with the number of antennas. Clever channel estimation techniques and pilot-contamination precoding techniques are needed to be developed to reap the full benefits of massive MIMO technology.

1.3.2 Cognitive radio networks

Surveys suggest that the spectrum allocated to licensed operators is sometimes unutilized due to the inactivity of the primary users (PUs) [24]. Such vacant bands are known as spectrum holes. The main feature of a cognitive radio (CR) transceiver (secondary user (SU)) is the spectrum awareness to identify spectrum holes and use them for data transmission. Whenever PU activity is detected in the spectrum in use, the SUs must vacate the spectrum. Therefore, SUs must monitor the spectrum for PU activity.

Significant progress has been made in CR technologies and the Federal Communications Commission (FCC) has allowed the TV broadcasting bandwidth (54-806 MHz) for CR communications. Furthermore, the IEEE 802.22 standard was released with specifications for physical and medium access control layer spec-

ifications for CR networks. Although CR networks are yet to be commercially implemented, it is expected that they will be more commonplace in 5G networks.

1.3.3 Full-duplex networks

Wireless communication systems that were built up to the present day, use orthogonal resources for uplink and downlink communications. Orthogonality achieved in the time domain using different time slots for uplink and downlink communications is known as TDD and the orthogonality achieved using non overlapping frequency band in the frequency domain is known as frequency division duplexing (FDD). However, due to spectrum scarcity, it is considered as a waste of resources to use orthogonal time or frequency resources for uplink and downlink. Therefore, recently, there is a surge of interest in developing wireless systems which can transmit and receive simultaneously using the same time and frequency resources. These systems are known as full-duplex (FD), while the conventional TDD and FDD systems are considered half-duplex (HD).

The major challenge for FD systems is the self-interference (SI) between its own transmission and reception. Therefore, the main focus of FD research was focused on developing SI cancellation techniques. Recent advances of SI cancellation techniques have achieved more than 90 dB isolation between the Tx and Rx. With sophisticated SI cancellation capabilities, FD is identified as a key technology for beyond 4th generation (4G) wireless communications. The European Union has included FD as a framework of METIS, their flagship project for 5G wireless research.

1.4 Motivation

As mentioned in previous sections, it is evident that spectrum scarcity has become a major challenge for future wireless system designers. After reviewing the current advancements in interference coordination techniques and SE improvement schemes, following observations can be made.

- Theoretical analyses are required to identify the performance limits imposed

by CCI on cellular wireless communications. The results for conventional single-input single-output (SISO) and single-input multiple-output (SIMO) systems can be found in [25–30]. However, future wireless standards are expected to be equipped with novel techniques such as relay communications and distributed antenna systems. Therefore, the theoretical performance limits for these novel techniques are required to assess their feasibility in a cellular wireless network setting.

- Interference coordination techniques should be developed to accommodate relay communications. Since relay based wireless networks are expected to be deployed in LTE-A, interference coordination of relay networks is an interesting topic to investigate.

- Theoretical performance limits of FD communications in a cellular network setting have not been investigated. Although it is common to believe that implementing FD communications in cellular networks will ideally increase the SE by a factor of two, the achievable gains could be lower due to the interference limited nature of cellular systems. Therefore, it is important to find ways to integrate FD communications in cellular systems without producing additional interference. A possible application will be to use FD communications only for short range links. A study on the feasibility of FD communications for short range communications in cellular systems is a worthwhile contribution to wireless communications research.

The problems addressed in this thesis are motivated by the above given observations.

1.5 Problem Statement

The specific research problems addressed in this thesis are presented in this section. The main contributions of this thesis are divided into 3 parts.

1. The first part of this thesis focuses on theoretical performance limits of cooperative relay networks and distributed antenna systems, when they operate in

a cellular network with CCI.

2. The second part of this thesis presents low-complexity interference coordination schemes for two-hop relay networks. The performance limits of the proposed schemes are theoretically investigated.

3. The third part of this thesis studies the potential of FD communications in device-to-device (D2D) networks, as a measure of increasing the overall spectral efficiency of wireless networks.

The contributions highlighted above are formulated as five research problems **P1-P5**.

- **P1**- *Outage probability analysis of multiuser relay networks in the presence of CCI*: Relay assisted communications are incorporated in wireless standards such as IEEE 802.16j and 3GPP LTE-A. Therefore, relay networks with multiple users will be implemented in future wireless networks. The performance of multiuser relay networks in the presence of CCI has not been investigated in the literature. This thesis addresses this problem by analyzing the outage probability performance of a multiuser relay network in the presence of CCI.

- **P2**- *Average rate analysis of distributed antenna systems in the presence of CCI*: In DASs, the transmit capabilities of a BS are increased using geographically distributed remote antenna units connected to the BS using backhaul links. This approach helps to achieve macrodiversity, reduce coverage dead spots and improve the per-user throughput in cellular networks. Only few works exist related to the performance of DASs in a cellular network setting. This thesis addresses the identified limitation by developing a theoretical framework to investigate the average rate performance of a DAS with quantized CSI in the presence of CCI.

- **P3**- *Relay coordination schemes for two-cell two-hop networks*: From the results of **P1**, one can identify the performance limits of two-hop relay networks in the presence of CCI may not satisfy the requirements specified for

an acceptable quality-of-service (QoS). To achieve better performance in the presence of CCI, this thesis proposes techniques to coordinate interference from the dominant co-channel interferer in two-hop networks with infrastructure relay nodes. A theoretical framework is presented to evaluate the outage probability achievable with each coordination scheme.

- **P4**- *Interference coordination using a shared relay*: Interference coordination schemes in **P3** require information exchange between the relays in interfering cells. This approach increases the network complexity. Therefore, it is desirable to develop interference coordination schemes that do not require information exchange between cells. To facilitate this, shared relay networks with linear transceivers are proposed and their performance is evaluated in terms of the outage probability and the average rate.

- **P5**- *Average rate analysis of full-duplex device-to-device networks*: Full-duplex communications are emerging as a method of improving SE of wireless networks. However, theoretical results on the achievable SE improvement of FD communications are not found in literature. It is beneficial to have a theoretical framework to identify the feasibility of FD communications over HD communication systems with equal hardware complexity and power consumption. This thesis presents an analytical framework to evaluate the performance of FD D2D networks in terms of the average achievable rate.

1.6 Thesis Structure

This thesis is written in the paper-based thesis format with the exception of Chapters 1, 2 and 8. The material presented in Chapters 3-7 are peer-reviewed research publications published in IEEE journals and IEEE international conference proceedings[1]. Due to the adoption of this paper-based style, each chapter contains its own background, literature review and a list of references.

[1]The results presented Chapters 3-6 of this thesis are published in top journals of IEEE Communications Society such as *IEEE Transactions on Communications* and *IEEE Communications Letters*, while the results of Chapter 7 are published in the proceedings of *IEEE Wireless Communications and Networking Conference*.

Chapter 2 presents background information related to the topics discussed in this thesis. For each topic, previous works and their limitation are mentioned.

Chapter 3 addresses **P1** by developing an analytical framework to evaluate the outage probability performance of an AF relay network with multiple users in the presence of CCI. Multiple users are served based on the principles of opportunistic scheduling. Apart from the impact of CCI, the performance degradation due to CSI feedback delay is also investigated. A version of Chapter 3 is published in *IEEE Transactions on Communications* [31].

Chapter 4 addresses **P2** by proposing a simple technique to accurately estimate the ergodic rate of a DAS operating in the presence of CCI. Apart from the impact of CCI, the worst-case performance achievable with quantized CSI in the presence of CCI is studied. With quantized CSI, the probability distribution of the signal-to-interference plus noise ratio (SINR) has a complicated mathematical form. Therefore, further analysis using this exact distribution becomes mathematically intractable. To alleviate this problem, it is proposed to approximate the distributions of the desired signal power and the cumulative interference power using a more tractable gamma distribution. The accuracy of this approximation is verified using extensive Monte-Carlo simulations. A version of Chapter 4 is published in *IEEE Communications Letters* [32].

Chapter 5 addresses **P3** with an outage probability analysis of relay coordination schemes for two-hop networks. Four relay coordination scenarios based on the backhaul capacity and the availability of CSI are defined and their outage probabilities are evaluated using closed-form expressions. An approximation technique is proposed to account for the user location randomness in outage probability evaluations. A version of Chapter 5 is accepted for publication in *IEEE Transactions on Communications* [33].

Chapter 6 proposes to coordinate CCI by sharing a relay station among the interfering cells. Shared relay CCI coordination can be implemented without CSI and user data exchange between the cells. The outage probability and ergodic rate behaviour of a two-cell shared relay network model is investigated. Two-cell network model can be considered as the case where CCI coordination is performed only

with the dominant interferer. The impact of CSI quantization is also investigated. A version of Chapter 6 is published in *IEEE Transactions on Communications* [34].

Chapter 7 studies the ergodic rate performance of FD D2D networks when they operate as an underlay of conventional cellular networks. A theoretical framework is presented to compare the performance of FD system with a HD system containing equivalent hardware complexity and energy consumption. The results can be used to identify the conditions required for FD systems to outperform HD systems. A version of Chapter 7 is published in the proceedings of the *IEEE Wireless Communications and Networking Conference* 2014 [35].

Chapter 8 presents concluding remarks and possible future research directions based on the results of this thesis.

References

[1] Cisco, "Cisco visual networking index: Global mobile data traffic forecast update, 2013–2018," 2013.

[2] G. L. Stüber, *Principles of Mobile Communication*. Norwell: Kluwer Academic, 2001.

[3] W. C. Jakes, *Microwave Mobile Communications*. New York: IEEE press, 1994.

[4] E. Telatar, "Capacity of multi-antenna Gaussian channels," *Europ. Trans. Telecommun.*, pp. 585–596, Nov.-Dec. 1999.

[5] J. G. J. Foschini and M. J. Gans, "On limits of wireless communication in a fading environment when using multiple antennas," *Wireless Personal Commun.*, no. 3, pp. 311–355, Mar. 1998.

[6] J. G. J. Foschini, "Layered space-time architecture for wireless communication in a fading environment when using multi-element antennas," *Bell Labs Tech. J.*, pp. 41–59, 1996.

[7] V. Tarokh, H. Jafarkhani, and A. R. Calderbank, "Space-time block codes from orthogonal designs," *IEEE Trans. Inf. Theory*, vol. 45, no. 5, pp. 1456–1467, Jul. 1999.

[8] H. Sampath, P. Stoica, and A. Paulraj, "Generalized linear precoder and decoder design for MIMO channels using the weighted MMSE criterion," *IEEE Trans. Commun.*, vol. 49, no. 12, pp. 2198–2206, 2001.

[9] A. F. Molisch and M. Z. Win, "MIMO systems with antenna selection," *IEEE Microw. Mag.*, vol. 5, no. 1, pp. 46–56, Mar. 2004.

[10] S. Sanayei and A. Nosratinia, "Antenna selection in MIMO systems," *IEEE Commun. Mag.*, vol. 42, no. 10, pp. 68–73, Oct. 2004.

[11] J. N. Laneman, D. N. C. Tse, and G. W. Wornell, "Cooperative diversity in wireless networks: Efficient protocols and outage behavior," *IEEE Trans. Inf. Theory*, vol. 50, no. 12, pp. 3062–3080, 2004.

[12] A. Sendonaris, E. Erkip, and B. Aazhang, "User cooperation diversity - part I: System description," *IEEE Trans. Commun.*, vol. 51, no. 11, pp. 1927–1938, 2003.

[13] A. Sendonaris, E. Erkip, and B. Aazhang, "User cooperation diversity - part II: Implementation aspects and performance analysis," *IEEE Trans. Commun.*, vol. 51, no. 11, pp. 1939–1948, 2003.

[14] K. T. Truong and R. W. Heath, "Joint transmit precoding for the relay interference broadcast channel," *IEEE Trans. Veh. Technol.*, vol. 62, no. 3, pp. 1201–1215, Mar. 2013.

[15] "3GPP TR 36.814. Evolved universal terrestrial radio access (E-UTRA); further advancements for E-UTRA (LTE-Advanced)." [Online]. Available: http://www.3gpp.org/ftp/Specs/html-info/36814.htm.

[16] A. Saleh, A. Rustako, and R. Roman, "Distributed antennas for indoor radio communications," *IEEE Trans. Commun.*, vol. 35, no. 12, pp. 1245 –1251, Dec. 1987.

[17] W. Choi and J. Andrews, "Downlink performance and capacity of distributed antenna systems in a multicell environment," *IEEE Trans. Wireless Commun.*, vol. 6, no. 1, pp. 69–73, Jan. 2007.

[18] S. W. Peters, A. Y. Panah, K. T. Truong, and R. W. Heath, "Relay architectures for 3GPP LTE-advanced," *EURASIP J. Wirel. Commun. Netw.*, vol. 2009, pp. 1:1–1:14, Mar. 2009.

[19] M. K. Karakayali, G. J. Foschini, and R. A. Valenzuela, "Network coordination for spectrally efficient communications in cellular systems," *IEEE Wireless Commun.*, vol. 13, no. 4, pp. 56–61, 2006.

[20] D. Lee, H. Seo, B. Clerckx, E. Hardouin, D. Mazzarese, S. Nagata, and K. Sayana, "Coordinated multipoint transmission and reception in LTE-advanced: deployment scenarios and operational challenges," *IEEE Commun. Mag.*, vol. 50, no. 2, pp. 148–155, Feb. 2012.

[21] S. Rangan, T. S. Rappaport, and E. Erkip, "Millimeter-wave cellular wireless networks: Potentials and challenges," *Proc. IEEE*, vol. 102, no. 3, pp. 366–385, Mar. 2014.

[22] E. Larsson, O. Edfors, F. Tufvesson, and T. Marzetta, "Massive MIMO for next generation wireless systems," *IEEE Commun. Mag.*, vol. 52, no. 2, pp. 186–195, Feb. 2014.

[23] L. Lu, G. Y. Li, A. L. Swindlehurst, A. Ashikhmin, and R. Zhang, "An overview of massive MIMO: Benefits and challenges," *IEEE J. Sel. Topics Signal Process.*, vol. 8, no. 5, pp. 742–758, Oct 2014.

[24] S. Haykin, "Cognitive radio: Brain-empowered wireless communications," *IEEE J. Select. Areas Commun.*, vol. 23, no. 2, pp. 201–220, Feb. 2005.

[25] A. A. Abu-Dayya and N. C. Beaulieu, "Outage probabilities of diversity cellular systems with cochannel interference in Nakagami fading," *IEEE Trans. Veh. Technol.*, vol. 41, no. 4, pp. 343–355, Nov. 1992.

[26] A. A. Abu-Dayya and N. C. Beaulieu, "MDPSK on frequency-selective Ricean channels with diversity and cochannel interference," in *Proc. IEEE Vehicular Technology Conf. (VTC)*, Jun 1994, pp. 996–1000 vol.2.

[27] A. A. Abu-Dayya and N. C. Beaulieu, "Diversity MPSK receivers in cochannel interference," *IEEE Trans. Veh. Technol.*, vol. 48, no. 6, pp. 1959–1965, Nov 1999.

[28] A. A. Abu-Dayya and N. C. Beaulieu, "Diversity $\pi/4$-DQPSK on microcellular interference channels," *IEEE Trans. Commun.*, vol. 44, no. 10, pp. 1289–1297, Oct 1996.

[29] A. A. Abu-Dayya and N. C. Beaulieu, "Outage probabilities in the presence of correlated lognormal interferers," *IEEE Trans. Veh. Technol.*, vol. 43, no. 1, pp. 164–173, Feb 1994.

[30] V. A. Aalo and J. Zhang, "Performance analysis of maximal ratio combining in the presence of multiple equal-power cochannel interferers in a Nakagami fading channel," *IEEE Trans. Veh. Technol.*, vol. 50, no. 2, pp. 497–503, Mar 2001.

[31] K. T. Hemachandra and N. C. Beaulieu, "Outage analysis of opportunistic scheduling in dual-hop multiuser relay networks in the presence of interference," *IEEE Trans. Commun.*, vol. 61, no. 5, pp. 1786–1796, May 2013.

[32] K. T. Hemachandra and N. C. Beaulieu, "A moment matching technique to estimate the achievable ergodic rate for limited feedback distributed antenna systems in the presence of out-of-cell interference," *IEEE Commun. Lett.*, vol. 17, no. 7, pp. 1360–1363, July 2013.

[33] K. T. Hemachandra and N. C. Beaulieu, "Relay coordination schemes for two-hop networks: Two-cell case," *IEEE Trans. Commun.*, 2015, (accepted).

[34] K. T. Hemachandra and N. C. Beaulieu, "Shared relay networks with linear receivers at the relay: Two-cell case," *IEEE Trans. Commun.*, vol. 62, no. 4, pp. 1230–1239, Apr. 2014.

[35] K. T. Hemachandra, N. Rajatheva, and M. Latva-aho, "Sum-rate analysis for full-duplex underlay device-to-device networks," in *IEEE Wireless Commun. and Networking Conf. (WCNC)*, April 2014, pp. 514–519.

Chapter 2

Background

This chapter reviews technical fundamentals of the topics discussed in this thesis. These include theoretical basics of fading channel model, transceiver structures, performance metrics, and practical limitations of the system models studied in this thesis. Furthermore, the limitations of the currently available results related to each of the research problems **P1-P5** are discussed.

2.1 Fading Channel Model

Based on the properties of the transmit signal and the characteristics of the propagation channel, fading can be categorized into several forms. Two forms of fading can be defined based on the relation between the symbol duration and the channel coherence time, namely, slow fading and fast fading. The channel coherence time is the time period where we can consider the fading channel impulse response remains almost constant. Slow fading occurs when the symbol duration is relatively smaller than the channel coherence time. And fast fading is vice versa. Similarly another two forms of multipath fading can be identified as flat fading and frequency selective fading. These two types are defined based on the relation between the channel coherence bandwidth and the transmitted signal bandwidth. The channel coherence bandwidth is defined as the frequency range over which the fading channel response remain almost constant. If the transmitted signal bandwidth is relatively smaller than the channel coherence bandwidth, the fading is considered to be flat and otherwise it is frequency selective. In this thesis, it is assumed in all the results

that the fading is slow and flat and the signal amplitude fading is modeled using the Rayleigh distribution. The Rayleigh distribution is used to model the signal amplitude fading when the receiver does not have a line-of-sight (LOS) with the transmitter. The probability density function (PDF) of a Rayleigh distributed signal amplitude X is given by

$$f_X(x) = \frac{x}{\sigma^2}\exp\left(-\frac{x^2}{2\sigma^2}\right), \qquad 0 \leq x < \infty \tag{2.1}$$

where $2\sigma^2$ is the average envelope power ($\mathbb{E}[x^2]$).

2.2 Key Performance Metrics

The performance of a wireless system primarily depends on the receiver's ability to extract the desired signal from a mixture of signals and noise. The relative power of the desired signal compared to other interference (signal-to-interference-plus-noise ratio (SINR)) is a key factor determining this ability. Therefore, majority of the performance metrics defined for wireless systems are closely dependent on the SINR at the receiver. For noise limited systems the SINR is approximated using the signal-to-noise ratio (SNR), while in an interference limited system the SINR is approximated using the signal-to-interference ratio (SIR). The performance metrics studied in this thesis are the outage probability and the achievable ergodic rate.

2.2.1 Outage probability

The outage probability P_{out} of a wireless system is defined as the probability that the instantaneous output SINR, γ, falls below a predefined threshold SINR value γ_{th}. This probability is directly related to the reliability of a wireless link. It can be computed using the probability density function (PDF) of the output SINR as

$$P_{\text{out}}(\gamma_{\text{th}}) = \int_0^{\gamma_{\text{th}}} f_\gamma(\gamma)d\gamma = F_\gamma(\gamma_{\text{th}}) \tag{2.2}$$

where $F_\gamma(\gamma)$ is the cumulative distribution function (CDF) of the SINR. The outage probability serves as an important design factor for a wireless system as it gives the probability that a particular user does not experience an acceptable quality-of-service (QoS). A system designer must make sure that the outage probability

remains small for a large range of SINR values. Typical outage probabilities of current cellular networks fall in the range 10^{-2} to 10^{-3} [1]. It is expected that 5G wireless networks will have to operate with an outage probabilities in the order of 10^{-5} [2].

The user perception of outage probability can be interpreted in several ways. For an example, if the outage probability has a value of 10^{-2}, it suggests that 1% of the time, a user may not receive the desired minimum QoS. The outage probability values computed using (2.2) can be used to evaluate other performance indicators such as average fade duration, which specifies the average duration of an outage event.

2.2.2 Ergodic rate

The ergodic rate of a wireless system is defined as the probabilistic average when the instantaneous rate is averaged over the distributions of all the fading processes. It can be mathematically represented as

$$C_{\text{erg}} = \int_0^\infty B_w \log_2(1+\gamma) f_\gamma(\gamma) d\gamma \tag{2.3}$$

where B_w is the signal bandwidth. The unit of ergodic rate is bits per second. In certain scenarios, it is convenient to compute the ergodic rate using the CDF of γ as

$$C_{\text{erg}} = \frac{B_w}{\ln(2)} \int_0^\infty \frac{1 - F_\gamma(\gamma)}{1+\gamma} d\gamma \tag{2.4}$$

where (2.4) is obtained applying integration by parts in (2.3). In [3], C_{erg} is described as the rate-adaptive, power non-adaptive information rate. This rate is achievable when the transmitter can be informed of the maximum possible transmission rate and use rate adaptive modulation to match the maximum rate at each transmit instant. In practice, the codewords that achieve the ergodic rate could be very long and may not be suitable for delay sensitive applications. However, ergodic rate can be used as a qualitative measure to compare the performance of different systems.

2.3 Transceiver Structures

This section presents the technical background for the transceiver structures employed in this thesis.

2.3.1 Maximal ratio combining receiver

Maximal ratio combining (MRC) is a form of space diversity where receiver uses multiple antennas to obtain multiple copies of the transmitted signal through independently faded paths. The output of a MRC receiver is the weighted sum of received signals. The combining weights are computed to maximize the SNR of the output signal. In the absence of CCI, the input signal of a M-branch MRC receiver can be given as

$$\mathbf{r}_{\text{in}} = \sqrt{P_0}\mathbf{h}_0 s_0 + \mathbf{n} \tag{2.5}$$

where P_0 is the transmit power, s_0 is the unit energy data symbol, $\mathbf{h}_0$ is the M-dimensional complex channel coefficient vector and $\mathbf{n}$ is the AWGN at the receiver. The combiner weights the input signal with weight vector $\mathbf{w}$ and the output of the combiner is given by

$$\mathbf{r}_{\text{out}} = \mathbf{w}^H \mathbf{r}_{\text{in}}. \tag{2.6}$$

It can be shown that the output SNR is maximized when $\mathbf{w} = \mathbf{h}_0$. The resulting SNR is given by

$$\gamma_{\text{MRC}} = \frac{P_0 \left|\left|\mathbf{h}_0\right|\right|^2}{\sigma_2} \tag{2.7}$$

where σ^2 is the noise variance which is assumed to be the same over all the branches.

When N interference signals are present at the receiver, the input signal can be modeled as

$$\mathbf{r}_{\text{in}} = \sqrt{P_0}\mathbf{h}_0 s_0 + \sum_{k=1}^{N} \sqrt{P_I}\mathbf{h}_k s_k + \mathbf{n} \tag{2.8}$$

where P_I is the transmit power of the interferers, s_k is the unit energy data symbol of the k^{th} interferer, and $\mathbf{h}_k$ is the M-dimensional complex channel coefficient vector of the k^{th} interferer. Since the combiner is unaware of the presence of interference, it treats interference as additional AWGN. Therefore, the combining weight vector

is identical to $\mathbf{w}$. The resulting SINR is given by

$$\gamma_{\text{MRC}} = \frac{P_0 \left|\left|\mathbf{h}_0\right|\right|^2}{\sigma_2 + P_I \sum_{k=1}^{N} \frac{|\mathbf{h}_0^H \mathbf{h}_k|^2}{\left|\left|\mathbf{h}_0\right|\right|^2}}. \tag{2.9}$$

2.3.2 Selection combining receiver

Selection combining (SC) is another form of space diversity where the branch with the highest SNR is selected for data decoding. The output SNR of a SC receiver in a noise dominant environment can be given as

$$\gamma_{\text{SC}} = \max\left\{\frac{P_0|h_1|^2}{\sigma^2}\frac{P_0|h_2|^2}{\sigma^2}\cdots\frac{P_0|h_M|^2}{\sigma^2}\right\} \tag{2.10}$$

where $h_1, \cdots, h_M$ are the elements of $\mathbf{h}_0$. When CCI signals are present at the receiver, depending on the ability of the receiver to estimate the interference channels, three SC receiver types are studied in this thesis. If the receiver can estimate the instantaneous SINR, the output SINR is given by

$$\gamma_{\text{SC-SINR}} = \max\left\{\frac{P_0|h_1|^2}{\sigma^2 + \sum_{k=1}^{N} P_I|h_{1k}|^2}\cdots\frac{P_0|h_M|^2}{\sigma^2 + \sum_{k=1}^{N} P_I|h_{Mk}|^2}\right\} \tag{2.11}$$

where h_{jk} is the channel coefficient between the k^{th} interferer and the j^{th} antenna.

If the receiver is capable of estimating only the average powers of the interferer signals, the combiner selects the branch which has the largest ratio of $\frac{|h_j|^2}{\sigma^2+\sigma_{jI}}$, and the resulting output SINR is given by

$$\gamma_{\text{SC-SINR}} = \max_{\frac{|h_j|^2}{\sigma^2+\sigma_{jI}}}\left\{\frac{P_0|h_1|^2}{\sigma^2 + \sum_{k=1}^{N} P_I|h_{1k}|^2}\cdots\frac{P_0|h_M|^2}{\sigma^2 + \sum_{k=1}^{N} P_I|h_{Mk}|^2}\right\} \tag{2.12}$$

where $\sigma_{jI} = \sum_{k=1}^{M} P_I|h_{jk}|$ is the average interference power at the j^{th} antenna. If the receiver has no knowledge regarding the CSI of the interferers, it selects the branch with the largest $|h_k|^2$, treating interference as additional AWGN.

2.3.3 Zero-forcing receiver

Zero-forcing (ZF) is a simple linear receiver technique used in multi-user communications with multiple antenna receivers. In this thesis, it is used with multi-user

networks where users are equipped with only a single antenna. Assuming a system with a M antenna receiver and N single antenna users ($M \geq N$), the $M \times 1$ receive signal vector can be represented as

$$\mathbf{r} = \mathbf{H}\mathbf{s} + \mathbf{n} \tag{2.13}$$

where $\mathbf{s} = (s_1, s_2, \cdots, s_N)^T$ is the $N \times 1$ data vector, $\mathbf{n} \sim \mathcal{CN}(0, \sigma^2\mathbf{I})$ is the AWGN vector, $\mathbf{H} = [\mathbf{h}_1 \cdots \mathbf{h}_N]$ is the $M \times N$ channel matrix with columns representing the channel vector from each user. The output of a ZF receiver can be given as

$$\hat{\mathbf{r}} = \mathbf{W}^H\mathbf{r} \tag{2.14}$$

where the weight matrix $\mathbf{W} = \mathbf{H}(\mathbf{H}^H\mathbf{H})^{-1}$ is given by the pseudoinverse of the matrix $\mathbf{H}$. The resulting SNR for the k^{th} data stream can be found as

$$\gamma_{k,\text{ZF}} = \frac{1}{\sigma^2[(\mathbf{H}^H\mathbf{H})^{-1}]_{kk}} \tag{2.15}$$

where $[(\mathbf{H}^H\mathbf{H})^{-1}]_{kk}$ is the $(k,k)^{\text{th}}$ element of the matrix $(\mathbf{H}^H\mathbf{H})^{-1}$.

2.3.4 Minimum mean-square error receiver

Minimum mean-square error (MMSE) receiver is another linear combining technique used in multi-user wireless systems to suppress multiple access interference [4]. The MMSE receiver is also known as the optimal combiner [5, 6] where it was first proposed as a technique to maximize the output SINR in the presence of CCI signals. In a multiuser network with N single antenna users and an M-antenna receiver, using the same signal model as (2.13), the weight vector for the data detection of the k^{th} user is computed as

$$\mathbf{w}_k = \left(\mathbf{H}\mathbf{H}^H + \sigma^2\mathbf{I}\right)^{-1}\mathbf{h}_1. \tag{2.16}$$

The resulting SINR of the k^{th} user is given by

$$\gamma_{k,\text{MMSE}} = \mathbf{h}_k^H\mathbf{R}^{-1}\mathbf{h}_k \tag{2.17}$$

where

$$R = \sum_{\substack{i=1 \\ i\neq k}}^{N} \mathbf{h}_i\mathbf{h}_i^H + \sigma^2\mathbf{I}. \tag{2.18}$$

2.3.5 Maximal ratio transmission

Maximal ratio transmission (MRT) can be considered as the extension of MRC for multiple transmitting antennas. When a transmitter is equipped with multiple antennas and have the knowledge of the propagation channel to the receiver, it can use MRT to obtain a diversity gain even when the receiver is equipped with only a single antenna. The transmit signal should be appropriately weighted such that the signals from multiple antennas are coherently combined at the receiver. Assuming a single antenna receiver, the received signal of a MRT system with M transmit antennas can be given as

$$r = \mathbf{w}_{\text{MRT}}^{H}\mathbf{h} + n \tag{2.19}$$

where $\mathbf{w}_{\text{MRT}}$ is the MRT weight vector, $\mathbf{h}$ is the $M \times 1$ channel vector and $n \sim \mathcal{CN}(0, \sigma^2)$ is the AWGN. The SNR of the received signal is given by

$$\gamma_{\text{MRT}} = \frac{|\mathbf{w}_{\text{MRT}}^{H}\mathbf{h}|^2}{\sigma^2}. \tag{2.20}$$

It has been shown in [7] that γ_{MRT} is maximized when $\mathbf{w}_{\text{MRT}} = \frac{\mathbf{h}}{||\mathbf{h}||}$. The SNR of the received signal is given by

$$\gamma_{\text{MRT}} = \frac{||\mathbf{h}||^2}{\sigma^2} \tag{2.21}$$

which is equivalent to a MRC receiver with same number of antennas.

2.3.6 Transmit antenna selection

Implementing MRT requires multiple RF chains in the transmitter. However, implementing multiple RF chains are generally expensive and consume extra power. Furthermore, MRT requires full CSI feedback from the receiver. Transmit antenna selection (TAS) serves as a low complexity transmit diversity scheme with lower device cost, power consumption and feedback load. In TAS, the transmitter selects a subset of transmit antennas and applies MRT on the selected subset. With this approach, the number of RF chains required at the transmitter can be reduced and the amount of CSI feedback is also reduced [8,9]. If only a single antenna is selected at the transmitter, only the antenna index needs to be fed back. The TAS scheme used

in this thesis only selects the best antenna, which maximizes SNR at the receiver. In a TAS system with N_t transmit antennas and N_r receiver antennas, the transmit antenna index is found using

$$t_1 = \underset{1 \leq n \leq N_t}{\arg\max} \{||\mathbf{h}_n||^2\} \tag{2.22}$$

where $\mathbf{h}_n$ is the $N_r \times 1$ channel vector between the n^{th} transmit antenna and the receiver. The SNR of this TAS scheme can be given as

$$\gamma_{\text{TAS}} = \max \left\{ \frac{P_0||\mathbf{h}_1||^2}{\sigma^2} \frac{P_0||\mathbf{h}_2||^2}{\sigma^2} \cdots \frac{P_0||\mathbf{h}_{N_t}||^2}{\sigma^2} \right\}. \tag{2.23}$$

2.3.7 Transmit zero forcing

Transmit zero-forcing is a linear precoding scheme used in multiuser MIMO (MU-MIMO) systems to precancel the inter-user interference at the transmitter [10]. Although transmit ZF is suboptimal compared to dirty-paper coding, it is the best precoding scheme among all the linear precoding schemes in the high SNR regime for single antenna users [11]. Consider an MU-MIMO system with M single antenna users and a transmitter with N_t antennas ($N_t \geq M$). The received signal at the u^{th} user can be given as

$$r_u = \mathbf{h}_u^H \sum_{k=1}^{M} \mathbf{f}_k x_k + n_u \tag{2.24}$$

where $\mathbf{h}_u$ is the $N_t \times 1$ channel vector between the transmitter and the u^{th} user, $n_u \sim \mathcal{CN}(0, \sigma^2)$ is the AWGN at the u^{th} user, $\mathbf{f}_k$ and x_k, are the $N_t \times 1$ precoding vector and the transmit symbol of the the k^{th} user, respectively. The transmit power constraint is given by $\mathbb{E}[\mathbf{x}^H \mathbf{x}] = P$, where $\mathbf{x} = [x_1^*, x_2^*, \cdots, x_M^*]^H$. The SINR for the u^{th} user can be given as

$$\gamma_{\text{TZF,u}} = \frac{\frac{P}{M}|\mathbf{h}_u^H \mathbf{f}_u|^2}{\sigma^2 + \frac{P}{M}\sum_{k \neq u}|\mathbf{h}_u^H \mathbf{f}_k|^2}. \tag{2.25}$$

In ZF precoding, the vectors $\mathbf{f}_k$ are computed such that the multiuser interference term $\frac{P}{M}\sum_{k \neq u}|\mathbf{h}_u^H \mathbf{f}_k|^2$ is equal to zero. To achieve this condition, precoding vectors are obtained from the normalized columns of the pseudoinverse of the concatenated channel matrix $\hat{\mathbf{H}} = [\mathbf{h}_1, \mathbf{h}_2, \cdots, \mathbf{h}_M]$. The precoding vector for the u^{th} user is the

normalized u^{th} column of $\hat{\mathbf{H}}^H(\hat{\mathbf{H}}\hat{\mathbf{H}}^H)^{-1}$. When BSs are equipped with multiple antennas and the users are single antenna devices, transmit ZF is suitable for downlink communications while ZF reception can be used for uplink signal reception.

2.4 Practical Limitations

From the details given in Sec. 2.3, it can be observed that multiuser interference cancellation schemes and transmit diversity schemes such as MRT and TAS, require the transmitter to have channel knowledge. In a TDD system, CSI at the transmitter can be obtained from the channel reciprocity. However, in a FDD network, the receivers have to estimate the channels and feedback the estimated CSI to the transmitter via a feedback channel. Channel estimating errors at the receivers, delays in the feedback channel and the limited information rate of the feedback channels are common limitations found in wireless systems. These limitations cause imperfect CSI at the transmitter. Therefore, it is of practical importance to consider the impact of these limitations in the performance evaluations and system designs. The results of this thesis have incorporated the impact of CSI feedback delay and the impact of CSI quantization due to the limited rate supported in the feedback channel.

2.4.1 CSI feedback delay

In FDD systems, initially, the transmitter sends pilot symbols and the receiver estimates the channel. The estimated CSI is fed back to the transmitter via a feedback channel. If the process of CSI estimation and feedback takes a time T_d, due to the time-varying nature of the wireless channels caused by Doppler shifts and other phenomena discussed in Sec.1.2, the actual channel response may be different than the CSI fed back to the transmitter. The correlation coefficient between the estimated channel SNR $\tilde{\gamma}$ and the actual channel γ_a is determined by the time correlation characteristics of the fading process. The most widely used time correlation model was proposed in [12] in which the correlation coefficient ρ is given by $\rho = \mathcal{J}_0^2(2\pi f_d T_d)$, where $\mathcal{J}_0(\cdot)$ is the zeroth-order Bessel function of the first kind

and f_d is the Doppler frequency. The PDF of $\tilde{\gamma}$ can be computed using [13] as

$$f_{\tilde{\gamma}}(\tilde{\gamma}) = \int_0^\infty f_{\tilde{\gamma}|\gamma_a}(\tilde{\gamma}|\gamma_a) f_{\gamma_a}(\gamma_a) d\gamma_a \tag{2.26}$$

where $f_{\tilde{\gamma}|\gamma_a}(\tilde{\gamma}|\gamma_a)$ is the PDF of $\tilde{\gamma}$ conditioned on γ_a. For Rayleigh fading channels considered in this thesis,

$$f_{\tilde{\gamma}|\gamma_a}(\tilde{\gamma}|\gamma_a) = \frac{\exp\left(-\frac{\rho\gamma_a+\tilde{\gamma}}{(1-\rho)\bar{\gamma}}\right)}{(1-\rho)\bar{\gamma}} \mathcal{I}_0\left(\frac{2\sqrt{\rho\tilde{\gamma}\gamma_a}}{(1-\rho)\bar{\gamma}}\right) \tag{2.27}$$

where $\bar{\gamma} = \mathbb{E}[\gamma_a]$ and $\mathcal{I}_0$ is the zeroth-order modified Bessel function of the first kind.

2.4.2 CSI quantization

Feedback channels in wireless systems are expected to have limited resources. Therefore, the information rate supported by feedback channels will be quite low. This imposes restrictions on the codebook size that can be used to quantize the CSI estimated at the receiver. The codebook size and the codeword generation technique are key factors determining the performance of transmit diversity techniques such as ZF precoding and MRT. Consider an MU-MIMO system with M single antenna users and a transmitter with N_t antennas ($N_t \geq M$). Assume that the users can perfectly estimate the CSI of the downlink channel from the pilot symbols. For applications considered in this thesis, only the channel direction $\hat{\mathbf{h}}_u = \frac{\mathbf{h}_u}{||\mathbf{h}_u||}$ is quantized and fed back. The users quantize the estimated channel directions using codebooks of size $L = 2^B$ with $N_t \times 1$ unit norm vectors [10]. The codebook of the u^{th} user is $\mathcal{C}_u = \{\mathbf{c}_{u,1}, \mathbf{c}_{u,2}, \cdots, \mathbf{c}_{u,L}\}$. Since the optimal technique to design the quantization codebooks is not known, random vector quantization (RVQ) is used to generate the codewords. With RVQ, each codeword is independently chosen from an isotropic distribution on the N_t-dimensional unit sphere [14]. The codebooks are known at the transmitter and the users select the index of the codeword closest to the estimated channel direction $\hat{\mathbf{h}}_u$ measured by the inner product

$$i_u = \underset{1 \leq k \leq L}{\arg\max} |\hat{\mathbf{h}}_u^H \mathbf{c}_{u,k}|. \tag{2.28}$$

The users feedback the B-bits corresponding to i_u and the transmitter obtains the CSI for the u^{th} user as $\tilde{\mathbf{h}}_u = \mathbf{c}_{u,i_u}$. Transmit ZF is performed with the normalized columns of the pseudoinverse of the matrix $\tilde{\mathbf{H}} = [\tilde{\mathbf{h}}_1, \tilde{\mathbf{h}}_2, \cdots \tilde{\mathbf{h}}_M]^H$. The SINR for the u^{th} user is given by

$$\gamma_{\text{QZF,u}} = \frac{\frac{P}{M}|\mathbf{h}_u^H \mathbf{f}_u^q|^2}{\sigma^2 + \frac{P}{M}\sum_{k \neq u}|\mathbf{h}_u^H \mathbf{f}_k^q|^2} \tag{2.29}$$

where $\mathbf{f}_k^q$ is the precoding vector of the k^{th} user. In contrast to the perfect CSI case, with quantized CSI the multiuser interference is not completely eliminated. If the elements of $\mathbf{h}_u$ are independent and identically distributed (i.i.d), the distribution of the desired signal is well approximated by a chi-square distribution with $N_t - M$ degrees of freedom. The distribution of the multiuser interference term is approximated using an exponential distribution with mean $\delta = 2^{-\frac{B}{N_t - 1}}$ [15].

2.5 Current State of Research

This section highlights the current state of research work related to each research problem addressed in this thesis.

- The performance limits of SIMO and MIMO systems in the presence of CCI have been characterized extensively in the literature. However, until recently, the research work on relay networks in the presence of CCI were quite limited [16–23]. These works only consider single-user relay networks in their analysis. It is well known that in the absence of CCI, multiuser wireless systems can benefit by introducing relays [24–29]. It is beneficial to have analytical results on the performance of multiuser relay networks (MRNs) in the presence of CCI, since they help the system designers to identify the performance limits of uncoordinated MRNs prior to designing coordinated MRNs. In addition to the impact of CCI, MRN performance depends on the CSI quality available for user scheduling [30]. However, previous studies have not considered the joint impact of CCI and CSI imperfections on the performance of MRNs. These limitations are addressed in Chapter 3.

- The performance of DASs in single-cell networks as well as multi-cell DAS networks have been studied extensively [31, 32]. Recently, interference coordination has been introduced into DASs [33, 34]. However, the main limitation of these works is that they assume the availability of perfect CSI at the transmitters, which is not feasible in practice. Therefore it is important to understand the performance of multi-cell DASs with imperfect CSI at transmitters. This is essential to identify realistic estimates for network design parameters such as number of distributed antenna units and CSI feedback quality required to achieve a particular performance target. Furthermore, the analytical results can be used to identify the sub-optimality of the CSI quantization schemes used in conventional MISO systems and the need of better CSI quantization schemes optimized for DASs. The results presented in Chapter 4 attempt to contribute towards these issues.

- Relay communications and network coordination are two novel features proposed in LTE-A. However, the combination of relay communications with network coordination has not received a significant attention in the literature. A limited number of works on coordinated dual-hop relay systems have been presented in [35–38]. References [35–37] develop transmission techniques for coordinated AF relay networks, while [38] study the capacity performance of coordinated DF relay networks. Although previous work on coordinated relay networks proposed sophisticated transmitter and receiver structures for source and relay nodes, there have been almost no analytical studies related to performance evaluation of relay coordination schemes. Furthermore, the previous studies do not consider the direct link between the source and the destination. Furthermore, it is important to account for the user location randomness in the performance evaluations. The results of Chapter 5 are focused on addressing these issues.

- Shared relay networks have not received significant research attention in the literature [39–41]. Reference [42] have shown that SRNs can approach the gains of network MIMO systems with a much simpler network architecture.

However, the work in [42] used complex techniques such as multiuser detection and dirty paper coding at the relay station, and ignore the existence of a direct link between the BSs and MSs. A transmission technique to maximize the sum capacity of two cell networks using a shared relay was proposed in [39]. The authors assumed that the two BSs exchange data and CSI with each other. The work in [41] studied user scheduling and power allocation schemes to ensure fairness in a multi-cell multiple user SRN. All these previous results on SRNs assumed perfect CSI availability at the relay. However, this condition is difficult to satisfy in practice. Therefore, it is important to consider these limitations for performance studies of SRNs. Furthermore, analytical studies on SRNs are not found in literature. Therefore, it is beneficial to have a theoretical framework to investigate the performance of SRNs. The results of Chapter 6 are focused on addressing these issues.

- Many research efforts in FD communications are focused on SI reduction techniques. Recent advancements in SI cancellation [43, 44] have proposed schemes that can achieve up to 110 dB isolation between the Tx and the Rx. The experimental results of [45] have shown that FD systems are capable of achieving higher spectral efficiencies than HD systems for SI isolation above 74 dB. Efficient SI cancellation filters for multiple antenna systems have been introduced in [46]. In general, these results have been observed in point-to-point FD systems with short distances between the nodes. Exploiting this fact, Chapter 7 investigate the applicability of FD techniques in D2D networks, where the communications are generally short range. In D2D networks, users in close proximity communicate with each other directly, instead of communicating through a central BS. The most common approach to deploy D2D communications in traditional cellular networks is the underlay approach, where D2D users coexist with conventional cellular users while maintaining a maximum allowed interference level on the cellular users. The authors in [47] pointed out the feasibility of underlay D2D networks in 3GPP LTE-A systems. Several works have proposed efficient communication techniques for D2D networks including resource allocation [48], and power opti-

mization [49]. It is interesting to combine the concepts of FD and D2D, since it may allow us to harvest the benefits of both technologies to improve the spectral efficiency of wireless communications. Apart from [50], there have been no prior work related to the performance of FD D2D networks. Chapter 7 presents an analytical framework to evaluate the ergodic rate performance of a FD D2D network.

References

[1] E. Beres and R. Adve, "Outage probability of selection cooperation in the low to medium SNR regime," *IEEE Commun. Lett.*, vol. 11, no. 7, pp. 589–597, 2007.

[2] A. Osseiran, F. Boccardi, V. Braun, K. Kusume, P. Marsch, M. Maternia, O. Queseth, M. Schellmann, H. Schotten, H. Taoka, H. Tullberg, M. A. Uusitalo, B. Timus, and M. Fallgren, "Scenarios for 5G mobile and wireless communications: the vision of the METIS project," *IEEE Commun. Mag.*, vol. 52, no. 5, pp. 26–35, May 2014.

[3] A. J. Goldsmith and P. P. Varaiya, "Capacity of fading channels with channel side information," *IEEE Trans. Inf. Theory*, vol. 43, no. 6, pp. 1986–1992, Nov. 1997.

[4] S. Verdu, *Multiuser Detection*, 1st ed. Cambridge University Press, 1998.

[5] V. M. Bogachev and I. G. Kiselev, "Optimal combination of signals in space-diversity reception," *Radiotekhnika*, vol. 35, pp. 32–34, Oct. 1980.

[6] J. Winters, "Optimum combining in digital mobile radio with cochannel interference," *IEEE J. Select. Areas Commun.*, vol. 2, no. 4, pp. 528–539, 1984.

[7] T. K. Y. Lo, "Maximum ratio transmission," *IEEE Trans. Commun.*, vol. 47, pp. 1458–1461, Oct. 1999.

[8] S. Sanayei and A. Nosratinia, "Antenna selection in MIMO systems," *IEEE Commun. Mag.*, vol. 42, no. 10, pp. 68–73, Oct. 2004.

[9] A. F. Molisch and M. Z. Win, "MIMO systems with antenna selection," *IEEE Microw. Mag.*, vol. 5, no. 1, pp. 46–56, Mar. 2004.

[10] N. Jindal, "MIMO broadcast channels with finite-rate feedback," *IEEE Trans. Inf. Theory*, vol. 52, pp. 5045–5060, Nov. 2006.

[11] N. Jindal, "High SNR analysis of MIMO broadcast channels," in *Proc. 2005 IEEE International Symposium on Information Theory*, Sep. 2005, pp. 2310–2314.

[12] W. C. Jakes, *Microwave Mobile Communications*. New York: IEEE press, 1994.

[13] J. Tang and X. Zhang, "Transmit selection diversity with maximal-ratio combining for multicarrier DS-CDMA wireless networks over Nakagami-*m* fading channels," *IEEE J. Select. Areas Commun.*, vol. 24, no. 1, pp. 104–112, Jan. 2006.

[14] W. Santipach and M. L. Honig, "Signature optimization for CDMA with limited feedback," *IEEE Trans. Inf. Theory*, vol. 51, no. 10, pp. 3475–3492, Oct. 2005.

[15] J. Zhang, R. W. Heath, M. Kountouris, and J. G. Andrews, "Mode switching for the multi-antenna broadcast channel based on delay and channel quantization," *EURASIP J. Adv. Signal Process*, vol. 2009, pp. 1:1–1:15, Feb. 2009.

[16] H. A. Suraweera, H. K. Garg, and A. Nallanathan, "Performance analysis of two hop amplify-and-forward systems with interference at the relay," *IEEE Commun. Lett.*, vol. 14, no. 8, Aug. 2010.

[17] S. S. Ikki and S. Aïssa, "Performance analysis of dual-hop relaying systems in the presence of co-channel interference," in *Proc. IEEE Global Telecommunications Conference, GLOBECOM 2010*, Miami, FL.

[18] D. B. da Costa, H. Ding, and J. Ge, "Interference-limited relaying transmissions in dual-hop cooperative networks over Nakagami-*m* fading," *IEEE Commun. Lett.*, vol. 15, pp. 503–505, May 2011.

[19] D. Lee and J. H. Lee, "Outage probability of decode-and-forward opportunistic relaying in a multicell environment," *IEEE Trans. Veh. Technol.*, vol. 60, pp. 1925–1930, May 2011.

[20] C. Zhong, S. Jin, and K.-K. Wong, "Dual-hop systems with noisy relay and interference-limited destination," *IEEE Trans. Commun.*, vol. 58, no. 3, Mar. 2010.

[21] D. Lee and J. H. Lee, "Outage probability for dual-hop relaying systems with multiple interferers over Rayleigh fading channels," *IEEE Trans. Veh. Technol.*, vol. 60, no. 1, Jan. 2011.

[22] D. B. da Costa and M. D. Yacoub, "Outage performance of two hop AF relaying systems with co-channel interferers over Nakagami-*m* fading," *IEEE Commun. Lett.*, vol. 15, pp. 980–982, Sep. 2011.

[23] F. S. Al-Qahtani, T. Q. Duong, C. Zhong, K. A. Qaraqe, and H. Alnuweiri, "Performance analysis of dual-hop AF systems with interference in Nakagami-*m* fading channels," *IEEE Signal Process. Lett.*, vol. 18, pp. 454–457, Aug. 2011.

[24] J. B. Kim and D. Kim, "Comparison of two SNR-based feedback schemes in multiuser dual-hop amplify-and-forward relaying networks," *IEEE Commun. Lett.*, vol. 12, no. 8, pp. 557 –559, Aug. 2008.

[25] N. Yang, M. Elkashlan, and J. Yuan, "Outage probability of multiuser relay networks in Nakagami-*m* fading channels," *IEEE Trans. Veh. Technol.*, vol. 59, no. 5, pp. 2120 –2132, Jun. 2010.

[26] C. K. Sung and I. B. Collings, "Multiuser cooperative multiplexing with interference suppression in wireless relay networks," *IEEE Trans. Wireless Commun.*, vol. 9, no. 8, pp. 2528 –2538, Aug. 2010.

[27] N. Yang, M. Elkashlan, and J. Yuan, "Impact of opportunistic scheduling on cooperative dual-hop relay networks," *IEEE Trans. Commun.*, vol. 59, no. 3, pp. 689 –694, Mar. 2011.

[28] N. Yang, P. L. Yeoh, M. Elkashlan, J. Yuan, and I. B. Collings, "Cascaded TAS/MRC in MIMO multiuser relay networks," *IEEE Trans. Commun.*, vol. 11, no. 10, pp. 3829 –3839, Oct. 2012.

[29] N. Yang, M. Elkashlan, P. Yeoh, and J. Yuan, "Multiuser MIMO relay networks in Nakagami-*m* fading channels," *IEEE Trans. Commun.*, vol. 60, no. 11, pp. 3298–3310, Nov. 2012.

[30] M. Soysa, H. Suraweera, C. Tellambura, and H. Garg, "Multiuser amplify-and-forward relaying with delayed feedback in Nakagami-*m* fading," in *IEEE Wireless Communications and Networking Conference (WCNC), 2011*, Mar. 2011, pp. 1724 –1729.

[31] W. Choi and J. Andrews, "Downlink performance and capacity of distributed antenna systems in a multicell environment," *IEEE Trans. Wireless Commun.*, vol. 6, no. 1, pp. 69–73, Jan. 2007.

[32] R. Heath, T. Wu, Y. H. Kwon, and A. Soong, "Multiuser MIMO in distributed antenna systems with out-of-cell interference," *IEEE Trans. Signal Process.*, vol. 59, no. 10, pp. 4885–4899, Oct. 2011.

[33] T. Ahmad, R. Gohary, H. Yanikomeroglu, S. Al-Ahmadi, and G. Boudreau, "Coordinated port selection and beam steering optimization in a multi-cell distributed antenna system using semidefinite relaxation," *IEEE Trans. Wireless Commun.*, vol. 11, no. 5, pp. 1861–1871, 2012.

[34] O. Haliloglu, C. Toker, G. Bulu, and H. Yanikomeroglu, "Radio resource management in a coordinated cellular distributed antenna system by using particle swarm optimization," in *IEEE Veh. Technol. Conf. (VTC - 2013 spring),*, 2013, pp. 1–5.

[35] K. Truong and R. Heath, "Interference alignment for the multiple-antenna amplify-and-forward relay interference channel," in *Signals, Systems and Computers (ASILOMAR), 2011 Conference Record of the Forty Fifth Asilomar Conference on*, 2011, pp. 1288–1292.

[36] K. Truong, P. Sartori, and R. Heath, "Cooperative algorithms for mimo amplify-and-forward relay networks," *IEEE Trans. Signal Process.*, vol. 61, no. 5, pp. 1272–1287, 2013.

[37] K. T. Truong and R. W. Heath, "Relay beamforming using interference pricing for the two-hop interference channel," in *IEEE Global Telecommunications Conference (GLOBECOM 2011),*, 2011, pp. 1–5.

[38] J. Zhang and K. Letaief, "Interference management with relay cooperation in two-hop interference channels," *IEEE Trans. Wireless Commun.*, vol. 1, no. 3, pp. 165–168, 2012.

[39] J.-W. Kwon, K.-H. Park, Y.-C. Ko, and H.-C. Yang, "Cooperative joint precoding in a downlink cellular system with shared relay: Design and performance evaluation," *IEEE Trans. Wireless Commun.*, vol. 11, no. 10, pp. 3462 –3473, Oct. 2012.

[40] T. Hui, W. Xi-jun, J. Fan, D. Gang, and Z. Jie-Tao, "An inter-cell interference mitigation scheme based on MIMO-relay technique," in *Proc. 71st IEEE Veh. Tech. Conf.*, May 2010.

[41] Y. Lin and W. Yu, "Fair scheduling and resource allocation for wireless cellular network with shared relays," *IEEE J. Select. Areas Commun.*, vol. 30, no. 8, pp. 1530–1540, Sep. 2012.

[42] S. W. Peters, A. Y. Panah, K. T. Truong, and R. W. Heath, "Relay architectures for 3GPP LTE-advanced," *EURASIP J. Wirel. Commun. Netw.*, vol. 2009, pp. 1:1–1:14, Mar. 2009.

[43] E. Everett, *Full-Duplex Infrastructure Nodes: Achieving Long Range with Half-duplex Mobiles.* Masters Thesis, Rice University., 2012, available: http://hdl.handle.net/1911/64704.

[44] D. Bharadia, E. McMilin, and S. Katti, "Full duplex radios," in *Proc. ACM 2013 Conference on SIGCOMM*, Hong Kong, China, 2013, pp. 375–386. [Online]. Available: http://doi.acm.org/10.1145/2486001.2486033

[45] M. Duarte, C. Dick, and A. Sabharwal, "Experiment-driven characterization of full-duplex wireless systems," *IEEE Trans. Wireless Commun.*, vol. 11, no. 12, pp. 4296–4307, 2012.

[46] D. Bharadia and S. Katti, "Full duplex MIMO radios," in *Proc. 11th USENIX Symposium on Networked Systems Design and Implementation (NSDI 14)*, Seattle, WA, Apr. 2014, pp. 359–372. [Online]. Available: https://www.usenix.org/conference/nsdi14/technical-sessions/bharadia

[47] K. Doppler, M. Rinne, C. Wijting, C. B. Ribeiro, and K. Hugl, "Device-to-device communication as an underlay to LTE-Advanced networks," *IEEE Commun. Mag.*, vol. 47, no. 12, pp. 42–49, 2009.

[48] C.-H. Yu, O. Tirkkonen, K. Doppler, and C. Ribeiro, "Power optimization of device-to-device communication underlaying cellular communication," in *Proc. IEEE International Conference on Communications, 2009. (ICC 09)*, 2009.

[49] X. Chen, L. Chen, M. Zeng, X. Zhang, and D. Yang, "Downlink resource allocation for device-to-device communication underlaying cellular networks," in *Proc. IEEE 23rd International Symposium on Personal Indoor and Mobile Radio Communications (PIMRC), 2012*, 2012, pp. 232–237.

[50] S. Ali, N. Rajatheva, and M. Latva-aho, "Full duplex device-to-device communication in cellular networks," in *Proc. 2014 European Conference on Networks and Communications*, Bologna, Italy.

Chapter 3

Opportunistic Scheduling in Dual-Hop Multiuser Relay Networks in the Presence of Interference

The outage probability of a multiuser two-hop amplify-and-forward relaying system employing opportunistic scheduling is investigated. A practically important case where there are cochannel interference signals present at the network is considered for the analysis. Exact expressions and closed-form lower bounds are derived for the outage probability. Exact closed-form expressions are derived for the system outage probability when interference signals are present at the relay and at the destination separately. A closed-form lower bound is derived for the outage probability when the relay and the destination nodes are affected by interference simultaneously. The effects of channel state information feedback delay are investigated for special cases. In addition, asymptotic outage probability results are derived to obtain useful insights on the effects of interference and feedback delay. The novel expressions can be used by practicing engineers to obtain reliable and realistic performance estimates for dual-hop multiuser relay networks. The results are useful for understanding the capabilities of the feedback channel required in this system.

3.1 Introduction

Dual-hop relay assisted wireless communications has been an active research topic for the last decade. Numerous studies have examined and improved the benefits which can be gained by using dual-hop relaying in the sense of spatial diversity, multiplexing and extending network coverage. Recently, there has been a surge in research related to investigating the effects of cochannel interference (CCI) on dual-hop relay networks. Many results have been published on the effects of CCI on the performance of dual-hop relay networks [1–9]. All these works assume that the network under consideration consists of a single user. However, it has been shown in many studies that multiuser wireless networks can benefit by introducing relaying into the network. These networks are commonly known as multiuser relay networks (MRNs), and their performance has been investigated extensively in the literature [10–15].

In all the previous studies on MRNs, it was assumed that the only additive interference present in the network is additive white Gaussian noise (AWGN). However, due to the practice of frequency reuse adopted to improve the spectral efficiency of cellular wireless networks, the performance of the network can be significantly affected by CCI. Therefore, it is necessary to examine the effects of CCI when we consider the performance of MRNs since it is essential for design of spectrally efficient MRNs.

In this chapter, we investigate the outage probability of an amplify-and-forward (AF) MRN operating in the presence of CCI. Our model is a scaled down version of the model analyzed with only AWGN in [14] in the following sense. Instead of multiple antenna nodes, we assume the source, relay and the destinations are single-antenna nodes. Similar to [14], the principles of opportunistic scheduling are used to determine the user to be served from the source. The relay is responsible for determining the user to be served based on the channel state information available at the relay. We derive closed-form expressions for the outage probability of the MRN when CCI is present at the relay and at the destinations separately. The effect of channel state information (CSI) feedback delays will be investigated for

the case when the interference signals are present only at the relay. When the interference signals are present only at the destination nodes, we study the performance of two possible user scheduling criteria and derive closed-form outage probability expressions for each case. Furthermore, we analyze the most general case when the CCI and AWGN are present at the relay and the destinations simultaneously; tight lower bounds for the outage probability are derived for this case. To the best of the authors' knowledge, there have been no analytical performance results reported for MRNs with CCI.

In wireless networks which employ opportunistic scheduling, the quality of the available CSI can be a critical factor affecting the performance of the system. In practical implementations, CSI feedback is obtained using a control channel and these channels are never perfect. Often they can have delays. Therefore, in order to obtain a realistic estimate of the performance achievable using a particular wireless system, it is important to consider the impact of this delay on the system performance. There are several works that deal with the impact of feedback delay on dual-hop relay networks [16–20], but most of the available works consider relay networks without CCI. A recent work [21] considered the impact of feedback delay on beamforming in a single user relay network. It was shown in [21] that the CCI does not destroy the diversity gain of the system, whereas the feedback delay can destroy the diversity order of the system. However, we are not aware of any works investigating the effects of feedback delay on MRNs operating in the presence of CCI. In this chapter, we derive an exact expression for the outage probability of a MRN with CCI present at the relay node.

The remainder of this chapter is organized as follows. In Section 3.2, we present three possible cases that may prevail in MRNs. Section 3.3 presents outage probability analyses for the three cases. Section 3.5 presents numerical results and comparisons while Section 3.6 concludes this chapter. The detailed derivations are presented in appendices.

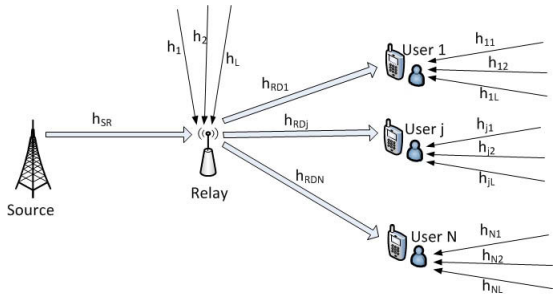

Figure 3.1: The general system model used for analysis.

3.2 System Models

In this section, we present the network configurations used for our analysis. We consider two multiuser relay network protocols, where the relay selects the user to be scheduled based on the available CSI. The relay is assumed to operate in the AF mode with variable amplifying gain. In both models, the source (S), the relay (R) and the users ($D_1, \cdots, D_N$) are single antenna nodes. The direct links between the source and the users (destinations) are assumed to be heavily shadowed and the communications between the source and destinations are possible only with the assistance of the relay. Destination nodes are assumed to be sufficiently spatially separated such that the fading channels from the relay to each destination are mutually independent. All the fading channels ($S - R$, $R - D_i$ and the fading channels of the interference signals) are assumed to be Rayleigh distributed. The source transmission and the relay transmission occur at two different time slots.

Notations

We will use the following notations throughout this chapter. The probability density function (PDF) and the cumulative distribution function (CDF) of a random variable (RV) X are denoted as $f_X(x)$ and $F_X(x)$, respectively. The symbol $\mathbb{E}[\cdot]$ denotes mathematical expectation while the probability of an event $\mathcal{A}$ is denoted $\Pr(\mathcal{A})$.

3.2.1 Interference at the relay

We first consider the case where the cochannel interference signals are present only at the relay while the only additive interference at the destination nodes is AWGN.

This situation can be experienced when a relay node which is located near the edge of a cell, serves shadowed user terminals. In the first time slot, the source transmits the signal to the relay. The signal received at the relay can be modeled as

$$y_{R1} = \sqrt{E_S} h_{SR} x + \sum_{j=1}^{L} \sqrt{E_j} h_j x_j + n_R \tag{3.1}$$

where E_S is the transmitted signal energy at the source, h_{SR} is the fading channel gain between the source and the relay, x is the unit energy data symbol of the scheduled user, E_j is the energy of the j^{th} CCI signal, h_j is the fading channel gain between the j^{th} interferer and the relay, x_j is the unit energy data symbol of the j^{th} interferer, L is the number of interference signals and n_R is the AWGN at the relay with variance σ_R^2.

The relay applies a gain G_1 to the received signal and forwards it to the scheduled destination. The received signal at the k^{th} destination node can be described as

$$y_{D_k} = h_{RD_k} G_1 \left(\sqrt{E_S} h_{SR} x + \sum_{j=1}^{L} \sqrt{E_j} h_j x_j + n_R \right) + n_{D_k} \tag{3.2}$$

where h_{RD_k} is the fading channel gain (with mean-square value Ω_{RD} for all $k \in [1, \cdots, N]$) between the relay and the k^{th} destination node, and n_{D_k} is the AWGN at the k^{th} destination node with variance σ_D^2 (the noise variances at all the destination nodes are assumed to be equal). The relay amplifying factor G_1 is given by [2]

$$G_1 = \sqrt{\frac{E_R}{E_S |h_{SR}|^2 + \sum_{j=1}^{L} E_j |h_j|^2 + \sigma_R^2}} \tag{3.3}$$

where E_R is the energy of the signal transmitted by the relay.

It is assumed that the noise power at the relay is negligible compared to the total interference power. This is a common assumption made in the literature for wireless systems operating under the influence of dominant CCI [2, 22]. Then, the end-to-end (e2e) signal-to-interference-plus-noise ratio (SINR) for the k^{th} destination node can be found as [2]

$$\gamma_k = \frac{\gamma_{SR} \gamma_{RD_{1,k}}}{\gamma_I (\gamma_{RD_{1,k}} + 1) + \gamma_{SR}} \tag{3.4a}$$

where

$$\gamma_{SR} = E_S |h_{SR}|^2 \tag{3.4b}$$

$$\gamma_{RD_{1,k}} = \frac{E_R|h_{RD_k}|^2}{\sigma_D^2} \tag{3.4c}$$

$$\gamma_I = \sum_{j=1}^{L} E_j|h_j|^2. \tag{3.4d}$$

Since it was assumed that the relay operates in the variable gain mode, the relay has access to perfect CSI for the $S-R$ link and knowledge of the instantaneous total interference power. Furthermore, it is assumed that the relay has perfect knowledge of all the $R - D_i, i \in [1, \cdots, N]$ links. Therefore, the relay uses the principle of opportunistic scheduling to determine which destination node signal is to be transmitted. The relay selects the user which maximizes the e2e SINR and feeds back the index of the selected destination to the source. In this system setting, the user with the best $R-D$ link will be the user with the highest e2e SINR. Therefore, the scheduled user's SINR is given by

$$\gamma_{e1} = \frac{\gamma_{SR}\gamma_{RD_{\max}}}{\gamma_I(\gamma_{RD_{\max}} + 1) + \gamma_{SR}} \tag{3.5a}$$

where

$$\gamma_{RD_{\max}} = \max_{k\in[1,\cdots,N]} \{\gamma_{RD_{1,k}}\}. \tag{3.5b}$$

3.2.2 Interference at the destination nodes

Now assume that multiple CCI signals are present only at the destination nodes, while the reception at the relay is corrupted only with AWGN. The signal received at the relay can be given as

$$y_{R2} = E_S h_{SR} x + n_R. \tag{3.6}$$

The relay amplifies the received signal with the gain G_2 given as

$$G_2 = \sqrt{\frac{E_R}{E_S|h_{SR}|^2 + \sigma_R^2}}. \tag{3.7}$$

The received signal at the k^{th} destination node can be given as

$$y_{D_k} = h_{RD_k} G_2 \left(\sqrt{E_S} h_{SR} x + n_R\right) + \sum_{l=1}^{L_k} \sqrt{E_{kl}} h_{kl} x_{kl} + n_{D_k} \tag{3.8}$$

where E_{kl}, h_{kl} and L_k are the energy and the fading channel gain of the l^{th} interferer and the number of interference signals at the k^{th} destination node, respectively. Assuming that the noise powers at the destination nodes are small compared to the CCI powers, the e2e SINR at the k^{th} destination node can be found as

$$\gamma_{2,k} = \frac{\gamma_{SR_2}\gamma_{RD_{2,k}}}{\gamma_{I_k}(\gamma_{SR_2}+1)+\gamma_{RD_{2,k}}} = \frac{\gamma_{SR_2}\gamma_{D_k}}{\gamma_{SR_2}+1+\gamma_{D_k}} \tag{3.9a}$$

where

$$\gamma_{SR_2} = \frac{E_S|h_{SR}|^2}{\sigma_R^2} \tag{3.9b}$$

$$\gamma_{RD_{2,k}} = E_R|h_{RD_k}|^2 \tag{3.9c}$$

$$\gamma_{I_k} = \sum_{l=1}^{L_k} E_{kl}|h_{kl}|^2 \tag{3.9d}$$

and γ_{D_k} is the signal-to-interference ratio (SIR) of the $R-D$ link at the k^{th} destination node given by $\gamma_{D_k} = \frac{\gamma_{RD_{2,k}}}{\gamma_{I_k}}$.

For this system setting, we consider two possible methods of user scheduling namely, a desired signal power algorithm, and a SIR based algorithm. We describe and analyze each of these algorithms in the following.

In desired signal power based selection, the relay has perfect CSI of the $S-R$ link and all the $R-D_i$, $i \in [1,\cdots,N]$ links but it may not have knowledge of the instantaneous interference power at each destination node. Then, the relay cannot apply the opportunistic scheduling principles using the e2e SINR. Therefore, the relay selects the user with the best $R-D$ link and feeds back the index of the selected destination to the source. Then, the e2e SINR of the system becomes

$$\gamma_{e2_D} = \frac{\gamma_{SR_2}\gamma_{RD_{2,\max}}}{\gamma_{I_{D_s}}(\gamma_{SR_2}+1)+\gamma_{RD_{2,\max}}} = \frac{\gamma_{SR_2}\gamma_{D_s}}{\gamma_{SR_2}+1+\gamma_{D_s}} \tag{3.10a}$$

with

$$\gamma_{RD_{2,\max}} = \max_{k\in[1,\cdots,N]}\{\gamma_{RD_{2,k}}\} \tag{3.10b}$$

where $\gamma_{I_{D_s}}$ and γ_{D_s} are the interference power and the SIR at the selected destination node.

If the user terminals are capable of identifying the desired signal and the interference signals, the relay has knowledge of the $R-D$ link SIRs of each user and

SIR based selection is implemented. Then the relay selects the user with the highest $R-D$ SIR and the e2e SINR of the system is given by

$$\gamma_{e2_{SIR}} = \frac{\gamma_{SR_2}\gamma_{D_{\max}}}{\gamma_{SR_2}+1+\gamma_{D_{\max}}} \tag{3.11}$$

where

$$\gamma_{D_{\max}} = \max_{k\in[1,\cdots,N]}\{\gamma_{D_k}\}. \tag{3.12}$$

3.2.3 Interference at the relay and the destinations

The most general case is where both the relay and the destination nodes are affected by CCI and AWGN. The received signal at the relay is same as (3.1) and the relay amplifying gain is given by (3.3). The received signal at the k^{th} destination node is given by

$$y_{D_k} = h_{RD_k}G_1\left(\sqrt{E_S}h_{SR}x+\sum_{j=1}^{L}\sqrt{E_j}h_jx_j+n_R\right)+\sum_{l=1}^{L_k}\sqrt{E_{kl}}h_{kl}x_{kl}+n_{Dk}. \tag{3.13}$$

After some simple manipulation, it can be shown that the SINR at the k^{th} destination can be found as [3]

$$\gamma_k^{\text{eff}} = \frac{\gamma_{SR}^{\text{eff}}\gamma_{RD_k}^{\text{eff}}}{\gamma_{SR}^{\text{eff}}+\gamma_{RD_k}^{\text{eff}}+1} \tag{3.14}$$

where γ_{SR}^{eff} and $\gamma_{RD_k}^{\text{eff}}$ are the effective SINRs of the $S-R$ and $R-D_k$ links, defined as

$$\gamma_{SR}^{\text{eff}} = \frac{\frac{E_S|h_{SR}|^2}{\sigma_R^2}}{1+\sum_{j=1}^{L}\frac{E_j|h_j|^2}{\sigma_R^2}} \tag{3.15}$$

and

$$\gamma_{RD_k}^{\text{eff}} = \frac{\frac{E_R|h_{RD_k}|^2}{\sigma_D^2}}{1+\sum_{l=1}^{L_k}\frac{E_{lk}|h_{lk}|^2}{\sigma_D^2}}. \tag{3.16}$$

In this scenario, the relay has perfect knowledge of the $S-R$ link and all the $R-D_i$, $i\in[1,\cdots,N]$ links and the instantaneous interference power at the relay. However, it may not have access to information on the instantaneous interference powers at the destination nodes. Therefore, the relay selects the user to be scheduled based only on the quality of the $R-D_i$ links. Similar to the case when CCI is present only at the destination nodes, the relay selects the user with the best $R-D$

link and feeds back the user index to the source. The e2e SINR of the scheduled user is given by (3.14) with $\gamma_{RD_k}^{\text{eff}}$ replaced with

$$\gamma_{RD_k}^{\text{eff}} = \frac{\gamma_{RD_{\max}}}{1 + \sum_{l=1}^{L_k} \gamma_{I_{lk}}} \tag{3.17}$$

where $\gamma_{I_{lk}} = \frac{E_{lk}|h_{lk}|^2}{\sigma_D^2}$.

We point out that in the system model adopted here, the system cannot take advantage of factors such as the uneven number of interferers at different destination nodes, the non-identical powers of interference signals and the non-identical mean-square values of the fading channel gains of the interference signals at different destination nodes. Exploiting these issues may result in better e2e SINR at a different destination node other than the node with the best $R - D$ link. However, exploiting these issues will create tradeoffs between the performance and the amount of information feedback implemented in the network. An analysis of this full complexity system for an arbitrary number of users N appears to be intractable.

3.3 Outage Probability Analysis

In this section, we derive exact expressions for the outage probabilities of each system model described in Section 3.2.

3.3.1 Interference at the relay

We define the outage probability as the probability that the e2e SINR falls below a predetermined SINR threshold, γ_{th}. For the case when CCI only is present at the relay, the outage probability can be written as

$$P_{\text{out}}(\gamma_{\text{th}}) = \Pr(\gamma_{e1} < \gamma_{\text{th}}). \tag{3.18}$$

Assuming equal power interferers with independent and identically distributed (i.i.d) fading channels, the outage probability can be obtained as

$$P_{\text{out}}(\gamma_{\text{th}}) = 1 - N \sum_{u=0}^{N-1} \binom{N-1}{u} \frac{(-1)^u \Gamma(L+1)}{\bar{\gamma}_I^L (u+1)} \exp\left(\frac{-(u+1)\gamma_{\text{th}}}{\bar{\gamma}_2}\right) \left[\frac{\gamma_{\text{th}}}{\bar{\gamma}_1} + \frac{1}{\bar{\gamma}_I}\right]^{-L} \exp\left[\frac{\gamma_{\text{th}}(\gamma_{\text{th}}+1)(u+1)}{2\bar{\gamma}_1\bar{\gamma}_2\left(\frac{\gamma_{\text{th}}}{\bar{\gamma}_1} + \frac{1}{\bar{\gamma}_I}\right)}\right] \mathcal{W}_{-L,\frac{1}{2}}\left(\frac{\gamma_{\text{th}}(\gamma_{\text{th}}+1)(u+1)}{\bar{\gamma}_1\bar{\gamma}_2\left(\frac{\gamma_{\text{th}}}{\bar{\gamma}_1} + \frac{1}{\bar{\gamma}_I}\right)}\right) \tag{3.19}$$

where $\bar{\gamma}_1 = E_S\mathbb{E}(|h_{SR}|^2)$, $\bar{\gamma}_2 = \frac{E_S\Omega_{RD}}{\sigma_D^2}$, $\Gamma(\cdot)$ is the Gamma function defined in [23, 8.310.1], and $\mathcal{W}_{\alpha,\beta}(\cdot)$ is the Whittaker function defined in [23, 9.221.1]. The derivation of (3.19) is given in Appendix 3.A.

While the expression (3.19) gives the exact outage probability of the system, next we present an expression to understand the behaviour of the outage probability of the system for the case when $\bar{\gamma}_1, \bar{\gamma}_2 \to \infty$, maintaining the ratio $\frac{\bar{\gamma}_2}{\bar{\gamma}_1}$ a constant κ. Following reference [21], in the high SNR regime, we use an upper bound on the e2e SINR given by $\gamma_{\text{asy}} = \min(\frac{\gamma_{SR}}{\gamma_I}, \gamma_{RD_k})$. The asymptotic outage probability of the system when $N > 1$ is given by

$$P_{\text{out}}^{\infty}(\gamma_{\text{th}}) \approx \frac{L\bar{\gamma}_I\gamma_{\text{th}}}{\bar{\gamma}_1} + \mathcal{O}\left(\bar{\gamma}_1^{-2}\right). \tag{3.20}$$

For a single user system, the asymptotic outage probability is given by

$$P_{\text{su}}^{\infty}(\gamma_{\text{th}}) \approx \frac{L\bar{\gamma}_I\gamma_{\text{th}}}{\bar{\gamma}_1} + \left(\frac{\gamma_{\text{th}}}{\kappa\bar{\gamma}_1}\right) + \mathcal{O}\left(\bar{\gamma}_1^{-2}\right) \tag{3.21}$$

The derivations of (3.20) and (3.21) are given in Appendix 3.A. One can observe that the system performance in the high SNR regime is dominated by the $S - R$ link quality in the multiuser case and the diversity order of the system is 1.

3.3.2 Interference at destination nodes

For the case when CCI only is present at the destination nodes, the outage probability is defined as the probability that the e2e SINR of the scheduled user falls below a predetermined SINR threshold.

The system outage probability under desired signal power based user scheduling is computed using

$$P_{\text{out}}(\gamma_{\text{th}}) = \Pr(\gamma_{e2_D} < \gamma_{\text{th}}) = \Pr\left(\frac{\gamma_{SR_2}\gamma_{D_s}}{\gamma_{SR_2} + 1 + \gamma_{D_s}} < \gamma_{\text{th}}\right). \tag{3.22}$$

Assuming equal power interferers with i.i.d. fading channels and an equal number of interferers (L_D) at all the destination nodes, the outage probability for the system

is given by

$$P_{\text{out}}(\gamma_{\text{th}}) = 1 - N\text{exp}\left(\frac{-\gamma_{\text{th}}}{\bar{\gamma}_{SR_2}}\right)\sum_{k=0}^{N-1}\frac{(-1)^k L_D!\bar{\gamma}_{RD}^{L_D}}{(k+1)\left[(k+1)\bar{\gamma}_{I_D}\gamma_{\text{th}}+\bar{\gamma}_{RD}\right]^{L_D}}$$
$$\times\text{exp}\left(\frac{\gamma_{\text{th}}(\gamma_{\text{th}}+1)(k+1)\bar{\gamma}_{I_D}}{2\bar{\gamma}_{SR_2}((k+1)\bar{\gamma}_{I_D}\gamma_{\text{th}}+\bar{\gamma}_{RD})}\right)\mathcal{W}_{-L_D,-\frac{1}{2}}\left(\frac{\gamma_{\text{th}}(\gamma_{\text{th}}+1)(k+1)\bar{\gamma}_{I_D}}{\bar{\gamma}_{SR_2}((k+1)\bar{\gamma}_{I_D}\gamma_{\text{th}}+\bar{\gamma}_{RD})}\right) \tag{3.23}$$

where $\bar{\gamma}_{SR_2} = \frac{E_S\mathbb{E}(|h_{SR_2}|^2)}{\sigma_R^2}$, and $\bar{\gamma}_{RD} = E_R\Omega_{RD}$, $\bar{\gamma}_{I_D} = E_I\Omega_I$, with E_I and Ω_I the transmitted power and the mean-square value of the fading channel gain of each interferer at the k^{th} destination node, which are assumed to be equal at all the destination nodes. The derivation of (3.23) is presented in Appendix 3.B.

The outage probability of a MRN which uses SIR based user selection can be computed using

$$P_{\text{out}}(\gamma_{\text{th}}) = \Pr(\gamma_{e2_{SIR}} < \gamma_{\text{th}}) = \Pr\left(\frac{\gamma_{SR_2}\gamma_{D_{\max}}}{\gamma_{SR_2}+1+\gamma_{D_{\max}}} < \gamma_{\text{th}}\right). \tag{3.24}$$

Assuming equal power interferers with i.i.d. fading channels and an equal number of interferers (L_D) at all the destination nodes, a closed-form expression for the system outage probability can be found as

$$P_{\text{out}}(\gamma_{\text{th}}) = 1-\text{exp}\left(\frac{-y}{\bar{\gamma}_{SR_2}}\right)\sum_{v=1}^{N}\binom{N}{v}(-1)^v(-L_Dv)\left[\frac{\bar{\gamma}_{RD}}{\bar{\gamma}_{RD}+\bar{\gamma}_{I_D}y}\right]^{L_Dv}\Gamma(L_Dv)$$
$$\times\text{exp}\left[\frac{\frac{y}{\bar{\gamma}_{SR_2}}\left(1+\frac{y}{\bar{\gamma}_{SR_2}}\right)}{2\left(\frac{\bar{\gamma}_{RD}+\bar{\gamma}_{I_D}y}{\bar{\gamma}_{I_D}}\right)}\right]\mathcal{W}_{-L_Dv,\frac{1}{2}}\left[\frac{\frac{y}{\bar{\gamma}_{SR_2}}\left(1+\frac{y}{\bar{\gamma}_{SR_2}}\right)}{\left(\frac{\bar{\gamma}_{RD}+\bar{\gamma}_{I_D}y}{\bar{\gamma}_{I_D}}\right)}\right]. \tag{3.25}$$

The derivation of (3.25) is given in Appendix 3.C.

3.3.3 Interference at the relay and the destinations

For the most general case when the CCI and AWGN are present at the relay and the destinations, the e2e SINR was found as (3.14). In general, the exact expression for the e2e SINR is difficult to use in analytical studies. Therefore, we make use of a tight upper bound on the e2e SINR, introduced in [3]. The e2e SINR of the scheduled user can be tightly upper bounded by γ_{up} given by

$$\gamma_{\text{e2e}} \leq \gamma_{\text{up}} = \min\{\gamma_{SR}^{\text{eff}}, \gamma_{RD_k}^{\text{eff}}\}. \tag{3.26}$$

Then the CDF of γ_{up} can be found as

$$F_{\gamma_{\text{up}}}(\gamma) = F_{\gamma_{SR}^{\text{eff}}}(\gamma) + F_{\gamma_{RD_k}^{\text{eff}}}(\gamma) - F_{\gamma_{SR}^{\text{eff}}}(\gamma).F_{\gamma_{RD_k}^{\text{eff}}}(\gamma) \tag{3.27}$$

where $F_{\gamma_{SR}^{\text{eff}}}(\gamma)$ and $F_{\gamma_{RD_k}^{\text{eff}}}(\gamma)$ are the CDFs of γ_{SR}^{eff} and $\gamma_{RD_k}^{\text{eff}}$, respectively. The expressions for $F_{\gamma_{SR}^{\text{eff}}}(\gamma)$ and $F_{\gamma_{RD_k}^{\text{eff}}}(\gamma)$ are derived in Appendix 3.D. Then a closed-form outage probability lower bound for the system, assuming equal power interference signals with i.i.d fading channels and an equal number of interference signals (L_D) at all the destination nodes, can be derived as

$$P_{\text{out}}(\gamma_{\text{th}}) = 1 - \left(\frac{\Lambda}{\gamma_{\text{th}}+\Lambda}\right)^{L} \exp\left(-\frac{\gamma_{\text{th}}}{\bar{\gamma}_1}\right) + \left[\left(\frac{\Lambda}{\gamma_{\text{th}}+\Lambda}\right)^{L} \exp\left(-\frac{\gamma_{\text{th}}}{\bar{\gamma}_1}\right) \times \sum_{k=0}^{N} \binom{N}{k} (-1)^k \exp\left(-\frac{k\gamma_{\text{th}}}{\bar{\gamma}_2}\right) \left(\frac{\Upsilon}{k\gamma_{\text{th}}+\Upsilon}\right)^{L_D}\right] \tag{3.28}$$

where $\bar{\gamma}_1 = \frac{E_S \mathbb{E}(|h_{SR}|^2)}{\sigma_R^2}$, $\bar{\gamma}_2 = \frac{E_R \mathbb{E}(|h_{RD_k}|^2)}{\sigma_D^2} \forall k \in [1, \cdots, N]$, $\bar{\gamma}_{I_D} = \frac{E_I \Omega_I}{\sigma_D^2}$, $\Lambda = \frac{\bar{\gamma}_1}{\bar{\gamma}_{I_R}}$ and $\Upsilon = \frac{\bar{\gamma}_2}{\bar{\gamma}_{I_D}}$.

While the expression (3.28) gives the exact outage probability of the system, here we present also an expression to understand the behaviour of the outage probability of the system for the case when $\bar{\gamma}_1$, $\bar{\gamma}_2 \to \infty$, maintaining the ratio $\frac{\bar{\gamma}_2}{\bar{\gamma}_1}$ a constant κ. The outage probability in the high SNR regime can be found as

$$P_{\text{out}}^{\infty}(\gamma_{\text{th}}) \approx \frac{\gamma_{\text{th}}}{\bar{\gamma}_1}\left[1 + L\bar{\gamma}_{I_R}\right] + \mathcal{O}(\bar{\gamma}_1^{-2}). \tag{3.29}$$

The derivation of (3.29) is given in Appendix 3.D.

3.4 Impact of CSI Feedback Delay

For the analysis in Sec. 3.3.1, it was assumed that the CSI of the $R-D$ links reach the relay instantaneously. However, in practice, the control channels may have delay and the CSI obtained by the relay could be outdated. In this section, we investigate the impact of CSI feedback delay on the system setting considered in Sec. 3.2.1. We assume the feedback is delayed by T_d time units. To pursue the analysis, we rewrite (3.2) with a time index, namely

$$y_{D1}(t) = h_{RD_k}(t) G_1 \left(\sqrt{E_S} h_{SR}(t) x(t) + \sum_{j=1}^{L} \sqrt{E_j} h_j(t) x_j(t) + n_R(t)\right) + n_D(t). \tag{3.30}$$

The e2e SINR at the k^{th} destination node can be found as

$$\gamma_{k1} = \frac{\gamma_{SR}\tilde{\gamma}_{RD_{1,k}}}{\gamma_I(\tilde{\gamma}_{RD_{1,k}} + 1) + \gamma_{SR}} \tag{3.31}$$

where $\tilde{\gamma}_{RD_{1,k}} = \frac{|h_{RD_k}(t)|^2}{\sigma_D^2}$. We also define $\hat{\gamma}_{RD_{1,k}} = \frac{|h_{RD_k}(t-T_d)|^2}{\sigma_D^2}$. We follow the CSI feedback delay model used in [24]. Note that the user selection is based on $\hat{\gamma}_{RD_{1,k}}$, while the SNR experienced in the selected link is $\tilde{\gamma}_{RD_{1,k}}$, a delayed version of $\hat{\gamma}_{RD_{1,k}}$. In order to evaluate the system outage probability, one requires the PDF of $\tilde{\gamma}_{RD_{1,k}}$. This PDF is computed using the method given in [24], namely

$$\begin{aligned} f_{\tilde{\gamma}_{RD_{1,k}}}(x) &= \int_0^\infty f_{\tilde{\gamma}_{RD_{1,k}}|\hat{\gamma}_{RD_{1,k}}}(x|y) f_{\hat{\gamma}_{RD_{1,k}}}(y) dy \\ &= \int_0^\infty \frac{\exp\left(-\frac{\rho y + x}{(1-\rho)\bar{\gamma}_2}\right)}{(1-\rho)\bar{\gamma}_2} \mathcal{I}_0\left(\frac{2\sqrt{\rho x y}}{(1-\rho)\bar{\gamma}_2}\right) f_{\hat{\gamma}_{RD_{1,k}}}(y) dy \end{aligned} \tag{3.32}$$

where $\mathcal{I}_0(\cdot)$ is the modified Bessel function of the first kind of order zero, $\rho = \mathcal{J}_0^2(2\pi f_d T_d)$, f_d is the Doppler frequency and $\mathcal{J}_0(\cdot)$ is the zeroth-order Bessel function of the first kind. Since the relay selects the user with the best $R-D$ link SNR, the PDF of $\hat{\gamma}_{RD_{1,k}}$ is given by

$$\begin{aligned} f_{\hat{\gamma}_{RD_{1,k}}}(y) &= N\left[F_{\gamma_{RD_{1,k}}}(y)\right]^{N-1} f_{\gamma_{RD_{1,k}}}(y) \\ &= N\left[1 - \exp\left(-\frac{y}{\bar{\gamma}_2}\right)\right]^{N-1} \frac{1}{\bar{\gamma}_2} \exp\left(-\frac{y}{\bar{\gamma}_2}\right). \end{aligned} \tag{3.33}$$

Substituting (3.33) in (3.32), and solving the integral using the result [25, eq. (9)], the PDF of $\tilde{\gamma}_{RD_{1,k}}$ can be found as

$$\begin{aligned} f_{\tilde{\gamma}_{RD_{1,k}}}(x) = \frac{N\exp\left(\frac{-x}{(1-\rho)\bar{\gamma}_2}\right)}{(1-\rho)\bar{\gamma}_2^2} \sum_{l=0}^{N-1} \frac{(-1)^l \binom{N-1}{l}}{\left[\frac{l}{\bar{\gamma}_2} + \frac{\rho}{(1-\rho)\bar{\gamma}_2} + \frac{1}{\bar{\gamma}_2}\right]} \\ \times \exp\left(\frac{\rho x}{(1-\rho)^2\bar{\gamma}_2^2\left[\frac{l}{\bar{\gamma}_2} + \frac{\rho}{(1-\rho)\bar{\gamma}_2} + \frac{1}{\bar{\gamma}_2}\right]}\right). \end{aligned} \tag{3.34}$$

Using the PDF of $\tilde{\gamma}_{RD_{1,k}}$, a closed-form expression for the outage probability can be found as

$$P_{\text{out}}(\gamma_{\text{th}}) = 1 - \frac{N}{2\bar{\gamma}_I^L} \sum_{l=0}^{N-1} \frac{(-1)^l \binom{N-1}{l}}{2(l+1)} \exp\left[\frac{-\gamma_{\text{th}}(l+1)}{\bar{\gamma}_2((1-\rho)l+1)}\right] \left[\frac{1}{\bar{\gamma}_I} + \frac{\gamma_{\text{th}}}{\bar{\gamma}_1}\right]^{-L} \Gamma(L+1) \exp\left(\frac{\frac{\gamma_{\text{th}}(1+\gamma_{\text{th}})(l+1)}{\bar{\gamma}_1\bar{\gamma}_2((1-\rho)l+1)}}{2\left(\frac{1}{\bar{\gamma}_I} + \frac{\gamma_{\text{th}}}{\bar{\gamma}_1}\right)}\right) \mathcal{W}_{-L,\frac{1}{2}}\left(\frac{\frac{\gamma_{\text{th}}(1+\gamma_{\text{th}})(l+1)}{\bar{\gamma}_1\bar{\gamma}_2((1-\rho)l+1)}}{\left(\frac{1}{\bar{\gamma}_I} + \frac{\gamma_{\text{th}}}{\bar{\gamma}_1}\right)}\right). \quad (3.35)$$

The derivation of (3.35) is similar to the derivation of (3.19) and hence omitted.

3.4.1 Asymptotic outage probability

In order to obtain insights on how the CSI feedback delay affects the system performance in the high SNR regime, we present here the asymptotic outage probability of the system. The outage probability behaviour when $\bar{\gamma}_1, \bar{\gamma}_2 \to \infty$ while maintaining the ratio $\frac{\bar{\gamma}_2}{\bar{\gamma}_1}$ a constant κ, can be found as

$$P_{\text{out}}^{\infty}(\gamma_{\text{th}}) \approx \frac{L\bar{\gamma}_I\gamma_{\text{th}}}{\bar{\gamma}_1} + N \sum_{l=0}^{N-1} \frac{(-1)^l \binom{N-1}{l} \gamma_{\text{th}}}{\left[l + \frac{\rho}{1-\rho} + 1\right](1-\rho)\kappa\bar{\gamma}_1} + \mathcal{O}\left(\bar{\gamma}_1^{-2}\right). \quad (3.36)$$

The derivation of (3.36) is given in Appendix 3.E. From (3.36), one can observe that the diversity order of the system is 1.

3.5 Numerical Results

In this section, we present some numerical results obtained from the expressions derived in Sections 3.3 and 3.4. The outage probability of the system with the interference limited relay is plotted in Fig. 3.2 for different numbers of users in the system. The average SIR per interferer (defined as $\frac{\bar{\gamma}_1}{\bar{\gamma}_I}$) at the relay is 20 dB. We can clearly observe the multiuser diversity loss in the system, due to the presence of CCI at the relay. When the first hop SINR dominates the outage probability of the system, the outage probability reaches a floor value. This floor value depends on the number of interference signals present at the relay. Furthermore, the excellent agreement between the theoretical results and the simulation results can be observed.

Fig. 3.3 shows the system outage probability when CCI signals are present at the relay and the average power per interferer is fixed at 5 dB for all values of $\bar{\gamma}_1$ and $\bar{\gamma}_2$. One can observe that the outage probability does not depend significantly on the number of users in the system and as the per hop SNR $\bar{\gamma}_1(\bar{\gamma}_2)$ increases, the impact of the number of users in the system on the system outage probability diminishes. This observation agrees with the asymptotic outage probability expressions, since the system performance is dominated by the first hop.

Fig. 3.4 shows impact of number of CCI signals at the relay on the system outage probability when the total power of the interferers is fixed at 10 dB. The results show that the number of interferers does not have a significant effect on the outage probability of the system when the total interference power is constant. This observation is useful when designing cognitive radio networks with the underlay approach, where the primary network and the secondary users coexist in the same frequency spectrum.

Figs. 3.5 and 3.6 present the impact of feedback delay on the system outage probability when CCI is present only at the relay. The outage probability behaviour for a fixed feedback delay ($f_d T_d = 0.17$ or $\rho = 0.5$) is given in Fig. 3.5 for different values of the number of users in the system and different numbers of CCI signals at the relay when $\bar{\gamma}_I = 10$ dB. Asymptotic outage probability results show that the system diversity order is one, and system performance is less sensitive to the number of users in the system, when the SNR is large. Furthermore, from Fig. 3.6, it can be seen that increasing the number of users in the system does not improve the outage probability performance significantly when the feedback delay is large ($f_d T_d = 0.3$ or $\rho = 0.1$).

Fig. 3.7 shows the outage probability performance when CCI is present only at the destination nodes. The average SIR per interferer at the destinations (defined as $\frac{\bar{\gamma}_{RD}}{\bar{\gamma}_{I_D}}$) is assumed to be 20 dB. One can observe that the SIR based user scheduling outperforms desired signal power based user scheduling in the high SNR regime. The gain obtained with SIR based selection improves with the number of users in the system, when the average SNR is large. For an example, the lowering of the outage probability floor by the SIR based selection scheme is larger for $N = 4$ than

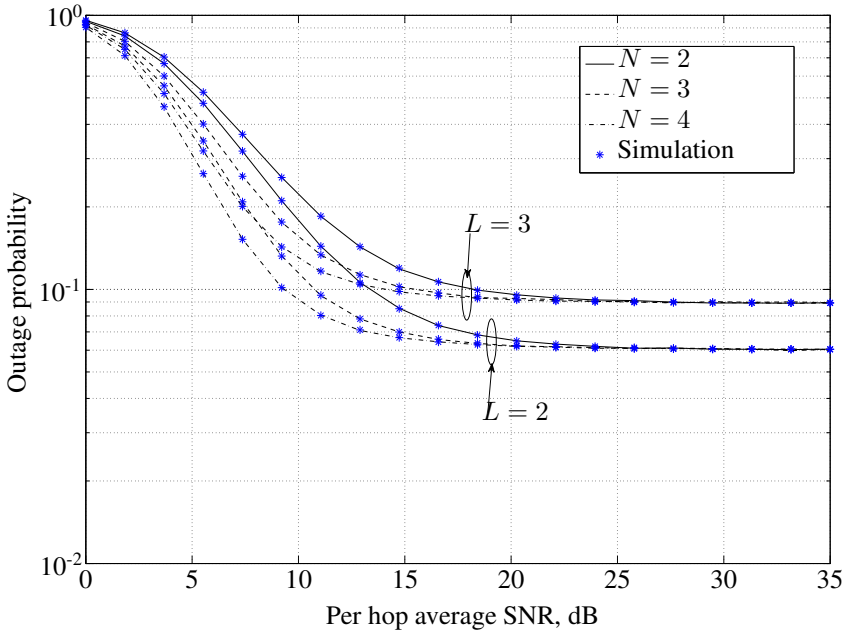

Figure 3.2: The outage probability of the system when interferers are present only at the relay for different numbers of N, L with $\frac{\bar{\gamma}_1}{\bar{\gamma}_I} = 20$ dB.

for the case when $N = 2$.

Fig. 3.8 presents the outage probability behaviour of the system with a fixed number of interferers at the relay. The outage probability lower bound is compared with the outage probability estimated by simulation. One can see that the bound is tight and that the maximum discrepancy does not exceed 0.5 dB in SNR. Observe that the outage probability is weakly dependent on the number of interferers at the destination, while it is dominated by the number of interferers at the relay.

Fig. 3.9 presents the outage probability characteristics of the system for changes in the number of users and the number of interferers at the relay. The results seen in Fig. 3.9 also confirm that the outage probability in the high SNR regime is mainly dependent on the number of interferers at the relay. This fact will be important in network designs for deciding the placement of relays, as it indicates that the interference at the relay tends to limit the performance of the system.

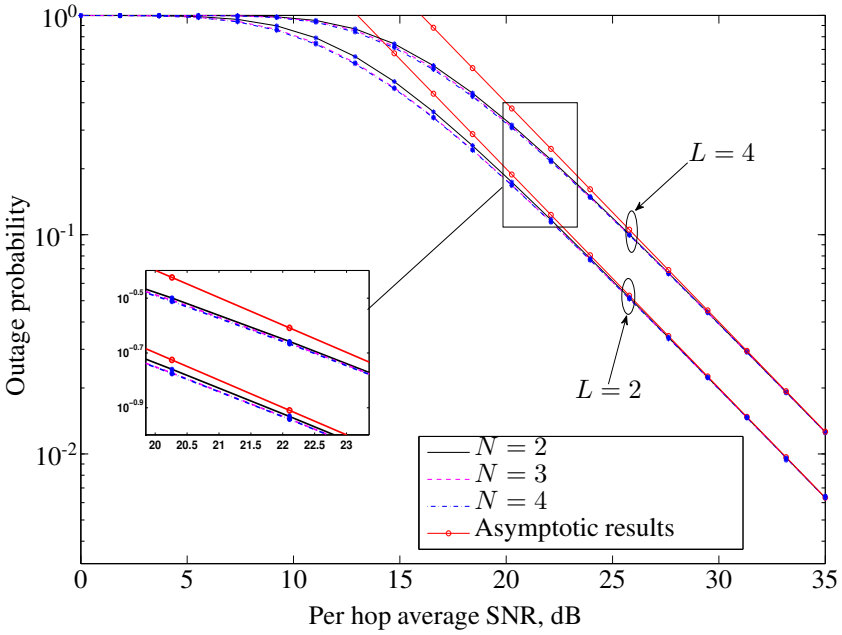

Figure 3.3: The outage probability of the system when interferers are present only at the relay for different numbers of users in the system with $\bar{\gamma}_{I_R} = 5$ dB.

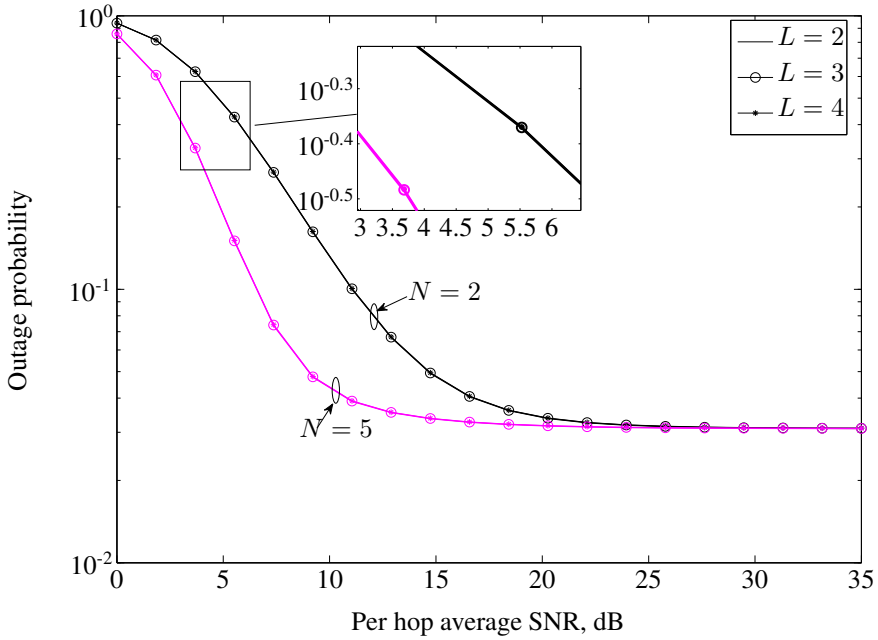

Figure 3.4: The outage probability for different numbers of interferers at the relay with a fixed interference power budget.

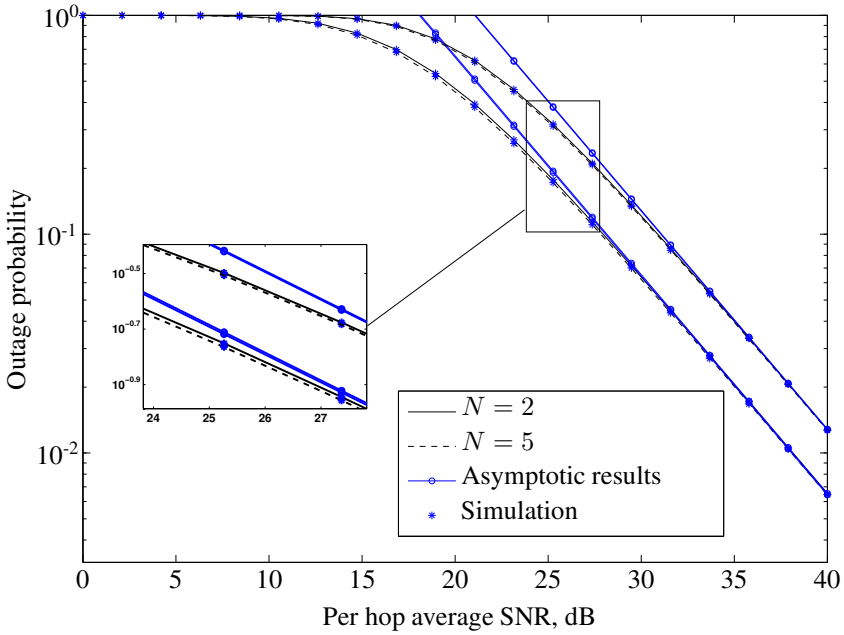

Figure 3.5: The impacts of feedback delay on the system outage probability when CCI signals are present at the relay, with $\rho = 0.5$.

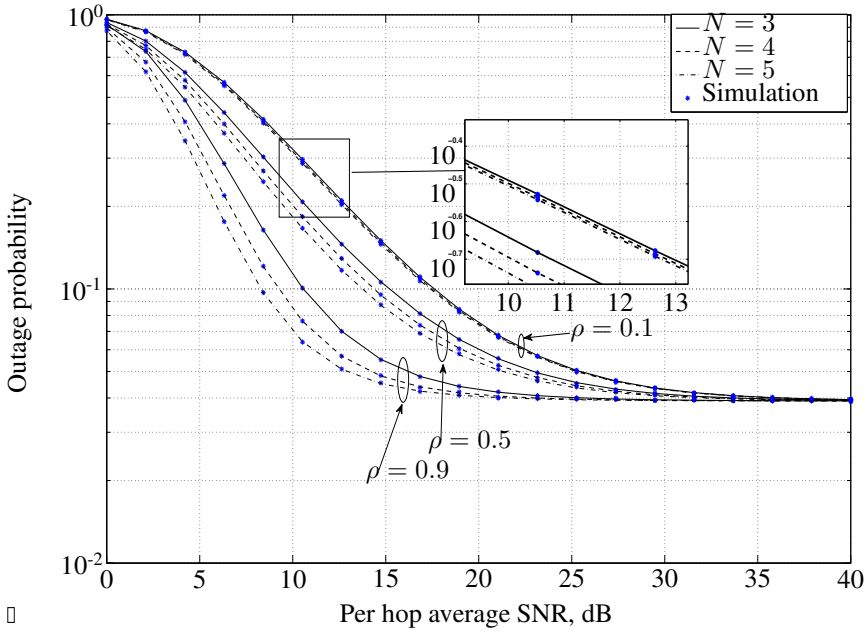

Figure 3.6: The impacts of feedback delay and the number of users in the system when CCI signals are present only at the relay with $\frac{\bar{\gamma}_1}{\bar{\gamma}_I} = 20$ dB.

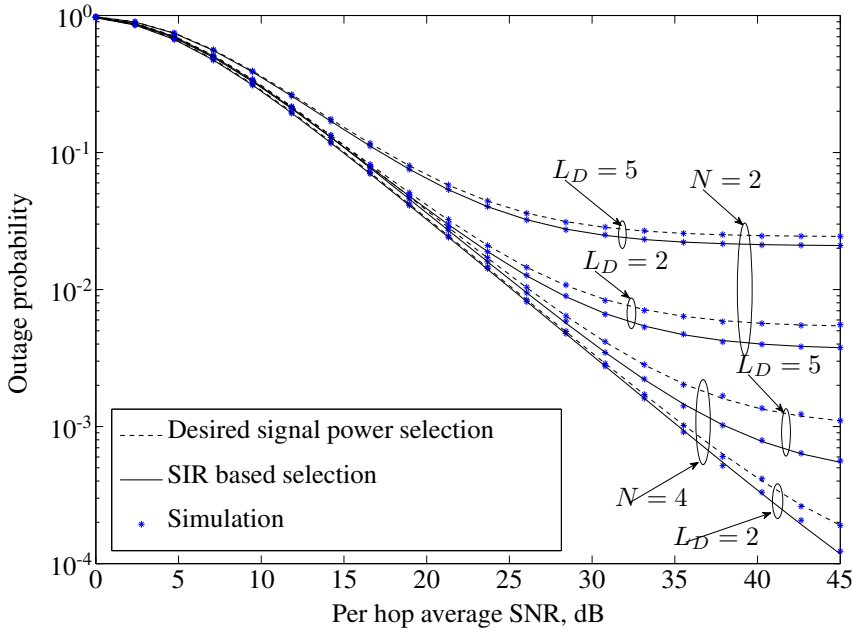

Figure 3.7: The outage probability for two user selection algorithms when interference signals are present only at the destination nodes. The SIR $\frac{\tilde{\gamma}_{RD}}{\tilde{\gamma}_{I_D}} = 20$ dB.

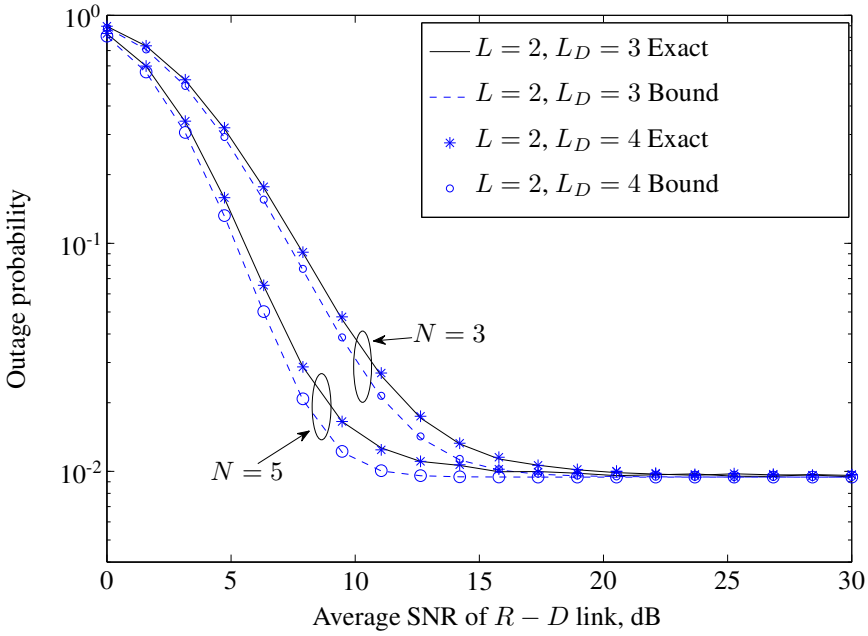

Figure 3.8: The outage probability for different numbers of users and for different numbers of interferers at the destination with $\Lambda = \Upsilon = 30$ dB.

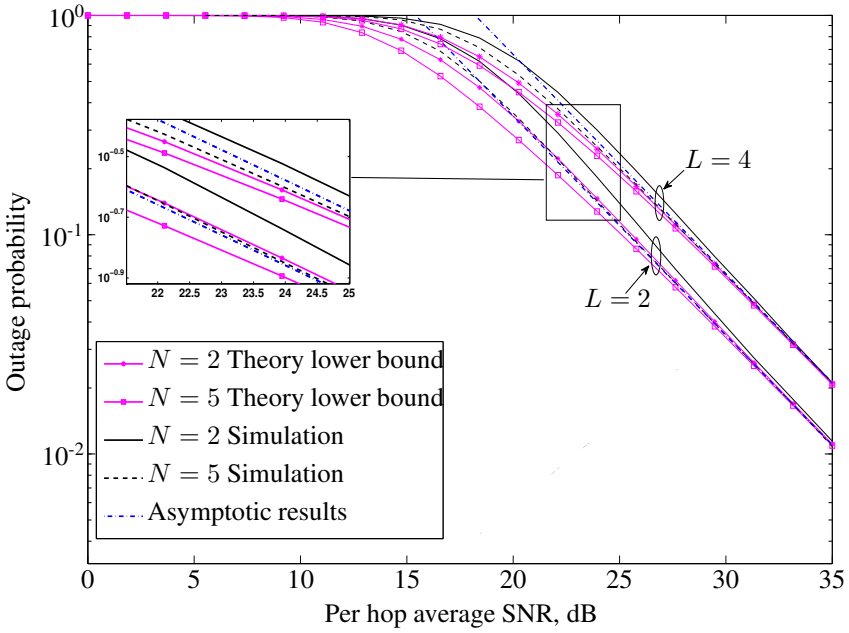

Figure 3.9: The outage probability when interferers are present at both the relay and the destination nodes for different numbers of interferers at the relay with $\bar{\gamma}_{I_R} = \bar{\gamma}_{I_D} = 5$ dB. The number of interferers at the user nodes $L_D = 2$.

3.6 Conclusion

This chapter presented an analysis of outage probability of multiuser relay networks in the presence of CCI. Closed-form expressions were derived for the outage probabilities of the network configurations assuming interference limited network entities. The most general case where the network entities are affected by both CCI and AWGN was also analyzed and a tight lower bound was derived for the outage probability. The lower bound was compared with the precise outage probability results obtained by simulation, and it was shown that the bound is tight at high $R-D$ average SNR values. From the numerical results it was clear that the outage probability is less sensitive to the number of interferers at the destination, while it is mainly dominated by the interference at the relay. Analytical results derived in this chapter can be used to evaluate the feedback channel capabilities of the network.

3.A The Derivations of (3.19), (3.20) and (3.21)

The expression in (3.18) can be rearranged as

$$P_{\text{out}}(\gamma_{\text{th}}) = \int_0^\infty \int_0^\infty \Pr\left(\gamma_{SR} \leq \frac{\gamma_{\text{th}} z(y+1)}{y-\gamma_{\text{th}}}\right) f_{\gamma_{RD}}(y) f_{\gamma_I}(z) dy dz$$
$$= 1 - \int_0^\infty \int_0^\infty \exp\left[\frac{-\gamma_{\text{th}} z(\omega+\gamma_{\text{th}}+1)}{\bar{\gamma}_1 \omega}\right] f_{\gamma_{RD}}(\omega+\gamma_{\text{th}}) f_{\gamma_I}(z) d\omega dz. \tag{3.37}$$

The RV γ_{SR} is exponentially distributed and the PDF of γ_{SR} is given by

$$f_{\gamma_{SR}}(\gamma_1) = \frac{1}{\bar{\gamma}_1} \exp\left(-\frac{\gamma_1}{\bar{\gamma}_1}\right). \tag{3.38}$$

The PDF of γ_{RD} is given by

$$f_{\gamma_{RD}}(y) = \frac{N}{\bar{\gamma}_2}\left[1 - \exp\left(\frac{-y}{\bar{\gamma}_2}\right)\right]^{N-1} \exp\left(\frac{-y}{\bar{\gamma}_2}\right). \tag{3.39}$$

For equal power interference signals in i.i.d. fading channels, the RV γ_I is gamma distributed and the PDF is given by

$$f_{\gamma_I}(\gamma) = \frac{\gamma^{L-1}}{\bar{\gamma}_I^L \Gamma(L)} \exp\left(-\frac{\gamma}{\bar{\gamma}_I}\right). \tag{3.40}$$

The double integral (3.37) can be solved with the help of the identities [23, eq. (3.471.9)] and [23, eq. (6.631.3)]. After some straightforward manipulations, the result in (3.19) is obtained.

In the high SNR regime, the e2e SINR is upper bounded as

$$\gamma_{\text{asy}} \approx \min\left(\frac{\gamma_{SR}}{\gamma_I}, \gamma_{RD_k}\right) = \min\left(\gamma_R, \gamma_{RD_k}\right). \tag{3.41}$$

Then the outage probability is given by

$$P_{\text{out}}^{\infty}(\gamma_{\text{th}}) \approx 1 - \left(1 - F_{\gamma_R}(\gamma_{\text{th}})\right)\left(1 - F_{\gamma_{RD_k}}(\gamma_{\text{th}})\right). \tag{3.42}$$

The CDF of γ_R can be found as

$$F_{\gamma_R}(x) = \int_0^\infty F_{\gamma_{SR}}(\gamma_I x) f_{\gamma_I}(\gamma_I) d\gamma_I = \int_0^\infty \left[1 - \exp\left(-\frac{\gamma_I x}{\bar{\gamma}_1}\right)\right] f_{\gamma_I}(\gamma_I) d\gamma_I \tag{3.43}$$

$$\overset{(a)}{=} \frac{L\bar{\gamma}_I \gamma_{\text{th}}}{\bar{\gamma}_1} + \mathcal{O}\left(\bar{\gamma}_1^{-2}\right) \tag{3.44}$$

where we have solved the integral (3.43) using [23, eq. 3.351.3] and applied the asymptotic expansion of a geometric series to obtain (3.44). The CDF of γ_{RD_k} is given by

$$F_{\gamma_{RD\text{max}}}(\gamma) = \left[1 - \exp\left(-\frac{\gamma}{\bar{\gamma}_2}\right)\right]^N. \tag{3.45}$$

The high-SNR representation of $F_{\gamma_{RD\text{max}}}(\gamma)$ can be found using the MacLaurin series expansion of the exponential function as

$$F_{\gamma_{RD\text{max}}}(\gamma) \approx \left(\frac{\gamma}{\bar{\gamma}_2}\right)^N + \mathcal{O}\left(\bar{\gamma}_2^{-2}\right). \tag{3.46}$$

Substituting (3.44) and (3.46) in (3.42), the expressions for the asymptotic outage probabilities can be obtained as (3.20) and (3.21).

3.B The Derivation of (3.23)

The outage probability (3.22) can be computed as

$$\begin{aligned}
P_{\text{out}}(\gamma_{\text{th}}) &= \int_0^{\infty} \Pr\left(\gamma_{SR_2} \le \frac{\gamma_{\text{th}}(y+1)}{y-\gamma_{\text{th}}}\right) f_{\gamma_{D_s}}(y)dy \\
&= \int_0^{\gamma_{\text{th}}} \Pr\left(\gamma_{SR_2} \le \frac{\gamma_{\text{th}}(y+1)}{y-\gamma_{\text{th}}}\right) f_{\gamma_{D_s}}(y)dy \\
&\qquad + \int_{\gamma_{\text{th}}}^{\infty} \Pr\left(\gamma_{SR_2} \le \frac{\gamma_{\text{th}}(y+1)}{y-\gamma_{\text{th}}}\right) f_{\gamma_{D_s}}(y)dy \qquad (3.47) \\
&\overset{(b)}{=} F_{\gamma_{D_s}}(\gamma_{\text{th}}) + \int_{\gamma_{\text{th}}}^{\infty} \left[1 - \exp\left(\frac{\gamma_{\text{th}}(y+1)}{\bar{\gamma}_{SR_2}(y-\gamma_{\text{th}})}\right)\right] f_{\gamma_{D_s}}(y)dy \qquad (3.48) \\
&\overset{(c)}{=} 1 - \int_0^{\infty} \exp\left(\frac{\gamma_{\text{th}}(\omega+\gamma_{\text{th}}+1)}{\bar{\gamma}_{SR_2}\omega}\right) f_{\gamma_{D_s}}(\omega+\gamma_{\text{th}})d\omega \qquad (3.49)
\end{aligned}$$

where (b) follows from the substitution of the CDF of γ_{SR_2} given by

$$F_{\gamma_{SR_2}}(\gamma) = 1 - \exp\left(-\frac{\gamma}{\bar{\gamma}_{SR_2}}\right) \tag{3.50}$$

into (3.47).

The PDF $f_{\gamma_{D_s}}(y)$ of the selected destination SIR is given by [26, p. 363],

$$f_{\gamma_{D_s}}(y) = N f_n(y, n) \tag{3.51}$$

where $f_n(y,n)$ is the joint PDF of the SIR for the n^{th} destination node and the event that the n^{th} destination is selected. The joint PDF $f_n(y,n)$ is given by [22]

$$f_n(y,n) = \int_0^\infty ds_n \left[\prod_{\substack{i=1 \\ i\neq n}}^{N} \int_0^{s_n} f_{S_i}(s_i) ds_i \right] f_n(y,s_n) \tag{3.52}$$

where the inner integral represents the probability that all other $N-1$ destination nodes have desired signal powers S_i, less than the desired signal power received by the n^{th} destination node, S_n, and $f_n(y,s_n)$ is the joint PDF of S_n and SIR for the n^{th} destination node. Following the steps given in [22, Appendix II], the joint PDF $f_n(y,s_n)$ can be derived as

$$f_n(y,s_n) = \frac{s_n^{L_D}}{\bar{\gamma}_{RD}\bar{\gamma}_{I_D}^{L_D}\Gamma(L_D)y^{L_D+1}} \exp\left[-s_n\left(\frac{1}{\bar{\gamma}_{RD}} + \frac{1}{y\bar{\gamma}_{I_D}}\right)\right]. \tag{3.53}$$

The term inside the brackets in (3.52) can be simplified to

$$\left[\prod_{\substack{i=1 \\ i\neq n}}^{N} \int_0^{s_n} f_{S_i}(s_i) ds_i \right] = \sum_{k=0}^{N-1} \binom{L-1}{k} (-1)^k \exp\left(\frac{-ks_n}{\bar{\gamma}_{RD}}\right). \tag{3.54}$$

Substituting (3.54) and (3.53) in (3.52), and solving the integral using [23, eq. 3.351.3], the joint PDF $f_n(y,n)$ can be found as

$$f_n(y,n) = \sum_{k=0}^{N-1} \binom{N-1}{k} \frac{(-1)^k L_D! \bar{\gamma}_{RD}^{L_D}\bar{\gamma}_{I_D}}{\Gamma(L_D)\left[(k+1)y\bar{\gamma}_{I_D} + \bar{\gamma}_{RD}\right]^{L_D+1}}. \tag{3.55}$$

Substituting (3.55) in (3.51) yields the PDF of γ_{D_s}. Substituting the PDF of γ_{D_s} in (3.49) and solving the integral using the identity [23, eq. 3.471.7] gives the closed-form expression (3.23) for the outage probability of the system.

3.C The Derivation of (3.25)

Using the steps executed in Appendix 3.B to arrive at (3.49), the outage probability expression in (3.24) can be simplified to the integral expression

$$P_{\text{out}}(\gamma_{\text{th}}) = 1 - \int_0^\infty \exp\left(\frac{\gamma_{\text{th}}(\omega+\gamma_{\text{th}}+1)}{\bar{\gamma}_{SR_2}\omega}\right) f_{\gamma_{D_{\max}}}(\omega+\gamma_{\text{th}}) d\omega. \tag{3.56}$$

The PDF $f_{\gamma_{D_{\max}}}(y)$ of the maximum $R-D$ link SIR can be found using [22, eq. (37)] as

$$f_{\gamma_{D_{\max}}}(y)=\sum_{v=1}^{N}\binom{N}{v}\frac{\bar{\gamma}_{RD}^{vL_D}\bar{\gamma}_{I_D}(-L_D v)}{\left(\bar{\gamma}_{I_D}y+\bar{\gamma}_{RD}\right)^{L_D v+1}}. \tag{3.57}$$

Substituting (3.57) in (3.56), and solving the integral using the identity [23, eq. 3.471.7], the closed-form expression (3.25) for the system outage probability is derived.

3.D The Derivation of (3.28)

In order to derive the CDF of γ_{up}, the CDFs of RVs γ_{SR}^{eff} and $\gamma_{RD_k}^{\text{eff}}$ are required. The CDF of γ_{SR}^{eff} was found in [3, eq. (17)], and is given by

$$F_{\gamma_{SR}^{\text{eff}}}(\gamma)=1-\left(\frac{\Lambda}{\gamma+\Lambda}\right)^{L}\exp\left(-\frac{\gamma}{\bar{\gamma}_1}\right). \tag{3.58}$$

The CDF of $\gamma_{RD_k}^{\text{eff}}$ can be derived as

$$\begin{aligned}F_{\gamma_{RD_k}^{\text{eff}}}(\gamma)&=\Pr\left(\frac{\gamma_{RD_{\max}}}{1+\sum_{l=1}^{L_k}\gamma_{I_{lk}}}\leq\gamma\right)\\&=\int_0^{\infty}F_{\gamma_{RD_{\max}}}\left(\gamma\left(1+y\right)\right)f_{\sum_{l=1}^{L_k}\gamma_{I_{lk}}}(y)dy.\end{aligned} \tag{3.59}$$

The CDF of $\gamma_{RD_{\max}}$ is given by

$$F_{\gamma_{RD_{\max}}}(\gamma)=\left[1-\exp\left(-\frac{\gamma}{\bar{\gamma}_2}\right)\right]^{N}. \tag{3.60}$$

Assuming the interferers at the selected destination node have equal powers and i.i.d fading channels, the PDF of $\sum_{l=1}^{L_k}\gamma_{I_{lk}}$ is given by a chi-square density

$$f_{\sum_{l=1}^{L_k}\gamma_{I_{lk}}}(y)dy=\frac{y^{L_k-1}}{\bar{\gamma}_{I_D}^{L_k}\Gamma(L_k)}\exp\left(-\frac{y}{\bar{\gamma}_{I_D}}\right). \tag{3.61}$$

Substituting (3.60) and (3.61) in (3.59), and using the result [23, eq. (3.351.3)], a closed-form expression can be derived for the CDF of $\gamma_{RD_k}^{\text{eff}}$, and is given by

$$F_{\gamma_{RD_k}^{\text{eff}}}(\gamma)=\sum_{n=0}^{N}\binom{N}{n}(-1)^n\exp\left(-\frac{n\gamma}{\bar{\gamma}_2}\right)\left[\frac{\Upsilon}{n\gamma+\Upsilon}\right]^{L_k}. \tag{3.62}$$

Substituting in (3.27), we obtain a closed-form lower bound for the outage probability of the system.

In the high SNR regime, we let $\bar{\gamma}_1, \bar{\gamma}_2 \to \infty$, maintaining the ratio $\frac{\bar{\gamma}_2}{\bar{\gamma}_1}$ a constant κ. We substitute asymptotic series expansions of the CDFs of γ_{SR}^{eff} and $\gamma_{RD_k}^{\text{eff}}$ given by

$$\begin{aligned} F_{\gamma_{SR}^{\text{eff}}}(x) &= 1 - \left(\frac{1}{1+\frac{x}{\Lambda}}\right)^L \exp\left(-\frac{x}{\bar{\gamma}_1}\right) \\ &\approx 1 - \left(1 - \frac{Lx}{\Lambda} + \mathcal{O}(\Lambda^{-2})\right)\left(1 - \frac{x}{\bar{\gamma}_1} + \mathcal{O}(\bar{\gamma}_1^{-2})\right) \\ &\approx \frac{x}{\bar{\gamma}_1}\left[1 + L\bar{\gamma}_{I_R}\right] + \mathcal{O}(\bar{\gamma}_1^{-2}) \end{aligned} \tag{3.63a}$$

and

$$\begin{aligned} F_{\gamma_{RD_k}^{\text{eff}}}(x) &= \sum_{n=0}^{N} \binom{N}{n} (-1)^n \exp\left(-\frac{nx}{\bar{\gamma}_2}\right) \left[\frac{1}{1+\frac{nx}{\Upsilon}}\right]^{L_k} \\ &\approx \sum_{n=0}^{N} \binom{N}{n} (-1)^n \left(1 - \frac{nx}{\bar{\gamma}_2} + \mathcal{O}(\bar{\gamma}_2^{-2})\right)\left[1 - \frac{L_k nx}{\Upsilon} + \mathcal{O}(\Upsilon^{-2})\right] \\ &\approx \sum_{n=0}^{N} \binom{N}{n} (-1)^n \left(1 - \left(\frac{L_k nx}{\Upsilon} + \frac{nx}{\bar{\gamma}_2}\right)\right) + \mathcal{O}(\bar{\gamma}_2^{-2}) \end{aligned} \tag{3.63b}$$

in (3.27) to obtain (3.29) as an expression for the outage probability in the high-SNR regime.

3.E The Derivation of (3.36)

Similar to [21], in the high SNR regime we upper bound the e2e SINR using

$$\gamma_{\text{asm}} = \min\left(\gamma_R, \tilde{\gamma}_{RD_{1,k}}\right). \tag{3.64}$$

Then the outage probability in the high SNR regime can be found in the form (3.42). The CDF of $\tilde{\gamma}_{RD_{1,k}}$ is given by

$$\begin{aligned} F_{\tilde{\gamma}_{RD_{1,k}}}(x) = N \sum_{l=0}^{N-1} & \frac{(-1)^l \binom{N-1}{l}}{\left[l + \frac{\rho}{1-\rho} + 1\right]\left[1 - \frac{\rho}{(1-\rho)\left[l+\frac{\rho}{1-\rho}+1\right]}\right]} \\ & \times \left[1 - \exp\left(\frac{-x}{(1-\rho)\bar{\gamma}_2}\left(1 - \frac{\rho}{(1-\rho)\left[l+\frac{\rho}{1-\rho}+1\right]}\right)\right)\right]. \end{aligned} \tag{3.65}$$

Using the approximation $\exp(-x) \approx 1 - x$ when $x \to 0$, and considering only the terms with the smallest exponent of $\frac{1}{\bar{\gamma}_1}$, the asymptotic outage probability expression (3.36) is obtained.

References

[1] C. Zhong, S. Jin, and K.-K. Wong, "Dual-hop systems with noisy relay and interference-limited destination," *IEEE Trans. Commun.*, vol. 58, no. 3, Mar. 2010.

[2] H. A. Suraweera, H. K. Garg, and A. Nallanathan, "Performance analysis of two hop amplify-and-forward systems with interference at the relay," *IEEE Commun. Lett.*, vol. 14, no. 8, Aug. 2010.

[3] S. S. Ikki and S. Aïssa, "Performance analysis of dual-hop relaying systems in the presence of co-channel interference," in *Proc. IEEE Global Telecommunications Conference, GLOBECOM 2010*, Miami, FL.

[4] D. Lee and J. H. Lee, "Outage probability for dual-hop relaying systems with multiple interferers over Rayleigh fading channels," *IEEE Trans. Veh. Technol.*, vol. 60, no. 1, Jan. 2011.

[5] D. B. da Costa, H. Ding, and J. Ge, "Interference-limited relaying transmissions in dual-hop cooperative networks over Nakagami-*m* fading," *IEEE Commun. Lett.*, vol. 15, pp. 503–505, May 2011.

[6] D. Lee and J. H. Lee, "Outage probability of decode-and-forward opportunistic relaying in a multicell environment," *IEEE Trans. Veh. Technol.*, vol. 60, pp. 1925–1930, May 2011.

[7] W. Xu, J. Zhang, and P. Zhang, "Outage probability of two-hop fixed-gain relay with interference at the relay and destination," *IEEE Commun. Lett.*, vol. 15, pp. 608–610, Jun. 2011.

[8] F. S. Al-Qahtani, T. Q. Duong, C. Zhong, K. A. Qaraqe, and H. Alnuweiri, "Performance analysis of dual-hop AF systems with interference in Nakagami-*m* fading channels," *IEEE Signal Process. Lett.*, vol. 18, pp. 454–457, Aug. 2011.

[9] H. A. Suraweera, D. S. Michalopoulos, R. Schober, G. K. Karagiannidis, and A. Nallanathan, "Fixed gain amplify-and-forward relaying with co-channel interference," in *Proc. IEEE International Conference on Communications (ICC), 2011*, Jun. 2011.

[10] J. B. Kim and D. Kim, "Comparison of two SNR-based feedback schemes in multiuser dual-hop amplify-and-forward relaying networks," *IEEE Commun. Lett.*, vol. 12, no. 8, pp. 557 –559, Aug. 2008.

[11] N. Yang, M. Elkashlan, and J. Yuan, "Outage probability of multiuser relay networks in Nakagami-*m* fading channels," *IEEE Trans. Veh. Technol.*, vol. 59, no. 5, pp. 2120 –2132, Jun. 2010.

[12] C. K. Sung and I. B. Collings, "Multiuser cooperative multiplexing with interference suppression in wireless relay networks," *IEEE Trans. Wireless Commun.*, vol. 9, no. 8, pp. 2528 –2538, Aug. 2010.

[13] N. Yang, M. Elkashlan, and J. Yuan, "Impact of opportunistic scheduling on cooperative dual-hop relay networks," *IEEE Trans. Commun.*, vol. 59, no. 3, pp. 689 –694, Mar. 2011.

[14] N. Yang, P. L. Yeoh, M. Elkashlan, J. Yuan, and I. B. Collings, "Cascaded TAS/MRC in MIMO multiuser relay networks," *IEEE Trans. Commun.*, vol. 11, no. 10, pp. 3829 –3839, Oct. 2012.

[15] N. Yang, M. Elkashlan, P. Yeoh, and J. Yuan, "Multiuser MIMO relay networks in Nakagami-*m* fading channels," *IEEE Trans. Commun.*, vol. 60, no. 11, pp. 3298–3310, Nov. 2012.

[16] H. Suraweera, M. Soysa, C. Tellambura, and H. Garg, "Performance analysis of partial relay selection with feedback delay," *IEEE Signal Process. Lett.*, vol. 17, no. 6, pp. 531 –534, Jun. 2010.

[17] D. Michalopoulos, H. Suraweera, G. Karagiannidis, and R. Schober, "Amplify-and-forward relay selection with outdated channel estimates," *IEEE Trans. Commun.*, vol. 60, no. 5, pp. 1278 –1290, May 2012.

[18] H. Suraweera, T. Tsiftsis, G. Karagiannidis, and A. Nallanathan, "Effect of feedback delay on amplify-and-forward relay networks with beamforming," *IEEE Trans. Veh. Technol.*, vol. 60, no. 3, pp. 1265 –1271, Mar. 2011.

[19] M. Soysa, H. Suraweera, C. Tellambura, and H. Garg, "Multiuser amplify-and-forward relaying with delayed feedback in Nakagami-*m* fading," in *IEEE Wireless Communications and Networking Conference (WCNC), 2011*, Mar. 2011, pp. 1724 –1729.

[20] M. Soysa, H. Suraweera, C. Tellambura, and H. Garg, "Partial and opportunistic relay selection with outdated channel estimates," *IEEE Trans. Commun.*, vol. 60, no. 3, pp. 840 –850, Mar. 2012.

[21] H. Phan, T. Duong, M. Elkashlan, and H.-J. Zepernick, "Beamforming amplify-and-forward relay networks with feedback delay and interference," *IEEE Signal Process. Lett.*, vol. 19, no. 1, pp. 16 –19, Jan. 2012.

[22] A. A. Abu-Dayya and N. C. Beaulieu, "Outage probabilities of diversity cellular systems with cochannel interference in Nakagami fading," *IEEE Trans. Veh. Technol.*, vol. 41, no. 4, pp. 343–355, Nov. 1992.

[23] I. Gradshteyn and I. Ryzhik, *Table of Integrals, Series, and Products, Seventh Edition*. Academic Press, 2007.

[24] J. Tang and X. Zhang, "Transmit selection diversity with maximal-ratio combining for multicarrier DS-CDMA wireless networks over Nakagami-*m* fading channels," *IEEE J. Select. Areas Commun.*, vol. 24, no. 1, pp. 104–112, Jan. 2006.

[25] A. H. Nuttall, "Some integrals involving the q-function," *Naval Underwater Systems Center (NUSC) Technical Report*, Apr. 1972.

[26] W. C. Jakes, *Microwave Mobile Communications*. New York: IEEE press, 1994.

Chapter 4

Ergodic Rate Performance of Limited Feedback Distributed Antenna Systems in the Presence of Interference

The performance of a random vector quantization based transmit precoding distributed antenna system is investigated in terms of the achievable ergodic rate. An approximate expression is derived for the ergodic rate of the system considering the effects of path loss, Rayleigh fading and out-of-cell interference. A moment matching technique is used to approximate the desired signal power and the total interference power distributions of the system using a Gamma distribution. The proposed approximation estimates the performance of the system accurately and saves computational time in simulations.

4.1 Introduction

Distributed antenna systems (DASs) where users are served using a set of geographically distributed antenna units (DAUs) connected to a central unit (CU), were first introduced as a solution to remove coverage dead-spots in indoor locations [1]. Later DASs emerged as a viable solution to provide reduced outages and higher throughputs in wireless networks [2–5]. A thorough analysis of the achievable ergodic rate of multiuser multiple antenna DASs with out-of-cell interference was presented in [6].

In the majority of the works examining the performance of DASs in multi-cell networks, it has been assumed that perfect channel state information (CSI) of all in-cell channels is available at the CU. However, this may impose heavy feedback requirements on the DASs. Reference [7] gave an overview of the feedback requirements and proposed a limited feedback precoding scheme for DASs. Random vector quantization (RVQ) limited feedback precoding, proposed in [8], has been identified as a less complex, suboptimal technique to reduce feedback in co-located multiple antenna systems. Although, RVQ limited feedback precoding is not optimal for DASs, the performance of DASs with RVQ based precoding can be used as a benchmark to compare other limited feedback precoding techniques. There are a limited number of studies that investigate RVQ based precoding in DASs [9, 10], considering only the cases where there are no sources of interference other than additive Gaussian noise. Since DASs have crucial application in heterogeneous networks, it is important to investigate their performance in the presence of out-of-cell interference.

In this chapter, we analyze the performance of DASs with RVQ limited feedback precoding in the presence of out-of-cell interference, in terms of achievable ergodic rate. Since an exact analysis is not mathematically tractable, we propose an approximate solution for the ergodic rate. We justify our approximations using extensive Monte Carlo simulations. The proposed approximations will be useful for practicing engineers to obtain realistic estimates for system design parameters such as codebook size, number of DAUs, and number of antennas at each DAU.

The remainder of this chapter is organized as follows. In Section 4.2, we present the DAS model used for our analysis. Section 4.3 presents the new performance approximations for DAS. Numerical and simulation results are given in Section 4.4, while Section 4.5 concludes this chapter.

The following notations will be used throughout this chapter. The probability density function (PDF) and the cumulative distribution function (CDF) of a random variable (RV) X are denoted as $f_X(x)$ and $F_X(x)$, respectively. The symbol $\mathbb{E}[\cdot]$ denotes expectation while the probability of an event $\mathcal{A}$ is denoted $\Pr(\mathcal{A})$. A complex Gaussian distribution with mean μ and variance σ^2 is denoted as $\mathcal{CN}(\mu, \sigma^2)$. A

Gamma distribution with parameters k and θ is denoted by $\Gamma(k, \theta)$. Euler's Gamma function is denoted as $\Gamma(\cdot)$, while the Whittaker function [11, 9.220.4] is denoted by $\mathcal{W}_{\lambda,\nu}(\cdot)$.

4.2 System Model

Consider a multi-cellular DAS with N DAUs and a central base station. Universal frequency reuse is assumed among the L neighboring cells. All the base stations and DAUs are equipped with N_t transmit antennas while the user equipments are single antenna devices. It is assumed that in each cell, there is only one active user. Without loss of generality, we consider a typical cell (cell 0 in Fig. 4.1) as our reference cell for the analysis, while the transmissions of neighboring cells are treated as co-channel interference.

The DAS uses blanket transmission [3] to serve the users and the macroscopic channel vector for the user in cell 0 (user 0) can be given as

$$\mathbf{h} = \left[\sqrt{L_0^{(0)}}\mathbf{h}_0^{(0)} \sqrt{L_1^{(0)}}\mathbf{h}_1^{(0)} \cdots, \sqrt{L_N^{(0)}}\mathbf{h}_N^{(0)}\right] \tag{4.1}$$

where $\mathbf{h}_i^{(j)}$ denotes the $1 \times N_t$ channel vector with independent and identically distributed (i.i.d.) $\mathcal{CN}(0, 1)$ components from the i^{th} DAU in the j^{th} cell and $L_i^{(j)}$ denotes the propagation path loss from the i^{th} DAU in the j^{th} cell. For simplicity, in theoretical computations and simulations, we use a free-space path loss model to compute $L_i^{(j)}$ as

$$L_i^{(j)} = P_i^{(j)} \frac{c^2}{(4\pi f_c d_i^{(j)})^2} \tag{4.2}$$

where $P_i^{(j)}$ is the power allocated to the i^{th} DAU in the j^{th} cell, $c = 3 \times 10^8$ m/s, f_c is the carrier frequency and $d_i^{(j)}$ is the distance from the i^{th} DAU in the j^{th} cell. Per cell power constraints are assumed such that $\sum_{i=0}^{N} P_i^{(j)} = P_c$, where P_c is the power constraint at each cell. The received signal at user 0 can be formulated as

$$Y^{(0)} = \mathbf{h}\mathbf{T}^{(0)}x^{(0)} + \textstyle\sum_{j=1}^{L} \mathbf{h}^{(j)}\mathbf{T}^{(j)}x^{(j)} + n \tag{4.3}$$

where $\mathbf{h}^{(j)}$ is the macroscopic channel vector from the j^{th} cell to the user 0, $\mathbf{T}^{(j)}$ and $x^{(j)}$ are the transmit precoding vector and the unit energy user data symbol at the j^{th} cell, and n is additive white Gaussian noise (AWGN) at user 0 distributed as

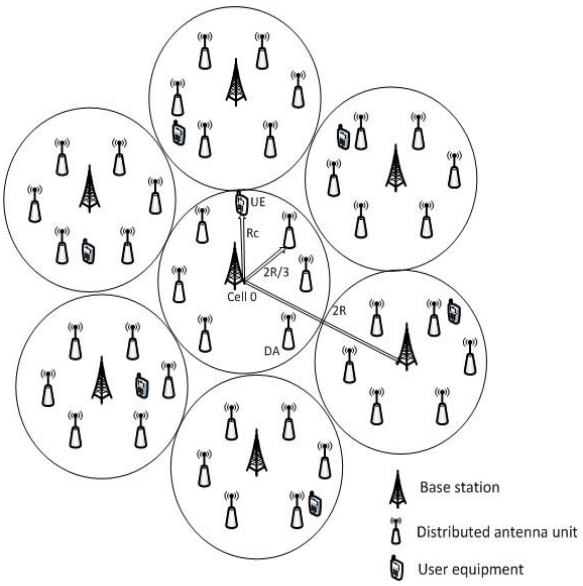

Figure 4.1: The multicell DAS model used for numerical and simulation results.

$\mathcal{CN}(0, \sigma_0^2)$. It is assumed that perfect knowledge of $\mathbf{h}$ is available at the user. However, due to feedback channel constraints, a quantized version $\hat{\mathbf{h}}$ of the estimated channel shape $\tilde{\mathbf{h}} = \frac{\mathbf{h}}{||\mathbf{h}||}$ is available at the CU of cell 0. The quantized channel shape is found using

$$\hat{\mathbf{h}} = \arg\max_{\mathbf{f} \in \mathcal{F}} |\tilde{\mathbf{h}}\mathbf{f}^H|^2 \tag{4.4}$$

where $\mathcal{F} = \{\boldsymbol{w}_k\}_{k=1}^{2^B}$ is the codebook with size 2^B, and $\boldsymbol{w}_k$ are $1 \times NN_t$ vectors. The user feeds back the index of the quantized channel to the processing station. Then, the precoding vector $\mathbf{T}^{(0)}$ is obtained as $\mathbf{T}^{(0)} = \hat{\mathbf{h}}^H$. We assume that codebook $\mathcal{F}$ is generated using the principles of RVQ [12]. The codewords $\boldsymbol{w}_k$ are independent and identically distributed on the unit sphere. The codebook is known at both the user and the AP, and it is changed pseudo-randomly for each symbol period.

4.3 Ergodic Rate Analysis

In this section, we present an approximate analysis of the ergodic rate of the DAS model given in Section 4.2. For our analysis, it is assumed that the covariance matrix of the interference channels is known at the user and no further coordination is assumed among the cells.

4.3.1 Limited feedback DAS

From (4.3) and (4.4), the received signal at user 0 can be written as

$$Y^{(0)} = \|\mathbf{h}\| vx + \sum_{j=1}^{L} \mathbf{h}^{(j)} \mathbf{T}^{(j)} x^{(j)} + n \tag{4.5}$$

with $v = \tilde{\mathbf{h}} \hat{\mathbf{h}}^H$. Assuming Gaussian signaling [6] and treating out-of-cell interference as noise, the ergodic rate of user 0 can be given as

$$\mathcal{I}_{\text{DAS}} = \mathbb{E}\left[\log_2\left(1 + \frac{\frac{1}{\sigma_0^2}\|\mathbf{h}\|^2 |v|^2}{1 + \frac{1}{\sigma_0^2}\sum_{j=1}^{L} \mathbf{h}^{(j)} \mathbf{T}^{(j)} (\mathbf{h}^{(j)} \mathbf{T}^{(j)})^H}\right)\right] \tag{4.6}$$

where the expectation is taken over the channel realizations and all the possible RVQ codebooks. In order to evaluate the expectation in (4.6), one requires the statistics of the signal terms and the total interference term.

Statistics of the Desired Signal Component

The desired signal power is given by

$$\gamma_D = \|\mathbf{h}\|^2 |v|^2 = |v|^2 \sum_{i=0}^{N} L_i^{(0)} \|\mathbf{h}_i^{(0)}\|^2. \tag{4.7}$$

It has been verified in [10] that $\|\mathbf{h}\|^2$ and $|v|^2$ are independent. According to (4.4), $|v|^2$ can be given as

$$|v|^2 = \max_{k=1,\cdots,2^B} \left| \left[\frac{\sqrt{L_0^{(0)}} \mathbf{h}_0^{(0)}}{\|\mathbf{h}\|}, , \cdots , \frac{\sqrt{L_N^{(0)}} \mathbf{h}_N^{(0)}}{\|\mathbf{h}\|} \right] \boldsymbol{w}_k^H \right|^2. \tag{4.8}$$

The CDF of $|v|^2$ for a distributed antenna system with RVQ based limited feedback was derived and verified in [10], and is given by

$$F_{|v|^2}(x) = \left(1 - (1-x)^{NN_t - 1}\right)^{2^B}, \quad 0 \le x < 1. \tag{4.9}$$

The CDF of γ_D can be given as

$$\Pr(\|\mathbf{h}\|^2 |v|^2 < y) = \left[F_{\|\mathbf{h}\|^2}\left(\frac{y}{x}\right) F_{|v|^2}(x) \right]_0^1 + \int_0^1 \frac{F_{|v|^2}(x) f_{\|\mathbf{h}\|^2}\left(\frac{y}{x}\right) y}{x^2} dx \tag{4.10}$$

where integration by parts is applied to obtain (4.10). The PDF of $\|\mathbf{h}\|^2$ can be found using [13, eq. (13)]. Substituting the PDF of $\|\mathbf{h}\|^2$ and using the identities [11, eq.

3.471.2 and eq. 3.381.1], the exact expression for the CDF of γ_D can be obtained as

$$F_{\gamma_D}(y) = \sum_{k=1}^{r}\sum_{l=1}^{v_k} \frac{(-1)\phi_{kl}\eta_k^k}{(l-1)!}\gamma\left(k, \frac{y}{\eta_k}\right) + \sum_{i=0}^{2^B}\sum_{k=1}^{r}\sum_{l=1}^{v_k}\binom{2^B}{i}\frac{(-1)^{i+1}\phi_{kl}}{(l-1)!}(y\eta_k)^{\frac{k-1}{2}} \times \exp\left(\frac{-y}{2\eta_k}\right)\Gamma(i(NN_t-1)+1)\mathcal{W}_{\lambda,\mu}\left(\frac{y}{\eta_k}\right) \quad (4.11)$$

where $\lambda = \frac{1-2(i(NN_t-1)+1)-(2-k)}{2}$ and $\mu = \frac{2-k}{2}$, and with

$$\phi_{kl} = \frac{(-1)^{v_k}}{\eta^{v_k}} \sum_{\tau(k,l)} \prod_{\substack{m=1 \\ m\neq k}}^{r} \binom{v_m + q_m - 1}{q_m} \frac{\eta_m^{q_m}}{\left(1-\frac{\eta_m}{\eta_k}\right)^{v_m+q_m}}$$

$\gamma(\cdot,\cdot)$ is the incomplete Gamma function defined in [11, eq. 8.350.1], $\eta_1, \eta_2, \cdots, \eta_r$ are the distinct values of $L_i^{(0)}$ with multiplicities $v_1, v_2, \cdots, v_r$ respectively, so that $\sum_{k=1}^{r} v_k = NN_t$, $\tau(k,l)$ is the set of r-tuples such that $\tau(k,l) = \{q = (q_1, q_2, \cdots, q_r) \in \mathbb{N}^r : q_k \neq 0, \sum_{m=1}^{r} q_m = v_k - l\}$ and $\mathbb{N}^r$ denotes the set of non-negative integers..

One can identify that the exact form of $F_{\gamma_D}(y)$ is complicated and the usability of (4.11) for performance evaluations is quite low. Therefore, we propose to approximate the distribution of γ_D using a Gamma distribution. Due to the mathematical tractability of the Gamma distribution, it is a common practice in wireless communications literature to approximate complicated distributions with the Gamma distribution [6, 14]. We follow an approach similar to references [6, 14], and use the second-order moment matching technique to approximate the distribution of γ_D with a Gamma distribution.

According to the principles of second-order moment matching, the approximate Gamma distribution $\Gamma(k,\theta)$ for a distribution with mean μ and variance σ^2 will have parameter values $k = \frac{\mu^2}{\sigma^2}$ and $\theta = \frac{\sigma^2}{\mu}$ [6]. Therefore, in order to find the appropriate Gamma approximation, one should compute the mean and variance of γ_D. Using the independence of $\|\mathbf{h}\|^2$ and $|v|^2$ the mean can be found as [10]

$$\mu = \textstyle\sum_{i=0}^{N} L_i^{(0)} N_t \left(1 - 2^B\beta\left(2^B, \frac{NN_t}{NN_t-1}\right)\right) \quad (4.12)$$

where $\beta(\cdot,\cdot)$ is the beta function defined in [11, 8.380.1]. The variance of γ_D can be found using the relations

$$\sigma^2 = [\mathbb{E}(|v|^2)]^2\text{Var}(\|\mathbf{h}\|^2) + [\mathbb{E}(\|\mathbf{h}\|^2)]^2\text{Var}(|v|^2) + \text{Var}(\|\mathbf{h}\|^2)\text{Var}(|v|^2) \quad (4.13a)$$

$$\text{Var}(|v|^2) = 1 - \sum_{t=0}^{2^B} \binom{2^B}{t} \frac{(-1)^t}{(t(NN_t-1))^2+3t(NN_t-1)+2} \tag{4.13b}$$

$$\text{Var}(\|\mathbf{h}\|^2) = N_t \sum_{i=0}^{N} \left(L_i^{(0)}\right)^2. \tag{4.13c}$$

Statistics of the Interference Component

The total interference power at user 0 is given by

$$P_I = \sum_{j=1}^{L} \mathbf{h}^{(j)}\mathbf{T}^{(j)}(\mathbf{h}^{(j)}\mathbf{T}^{(j)})^H. \tag{4.14}$$

We assume identical transmission techniques in neighboring cells, where transmit precoding vectors $\mathbf{T}^{(j)}$ are computed using RVQ based codebooks. To the best of the authors' knowledge, the exact distribution of P_I is not known. However, exploiting the fact that the precoding vectors $\mathbf{T}^{(j)}$ are independent from the channel vectors $\mathbf{h}^{(j)}$ and using the properties of isotropic random vectors, we approximate the distribution of P_I using a Gamma distribution following reference [6], which used second-order moment matching to approximate a total interference power distribution in multi-cell DAS.

First we approximate the distribution of $\nu_j = \|\mathbf{h}^{(j)}\mathbf{T}^{(j)}\|^2$ using a Gamma distribution. In order to proceed with this approach, one must have the mean and the variance of ν_j. The elements of $\mathbf{h}^{(j)}$ are independent but not necessarily identically distributed complex Gaussian RVs. The precoding vectors $\mathbf{T}^{(j)}$ are independent isotropic random vectors. It was shown in [6, Proposition 11] that the mean and the variance of ν generated by such random vectors can be calculated using

$$\mu_{v_j} = \frac{1}{NN_t} \sum_{n=1}^{NN_t} \sigma_n^2 \quad \text{and}$$

$$\sigma_{v_j}^2 = \frac{2}{(NN_t)(NN_t+1)} \left(2 \sum_{n=1}^{NN_t} \sigma_n^4 + \sum_{n=1}^{NN_t} \sum_{k \neq n} \sigma_n^2 \sigma_k^2\right)$$

where σ_n^2 is the variance of the n^{th} component of $\mathbf{h}^{(j)}$. The approximate Gamma distribution for v_j is then given by $\Gamma(k_j, \theta_j)$ with $k_j = \frac{\mu_{v_j}^2}{\sigma_{v_j}^2}$ and $\theta_j = \frac{\sigma_{v_j}^2}{\mu_{v_j}}$.

Now, the distribution of total interference power $V = \sum_j v_j$, can be derived as the distribution of a sum of independent and not necessarily identically distributed $\Gamma(k_j, \theta_j)$, and is given by [15, eq. (2.9)]. However, the PDF given in [15] has limited usage for the purpose of ergodic rate analysis due to its complicated form. Therefore, we propose to approximate the distribution of V using the second-order

moment matching for a sum of Gamma random variables introduced in [6, Proposition 8]. Following the principles of second-order moment matching, the approximate Gamma distribution for V is given as $\Gamma(k_y, \theta_y)$ with $k_y = \frac{\left(\sum_j k_j \theta_j\right)^2}{\sum_j k_j \theta_j^2}$ and $\theta_y = \frac{\sum_j k_j \theta_j^2}{\sum_j k_j \theta_j}$.

Rate Computation

The approximate ergodic rate of the system is given by

$$\mathcal{I}_{\text{DAS}} = \mathbb{E}\left[\log_2\left(1 + \frac{\frac{\gamma_D}{\sigma_0^2}}{1+\frac{V}{\sigma_0^2}}\right)\right] \tag{4.15}$$

where γ_D and V are approximately Gamma distributed RVs. However, the expression (4.15) in its original form is difficult to evaluate analytically. A high signal-to-noise ratio (SNR) approximation for the ergodic rate when γ_D and V are Gamma distributed RVs was proposed in [6]. Applying this approach, the ergodic rate can be computed using

$$\mathcal{I}_{\text{DAS}} \approx \mathbb{E}\left[\log\left(\gamma_D + V\right)\right] - \mathbb{E}[\log(V)]. \tag{4.16}$$

The proof of (4.16) is straightforward and given in [6, Proposition 9]. The expectation of the logarithm of a Gamma RV $X \sim \Gamma(k, \theta)$ is given by

$$\mathbb{E}\log_2(X) = \psi(k)\log_2 e + \log_2(\theta) \tag{4.17}$$

where $\psi(\cdot)$ is the digamma function [11, eq. 8.360.1]. Approximating the signal-plus-interference term $\gamma_D + V$ using a Gamma distribution $\Gamma(k_{xy}, \theta_{xy})$ where $k_{xy} = \frac{(k\theta + k_y\theta_y)^2}{k\theta^2 + k_y\theta_y^2}$ and $\theta_{xy} = \frac{k\theta^2 + k_y\theta_y^2}{k\theta + k_y\theta_y}$. and substituting k_{xy}, θ_{xy} and (4.17) in (4.16), the approximate expression for the system ergodic rate can be found as

$$\mathcal{I}_{\text{DAS}} \approx \psi(k_{xy})\log_2 e + \log_2(\theta_{xy}) - \psi(k_y)\log_2 e - \log_2(\theta_y). \tag{4.18}$$

4.3.2 Conventional limited feedback MISO system

Next, we analyze the ergodic rate when there is a single transmit unit in each cell and a common per cell power constraint P_c. Without loss of generality, we assume that only the base station is active in each cell.

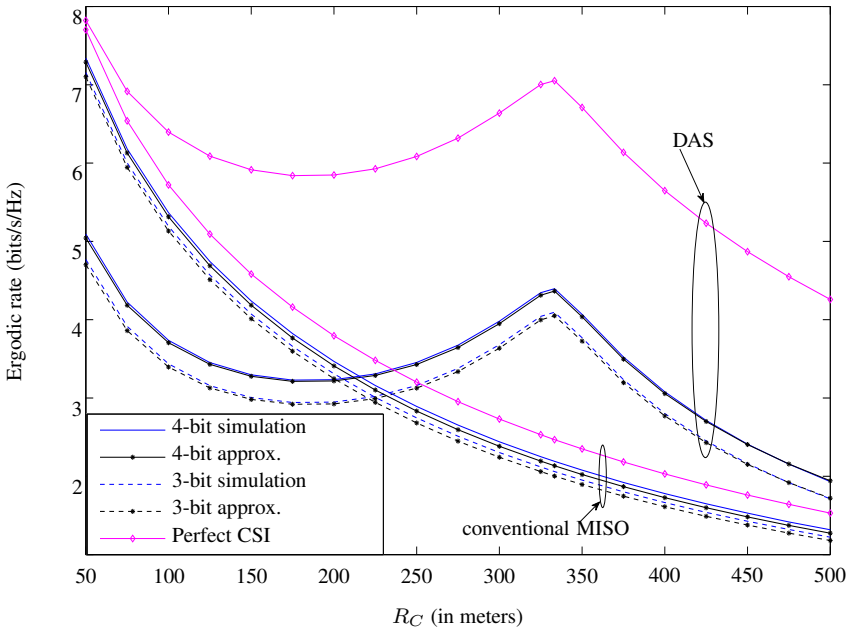

Figure 4.2: Ergodic rate comparisons using different codebook sizes for DAS and MISO systems.

The exact CDF of the desired signal component is given in [12, eq. 20]. However, due to the complicated structure of this CDF, it is not readily usable for ergodic rate computations. Therefore, again we approximate the distribution of γ_D using a Gamma distribution with $\Gamma(k_c, \theta_c)$, where the parameters k_c and θ_c can be readily obtained from (4.12) and (4.13a) by letting $N = 1$.

An exact solution for the total out-of-cell interference power in this scenario is not known. Therefore, we approximate the total interference power distribution using a Gamma distribution as discussed in Section 4.3.1. Then, employing the high SNR rate approximation (4.16), the approximate ergodic capacity of the system can be evaluated.

4.4 Numerical and Simulation Results

The network model used for numerical and simulation results is given in Fig. 4.1. The cell radius is $R = 500$ m and we use DASs with one base station and 6 DAUs (equipped with N_t=3) in each cell, where DAUs are deployed such that they are

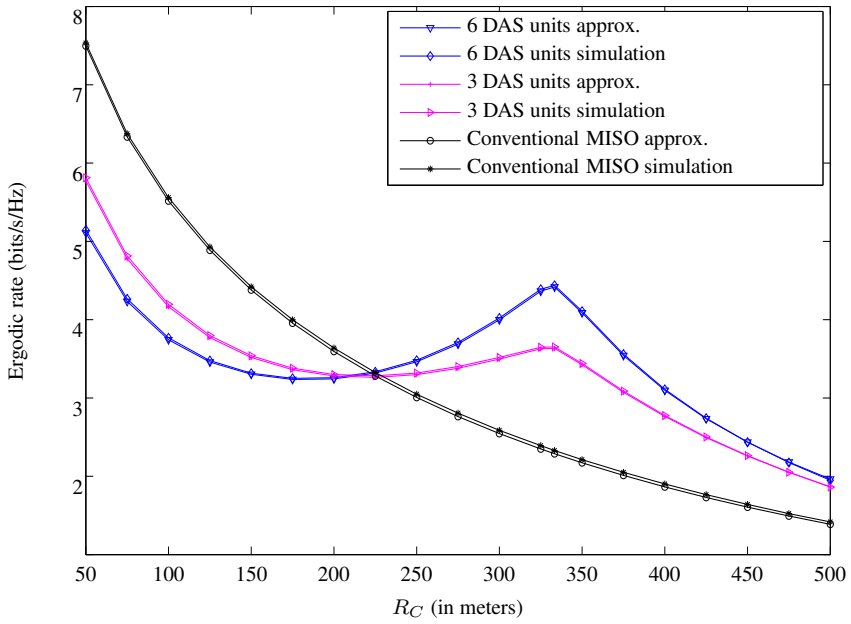

Figure 4.3: Ergodic rate comparisons with different DAS topologies.

uniformly spaced on a ring with radius $\frac{2R}{3}$ from the base station. The cell of interest (cell 0) is assumed to be affected by 6 interfering cells, uniformly spaced on a ring of radius $2R$ from the center of cell 0. The user in cell 0 is located on a ring with radius R_c and the position of the user on this ring is selected randomly. Each cell operates with a total power constraint of 1 W. The carrier frequency f_c of the network is assumed to be 2 GHz and the noise power is computed assuming a bandwidth of 5 MHz and a temperature of 290 K. The ergodic rate of user 0 is estimated as a function of R_c where we average over 1000 random user locations for each value of R_c. To estimate the ergodic rate by simulation, we use 10,000 channel realizations. The ergodic rates of a DAS with one base station and 3 DAUs at each cell, as well as a limited feedback conventional multicell MISO system where only the base station is transmitting with transmit power 1 W, are also computed for comparison. Furthermore, we conducted rate computations with lower transmit power constraints and found that the approximation is accurate when the total interference-to-noise power ratio is larger than 15 dB.

Fig. 4.2 shows the ergodic rates for user 0 as a function of distance from the cell center, calculated using proposed approximation (4.18) and with the rates estimated

using Monte Carlo simulation. One can observe that the approximations follow extremely closely the results estimated with simulation. In Fig. 4.3 we compare the ergodic rate of 3 different network topologies when 4-bit codebook is used for precoding. Results show that each configuration has superior ergodic rate performance over the other configurations in a particular range of user distance from the cell center. This fact can be used in network design to determine the optimal number of DAUs that need to be implemented based on user densities.

The performances with different codebook sizes are compared with the case where the system uses perfect in-cell CSI at the CU calculated using the results given in [6]. The performance loss due to limited feedback is significant in DAS while conventional MISO suffers lesser rate loss with RVQ based precoding. The asymptotic optimality of RVQ precoding for conventional MISO systems explains the lower rate loss in MISO systems while DASs suffer higher rate losses with RVQ precoding. The proposed approximations can be used as a tool to quantify performance losses with RVQ precoding in DASs and multicell MISO systems. Furthermore, they can be used to obtain accurate estimates for the system design parameters such as RVQ codebook size, number of DAUs, and number of antennas at each DAU, without using time consuming Monte Carlo simulations.

4.5 Conclusion

Simple approximations were derived for the ergodic rate of DASs operating in the presence of out-of-cell interference. The moment matching technique was used to approximate the distribution of the desired signal power and the total interference power of the system. Simulation results were presented to validate the proposed approximations.

References

[1] A. Saleh, A. Rustako, and R. Roman, "Distributed antennas for indoor radio communications," *IEEE Trans. Commun.*, vol. 35, no. 12, pp. 1245 –1251, Dec. 1987.

[2] W. Roh and A. Paulraj, "Performance of the distributed antenna systems in a multi-cell environment," in *Proc. IEEE Veh. Technol. Conf., 2003. VTC 2003-Spring*, Apr. 2003, pp. 587 – 591.

[3] W. Choi and J. Andrews, "Downlink performance and capacity of distributed antenna systems in a multicell environment," *IEEE Trans. Wireless Commun.*, vol. 6, no. 1, pp. 69–73, Jan. 2007.

[4] Y. Liu, J. Liu, H. Chen, L. Zheng, G. Zhang, and W. Guo, "Downlink performance of distributed antenna systems in multicell environment," *IET Communications*, vol. 5, no. 15, pp. 2141 –2148, 2011.

[5] L. Li, G. Li, F. Zhou, and M. Wu, "Downlink performance evaluation of centralized and distributed antenna systems in multicell multiuser spatial multiplexing environment," in *Proc.4th Int. Conf. on Wireless Commun., Networking and Mobile Computing, 2008. WiCOM '08.*, Oct. 2008.

[6] R. Heath, T. Wu, Y. H. Kwon, and A. Soong, "Multiuser MIMO in distributed antenna systems with out-of-cell interference," *IEEE Trans. Signal Process.*, vol. 59, no. 10, pp. 4885–4899, Oct. 2011.

[7] X. Chen, Z. Zhang, and H.-H. Chen, "On distributed antenna systems with limited feedback precoding: Opportunities and challenges," *IEEE Wireless Commun.*, vol. 17, no. 2, pp. 80–88, Apr. 2010.

[8] W. Santipach and M. Honig, "Asymptotic performance of MIMO wireless channels with limited feedback," in *Proc. IEEE Military Communications Conference, 2003. MILCOM '03*, vol. 1, Oct. 2003, pp. 141–146.

[9] N. Zhang, G. Kang, Y. Guo, and X. Gui, "Symbol error rate analysis and antenna selection in limited feedback distributed antenna systems," in *Proc. IEEE Veh. Technol. Conf. Fall (VTC 2010-Fall)*, Sep. 2010.

[10] E. Zeng, S. Zhu, and Z. Zhong, "On the performance of adaptive limited feedback beamforming in distributed MIMO systems," in *Proc. IEEE Global Telecommun. Conf., GLOBECOM 2008.*, Dec. 2008.

[11] I. Gradshteyn and I. Ryzhik, *Table of Integrals, Series, and Products, Seventh Edition*. Academic Press, 2007.

[12] C. K. Au-Yeung and D. J. Love, "On the performance of random vector quantization limited feedback beamforming in a MISO system," *IEEE Trans. Wireless Commun.*, vol. 6, no. 2, pp. 458–462, Feb. 2007.

[13] X. W. Cui and Z. M. Feng, "Lower capacity bound for MIMO correlated fading channels with keyhole," *IEEE Commun. Lett.*, vol. 8, no. 8, pp. 500–502, Aug. 2004.

[14] S. Al-Ahmadi and H. Yanikomeroglu, "On the approximation of the generalized-K distribution by a Gamma distribution for modeling composite fading channels," *IEEE Trans. Wireless Commun.*, vol. 9, no. 2, pp. 706 –713, Feb. 2010.

[15] P. Moschopoulos, "The distribution of sum of independent Gamma random variables," *Ann. Inst. Statist. Math.*, vol. 37, pp. 541–544, 1985.

Chapter 5

Relay Coordination Schemes for Two-Hop Networks: Two-Cell Case

The outage probability of a two-hop coordinated decode-and-forward relay network is investigated. The case of two interfering cells is considered. This is analogous to the case when network coordination is performed with the dominant cochannel interfering cell. Different levels of network coordination are studied and their performances are compared. Exact expressions are derived for the outage probability of the system for each coordination method. The impact of user location randomness on the outage probability is investigated.

5.1 Introduction

Dual-hop relay assisted wireless communications has been an active research topic for the last decade. Performance gains identified through theoretical studies and experimental implementations have led to consideration of relay assisted communications for upcoming wireless standards such as 3GPP LTE-Advanced (LTE-A) [1,2]. Another novel technique that has been proposed for LTE-A is coordination of network entities to minimize the level of harmful inter-cell interference (ICI). Therefore, there have been several works recently on wireless systems which combine network coordination techniques with relay communications.

Reference [3] studied the achievable degrees of freedom when the relays of two neighbouring cells are coordinated using a zero-forcing (ZF) strategy. In [3], both the source and the relay nodes were equipped with multiple antennas and the trans-

mit precoding matrices for source nodes and receiver decoding matrices for relay nodes were designed based on a zero interference constraint. Reference [4] extended the results of [3] to support multiple cells with multiple relays and multiple users. In [4], suboptimal solutions were found for the first- and second-hop transmit precoders such that the sum-rate of the network is maximized. Reference [5] studied interference neutralization beamforming for coordinated relay networks. Although previous work on coordinated relay networks proposed sophisticated transmitter and receiver structures for source and relay nodes, there have been almost no analytical studies related to performance evaluation of relay coordination schemes. Furthermore, the previous studies do not consider the direct link between the source and the destination.

In this chapter, we investigate the outage probability of two-hop decode-and-forward (DF) relay networks, where network coordination is performed with the cell which causes strongest cochannel interference. Two-cell network models are practically important, and have been studied in [6–11]. In each cell, we assume infrastructure relays with multiple antennas, while the source and destination nodes are single antenna devices. The relay nodes of two cells are coordinated by exchanging information between them, while the source nodes do not share any information among themselves. Different levels of relay coordination are investigated based on the type and amount of information available at the relays. Compared to previous studies on the performance analysis of two-hop relay networks in the presence of ICI [12–16], we analyze the performance of ICI mitigation schemes for two-hop networks. Our contributions are highlighted below.

- Exact expressions are derived for the outage probability of the system for four coordination scenarios.

- In certain applications, complex exact outage probability expressions may not provide direct insights regarding how system parameters affect the system performance. To facilitate insight and oversight, we derive asymptotic results for the outage probability of the system in the high signal-to-noise ratio (SNR) regime.

- It is important to consider the randomness of the mobile station (MS) locations in performance evaluations to obtain a realistic estimate on the service quality achievable in a network. We propose approximation techniques to account for user location randomness in outage probability computations by evaluating the area outage probability of the system.

The remainder of this chapter is organized as follows. In Section 5.2, we present the system models for each relay coordination method considered in our analysis. For each model, the resultant signal-to-interference plus noise ratios (SINRs) at the MSs are presented. In Section 5.3, we derive expressions for the outage probability of each scenario described in Section 5.2. Section 5.4 presents the outage probability analysis for the asymptotically high SNR regime. The performance improvements achievable by implementing multiple antennas at the source nodes are studied in Section 5.5. Performance approximations that account for the user location randomness are given in Section 5.6. Some numerical and simulation results are presented in Section 5.7, while Section 5.8 concludes this chapter. The derivations of the outage probability expressions are presented in appendices.

We will use the following notations throughout this chapter. The probability density function (PDF) and the cumulative distribution function (CDF) of a random variable (RV) X are denoted as $f_X(x)$ and $F_X(x)$, respectively. The symbol $\mathbb{E}[\cdot]$ denotes mathematical expectation while the probability of an event $\mathcal{A}$ is denoted $\Pr(\mathcal{A})$. Lowercase bold letters and uppercase bold letters are used to denote column vectors and matrices, respectively. A complex Gaussian distribution with mean μ and variance σ^2 is represented as $\mathcal{CN}(\mu, \sigma^2)$, and a gamma distribution with parameters k and m is represented as $\mathcal{G}(k, m)$. The gamma function is denoted as $\Gamma(\cdot)$. An identity matrix with size $l \times l$ is denoted $\boldsymbol{I}_l$.

5.2 System Models

We consider a network model where two interfering cells which use infrastructure relay assisted two-hop communications to serve mobile users, try to coordinate the ICI using relay coordination. In a practical network point of view, this scenario is

similar to a case where ICI coordination is performed only with the cochannel cell with the most dominant interference. Once the dominant component of the ICI is mitigated, the remaining interference can be considered as an increase in the thermal noise level. We assume that the two-hop communication is performed with the aid of infrastructure based DF relays with multiple antennas ($N_r \geq 2$) [2, 17–21] while the source nodes (BSs) and destination nodes (MSs) are single antenna devices. For comparisons, we also present an analysis for the case where source nodes are equipped with multiple antennas as well. The source nodes, relays and destination modes are denoted as $\mathrm{BS}_k, \mathrm{R}_k$ and MS_k for $k \in \{1, 2\}$. The communication between the BSs and the MSs occurs in two time slots. In the first time slot, BSs transmit their data to MSs and relays. The relays decode the data they received in the first time slot and retransmit the decoded data in the second time slot. The relays operate in the selective DF mode where the relay transmits in the second hop only if the first-hop transmission was correctly decoded. If the first-hop reception was not correctly decoded, the relay informs the MS via a control channel and the MS uses only the signal received in first time slot for data decoding. For analytical tractability, we assume that the MSs apply selection combining (SC) on the signals they received in two time slots. We consider two SC schemes, namely SINR based selection [22], where the MSs select the signal with the largest SINR, and desired signal power based selection, where the MSs have only the statistical channel state information (CSI) of the interference links. Without loss of generality, we select MS_1 for our analysis. The performance metrics for MS_2 can be deduced in a straightforward manner from the results for MS_1. The model used in the analysis can be identified as a scenario where infrastructure nodes are being used to coordinate interference among the small cells where peer-to-peer or device-to-device (D2D) type communications are taking place. D2D communications are expected to be more commonplace in LTE-A and 5th generation (5G) networks. Although, we refer to the infrastructure nodes as 'relays', these nodes could be any remote radio unit (RRU) connected to the other RRUs via a backhaul. The received signal at R_1 and MS_1 during the first time slot can be given as

$$\boldsymbol{y}_{R1} = \boldsymbol{h}_{B1,R1}\, s_1 + \boldsymbol{h}_{B2,R1}\, s_2 + \boldsymbol{n}_{R,1} \tag{5.1a}$$

$$y_{M1,1} = g_{B1,M1}s_1 + g_{B2,M1}s_2 + n_{M1,1} \tag{5.1b}$$

where $\boldsymbol{h}_{B1,R1}$ is the $N_r \times 1$ channel vector between BS_1 and R_1 with elements distributed as $\mathcal{CN}(0, L_{B1,R1})$, $\boldsymbol{h}_{B2,R1}$ is the $N_r \times 1$ channel vector between BS_2 and R_1 with elements distributed as $\mathcal{CN}(0, L_{B2,R1})$, $\boldsymbol{n}_{R,1} \sim \mathcal{CN}(0, N_0\boldsymbol{I}_{N_r})$ is the additive white Gaussian noise (AWGN) at R_1, $g_{B1,M1} \sim \mathcal{CN}(0, L_{B1,M1})$ is the channel gain between BS_1 and MS_1, $g_{B2,M1} \sim \mathcal{CN}(0, L_{B2,M1})$ is the channel gain between BS_2 and MS_1, $n_{M1,1} \sim \mathcal{CN}(0, N_0)$ is the AWGN at MS_1, and s_1 and s_2 are the unit energy data symbols intended for MS_1 and MS_2, respectively. The values of $L_{B1,R1}$, $L_{B2,R1}$, $L_{B1,M1}$ and $L_{B2,M1}$ are determined by a simplified path loss model

$$L_{a,b} = P_a K \left[\frac{d_0}{d_{a,b}}\right]^{\eta} \tag{5.2}$$

where P_a is the transmit power of node a, $d_{a,b}$ is the distance between nodes, d_0 is a reference distance for the antenna far field, $K(dB) = 20\log_{10}\frac{\lambda}{4\pi d_0}$, λ is the wavelength of the carrier signal, and η is the path loss exponent.

Depending on the level of coordination between the relays, we consider four scenarios. They are summarized in Table 5.1.

Table 5.1: Relay coordination schemes

Scenario	**Description**
1	Local CSI available at the infrastructure relays and the MSs. Relay backhaul is not available. Maximal ratio combining (MRC) and maximal ratio transmission (MRT) are used at the relays.
2	Relays estimate the first-hop interference channel while MSs only estimate and feedback the local CSI. Relay backhaul is not available. Minimum mean-square error (MMSE) receiver and MRT are used at the relays.
3	Relays and MSs estimate the interference CSI and the MSs feedback the local and interference CSI separately. CSI of the interference channels are shared. MMSE and ZF used at the relays.
4	Relays and MSs estimate the interference CSI and the MSs feedback the CSI of the superimposed channel. Decoded data at the relays and the CSI of the superimposed channel are shared.

5.2.1 Scenario 1: No network coordination

When no network coordination is implemented, the relays use MRC for the signals they received during the first hop and the resulting SINR at R_1 can be found as [23]

$$\gamma_{\text{MRC},1} = \frac{||\boldsymbol{h}_{B1,R1}||^2}{N_0 + \frac{|\boldsymbol{h}_{B1,R1}^H \boldsymbol{h}_{B2,R1}|^2}{||\boldsymbol{h}_{B1,R1}||^2}}. \tag{5.3}$$

The SINR at MS_1 from the signals received in the first time slot is given by

$$\gamma_{M1,1} = \frac{|g_{B1,M1}|^2}{N_0 + |g_{B2,M1}|^2}. \tag{5.4}$$

We assume that the relay is able to successfully decode the transmitted symbols if the SINR at the relay is greater than or equal to a predetermined SINR threshold, γ_{th}. When the relays do not coordinate, the second-hop transmission is equivalent to a multiple input single output (MISO) interference channel. The best strategy for each relay is to use MRT, which is the Nash equilibrium solution for a MISO interference channel [24]. Then, the received signal at MS_1 is given by

$$y_{M1,2} = \boldsymbol{h}_{R1,M1}^T \boldsymbol{w}_{R1} s_1 + \boldsymbol{h}_{R2,M1}^T \boldsymbol{w}_{R2} s_2 + n_{M1,2}$$

where $\boldsymbol{h}_{R1,M1}$ is the $N_r \times 1$ channel vector between R_1 and MS_1 with elements distributed as $\mathcal{CN}(0, L_{R1,M1})$, $\boldsymbol{h}_{R2,M1}$ is the $N_r \times 1$ channel vector between R_2 and MS_1 with elements distributed as $\mathcal{CN}(0, L_{R2,M1})$, $\boldsymbol{w}_{Rk} = \frac{\boldsymbol{h}_{Rk,Mk}^*}{||\boldsymbol{h}_{Rk,Mk}||}$ is the MRT weight vector of the k^{th} relay, and $n_{M1,2} \sim \mathcal{CN}(0, N_0)$ is the AWGN at MS_1 during the second time slot. If R_2 could not decode the first-hop data symbols, the received signal at MS_1 during the second time slot is interference free. The resulting SINRs can be found as

$$\gamma_{M1,2}^I = \frac{||\boldsymbol{h}_{R1,M1}||^2}{N_0 + \frac{|\boldsymbol{h}_{R2,M2}^h \boldsymbol{h}_{R2,M1}|^2}{||\boldsymbol{h}_{R2,M2}||^2}} \tag{5.5}$$

for the case when R_2 decoded s_2 correctly and

$$\gamma_{M1,2}^{\text{NI}} = \frac{||\boldsymbol{h}_{R1,M1}||^2}{N_0} \tag{5.6}$$

for the case when R_2 is silent in the second time slot.

If MS_1 uses SINR based SC, the output SINR at MS_1 is given by

$$\gamma_{M1} = \max\left(\gamma_{M1,1}, \gamma_{M1,2}\right) \tag{5.7}$$

where $\gamma_{M1,2}$ is either $\gamma^{I}_{M1,2}$ or $\gamma^{\text{NI}}_{M1,2}$. We refer to this scheme as SC-1.

When MS_1 uses the CSI of the R_1-MS_1 channel and the statistical CSI of the R_2-MS_1 link, the output SINR is given by

$$\gamma^{\text{SI}}_{M1} = \begin{cases} \gamma_{M1,1} & \text{if } \frac{|g_{B1,M1}|^2}{N_0+L_{B2,M1}} > \frac{\left|\left|\boldsymbol{h}_{R1,M1}\right|\right|^2}{N_0+L_{R2,M1}} \\ \gamma^{I}_{M1,2} & \text{if } \frac{|g_{B1,M1}|^2}{N_0+L_{B2,M1}} \leq \frac{\left|\left|\boldsymbol{h}_{R1,M1}\right|\right|^2}{N_0+L_{R2,M1}} \end{cases} \tag{5.8}$$

for the case when R_2 decoded s_2 correctly. When R_2 is silent during the second time slot, the output SINR at MS_1 is given by

$$\gamma^{\text{S}}_{M1} = \begin{cases} \gamma_{M1,1} & \text{if } \frac{|g_{B1,M1}|^2}{N_0+L_{B2,M1}} > \frac{\left|\left|\boldsymbol{h}_{R1,M1}\right|\right|^2}{N_0} \\ \gamma^{\text{NI}}_{M1,2} & \text{if } \frac{|g_{B1,M1}|^2}{N_0+L_{B2,M1}} \leq \frac{\left|\left|\boldsymbol{h}_{R1,M1}\right|\right|^2}{N_0} \end{cases} \tag{5.9}$$

where we assume that the MSs are capable of determining whether interference is present or not. We refer to this scheme as SC-2. Since the SC-2 scheme requires only the statistical CSI of the interference links, SC-2 is preferred over SC-1 for uncoordinated networks.

5.2.2 Scenario 2: First-hop interference CSI estimation

When R_k has the CSI of the $\text{BS}_j - \text{R}_k$ link, it applies MMSE reception on the signals received in the first time slot. The receiver weight vector at the k^{th} relay is computed as

$$\boldsymbol{w}_{\text{MMSE}} = \boldsymbol{R}_k^{-1}\boldsymbol{h}_{Bk,Rk} \tag{5.10}$$

where $\boldsymbol{R}_k = \boldsymbol{h}_{Bj,Rk}\boldsymbol{h}^H_{Bj,Rk} + N_0\boldsymbol{I}_{N_r}$, $j,k \in \{1,2\}$, $j \neq k$. The resulting SINR at R_1 is given by

$$\gamma_{\text{MMSE},1} = \boldsymbol{h}^H_{B1,R1}\boldsymbol{R}_1^{-1}\boldsymbol{h}_{B1,R1}. \tag{5.11}$$

Since only the CSIs of the first hop are estimated, the second hop transmission and the resulting SINRs are identical to Scenario 1.

5.2.3 Scenario 3: Sharing second-Hop CSI

In this scenario, the relays use MMSE reception in the first time slot. We assume that MS_k estimates the CSI of the interference link R_j-MS_k and feeds this CSI back to R_k. The relays exchange these CSIs through a backhaul link. Now, the relays use a transmit strategy which creates no interference for the MS in the cochannel cell. We select ZF transmission at the relays. The transmit beamforming vector at R_1 is computed as

$$\boldsymbol{w}_{R1}^{\mathrm{ZF}} = \frac{\Pi^{\perp}_{\boldsymbol{h}^{*}_{R1,M2}} \boldsymbol{h}^{*}_{R1,M1}}{\left|\left| \Pi^{\perp}_{\boldsymbol{h}^{*}_{R1,M2}} \boldsymbol{h}^{*}_{R1,M1} \right|\right|^2} \tag{5.12}$$

where $\Pi^{\perp}_{X} = \boldsymbol{I}_l - \boldsymbol{X}(\boldsymbol{X}^H\boldsymbol{X})^{-1}\boldsymbol{X}^H$ is the projection onto the orthogonal complement of the column space of $\boldsymbol{X}$ [24], and l is the length of $\boldsymbol{X}$. The SINR of the received signal at MS_1 for the second time slot is given by

$$\gamma_{M1,2}^{\mathrm{ZF}} = \frac{|(\boldsymbol{w}_{R1}^{\mathrm{ZF}})^T \boldsymbol{h}_{R1,M1}|^2}{N_0}. \tag{5.13}$$

In addition to CSI exchange, the relays can include a one-bit flag declaring whether the first-hop decoding was successful or not. If R_2 informs that s_2 was not decoded successfully, then R_1 can use MRT for second-hop transmission. When this occurs, the SINR of the received signal at MS_1 for the second time slot is given by

$$\gamma_{M1,2}^{\mathrm{MRT}} = \frac{||\boldsymbol{h}_{R1,M1}||^2}{N_0}. \tag{5.14}$$

5.2.4 Scenario 4: Sharing CSI and data

Similar to Scenarios 2 and 3, the relays use MMSE reception to decode data symbols from the first time slot transmissions. If both relays have access to codebooks of both BSs, each relay is able to decode both s_1 and s_2. However, if R_k only has knowledge of the codebook of BS_k, the relay can decode only s_k. Then the relays exchange decoded data and CSI through a backhaul link. In the second time slot, two relays operate as a DAS. We assume the suboptimal ZF multiuser blanket transmission (BT) scheme proposed for DASs in [25]. Both relays transmit identical data symbols using identical beamforming vectors. To implement this scheme, MS_k has to feedback the CSI of the superimposed channel $\boldsymbol{h}_k = \boldsymbol{h}_{Rk,Mk} + \boldsymbol{h}_{Rj,Mk}$.

Therefore, this scheme reduces the CSI estimation and feedback overhead. The macroscopic multiuser channel matrix can be given as

$$\boldsymbol{H}_R = [\boldsymbol{h}_1\ \boldsymbol{h}_2]^H . \tag{5.15}$$

The ZF precoder matrix $\boldsymbol{Z}_R$ is obtained by finding the pseudo-inverse of $\boldsymbol{H}_R$ and normalizing the columns. The k^{th} column of $\boldsymbol{Z}_R$, $\boldsymbol{z}_k$, is used as the precoding vector for MS_k. The resulting SINR at MS_1 during the second time slot is given by [25]

$$\gamma_{M1,2}^{\text{BT,ZF}} = \frac{\frac{1}{2}|\boldsymbol{h}_1^T \boldsymbol{z}_1|^2}{N_0}. \tag{5.16}$$

If R_2 could not decode the first-hop data symbols, both relays transmit s_1 by applying MRT on the superimposed channel $\boldsymbol{h}_1$. The corresponding MRT weight vector is given by $\boldsymbol{w}_R^{\text{BT,MRT}} = \frac{\boldsymbol{h}_1^*}{||\boldsymbol{h}_1||}$. We refer to this as the BT-1 scheme. The resulting SINR at MS_1 during the second time slot is given by

$$\gamma_{M1,2}^{\text{BT,MRT}} = \frac{||\boldsymbol{h}_1||^2}{N_0}. \tag{5.17}$$

In the BT-2 scheme, both relays have the knowledge of the codebooks used by both BSs. Therefore, MS_k will not be served by the relays only if both relays couldn't decode s_k in the first time slot. If only s_k is decoded by the relays, then MS_k will be served by applying MRT on the superimposed channel $\boldsymbol{h}_k$. The resulting SINR is equivalent to (5.17). If s_1 and s_2 were successfully decoded by at least one relay, then both MSs are served by applying ZF precoding similar to the BT-1 scheme.

5.3 Outage Probability Analysis

In this section, we present the statistical characterization of output SINR for each of the four scenarios introduced in Sec. 5.2, and use the statistics to derive expressions for the system outage probability for each scenario.

5.3.1 Scenario 1: No network coordination

The RV $||\boldsymbol{h}_{B1,R1}||^2$ is distributed as $\mathcal{G}(N_r, L_{B1,R1})$ and the interference power $\frac{|\boldsymbol{h}_{B1,R1}^H \boldsymbol{h}_{B2,R1}|^2}{||\boldsymbol{h}_{B1,R1}||^2}$ is distributed as $\mathcal{G}(1, L_{B2,R1})$ [24]. The CDF of a gamma distributed RV X with

$\mathcal{G}(N, \bar{\gamma})$ is given by

$$F_X(x) = 1 - \exp\left(-\frac{x}{\bar{\gamma}}\right) \sum_{n=0}^{N-1} \frac{x^n}{n!\bar{\gamma}^n} \tag{5.18}$$

when N is an integer. The CDF of $\gamma_{\text{MRC},1}$ can be found as [23]

$$F_{\gamma_{\text{MRC},1}}(x) = 1 - e^{\frac{-x}{\bar{\gamma}_R}} \sum_{n=0}^{N_r-1} \sum_{k=0}^{n} \binom{n}{k} \frac{k! x^n \Phi}{n! \bar{\gamma}_R^{n-k} (x+\Phi)^{k+1}} \tag{5.19}$$

where $\bar{\gamma}_R = \frac{L_{B1,R1}}{N_0}$ and $\bar{\gamma}_{IR} = \frac{L_{B2,R1}}{N_0}$ and $\Phi = \frac{\bar{\gamma}_R}{\bar{\gamma}_{IR}}$. The CDF of $\gamma_{M1,1}$ can be derived as [26]

$$F_{\gamma_{M1,1}}(x) = 1 - \left(\frac{\Upsilon}{x+\Upsilon}\right) \exp\left(\frac{-x}{\bar{\gamma}_{B1}}\right) \tag{5.20}$$

where $\Upsilon = \frac{L_{B1,M1}}{L_{B2,M1}}$ and $\bar{\gamma}_{B1} = \frac{L_{B1,M1}}{N_0}$. The CDF of $\gamma^I_{M1,2}$ is given by

$$F_{\gamma^I_{M1,2}}(x) = 1 - e^{\frac{-x}{\bar{\gamma}_M}} \sum_{n=0}^{N_r-1} \sum_{k=0}^{n} \binom{n}{k} \frac{k! x^n \Omega}{n! \bar{\gamma}_M^{n-k} (x+\Omega)^{k+1}} \tag{5.21}$$

where $\bar{\gamma}_M = \frac{L_{R1,M1}}{N_0}$ and $\bar{\gamma}_{IM} = \frac{L_{R2,M1}}{N_0}$ and $\Omega = \frac{\bar{\gamma}_M}{\bar{\gamma}_{IM}}$. The RV $\gamma^{\text{NI}}_{M1,2}$ is distributed as $\mathcal{G}\left(N_r, \frac{L_{R1,M1}}{N_0}\right)$. The CDF of the output SINR with the SC-1 scheme is given by

$$F_{\gamma_{M1}}(x) = F_{\gamma_{M1,1}}(x) \times F_{\gamma_{M1,2}}(x). \tag{5.22}$$

For the SC-2 scheme, the CDF of the output SINR is given by

$$\begin{aligned} F_{\gamma^{\text{SI}}_{M1}}(x) = {} & F_{\gamma_{M1,1}}(x) \times F_{\gamma_{M1,2}}(x) \\ & + \int_0^\infty \int_0^\infty \int_{Ax}^{\frac{CBx}{D}} \int_{\frac{D\gamma_1}{C}}^{Bx} f_{G_1,G_2}(\gamma_1, \gamma_2) f_{\gamma_{I1}}(\gamma_{I1}) f_{\gamma_{I2}}(\gamma_{I2}) \\ & \qquad d\gamma_2 d\gamma_1 d\gamma_{I1} d\gamma_{I2} \end{aligned} \tag{5.23}$$

where $G_1 = \frac{|g_{B1,M1}|^2}{N_0}$, $G_2 = \gamma^{\text{NI}}_{M1,2}$, $A = 1 + \gamma_{I1}$, $B = 1 + \gamma_{I2}$, $C = 1 + \bar{\gamma}_{IM}$, $D = 1 + \bar{\gamma}_{IR}$, $\gamma_{I1} = \frac{|g_{B2,M1}|}{N_0}$ and $\gamma_{I2} = \frac{|\boldsymbol{h}^H_{R1,M1} \boldsymbol{h}_{R2,M1}|^2}{N_0 \left|\left|\boldsymbol{h}_{R1,M1}\right|\right|^2}$. A closed-form solution for

(5.23) can be found as

$$F_{\gamma_{M1}^{\text{SI}}}(x) = \exp\left[-x\left(\frac{C}{D\bar{\gamma}_{B1}} + \frac{1}{\bar{\gamma}_M}\right)\right] \sum_{k=0}^{N_1-1}\sum_{n=0}^{k}\binom{k}{n}\frac{x^k n!}{k!\bar{\gamma}_M^{k-n}}\frac{D^{n+1}\Omega}{\left(xC\frac{\bar{\gamma}_M}{\bar{\gamma}_{B1}} + xD + \Omega\right)^{n+1}}$$

$$-\exp\left[-\frac{xC}{D}\left(\frac{1}{\bar{\gamma}_{B1}} + \frac{D}{C\bar{\gamma}_M}\right)\right] \sum_{k=0}^{N1-1}\sum_{n=0}^{k}\sum_{j=0}^{n}\frac{\binom{n}{j}x^n C^{n-k} j!\left[\frac{1}{\bar{\gamma}_{B1}} + \frac{D}{C\bar{\gamma}_M}\right]^{n-k-1}}{n!D^{n-k-j-1}\bar{\gamma}_{B1}}\frac{\Omega\bar{\gamma}_M^j}{\left(Cx\frac{\bar{\gamma}_M}{\bar{\gamma}_{B1}} + xD + \Omega\right)^{j+1}}$$

$$+\exp\left[-x\left(\frac{1}{\bar{\gamma}_{B1}} + \frac{D}{C\bar{\gamma}_M}\right)\right] \sum_{k=0}^{N1-1}\sum_{n=0}^{k}\sum_{j=0}^{n}\frac{\binom{n}{j}x^n D^k j!\left[\frac{1}{\bar{\gamma}_{B1}} + \frac{D}{C\bar{\gamma}_M}\right]^{n-k-1}}{n!C^{n-j-1}\bar{\gamma}_M^k}\frac{\Upsilon\bar{\gamma}_{B1}^{j-1}}{\left(\frac{xD\bar{\gamma}_{B1}}{C\bar{\gamma}_M} + xC + C\Upsilon\right)^{j+1}}$$
$$+ F_{\gamma_{M1,1}}(x) + F_{\gamma_{M1,2}^I}(x) - 1. \quad (5.24)$$

The derivation steps for (5.24) are shown in Appendix 5.A. A closed-form expression for the CDF of γ_{M1}^{S} can be found as

$$F_{\gamma_{M1}^{\text{S}}}(x) = \exp\left[-Cx\left(\frac{1}{\bar{\gamma}_{B1}} + \frac{1}{C\bar{\gamma}_M}\right)\right] \sum_{n=0}^{N_1-1}\sum_{k=0}^{n}\frac{x^k}{k!C^{n-k}\bar{\gamma}_M^n\bar{\gamma}_{B1}}\left(\frac{1}{\bar{\gamma}_{B1}} + \frac{1}{C\bar{\gamma}_M}\right)^{k-n-1}$$

$$+\exp\left[-x\left(\frac{1}{\bar{\gamma}_{B1}} + \frac{1}{C\bar{\gamma}_M}\right)\right] \sum_{n=0}^{N1-1}\sum_{k=0}^{n}\sum_{j=0}^{k}\frac{\binom{k}{j}x^k j!\left[\frac{1}{\bar{\gamma}_{B1}} + \frac{1}{C\bar{\gamma}_M}\right]^{n-k-1}}{k!C^{n-j-1}\bar{\gamma}_M^n}\frac{\Upsilon\bar{\gamma}_{B1}^{j-1}}{\left(\frac{x\bar{\gamma}_{B1}}{C\bar{\gamma}_M} + xC + C\Upsilon\right)^{j+1}}$$
$$+ F_{\gamma_{M1,1}}(x) + F_{G_1}(x)F_{G_2}(Cx) - F_{G_1}(Cx) \quad (5.25)$$

We recognize that the system is in outage when the resultant SINR at MS_1 drops below a predetermined threshold γ_{th}. Then, the outage probability is calculated as

$$\begin{aligned} P_{\text{out},S1} &= \Pr(\gamma_{\text{MRC},1} \geq \gamma_{\text{th}} \text{ and } \gamma_{\text{MRC},2} \geq \gamma_{\text{th}})F_{\gamma_{M1,1}}(\gamma_{\text{th}})F_{\gamma_{M1,2}^I}(\gamma_{\text{th}}) \\ &\quad + \Pr(\gamma_{\text{MRC},1} \geq \gamma_{\text{th}} \text{ and } \gamma_{\text{MRC},2} < \gamma_{\text{th}})F_{\gamma_{M1,1}}(\gamma_{\text{th}})F_{\gamma_{M1,2}^{\text{NI}}}(\gamma_{\text{th}}) \\ &\quad + \Pr(\gamma_{\text{MRC},1} < \gamma_{\text{th}})F_{\gamma_{M1,1}}(\gamma_{\text{th}}) \end{aligned} \quad (5.26)$$

where we have used the total probability theorem [27]. Since the events $\gamma_{\text{MRC},1} \geq \gamma_{\text{th}}$ and $\gamma_{\text{MRC},2} \geq \gamma_{\text{th}}$ are independent, the outage probability can be evaluated using

$$\begin{aligned} P_{\text{out},S1} &= (1 - F_{\gamma_{\text{MRC},1}}(\gamma_{\text{th}}))(1 - F_{\gamma_{\text{MRC},2}}(\gamma_{\text{th}}))F_{\gamma_{M1,1}}(\gamma_{\text{th}})F_{\gamma_{M1,2}^I}(\gamma_{\text{th}}) \\ &\quad + (1 - F_{\gamma_{\text{MRC},1}}(\gamma_{\text{th}}))F_{\gamma_{\text{MRC},2}}(\gamma_{\text{th}})F_{\gamma_{M1,1}}(\gamma_{\text{th}})F_{\gamma_{M1,2}^{\text{NI}}}(\gamma_{\text{th}}) \\ &\quad + F_{\gamma_{\text{MRC},1}}(\gamma_{\text{th}})F_{\gamma_{M1,1}}(\gamma_{\text{th}}). \end{aligned} \quad (5.27)$$

The outage probability expression for the SC-2 scheme can be deduced from (5.27) as

$$P_{\text{out},S1} = (1 - F_{\gamma_{\text{MRC},1}}(\gamma_{\text{th}}))(1 - F_{\gamma_{\text{MRC},2}}(\gamma_{\text{th}}))F_{\gamma_{M1}^{\text{SI}}}(\gamma_{\text{th}}) + (1 - F_{\gamma_{\text{MRC},1}}(\gamma_{\text{th}}))F_{\gamma_{\text{MRC},2}}(\gamma_{\text{th}})F_{\gamma_{M1}^{\text{S}}}(\gamma_{\text{th}}) + F_{\gamma_{\text{MRC},1}}(\gamma_{\text{th}})F_{\gamma_{M1,1}}(\gamma_{\text{th}}). \quad (5.28)$$

5.3.2 Scenario 2: First-hop interference CSI estimation

We simplify (5.11) using eigendecomposition of $\boldsymbol{R}_1$ to obtain

$$\gamma_{\text{MMSE},1} = \boldsymbol{h}_{B1,R1}^H \boldsymbol{U}\boldsymbol{\Lambda}^{-1}\boldsymbol{U}^{-1}\boldsymbol{h}_{B1,R1} = \boldsymbol{\alpha}^H\boldsymbol{\Lambda}^{-1}\boldsymbol{\alpha} \quad (5.29)$$

where $\boldsymbol{\alpha} = \boldsymbol{U}^{-1}\boldsymbol{h}_{B1,R1}$, $\boldsymbol{U}$ is a unitary matrix, and $\boldsymbol{\Lambda}$ is a diagonal matrix of eigenvalues of $\boldsymbol{R}$. The matrix $\boldsymbol{R}$ can be identified as an addition of a rank-1 matrix and a diagonal matrix. The eigenvalues of $\boldsymbol{R}$ have a special structure where one eigenvalue is equal to $N_0 + ||\boldsymbol{h}_{B2,R1}||^2$ and the other $N_r - 1$ eigenvalues are equal to N_0. Then, $\gamma_{\text{MMSE},1}$ can be given as

$$\gamma_{\text{MMSE},1} = \frac{|\alpha_1|^2}{N_0 + ||\boldsymbol{h}_{B2,R1}||^2} + \underbrace{\sum_{k=2}^{N_r} \frac{|\alpha_k|^2}{N_0}}_{Z} \quad (5.30)$$

where α_k, $k \in \{1, 2, \cdots, N_r\}$ are the elements of $\boldsymbol{\alpha}$. Due to the fact that the product of a Gaussian random vector and a unitary matrix has statistics identical to the original Gaussian random vector, the elements in $\boldsymbol{\alpha}$ have identical statistics as the elements in $\boldsymbol{h}_{B1,R1}$. Using [28, 1.2.4.3] and [29], the CDF of $\gamma_{\text{MMSE},1}$ can be derived as

$$F_{\gamma_{\text{MMSE},1}}(x) = F_Z(x) - \left[\frac{\bar{\gamma}_R e^{\frac{-x}{\bar{\gamma}_R}} x^{N_r-1}\Phi^{-N_r+1}}{\bar{\gamma}_{IR}^{N_r}(\Phi + x)\,\Gamma(N_r)}\right] \quad (5.31)$$

where $Z \sim \mathcal{G}(N_r - 1, \bar{\gamma}_R)$.

The system outage probability for Scenario 2 can be deduced by replacing $F_{\gamma_{\text{MRC},1}}(x)$ and $F_{\gamma_{\text{MRC},2}}(x)$ with $F_{\gamma_{\text{MMSE},1}}(x)$ and $F_{\gamma_{\text{MMSE},2}}(x)$, respectively.

5.3.3 Scenario 3: Sharing second-hop CSI

In this scenario, the CDFs of the first-hop SINRs are equivalent to $F_{\gamma_{\text{MMSE},1}}(x)$ and $F_{\gamma_{\text{MMSE},2}}(x)$. The RV $\gamma_{M1,2}^{\text{ZF}}$ is distributed as $\mathcal{G}\left(N_r - 1, \frac{L_{R1,M1}}{N_0}\right)$ [24] and the RV

$\gamma_{M1,2}^{\text{MRT}}$ is distributed as $\mathcal{G}\left(N_r, \frac{L_{R1,M1}}{N_0}\right)$. When the relays do not share the information regarding their success or failure of decoding the first-hop data symbols, the system outage probability can be found as

$$\begin{aligned} P_{\text{out},S3} &= (1 - F_{\gamma_{\text{MMSE},1}}(\gamma_{\text{th}}))F_{\gamma_{M1,1}}(\gamma_{\text{th}})F_{\gamma_{M1,2}^{\text{ZF}}}(\gamma_{\text{th}}) \\ &\quad + F_{\gamma_{\text{MMSE},1}}(\gamma_{\text{th}})F_{\gamma_{M1,1}}(\gamma_{\text{th}}). \end{aligned} \tag{5.32}$$

When relays use an additional bit to indicate the success or failure of decoding the first-hop data symbols, the system outage probability can be found as

$$\begin{aligned} P_{\text{out},S3} &= (1 - F_{\gamma_{\text{MMSE},1}}(\gamma_{\text{th}}))(1 - F_{\gamma_{\text{MMSE},2}}(\gamma_{\text{th}}))F_{\gamma_{M1,1}}(\gamma_{\text{th}})F_{\gamma_{M1,2}^{\text{ZF}}}(\gamma_{\text{th}}) \\ &\quad + (1 - F_{\gamma_{\text{MMSE},1}}(\gamma_{\text{th}}))F_{\gamma_{\text{MMSE},2}}(\gamma_{\text{th}})F_{\gamma_{M1,1}}(\gamma_{\text{th}})F_{\gamma_{M1,2}^{\text{MRT}}}(\gamma_{\text{th}}) \\ &\quad + F_{\gamma_{\text{MMSE},1}}(\gamma_{\text{th}})F_{\gamma_{M1,1}}(\gamma_{\text{th}}). \end{aligned} \tag{5.33}$$

5.3.4 Scenario 4: Sharing CSI and data

The distributions of the RVs $\gamma_{M1,2}^{\text{BT,ZF}}$ and $\gamma_{M1,2}^{\text{BT,MRT}}$ can be found as $\mathcal{G}\left(N_r - 1, \frac{L_{R1,M1}+L_{R2,M1}}{2N_0}\right)$ and $\mathcal{G}\left(N_r, \frac{L_{R1,M1}+L_{R2,M1}}{N_0}\right)$, respectively [25]. The factor $\frac{1}{2}$ appears because the relay divides it's available power for two user symbols. For the BT-1 scheme, the system outage probability can be found as

$$\begin{aligned} P_{\text{out},S4} &= \Pr(\gamma_{\text{MMSE},1} \geq \gamma_{\text{th}} \text{ and } \gamma_{\text{MMSE},2} \geq \gamma_{\text{th}})F_{\gamma_{M1,1}}(\gamma_{\text{th}})F_{\gamma_{M1,2}^{\text{BT,ZF}}}(\gamma_{\text{th}}) \\ &\quad + \Pr(\gamma_{\text{MMSE},1} \geq \gamma_{\text{th}} \text{ and } \gamma_{\text{MMSE},2} < \gamma_{\text{th}})F_{\gamma_{M1,1}}(\gamma_{\text{th}})F_{\gamma_{M1,2}^{\text{BT,MRT}}}(\gamma_{\text{th}}) \\ &\quad + \Pr(\gamma_{\text{MMSE},1} < \gamma_{\text{th}})F_{\gamma_{M1,1}}(\gamma_{\text{th}}). \end{aligned} \tag{5.34}$$

Since the events $\gamma_{\text{MMSE},1} \geq \gamma_{\text{th}}$ and $\gamma_{\text{MMSE},2} \geq \gamma_{\text{th}}$ are independent, the outage probability can be evaluated using

$$\begin{aligned} P_{\text{out},S4} &= (1 - F_{\gamma_{\text{MMSE},1}}(\gamma_{\text{th}}))(1 - F_{\gamma_{\text{MMSE},2}}(\gamma_{\text{th}}))F_{\gamma_{M1,1}}(\gamma_{\text{th}})F_{\gamma_{M1,2}^{\text{BT,ZF}}}(\gamma_{\text{th}}) \\ &\quad + (1 - F_{\gamma_{\text{MMSE},1}}(\gamma_{\text{th}}))F_{\gamma_{\text{MMSE},2}}(\gamma_{\text{th}})F_{\gamma_{M1,1}}(\gamma_{\text{th}})F_{\gamma_{M1,2}^{\text{BT,MRT}}}(\gamma_{\text{th}}) \\ &\quad + F_{\gamma_{\text{MMSE},1}}(\gamma_{\text{th}})F_{\gamma_{M1,1}}(\gamma_{\text{th}}). \end{aligned} \tag{5.35}$$

For the BT-2 scheme, the system outage probability is given by

$$\begin{aligned} P_{\text{out},BT2} &= \Pr(s_1 \in \mathcal{D} \text{ and } s_2 \in \mathcal{D}) F_{\gamma_{M1,1}}(\gamma_{\text{th}}) F_{\gamma_{M1,2}^{\text{BT,ZF}}}(\gamma_{\text{th}}) \\ &\quad + \Pr(s_1 \in \mathcal{D} \text{ and } s_2 \notin \mathcal{D}) F_{\gamma_{M1,1}}(\gamma_{\text{th}}) F_{\gamma_{M1,2}^{\text{BT,MRT}}}(\gamma_{\text{th}}) \\ &\quad + \Pr(s_1 \notin \mathcal{D}) F_{\gamma_{M1,1}}(\gamma_{\text{th}}) \end{aligned} \tag{5.36}$$

where $\mathcal{D}$ is the set of decoded symbols. In general, the events $s_1 \in \mathcal{D}$ and $s_2 \in \mathcal{D}$ are not independent. Therefore, finding an exact expression for the outage probability for the case where relays share the codebooks, appears to be intractable. We derive a performance upper bound by assuming independence between $s_1 \in \mathcal{D}$ and $s_2 \in \mathcal{D}$, which can be computed as

$$\begin{aligned} &P_{\text{out},BT2} \approx \Pr(\gamma_{\text{R},1}^{s_1} < \gamma_{\text{th}} \text{ and } \gamma_{\text{R},2}^{s_1} < \gamma_{\text{th}}) F_{\gamma_{M1,1}}(\gamma_{\text{th}}) + \\ &\Big[\Pr(\gamma_{\text{R},1}^{s_1} \geq \gamma_{\text{th}} \text{ or } \gamma_{\text{R},2}^{s_1} \geq \gamma_{\text{th}}) \Pr(\gamma_{\text{R},1}^{s_2} \geq \gamma_{\text{th}} \text{ or } \gamma_{\text{R},2}^{s_2} \geq \gamma_{\text{th}}) \\ &F_{\gamma_{M1,1}}(\gamma_{\text{th}}) F_{\gamma_{M1,2}^{\text{BT,ZF}}}(\gamma_{\text{th}})\Big] + \Big[\Pr(\gamma_{\text{R},1}^{s_1} \geq \gamma_{\text{th}} \text{ or } \gamma_{\text{R},2}^{s_1} \geq \gamma_{\text{th}}) \\ &\Pr(\gamma_{\text{R},1}^{s_2} < \gamma_{\text{th}} \text{ and } \gamma_{\text{R},2}^{s_2} < \gamma_{\text{th}}) F_{\gamma_{M1,1}}(\gamma_{\text{th}}) F_{\gamma_{M1,2}^{\text{BT,MRT}}}(\gamma_{\text{th}})\Big] \end{aligned} \tag{5.37}$$

where $\gamma_{\text{R},j}^{s_k}$ is the SINR of k^{th} symbol at R_j, $j,k \in \{1,2\}$. The system outage probability can be lower bounded as

$$\begin{aligned} &P_{\text{out},BT2}^{\text{LB}} \approx F_{\gamma_{\text{R},1}^{s1}}(\gamma_{\text{th}}) F_{\gamma_{\text{R},2}^{s1}}(\gamma_{\text{th}}) F_{\gamma_{M1,1}}(\gamma_{\text{th}}) + \\ &\Big[\Big(1 - F_{\gamma_{\text{R},1}^{s1}}(\gamma_{\text{th}}) F_{\gamma_{\text{R},2}^{s1}}(\gamma_{\text{th}})\Big)\Big(1 - F_{\gamma_{\text{R},1}^{s2}}(\gamma_{\text{th}}) F_{\gamma_{\text{R},2}^{s2}}(\gamma_{\text{th}})\Big) \\ &F_{\gamma_{M1,1}}(\gamma_{\text{th}}) F_{\gamma_{M1,2}^{\text{BT,ZF}}}(\gamma_{\text{th}})\Big] + \Big[\Big(1 - F_{\gamma_{\text{R},1}^{s1}}(\gamma_{\text{th}}) F_{\gamma_{\text{R},2}^{s1}}(\gamma_{\text{th}})\Big) \\ &F_{\gamma_{\text{R},1}^{s1}}(\gamma_{\text{th}}) F_{\gamma_{\text{R},2}^{s1}}(\gamma_{\text{th}}) F_{\gamma_{M1,1}}(\gamma_{\text{th}}) F_{\gamma_{M1,2}^{\text{BT,MRT}}}(\gamma_{\text{th}})\Big] \end{aligned} \tag{5.38}$$

where $F_{\gamma_{\text{R},j}^{sk}}(x)$ is the CDF of the k^{th} symbol's SINR at R_j, $j,k \in \{1,2\}$. Following the derivation of $F_{\gamma_{\text{MMSE},1}}(x)$, $F_{\gamma_{\text{R},1}^{s2}}(x)$ and can be derived as

$$F_{\gamma_{\text{R},1}^{s2}}(x) = F_{Z_{B2,R1}}(x) - \frac{\bar{\gamma}_{B2,R1} e^{\frac{-x}{\bar{\gamma}_{B2,R1}}} x^{N_r - 1} \Psi^{1-N_r}}{\bar{\gamma}_{B1,R1}^{N_r} (\Psi + x) \Gamma(N_r)} \tag{5.39}$$

where $Z_{B2,R1} \sim \mathcal{G}(N_r - 1, \bar{\gamma}_{B2,R1})$, $\bar{\gamma}_{B2,R1} = \frac{L_{B2,R1}}{N_0} = \bar{\gamma}_{IR}$, $\bar{\gamma}_{B1,R1} = \frac{L_{B1,R1}}{N_0} = \bar{\gamma}_R$ and $\Psi = \frac{\bar{\gamma}_{B2,R1}}{\bar{\gamma}_{B1,R1}}$. The CDFs of $\gamma_{\text{R},2}^{s1}$, and $\gamma_{\text{R},2}^{s2}$ can be derived in a similar manner as used to derive (5.39).

5.3.5 Comparison with optimal combining at the MSs

In our analysis, we considered SC at the MSs for analytical tractability. However, for comparison, here we present the analysis for the case when the MSs use MMSE combining (optimal combining (OC)) to combine the signals received in two time slots for Scenarios 3 and 4. Following [11, Sec. III-B], we represent the received signals in the two time slots using vector notations

$$\boldsymbol{y}_{MS} = \boldsymbol{h}_d s_1 + \boldsymbol{h}_I s_2 + \boldsymbol{n} \tag{5.40}$$

where $\boldsymbol{h}_d = \left[||\boldsymbol{h}_{\text{eff}}||^2 \; g_{B1,M1}\right]^T$, $||\boldsymbol{h}_{\text{eff}}||^2$ is the effective channel from the RS to the MS, $\boldsymbol{h}_I = [0 \; g_{B2,M1}]^T$ and $\boldsymbol{n} = [n_{M1,1} \; n_{M1,2}]^T$. Following a similar procedure as used in [11], the SINR at the MS_1 can be represented as

$$\gamma_{MS1,OC} = \underbrace{\frac{|g_{B1,M1}|^2}{N_0 + |g_{B2,M1}|^2}}_{\gamma_{M1,1}} + \underbrace{\frac{||\boldsymbol{h}_{\text{eff}}||^2}{N_0}}_{\gamma^{RD}_{M1,2}} \tag{5.41}$$

where $\gamma^{RD}_{M1,2}$ is determined by the relay coordination scheme. We derive the cumulative distribution function (CDF) of $\gamma_{MS1,OC}$ for a general case where $\gamma^{RD}_{M1,2}$ is distributed as $\mathcal{G}\left(N_k, \bar{\gamma}_{RD}\right)$. The CDF of $\gamma_{MS1,OC}$ can be given as

$$\begin{aligned} F_{\gamma_{MS1,OC}}(x) &= \Pr\left(\frac{\gamma_{B1,M1}}{1+\gamma_{B2,M1}} + \gamma^{RD}_{M1,2} \leq x\right) \\ &= \int_0^x \int_0^\infty F_{\gamma_{B1,M1}}\left((x-Z)(1+Y)\right) f_{\gamma_{B2,M1}}(Y) f_{\gamma^{RD}_{M1,2}}(Z) dY dZ. \end{aligned} \tag{5.42}$$

After some manipulations, we obtain

$$F_{\gamma_{MS1,OC}}(x) = \frac{-e^{-\frac{x}{\bar{\gamma}_{B1}}}}{\Gamma(N_k)\bar{\gamma}^{N_k}_{RD}} \int_0^x \frac{\Upsilon Z^{N_k-1} e^{-\left(\frac{1}{\bar{\gamma}_{RD}} - \frac{1}{\bar{\gamma}_{B1}}\right)}}{-Z + (x+\Upsilon)} dZ + F_{\gamma^{RD}_{M1,2}}(x). \tag{5.43}$$

When $\bar{\gamma}_{RD} = \bar{\gamma}_{B1}$, the integral can be solved using [28, 1.2.4.3] to obtain

$$\begin{aligned} F_{\gamma_{MS1,OC}}(x) = F_{\gamma^{RD}_{M1,2}}(x) - \frac{e^{-\frac{x}{\bar{\gamma}_{B1}}} x^{N_k} \Upsilon}{\Gamma(N_k+1)\bar{\gamma}^{N_k}_{RD}(x+\Upsilon)} \\ {}_2F_1\left(1, N_k; N_k+1; \frac{x}{x+\Upsilon}\right). \end{aligned} \tag{5.44}$$

When $\bar{\gamma}_{RD} \neq \bar{\gamma}_{B1}$, we follow the approach used in [30] to obtain $F_{\gamma_{MS1,OC}}(x)$ as

$$F_{\gamma_{MS1,OC}}(x) = F_{\gamma_{M1,2}^{RD}}(x) + \frac{e^{-\frac{x}{\bar{\gamma}_{B1}}} e^{\frac{x+\Upsilon}{\bar{\gamma}}} \Upsilon}{\Gamma(N_k)\bar{\gamma}_{RD}^{N_k}} \sum_{j=0}^{N_k-1} \binom{N_k-1}{j} (x+\Upsilon)^{N_k-1-j} \hat{I}(\Upsilon, j, \bar{\gamma}) \quad (5.45)$$

where

$$\hat{I}(\Upsilon, j, \bar{\gamma}) = \int_{-(x+\Upsilon)}^{-\Upsilon} y^{j-1} e^{\frac{y}{\bar{\gamma}}} dy \quad (5.46a)$$

can be solved as

$$= \begin{cases} \text{Ei}\left(\frac{-\Upsilon}{\bar{\gamma}}\right) - \text{Ei}\left(\frac{-(x+\Upsilon)}{\bar{\gamma}}\right) & \text{if } j = 0 \\ \bar{\gamma}\left(e^{\frac{-\Upsilon}{\bar{\gamma}}} - e^{\frac{-(x+\Upsilon)}{\bar{\gamma}}}\right) & \text{if } j = 1 \\ e^{\frac{-\Upsilon}{\bar{\gamma}}}\left(\sum_{k=0}^{j-1} \frac{(-1)^k k! \binom{j}{k} (-1)^{j-k}}{\left(\frac{1}{\bar{\gamma}}\right)^{k+1}} \Upsilon^{j-k}\right) & \\ -e^{\frac{-(x+\Upsilon)}{\bar{\gamma}}}\left(\sum_{k=0}^{j-1} \frac{(-1)^k k! \binom{j}{k} (-1)^{j-k} (x+\Upsilon)^{j-k}}{\left(\frac{1}{\bar{\gamma}}\right)^{k+1}}\right) & \text{if } j > 1 \end{cases} \quad (5.46b)$$

$$\frac{1}{\bar{\gamma}} = \frac{1}{\bar{\gamma}_{B1}} - \frac{1}{\bar{\gamma}_{RD}} \quad (5.46c)$$

where $\text{Ei}(\cdot)$ is the exponential integral function defined in [31, eq. 8.211.1].

5.4 Performance Approximations for the High-SNR Regime

The expressions derived in Sec. 5.3 are useful for obtaining exact numerical values for the system outage probability. However, they may not provide direct insights into the system such as the diversity order and the array gain of the system. Therefore, we derive expressions for the outage probability when the transmit power is asymptotically large. The asymptotic outage probability expressions can be used to directly evaluate the diversity order and the array gain of the system. We assume $\bar{\gamma}_M = \nu\bar{\gamma}_R$, $\bar{\gamma}_{B_1} = \kappa\bar{\gamma}_R$, $\bar{\gamma}_{B1,R2} = \tau\bar{\gamma}_R$ and $\Phi_2 = \frac{\bar{\gamma}_{B2,R2}}{\bar{\gamma}_{B1,R2}}$, where $\bar{\gamma}_{B2,R2} = \frac{L_{B2,R2}}{N_0}$ and $\bar{\gamma}_{B1,R2} = \frac{L_{B1,R2}}{N_0}$. To identify the outage probability behaviour in the large SNR regime, we let $\bar{\gamma}_R \to \infty$. The asymptotic outage probability expressions are given in Table 5.2, where $\mathcal{O}\left(\bar{\gamma}_R^{-n}\right)$ denotes terms with the exponent of $\bar{\gamma}_R$ smaller than n.

Table 5.2: Asymptotic outage probability

Scenario	Asymptotic outage probability
1	$P_{S1}^{\infty} = \frac{\gamma_{\text{th}}^{N_r+1}}{(\gamma_{\text{th}}+\Upsilon)(\gamma_{\text{th}}+\Phi)^{N_r}} + \left(\frac{\gamma_{\text{th}}^{N_r+1}}{(\gamma_{\text{th}}+\Upsilon)(\gamma_{\text{th}}+\Omega)^{N_r}}\left(1-\left(\frac{\gamma_{\text{th}}}{\gamma_{\text{th}}+\Phi}\right)^{N_r}\right)\left(1-\left(\frac{\gamma_{\text{th}}}{\gamma_{\text{th}}+\Phi_2}\right)^{N_r}\right)\right) + \mathcal{O}\left(\bar{\gamma}_R^{-1}\right)$
2	$P_{S2}^{\infty} = \frac{\gamma_{\text{th}}^{N_r+1}}{(\gamma_{\text{th}}+\Upsilon)(\gamma_{\text{th}}+\Omega)^{N_r}} + \mathcal{O}\left(\bar{\gamma}_R^{-1}\right)$
3	$P_{S3}^{\infty} = \frac{\gamma_{\text{th}}^{N_r+1}}{\Gamma(N_r)\bar{\gamma}_R^{N_r-1}(\gamma_{\text{th}}+\Phi)(\gamma_{\text{th}}+\Upsilon)} + \frac{\gamma_{\text{th}}^{N_r}}{\Gamma(N_r)(\gamma_{\text{th}}+\Upsilon)(\nu\bar{\gamma}_R)^{N_r-1}} + \mathcal{O}\left(\bar{\gamma}_R^{-N_r}\right)$
BT-1	$P_{BT1}^{\infty} = \frac{\gamma_{\text{th}}^{N_r+1}}{\Gamma(N_r)\bar{\gamma}_R^{N_r-1}(\gamma_{\text{th}}+\Phi)(\gamma_{\text{th}}+\Upsilon)} + \frac{\gamma_{\text{th}}^{N_r}}{\Gamma(N_r)(\gamma_{\text{th}}+\Upsilon)\bar{\gamma}_R^{N_r-1}\left(\frac{\nu}{2}+\frac{\nu}{2\Omega}\right)^{N_r-1}} + \mathcal{O}\left(\bar{\gamma}_R^{-N_r}\right)$
BT-2	$P_{BT2}^{\infty} = \frac{\gamma_{\text{th}}^{N_r}}{\Gamma(N_r)(\gamma_{\text{th}}+\Upsilon)\bar{\gamma}_R^{N_r-1}\left(\frac{\nu}{2}+\frac{\nu}{2\Omega}\right)^{N_r-1}} + \mathcal{O}\left(\bar{\gamma}_R^{-N_r}\right)$

5.5 Performance Improvement With Multiple Antennas at the Source Nodes

In this section, we study the system outage probabilities with multiple antennas at the source nodes. We assume that the source nodes use transmit antenna selection (TAS) for the first-hop transmission. The motivation for the choice of TAS is that it requires only few bits of feedback between the source and relay nodes. We assume that TAS is performed with local CSI only. Joint TAS schemes are not considered in our analysis. We assume that each BS is equipped with N_t antennas. The transmit antenna selection at R_1 is performed as

$$t_1 = \underset{1\leq n\leq N_t}{\arg\max}\{||\boldsymbol{g}_{n,1}||^2\} \tag{5.47}$$

where $\boldsymbol{g}_{n,1}$ is the $N_r \times 1$ channel vector between the n^{th} source antenna and R_1. The elements of $\boldsymbol{g}_{n,1}$ are distributed as $\mathcal{CN}(0, L_{B1,R1})$.

5.5.1 Scenario 1: No network coordination

The SINR at R_1 is given by

$$\gamma_{\text{TAS},1}^{S1} = \frac{||\boldsymbol{g}_{t_1,R1}||^2}{N_0 + \frac{|\boldsymbol{g}_{t_1,R1}^H \boldsymbol{g}_{t_2,R1}|^2}{||\boldsymbol{g}_{t_1,R1}||^2}} \tag{5.48}$$

where $\boldsymbol{g}_{t_2,R1}$ is the channel vector between the selected antenna at BS_2 and R_1 with elements distributed as $\mathcal{CN}(0, L_{B2,R1})$. The interference power term $\frac{|\boldsymbol{g}_{t_1,R1}^H \boldsymbol{g}_{t_2,R1}|^2}{||\boldsymbol{g}_{t_1,R1}||^2}$ is distributed as $\mathcal{G}(1, L_{B2,R1})$. The CDF of $\gamma_{\text{TAS},1}^{S1}$ can be found using [32, eq. (17)] and [31, 3.351.3] as

$$F_{\gamma_{\text{TAS},1}^{S1}}(x) = 1 - \sum_{q=1}^{N_t} \binom{N_t}{q} (-1)^{q-1} e^{\frac{-qx}{\bar{\gamma}_R}} \sum_{m_1=1}^{N_r} \cdots \sum_{m_q=1}^{N_r} \sum_{r=0}^{m_s} \times \binom{m_s}{r} \frac{x^{m_s}}{\prod_{p=1}^{q}(m_p-1)!} \frac{r!\Phi}{\bar{\gamma}_R^{m_s-r}(\Phi+qx)^{r+1}} \quad (5.49)$$

where $m_s = \sum_{p=1}^{q}(m_q - 1)$. The CDF for the SINR at R_2 can be found similarly. The system outage probability can be computed by replacing $F_{\gamma_{\text{MRC},1}}(\gamma_{\text{th}})$ and $F_{\gamma_{\text{MRC},2}}(\gamma_{\text{th}})$ with $F_{\gamma_{\text{TAS},1}^{S1}}(\text{th})$ and $F_{\gamma_{\text{TAS},2}^{S1}}(\text{th})$ in (5.27) and (5.28).

5.5.2 Scenario 2: First-hop interference CSI estimation

Since the relays do not perform joint antenna selection, they use local CSI for determining the transmit antenna index. However, since the relays are capable of estimating the CSI of the interference link, they use a MMSE receiver for signal combining in the first hop. The SINR at R_1 is given by

$$\gamma_{\text{TAS},1}^{S2} = \frac{|\zeta_1|^2}{N_0 + ||\boldsymbol{g}_{t_2,R1}||^2} + \underbrace{\sum_{k=2}^{N_r} \frac{|\zeta_k|^2}{N_0}}_{Z_M} \quad (5.50)$$

where $\zeta_k,\ k \in [1, N_r]$ have the same statistics as the elements of $\boldsymbol{g}_{t_1,R1}$. Deriving an exact expression for the CDF of $\gamma_{\text{TAS},1}^{S2}$ appears to be intractable. Therefore, we derive a tight upper bound assuming that transmit antenna was selected to maximize SINR at R_1 as

$$t_1 = \underset{1 \le n \le N_t}{\arg\max} \left\{ \frac{|\zeta_{1,n}|^2}{N_0 + ||\boldsymbol{g}_{t_2,R1}||^2} + \sum_{k=2}^{N_r} \frac{|\zeta_{k,n}|^2}{N_0} \right\} \quad (5.51)$$

where $\zeta_{k,n},\ k \in [1, N_r],$ have the same statistics as the elements of $\boldsymbol{g}_{n,R1}$. Then, the approximate CDF of $\gamma_{\text{TAS},1}^{S2}$ can be found as

$$F_{\gamma_{\text{TAS},1}^{S2}}(x) = \left(F_{Z_M}(x) - \left[\frac{\bar{\gamma}_R e^{\frac{-x}{\bar{\gamma}_R}} x^{N_r-1} \Phi^{-N_r+1}}{\bar{\gamma}_{IR}^{N_r} (\Phi + x) \Gamma(N_r)} \right] \right)^{N_t}. \quad (5.52)$$

Using $F_{\gamma_{\text{TAS},1}^{S2}}(x)$, one can obtain a tight upper bound on the system outage probability. An expression for the system outage probability in the high-SNR regime can be derived by applying a Taylor series expansion on $F_{\gamma_{\text{TAS},1}^{S2}}(x)$ and considering only the terms with the largest exponent of $\bar{\gamma}_R$. The asymptotic outage probability is identical to P_{S2}^{∞}. Therefore, one can identify that implementing multiple antennas at the source does not improve the system performance in the high-SNR regime.

5.5.3 Scenario 3: Sharing second-hop CSI

Since the first-hop techniques are identical to Scenario 2, we use the same approximate CDF (5.52) derived in Scenario 2 to compute the system outage probability in Scenario 3. Using a Taylor series expansion of $F_{\gamma_{\text{TAS},1}^{S2}}(x)$ and considering only the terms with the largest exponent of $\bar{\gamma}_R$, the asymptotic outage probability for Scenario 3 can be found as

$$P_{S3,TAS}^{\infty} = \frac{\gamma_{\text{th}}^{N_r}}{\Gamma(N_r)(\gamma_{\text{th}} + \Upsilon)(\nu\bar{\gamma}_R)^{N_r-1}} + \mathcal{O}\left(\bar{\gamma}_R^{-N_r}\right). \tag{5.53}$$

From (5.53), one can identify the performance gain obtained by implementing multiple antennas at the source nodes. Another interesting observation is that increasing N_t from 1 to 2 provides performance gain and thereafter increasing N_t does not provide a significant performance gain in the high-SNR regime.

5.5.4 Scenario 4: Sharing CSI and data

For the BT-1 scheme, the first-hop techniques are identical to Scenario 2, and we use the same approximate CDF for the SINR at R_1 to compute the system outage probability. Similar to Scenario 3, the asymptotic outage probability can be derived as

$$P_{BT1}^{\infty} = \frac{\gamma_{\text{th}}^{N_r}}{\Gamma(N_r)(\gamma_{\text{th}} + \Upsilon)\bar{\gamma}_R^{N_r-1}\left(\frac{\nu}{2} + \frac{\nu}{2\Omega}\right)^{N_r-1}} + \mathcal{O}\left(\bar{\gamma}_R^{-N_r}\right). \tag{5.54}$$

One can observe the performance gain with multiple antennas at the source nodes. Similar to Scenario 3, a high-SNR outage probability improvement is observed when N_t increases from 1 to 2. Thereafter, a significant gain cannot be achieved in the high-SNR regime.

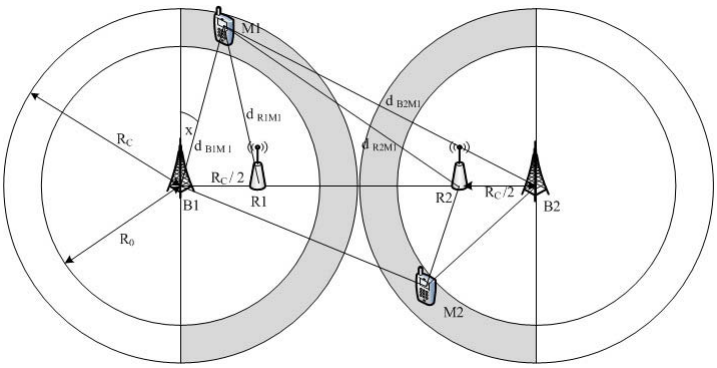

Figure 5.1: The two-cell network model used in the numerical results.

An outage probability analysis for the BT-2 scheme appears to be intractable. Therefore, we use simulations to compare its performance with the BT-1 scheme.

5.6 Performance Approximations for Random User Locations

In this section, we study the impact of user location randomness on the system outage probability for each scenario analyzed in Sections 5.2 and 5.3. We consider the case when the MSs of both cells are located close to the cell edge. We assume circular cells with radius R_c and the relays are located at a distance $\frac{R_c}{2}$ from the BSs of each cell. The MSs are uniformly distributed in the shaded region of each cell given in Fig. 5.1. Therefore, the distances d_{B1M1}, d_{R1M1}, d_{B2M1}, d_{R2M1} are RVs. Then, the path loss for each link is also an RV. We assume that the angle x is uniformly distributed in the interval $[0, \pi]$. Then, the PDF of d_{B1M1} can be deduced from [33] as

$$f_{d_{B1M1}}(r) = \frac{2r}{R_c^2 - R_0^2} \quad \text{for} \quad R_0 \leq r \leq R_c. \tag{5.55}$$

The mean distance between BS_1 and MS_1 can be computed as

$$\bar{d}_{B1M1} = \frac{2}{3}\frac{(R_c^3 - R_0^2)}{(R_c^2 - R_0^2)}. \tag{5.56}$$

Applying the law of cosines, the distances d_{R1M1}, d_{B2M1}, and d_{R2M1} can be found as

$$d_{R1M1}^2 = d_{B1M1}^2 + \left(\frac{R_c}{2}\right)^2 - d_{B1M1} R_c \sin(x) \tag{5.57a}$$

$$d_{B2M1}^2 = d_{B1M1}^2 + (2R_c)^2 - 4d_{B1M1}R_c\sin(x) \tag{5.57b}$$

$$d_{R2M1}^2 = d_{B1M1}^2 + \left(\frac{3R_c}{2}\right)^2 - 3d_{B1M1}R_c\sin(x). \tag{5.57c}$$

Finding exact expressions for the PDFs of d_{R1M1}, d_{B2M1}, and d_{R2M1} appear to be intractable. Therefore, we approximate their distributions by replacing d_{B1M1} with $\bar{d}_{B1M1}$. Applying standard transformation theory, the approximate PDF of d_{R1M1}^2 can be found as

$$f_{d_{R1M1}^2}(y) = \frac{1}{K_2\pi\sqrt{1-\left(\frac{y-K_1}{K_2}\right)^2}},\ y \in [K_1 - K_2, K_1 + K_2]$$

where $K_1 = (\bar{d}_{B1M1})^2 + \left(\frac{R_c}{2}\right)^2$ and $K_2 = \bar{d}_{B1M1}R_c$. The mean of d_{R1M1} is given by

$$\bar{d}_{R1M1} = \int_{K_1-K_2}^{K_1+K_2} \frac{\sqrt{y}}{K_2\pi\sqrt{1-\left(\frac{y-K_1}{K_2}\right)^2}}dy.$$

Applying the variable transformation $\frac{y-K_1}{K_2} = \cos(x)$ and solving the resulting integral using [31, eq. 3.670.1], the mean of d_{R1M1} can be found as

$$\bar{d}_{R1M1} = \frac{2\sqrt{K_1+K_2}}{\pi}\boldsymbol{K}\left(\sqrt{\frac{2K_2}{K_1+K_2}}\right) \tag{5.58}$$

where $\boldsymbol{K}(\cdot)$ is the complete elliptic integral of the second kind [31, 8.112]. The mean distances $\bar{d}_{B2M1}$, and $\bar{d}_{R2M1}$ can be found similarly.

To account for the user location randomness, one must average $L_{a,b}$ over the PDF of $d_{a,b}$. However, this approach appears to be mathematically intractable. Therefore, instead of averaging over the PDF of $d_{a,b}$, we substitute the average value $\bar{d}_{a,b}$ in path loss computations to account for the user location randomness. Then, the outage probability for each scenario can be evaluated by substituting the modified path loss figures in the expressions derived in Sec. 5.3. Outage probability computed in this manner is known as the area outage probability since it is the outage probability of the MS averaged over the geographical area. From simulation results, it can be observed that this approach leads to very good performance approximations for Scenarios 1, 2 and 3 when the users are located close to the cell edge.

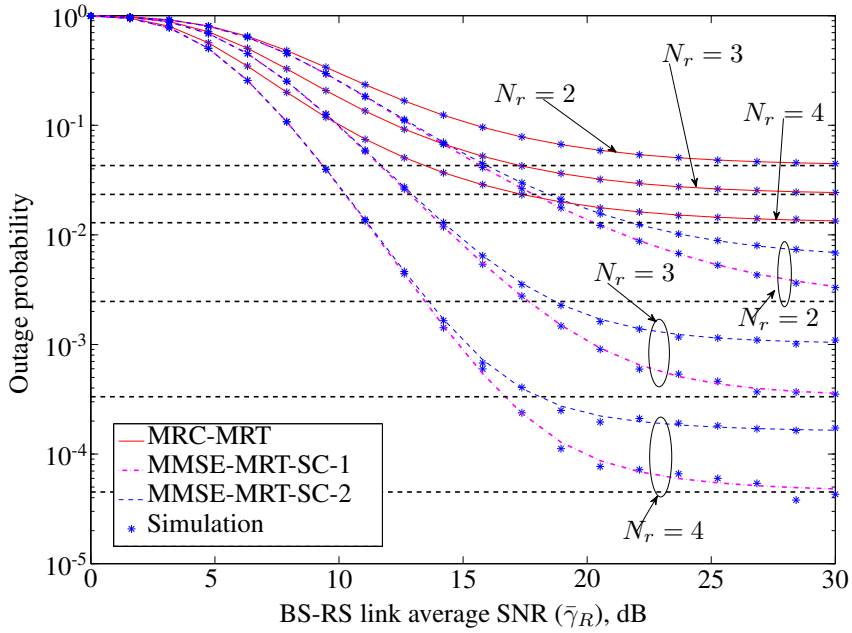

Figure 5.2: Outage probability for MRC-MRT and MMSE-MRT systems.

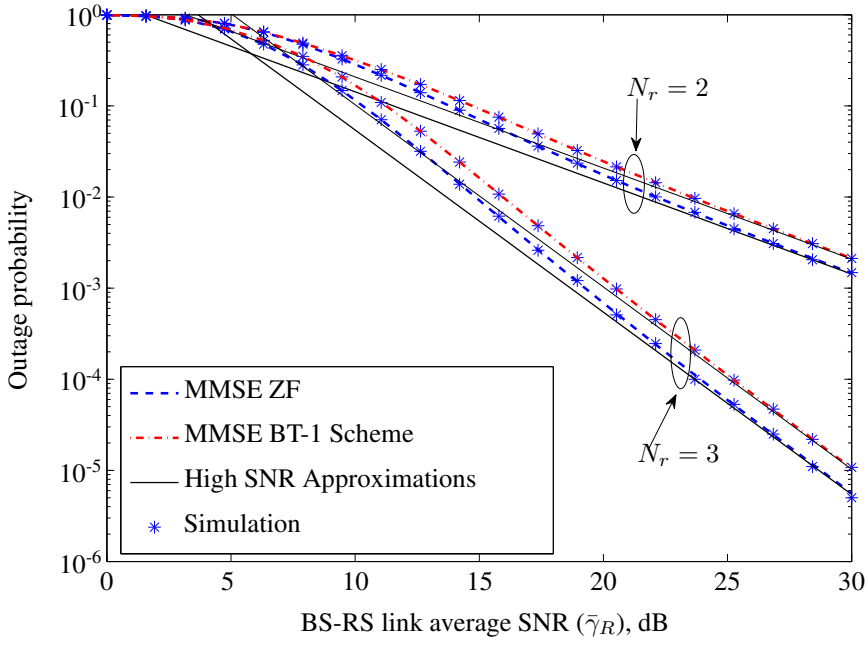

Figure 5.3: Outage probability comparisons for MMSE-ZF and MMSE-BT-1 schemes.

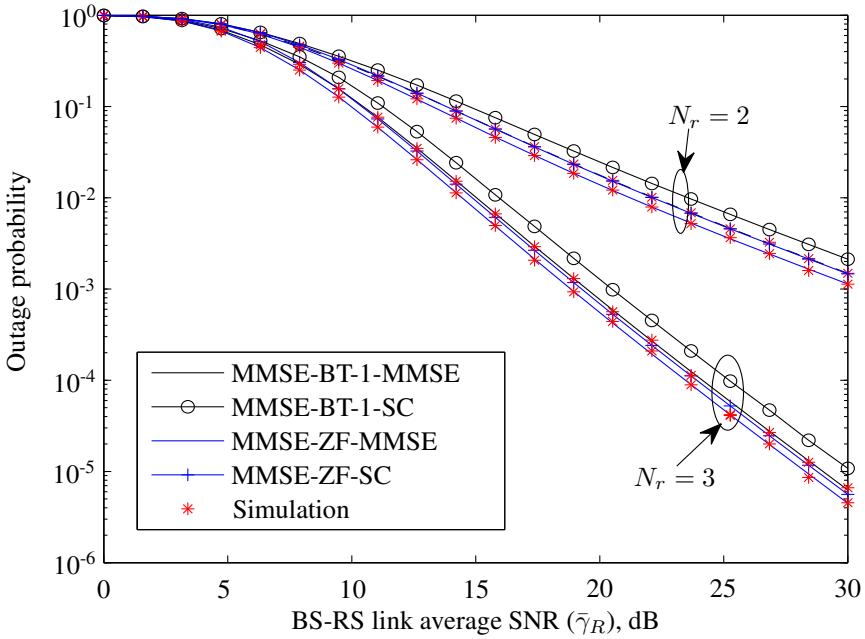

Figure 5.4: Outage probability comparisons for SC and OC for MMSE/ZF and MMSE/BT-1 schemes.

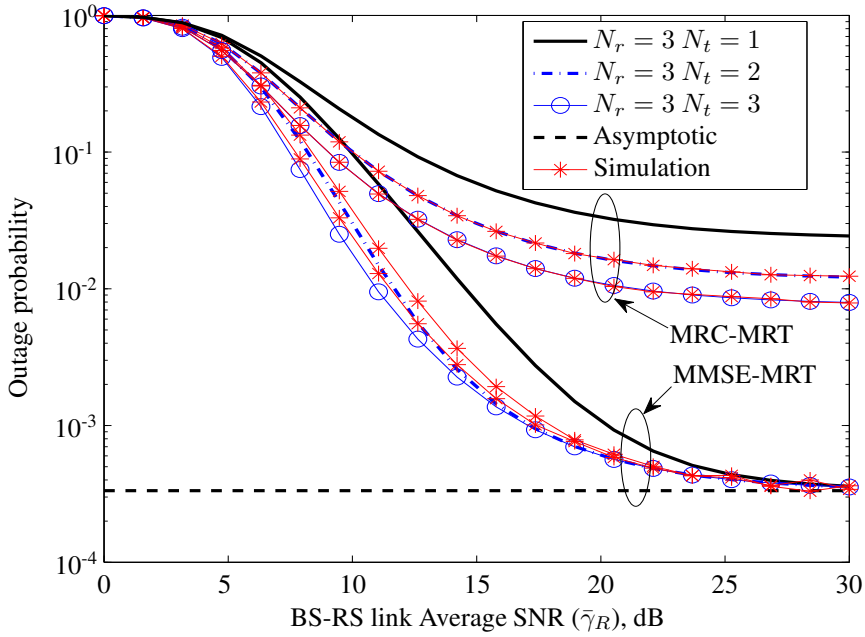

Figure 5.5: Outage probability for MRC-MRT and MMSE-MRT schemes with TAS.

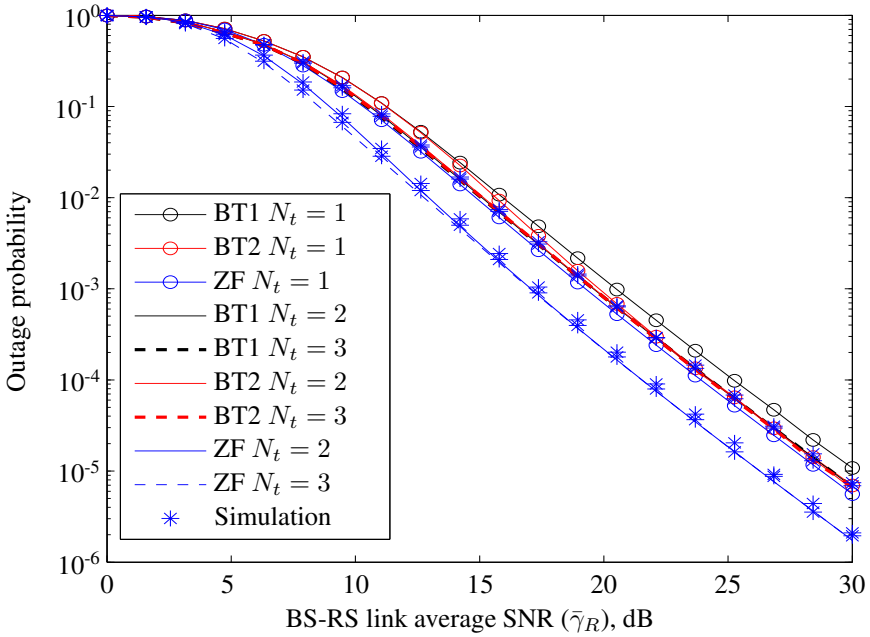

Figure 5.6: The outage probability comparisons for Scenario 3 and Scenario 4 with multiple antennas at the source nodes and $N_r = 3$.

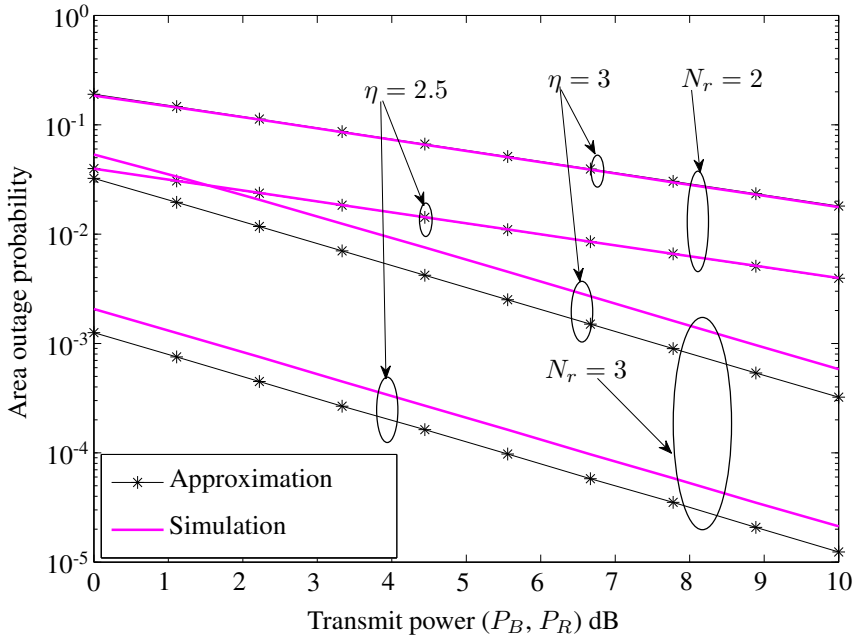

Figure 5.7: The area outage probability of the MMSE-ZF scheme with different path loss exponents.

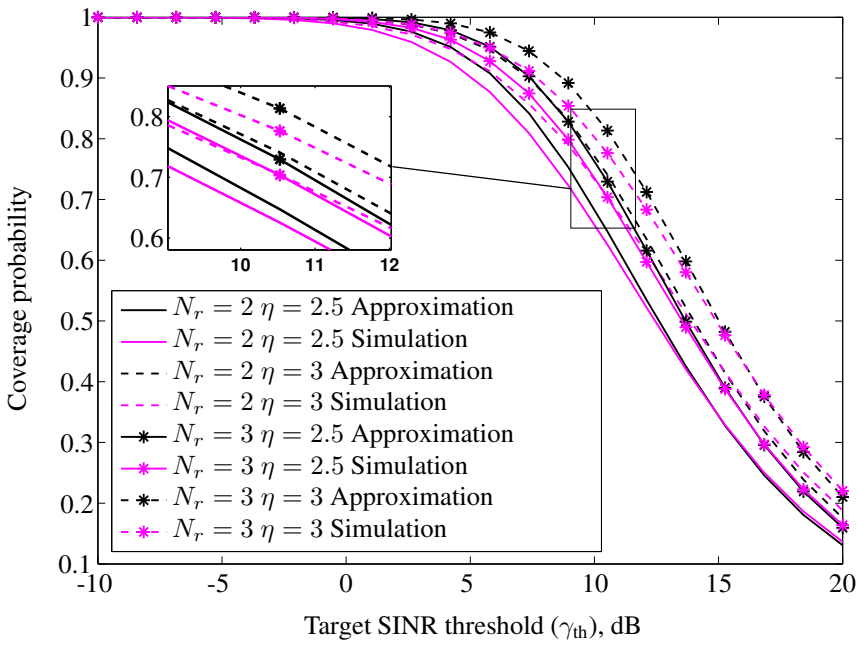

Figure 5.8: The coverage probability of the MMSE-MRT scheme with different path loss exponents.

5.7 Numerical Results and Discussion

In this section, we present some numerical results obtained using the analytical results presented in Sections 5.3, 5.4, 5.5 and 5.6. The results in Figs. 5.2, 5.3, and 5.4 are obtained assuming fixed positions for MSs close to the BSs, while the results of Figs. 5.7, and 5.8 are obtained using random locations for MSs close to the cell edge. The location of the relays are fixed at a distance $\frac{R_c}{2}$ from the center of the cell. The cell radius is assumed to be 250 m. In all numerical results, except for the results in Fig. 5.8, the predetermined SINR threshold γ_{th} for a successful reception to support the desired data rate, is assumed to be 10 dB. Unless otherwise mentioned, the path loss is calculated using a reference distance of 10 m, carrier frequency of 2.4 GHz and a path loss exponent of 2.5.

For the cases with fixed MS locations close to the BSs, we have used $\bar{\gamma}_M = 2\bar{\gamma}_R$, $\bar{\gamma}_{B_1} = 2\bar{\gamma}_R$, $\bar{\gamma}_{B1,R2} = \frac{\bar{\gamma}_R}{8}$, $\Upsilon = 64$, $\Omega = 64$, and $\Phi = \Phi_2 = 8$. For simulation results, we used 10^6 channel realizations per data point. For the cases with random MS locations, the MSs are assumed to be located in the shaded area of Fig. 5.1

with $R_0 = 220$ m. In the simulations, 50,000 random MS locations are considered and for each location 10,000 fading realizations were used to estimate the outage probability and the coverage probability. The noise power was set to -116 dBm and the transmit power per node was set to 40 dBm for the results in Fig. 5.8.

Fig. 5.2 shows the outage probability performance for Scenarios 1 and 2. High-SNR approximations are shown using dashed black lines. As predicted by the asymptotic analysis, the outage probability reaches a floor for these two scenarios. However, estimating the first-hop interference CSI provides a significant performance improvement over the MRC-MRT system. The two SC schemes perform almost identically for the MRC-MRT system since the performance is dominated by the first hop. However, in the MMSE-MRT system, the SC-1 scheme outperforms the SC-2 scheme in the high SNR regime. However, the SC-2 scheme does not require instantaneous CSI of the interference links, making it the sensible option for an uncoordinated network. Furthermore, one can observe excellent agreement between the theoretical results and the simulation results.

Fig. 5.3 compares the outage probability performance of the MMSE-ZF scheme and the BT-1 scheme. An interesting observation from the results of Fig. 5.3 is that the MMSE-ZF scheme outperforms the MMSE-BT scheme in the high SNR regime when $\bar{\gamma}_M > \bar{\gamma}_{IM}$. However, the CSI estimation and feedback overhead for the MS is higher in the MMSE-ZF scheme, since the MSs have to estimate and feedback the desired channel and interference channel information separately in the MMSE-ZF scheme, while the MMSE-BT scheme requires estimating and feeding back the only the CSI of the superimposed channel. Therefore, when selecting between the MMSE-ZF scheme and the MMSE-BT scheme, one must consider both the channel quality and the overheads of CSI estimation and feedback.

Fig. 5.4 compares the outage probability performance of MMSE-BT-1 and MMSE-ZF schemes with SC and OC at the MSs. One can observe that OC marginally outperforms SC. Both schemes require the same amount of memory while the computational complexity of OC is higher compared to SC since it requires a matrix inversion operation.

Figs. 5.5 and 5.6 compare the system outage probabilities with multiple anten-

nas at the source nodes. One can observe that implementing multiple antennas at the source nodes improves the performance of Scenario 1 significantly. However, for the MMSE-MRT scheme, a performance gain is observed only in the medium SNR regime, and in the high SNR regime, the performance approaches the performance of the single antenna source system. For the MMSE-BT1 and MMSE-ZF schemes, a performance gain is observed when N_t is increased from 1 to 2. For $N_t > 2$, the performance does not show an identifiable improvement. For the MMSE-BT2 scheme, a significant performance gain cannot be observed with multiple antenna source nodes.

Fig. 5.7 compares the area outage probability for the MMSE-ZF scheme computed using the proposed approximation technique with the simulation results. When $N_r = 2$, the approximation is extremely accurate and almost indistinguishable from the simulation results. When N_r is increased, there is a discrepancy between the approximate outage probability and the simulation results. However, this discrepancy is less than 1 dB. We used path loss exponent values 2.5 and 3 since these are the most commonly observed values of η. The accuracy of the approximations is reasonably good and they result in a significant amount of computational time savings compared to computer simulations.

Fig. 5.8 shows the coverage probability of MS_1 with the MMSE-MRT scheme, for different SINR threshold values. The coverage probability is computed as $1 - P_{\text{out}}$. The curves are magnified for clarity. One can observe that the the proposed approximations are capable of estimating the coverage probabilities with a reasonable accuracy, while saving significant amounts of computational time.

The numerical and theoretical results can be used to obtain the following basic rules of thumb for system design.

- From the view point of the MSs, with symmetric fading channels from R_1 and R_2, it is preferable to implement BT-1 or BT-2 schemes for relay coordination. If the MSs are located such that MS_k is closer to R_j, BT schemes are preferred. However, the backhaul capacity between the relays should be increased to exchange the user data symbols. With an M-ary modulation alphabet, the increase in feedback will be M bits.

- When MS_k is closer to R_k, the relay coordination scheme should be selected carefully. One must consider the increase in feedback load from MS_k to R_k to feedback the CSI of both channels separately. If this increase can be sufficiently supported by the feedback channel, it is desirable to use the MMSE-ZF scheme.

- Implementing multiple antennas at the source nodes will not change the system diversity order. However, it results in an improvement of the high-SNR performance in Scenario 1, 3 and the BT-1 scheme. In the high-SNR regime, the performance gain is significant only for the case when $N_t = 2$, and a further increase in N_t will be a waste of resources.

5.8 Conclusion

A comprehensive outage probability analysis was provided for relay coordination schemes in two-hop DF relay networks. A practically relevant case where the cells are coordinated only with the cell which causes the strongest interference was considered in the analysis. Closed-form outage probability expressions were derived for four relay coordination schemes. Simplified outage probability expressions were derived for the high-SNR regime to identify important parameters such as array gain and the diversity order of the system. Furthermore, an approximation technique was proposed to incorporate the impact of user location randomness in outage probability computations.

5.A The derivations of (5.24) and (5.25)

We consider the following general case where we derive the CDF of the RV V given as

$$V = \begin{cases} \frac{X}{A} & \text{if } \frac{X}{C} > \frac{Y}{D} \\ \frac{Y}{B} & \text{if } \frac{X}{C} \leq \frac{Y}{D}. \end{cases} \tag{5.59}$$

Following [27, 6-77], the CDF of the RV V can be obtained as

$$\begin{aligned} F_V(v) &= \Pr\left[X \le Av, \frac{X}{C} > \frac{Y}{D}\right] + \Pr\left[Y \le Bv, \frac{X}{C} \le \frac{Y}{D}\right] \\ &= \Pr\left[X \le Av, Y \le Bv\right] + \int_{\frac{CBv}{D}}^{Av} \int_{Bv}^{\frac{Dx}{C}} f_{X,Y}(x,y)dydx. \\ &= F_{X,Y}(Av, Bv) + \int_{\frac{CBv}{D}}^{Av} \int_{Bv}^{\frac{Dx}{C}} f_{X,Y}(x,y)dydx. \end{aligned} \tag{5.60}$$

The 4-fold integral in (5.23) is obtained by averaging over the distributions of γ_{I1} and γ_{I2}. It is solved using the binomial theorem and the identity [31, 3.351.3], and the CDF of γ_{M1}^{SI} can be found as (5.24). Setting $B = 1$, and $D = 1$, one can obtain a general form for the case when the reception at M1 is interference free. The CDF of γ_{M1}^{S} can be found as (5.25).

5.B The Derivations of Asymptotic Outage Probability Expressions

In this appendix, we present the derivations of asymptotic outage probability expressions given in Table 5.2. When $\bar{\gamma}_R \to \infty$, we only consider the terms with the largest exponent of $\bar{\gamma}_R$. We apply Taylor series expansions on the PDFs of the RVs $\gamma_{\text{MRC},1}$, $\gamma_{M1,1}$, $\gamma_{M1,2}^{I}$, $\gamma_{M1,2}^{\text{NI}}$, $\gamma_{\text{MMSE},1}$, $\gamma_{M1,2}^{\text{ZF}}$, $\gamma_{M1,2}^{\text{MRT}}$, $\gamma_{M1,2}^{\text{BT,ZF}}$, $\gamma_{M1,2}^{\text{BT,MRT}}$, and obtain their asymptotic CDF representations as

$$F_{\gamma_{\text{MRC},1}}^{\infty}(x) \approx \left(\frac{x}{x+\Phi}\right)^{N_r}, \quad F_{\gamma_{M1,1}}^{\infty}(x) \approx \left(\frac{x}{x+\Upsilon}\right)$$

$$F_{\gamma_{M1,2}^{I}}^{\infty}(x) \approx \left(\frac{x}{x+\Omega}\right)^{N_r}, \quad F_{\gamma_{M1,2}^{\text{NI}}}^{\infty}(x) \approx \frac{x^{N_r}}{\Gamma(N_r+1)\bar{\gamma}_M^{N_r}}$$

$$F_{\gamma_{\text{MMSE},1}}^{\infty}(x) \approx \frac{\gamma_{\text{th}}^{N_r+1}}{\Gamma(N_r)\bar{\gamma}_R^{N_r-1}(\gamma_{\text{th}}+\Phi)}$$

$$F_{\gamma_{M1,2}^{\text{ZF}}}^{\infty}(x) \approx \frac{x^{N_r-1}}{\Gamma(N_r)\bar{\gamma}_M^{N_r-1}}$$

$$F^{\infty}_{\gamma^{\text{BT,ZF}}_{M1,2}}(x) \approx \frac{x^{N_r-1}}{\Gamma(N_r)\left(\frac{\bar{\gamma}_M+\bar{\gamma}_{MI}}{2}\right)^{N_r-1}}$$

$$F^{\infty}_{\gamma^{\text{BT,MRT}}_{M1,2}}(x) \approx \frac{x^{N_r}}{\Gamma(N_r+1)\left(\frac{\bar{\gamma}_M+\bar{\gamma}_{MI}}{2}\right)^{N_r}}.$$

The asymptotic CDFs of $\gamma_{\text{MRC},2}$ and $\gamma_{\text{MMSE},2}$ can be deduced from the CDFs $F^{\infty}_{\gamma_{\text{MRC},1}}(x)$ and $F_{\gamma_{\text{MMSE},1}}$ in a straightforward manner. Substituting the relevant asymptotic CDFs and considering only the terms with the largest exponent of $\bar{\gamma}_R$, we obtain the outage probability expressions for the high-SNR regime.

References

[1] *3rd Generation Partnership Project-Technical Specification Group Radio Access Network-Evolved Universal Terrestrial Radio Access (E-UTRA)-relay architectures for E-UTRA (LTE-Advanced)(release 9)*, vol. 3GPP TR 36.806 V9.0.0, Mar. 2010.

[2] S. W. Peters, A. Y. Panah, K. T. Truong, and R. W. Heath, "Relay architectures for 3GPP LTE-advanced," *EURASIP J. Wirel. Commun. Netw.*, vol. 2009, pp. 1:1–1:14, Mar. 2009.

[3] J. Zhang and K. B. Letaief, "Interference management with relay cooperation in two-hop interference channels," *IEEE Wireless Commun. Lett.*, vol. 1, no. 3, pp. 165–168, June 2012.

[4] K. T. Truong and R. W. Heath, "Joint transmit precoding for the relay interference broadcast channel," *IEEE Trans. Veh. Technol.*, vol. 62, no. 3, pp. 1201–1215, Mar. 2013.

[5] Y. Shi, J. Zhang, and K. B. Letaief, "Coordinated relay beamforming for amplify-and-forward two-hop interference networks," in *IEEE Global Telecommun. Conf.*, Dec. 2012, pp. 2408–2413.

[6] N. Lee, W. Shin, R. W. Heath, and B. Clerckx, "Interference alignment with limited feedback for two-cell interfering MIMO-MAC," in *International Symposium on Wireless Communication Systems (ISWCS), 2012*, 2012, pp. 566–570.

[7] C.-B. Chae, I. Hwang, R. W. Heath, and V. Tarokh, "Jointly optimized two-cell MIMO systems," in *IEEE GLOBECOM Workshops (GC Wkshps), 2011*, 2011, pp. 421–425.

[8] C. Na, X. Hou, and A. Harada, "Two-cell coordinated transmission scheme based on interference alignment and MU-MIMO beamforming," in *75th IEEE Vehicular Technology Conference (VTC Spring), 2012*, 2012, pp. 1–5.

[9] J.-W. Kwon, K.-H. Park, Y.-C. Ko, and H.-C. Yang, "Cooperative joint precoding in a downlink cellular system with shared relay: Design and performance evaluation," *IEEE Trans. Wireless Commun.*, vol. 11, no. 10, pp. 3462 –3473, Oct. 2012.

[10] K. Lee, "Uplink interference alignment for two-cell MIMO interference channels," *IEEE Trans. Veh. Technol.*, vol. 62, no. 4, pp. 1861–1865, 2013.

[11] K. T. Hemachandra and N. C. Beaulieu, "Shared relay networks with linear receivers at the relay: Two-cell case," *IEEE Trans. Commun.*, vol. 62, no. 4, pp. 1230–1239, Apr. 2014.

[12] H. A. Suraweera, H. K. Garg, and A. Nallanathan, "Performance analysis of two hop amplify-and-forward systems with interference at the relay," *IEEE Commun. Lett.*, vol. 14, no. 8, Aug. 2010.

[13] D. B. da Costa, H. Ding, and J. Ge, "Interference-limited relaying transmissions in dual-hop cooperative networks over Nakagami-*m* fading," *IEEE Commun. Lett.*, vol. 15, pp. 503–505, May 2011.

[14] D. Lee and J. H. Lee, "Outage probability of decode-and-forward opportunistic relaying in a multicell environment," *IEEE Trans. Veh. Technol.*, vol. 60, pp. 1925–1930, May 2011.

[15] D. B. da Costa and M. D. Yacoub, "Outage performance of two hop AF relaying systems with co-channel interferers over Nakagami-*m* fading," *IEEE Commun. Lett.*, vol. 15, pp. 980–982, Sep. 2011.

[16] F. S. Al-Qahtani, T. Q. Duong, C. Zhong, K. A. Qaraqe, and H. Alnuweiri, "Performance analysis of dual-hop AF systems with interference in Nakagami-*m* fading channels," *IEEE Signal Process. Lett.*, vol. 18, pp. 454–457, Aug. 2011.

[17] Y. Fan, J. S. Thompson, A. Adinoyi, and H. Yanikomeroglu, "On the diversity-multiplexing tradeoff for multi-antenna multi-relay channels," in *IEEE International Conference on Communications,*, Jun. 2007, pp. 5252–5257.

[18] A. Adinoyi and H. Yanikomeroglu, "Cooperative relaying in multi-antenna fixed relay networks," *IEEE Trans. Wireless Commun.*, vol. 6, no. 2, pp. 533–544, Feb 2007.

[19] Y. Fan, A. Adinoyi, J. S. Thompson, H. Yanikomeroglu, and H. V. Poor, "A simple distributed antenna processing scheme for cooperative diversity," *IEEE Trans. Commun.*, vol. 57, no. 3, pp. 626–629, Mar. 2009.

[20] A. Talebi and W. A. Krzymień, "Multiple-antenna multiple-relay cooperative communication system with beamforming," in *IEEE Vehicular Technology Conference,*, May 2008, pp. 2350–2354.

[21] A. Talebi and W. A. Krzymień, "Cooperative MIMO multiple-relay system with optimised beamforming and power allocation," *IET Communications*, vol. 4, no. 14, pp. 1677–1686, Sep. 2010.

[22] A. A. Abu-Dayya and N. C. Beaulieu, "Outage probabilities of diversity cellular systems with cochannel interference in Nakagami fading," *IEEE Trans. Veh. Technol.*, vol. 41, no. 4, pp. 343–355, Nov. 1992.

[23] J. Cui and A. U. H. Sheikh, "Outage probability of cellular radio systems using maximal ratio combining in the presence of multiple interferers," *IEEE Trans. Commun.*, vol. 47, pp. 1121–1124, Aug. 1999.

[24] E. G. Larsson and E. A. Jorswieck, "Competition versus cooperation on the MISO interference channel," *IEEE J. Select. Areas Commun.*, vol. 26, no. 7, pp. 1059–1069, Sep. 2008.

[25] R. Heath, T. Wu, Y. H. Kwon, and A. Soong, "Multiuser MIMO in distributed antenna systems with out-of-cell interference," *IEEE Trans. Signal Process.*, vol. 59, no. 10, pp. 4885–4899, Oct. 2011.

[26] S. S. Ikki and S. Aïssa, "Performance analysis of dual-hop relaying systems in the presence of co-channel interference," in *Proc. IEEE Global Telecommunications Conference, GLOBECOM 2010*, Miami, FL.

[27] A. Papoulis and U. S. Pillai, *Probability, Random Variables and Stochastic Processes*, 4th ed. New York: McGraw-Hill, 2002.

[28] A. P. Prudnikov, Y. Brychkov, and O. Marichev, *Integrals and Series*. Gorden and Breach Science, 1998, vol. 1.

[29] Wolfram functions site, "Hypergeometric2F1." [Online]. Available: http://functions.wolfram.com/HypergeometricFunctions/Hypergeometric2F1%/03/06/01/0001/

[30] N. Suraweera and N. C. Beaulieu, "Performance analysis of amplify-and-forward relaying with optimum combining in the presence of co-channel interference," in *IEEE Global Communications Conference (GLOBECOM)*, Dec. 2013, pp. 3565–3570.

[31] I. Gradshteyn and I. Ryzhik, *Table of Integrals, Series, and Products, Seventh Edition*. Academic Press, 2007.

[32] P. L. Yeoh, M. Elkashlan, and I. B. Collings, "Exact and asymptotic SER of distributed TAS/MRC in MIMO relay networks," *IEEE Trans. Wireless Commun.*, vol. 10, no. 3, pp. 751–756, Mar. 2011.

[33] S. Srinivasa and M. Haenggi, "Distance distributions in finite uniformly random networks: Theory and applications," *IEEE Trans. Veh. Technol.*, vol. 59, no. 2, pp. 940–949, Feb. 2010.

Chapter 6

Shared Relay Networks With Linear Receivers at the Relay: Two-Cell Scenario

The downlink performance of a two-cell relay enhanced wireless network is investigated. A single relay is shared by the two base stations in the system. The relay is assumed to be placed in a geographic region covered by both base stations. The relay station is operating in the decode-and-forward mode. Closed-form approximations which estimate the exact results extremely closely are derived for the outage probability and the ergodic rate of the system. The impact of finite rate channel state information feedback on the user ergodic rate is examined.

6.1 Introduction

The performance of users at the cell edges in a cellular wireless network is generally degraded due to the high level of inter-cell interference (ICI). To overcome this problem, the idea of coordinated base stations (also known as coordinated multi-point (CoMP)) has been proposed [1]. However, CoMP schemes require high capacity backhaul capabilities among the coordinating base stations.

In [2], the concept of shared relays was introduced as a low complexity solution for the ICI problem. In shared relay networks, multiple interfering base stations (BSs) share a multi-antenna relay station to process the received signals from multiple base stations and retransmit the signals to corresponding users, such that the

effective ICI level for each user is minimized. The scheme proposed in [2] uses multiuser detection in the first hop to decode the signals from multiple base stations and uses dirty paper coding in the second hop transmission. A recent paper [3] proposed a sum rate maximizing precoding scheme for two-cell shared relay networks where the relay is equipped with a single antenna. However, [3] assumed that the base stations are connected using a high capacity backhaul link. Problems regarding scheduling and resource allocation in shared relay networks have been addressed in [4].

In this chapter, we investigate the performance of a two-cell shared relay system (SRS) with a multi-antenna decode-and-forward (DF) relay, in terms of outage probability and ergodic rate. We assume linear receivers at the relay with zero-forcing (ZF) and minimum mean-square error (MMSE) combining. Although more sophisticated receiver/transmitter structures have been proposed for shared relay networks [5, 6], we consider linear processing at the relay as a benchmark for performance comparisons. Analytical solutions for performance metrics of shared relay networks are rare in the literature. We derive exact closed-form expressions as well as closed-form approximations for the system outage probability and the ergodic rate. In our analyses, we include the direct links between the base stations and users, which have been ignored in previous studies [7]. Our contributions are highlighted below.

- Closed-form approximations are derived for the outage probability and the ergodic rate of the shared relay network model described in Section 6.2. We propose an analytically tractable alternative system model, which performs extremely close to the original system model and derive exact expressions for performance metrics of this alternative model.

- Although closed-form solutions are preferred for exact performance evaluations, they may not provide direct insights into the system performance. Therefore, we derive outage probability and ergodic rate expressions for the system in the asymptotically high signal-to-noise ratio (SNR) regime.

- The transmissions at the relay require channel state information (CSI) of the

relay-to-user links. We analyze the case when the available CSI at the relay is not perfect when CSI quantization is performed by the users to feedback the estimated CSI. This analysis helps to understand the feedback channel requirements for SRSs.

The remainder of this chapter is organized as follows. In Section 6.2, we describe the SRS model and different system configurations to be studied. Section 6.3 provides detailed analysis on the end-to-end (e2e) signal-to-interference plus noise ratio (SINR). In Section 6.4, we provide expressions to compute the outage probability of the SRS. Section 6.5 presents ergodic rate computations for the system. In Section 6.6, we investigate the impact of finite rate CSI feedback on the ergodic rate of the system. Some numerical and simulation results are provided in Section 6.7, and the chapter is concluded in Section 6.8. Detailed derivations are provided in the Appendices.

The following notations will be used throughout this chapter. The probability density function (PDF) and the cumulative distribution function (CDF) of a random variable (RV) X are denoted as $f_X(x)$ and $F_X(x)$, respectively. The symbol $\mathbb{E}[\cdot]$ denotes expectation while the probability of an event $\mathcal{A}$ is denoted $\Pr(\mathcal{A})$. A complex Gaussian distribution with mean μ and variance σ^2 is denoted as $\mathcal{CN}(\mu, \sigma^2)$. A Gamma distribution with parameters k and θ is denoted by $\Gamma(k, \theta)$. Euler's Gamma function is denoted as $\Gamma(\cdot)$. We use lowercase bold letters to denote column vectors and uppercase bold letters to denote matrices. The transpose and the conjugate transpose of a vector or a matrix are denoted $(\cdot)^T$ and $(\cdot)^H$, respectively. The 2-norm of vector $\boldsymbol{x}$ is denoted $||\boldsymbol{x}||$.

6.2 System Model

The network model used in this chapter consists of two BSs (BS1 and BS2) which use identical frequency bands to serve their selected mobile stations (MSs) (MS1 and MS2). A relay station (RS) is located at the edge of the cells where ICI is strong. The RS is equipped with $N_t \geq 2$ antennas and the BSs and MSs are single antenna devices. Single antenna BSs are used for analytical tractability. However,

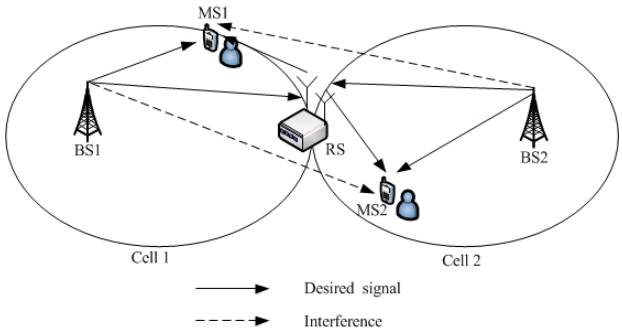

Figure 6.1: The shared relay model used for analysis.

the analysis can be extended for the case with multiple antenna BSs which use transmit antenna selection for transmission. It is assumed that the BSs are synchronized such that they transmit to their selected MSs at the same instant. In the first time slot, each BS transmits the data symbols intended for the MS it serves. No information is shared among the BSs. It is assumed that the relay has perfect knowledge of all the BS-RS channels and the RS-MS channels. The RS uses linear processing on the received signals and decodes the corresponding data symbols of two MSs. Without loss of generality, we select MS1 for our analysis.

The received signals at the RS and MS1 during the first time slot can be represented as

$$\boldsymbol{y}_R = \boldsymbol{H}\boldsymbol{s} + \boldsymbol{n}_R \tag{6.1a}$$

$$y_{MS1,1} = g_{1,1}s_1 + g_{2,1}s_2 + n_1 \tag{6.1b}$$

where $\boldsymbol{n}_R \sim \mathcal{CN}(0, N_0\boldsymbol{I}_{N_t})$ is a $N_t \times 1$ additive white Gaussian noise (AWGN) vector at the RS, $\boldsymbol{s} = [s_1\, s_2]^T$ is a symbol vector from each BS with unit energy symbols, $\boldsymbol{H}$ is the $N_t \times 2$ channel matrix between BSs and RS with columns $\boldsymbol{h}_1$ and $\boldsymbol{h}_2$, $g_{1,1}$ is the channel coefficient of the direct link from BS1 to MS1, $g_{2,1}$ is the channel coefficient of the direct link from BS2 to MS1 and $n_1 \sim \mathcal{CN}(0, N_0)$ is AWGN at MS1. Fading channel coefficients are modeled as complex Gaussian RVs whose variances are determined by the path-loss of the signal. The elements of the vectors $\boldsymbol{h}_1$ and $\boldsymbol{h}_2$ are distributed as $\mathcal{CN}(0, L_i)$, $i \in \{1, 2\}$ with L_i given by the free space propagation model,

$$L_i = P_i \frac{c^2}{(4\pi f_c d_i)^2} \tag{6.2}$$

where P_i is the transmit power of the i^{th} BS, $c = 3 \times 10^8$ m/s, f_c is the carrier frequency and d_i is the distance from the i^{th} BS to the RS. The RVs $g_{1,1}$ and $g_{2,1}$ are also complex Gaussian distributed with $\mathcal{CN}(0, L_{gi,1})$, and $i \in \{1, 2\}$ where L_{gi} can be computed by substituting the distances between BS1-MS1 and BS2-MS1 in (6.2) instead of d_i.

The RS applies linear combining on $\boldsymbol{y}_R$ by multiplying it with a $N_t \times 2$ weight matrix $\boldsymbol{W}$ to obtain the combiner output

$$\tilde{\boldsymbol{y}} = \boldsymbol{W}^H \boldsymbol{y}_R. \tag{6.3}$$

The structure of $\boldsymbol{W}$ is determined by the combining scheme used and we consider two well known receiver structures, namely ZF and MMSE. With ZF combining, the weight matrix is obtained from the pseudo-inverse of $\boldsymbol{H}$ as $\boldsymbol{W} = \boldsymbol{H}(\boldsymbol{H}^H\boldsymbol{H})^{-1}$, and the output SNR for BS1 can be obtained as

$$\gamma_{R_{ZF,1}} = \frac{1}{N_0 \left[(\boldsymbol{H}^H\boldsymbol{H})^{-1}\right]_{11}} \tag{6.4}$$

where $[\boldsymbol{B}]_{11}$ denotes the $(1,1)^{\text{th}}$ element of matrix $\boldsymbol{B}$. For MMSE combining, the first column $\boldsymbol{w}_1$ of the weight matrix $\boldsymbol{W}$ is found using

$$\boldsymbol{w}_1 = \boldsymbol{R}^{-1}\boldsymbol{h}_1 \tag{6.5a}$$

$$\boldsymbol{R} = \boldsymbol{h}_2\boldsymbol{h}_2^H + N_0\boldsymbol{I}_{N_t}. \tag{6.5b}$$

The output SINR for BS1's signal is given by

$$\gamma_{R_{MMSE,1}} = \boldsymbol{h}_1^H\boldsymbol{R}^{-1}\boldsymbol{h}_1. \tag{6.6}$$

It is assumed that if the SNR/SINR of a user is above a predefined threshold γ_{TR}, the RS can successfully decode the user symbol. In the second time slot, the RS will perform one of the following tasks, depending on the received signal SNRs in the first time slot.

- If the RS is able to decode both user symbols successfully, it uses ZF precoding for second hop transmission. We refer to this mode as the ZF mode.

- If RS is able to decode only one user symbol, it uses a control channel to inform the other user that there will be no transmission intended for that user in the next time slot, and uses maximal ratio transmission (MRT) [8] to transmit the symbol of the decoded user. We refer to this mode as the MRT mode.

- If the RS is able to decode only one user's symbol, it has the option to transmit the decoded user's symbol with MRT using only $N_t - 1$ number of antennas (for analytical tractability, we assume that the relay will use a fixed antenna set without considering the channel quality for selecting $N_t - 1$ antennas) and half the transmit power. It can be shown that this option also results in the same SNR distribution for the decoded user as in the ZF transmission mode. We call this mode the power save (PS) mode. This mode is proposed as an analytically tractable alternative system model for the SRS since exact performance measures can be derived for the SRS using PS mode.

- If the RS is not able to decode either user's symbol, it will inform the MSs using control channels and the MSs will use only the direct signal from the BSs to decode the data.

In the ZF mode, the RS precoding matrix $\boldsymbol{T}$ is derived by normalizing the columns of the pseudo-inverse of the multiuser channel matrix $\boldsymbol{H}_R$ given by [9]

$$\boldsymbol{H}_R = [\boldsymbol{h}_{R1}\, \boldsymbol{h}_{R2}]^H \tag{6.7}$$

where $\boldsymbol{h}_{R1}$ and $\boldsymbol{h}_{R2}$ are the $N_t \times 1$ channel vectors from the RS to MS1 and MS2, respectively. The elements of $\boldsymbol{h}_{Ri}$, $i \in \{1, 2\}$ are distributed as $\mathcal{CN}(0, L_{Ri})$, $i \in \{1, 2\}$ and the variance L_{Ri} can be calculated using the free space path-loss model given in (6.2). The received signal at MS1 can be represented as

$$y_{\text{ZF}} = \boldsymbol{h}_{R1}^H \boldsymbol{t}_1 s_1 + n_2 \tag{6.8}$$

where $\boldsymbol{t}_1$ denotes the 1^{st} column of $\boldsymbol{T}$ and $n_2 \sim \mathcal{CN}(0, N_0)$ is the AWGN at MS1 in the second time slot.

In the MRT mode, the RS weight vector $\boldsymbol{t}_{\text{MRT}}$ for MS1 is computed as

$$\boldsymbol{t}_{\text{MRT}} = \frac{\boldsymbol{h}_{R1}}{||\boldsymbol{h}_{R1}||}. \tag{6.9}$$

The received signal at the MS1 in this mode can be given as

$$y_{\text{MRT}} = ||\boldsymbol{h}_{R1}||s_1 + n_2. \tag{6.10}$$

If the RS used the power save mode for the second hop transmission, the precoding vector at the RS is computed similar to the MRT mode using only $N_t - 1$ number of transmit antennas. For simplicity, we do not consider antenna selection at the RS in the analysis, and assume that the $N_t - 1$ antennas are predetermined for the PS mode irrespective of the channel quality. The received signal at MS1 in this mode can be given as

$$y_{\text{PS}} = \sqrt{\frac{1}{2}}||\boldsymbol{h}_{PS}||s_1 + n_2 \tag{6.11}$$

where $\boldsymbol{h}_{PS}$ is the $N_t - 1 \times 1$ channel vector from the $N_t - 1$ transmit antennas used at the RS to MS1. The elements of $\boldsymbol{h}_{PS}$ are distributed as $\mathcal{CN}(0, L_{R1})$.

The MSs use a diversity combining scheme to combine the signals they received in the first and second time slots before they decode the data symbols. In this chapter, we consider two diversity combiners at the MSs, namely selection combining (SC) [10, 11] and MMSE combining (optimum combining (OC)) [12].

6.3 Output SINR Analysis

In this section, we present the statistical properties of the SNRs and the SINRs at the RS and MS1. Without loss of generality, we assume that $N_0 = 1$.

6.3.1 SNR/SINR analysis at the relay

When a ZF receiver is used at the RS, the distribution of $\gamma_{R_{ZF,1}}$ can be found as [13]

$$f_{\gamma_{R_{ZF,1}}}(x) = \frac{x^{N_t-2}e^{-\frac{x}{L_1}}}{\Gamma(N_t-1)L_1^{N_t-1}} \tag{6.12}$$

which is a gamma distribution with $\Gamma(N_t - 1, L_1)$. The distribution of $\gamma_{R_{ZF,2}}$ can be found similarly.

To find the statistics of $\gamma_{R_{MMSE,1}}$, we use eigendecomposition of $\boldsymbol{R}^{-1}$ and rewrite $\gamma_{R_{MMSE,1}}$ as

$$\gamma_{R_{MMSE,1}} = \boldsymbol{h}_1^H \boldsymbol{U}\boldsymbol{\Lambda}^{-1}\boldsymbol{U}^{-1}\boldsymbol{h}_1 = \boldsymbol{\alpha}^H\boldsymbol{\Lambda}^{-1}\boldsymbol{\alpha} \tag{6.13}$$

where $\boldsymbol{\alpha} = \boldsymbol{U}^{-1}\boldsymbol{h}_1$, $\boldsymbol{U}$ is a unitary matrix, and $\boldsymbol{\Lambda}$ is a diagonal matrix of eigenvalues of $\boldsymbol{R}$. The matrix $\boldsymbol{R}$ has a special structure where it is an addition of a rank-1 matrix and a diagonal matrix. Therefore, the eigenvalues of $\boldsymbol{R}$ have a special structure where one eigenvalue is equal to $1 + ||\boldsymbol{h}_2||^2$ and the other $N_t - 1$ eigenvalues are equal to 1. Then $\gamma_{R_{MMSE,1}}$ can be given as

$$\gamma_{R_{MMSE,1}} = \frac{|\alpha_1|^2}{1 + ||\boldsymbol{h}_2||^2} + \underbrace{\sum_{k=2}^{N_t} |\alpha_k|^2}_{Z} \tag{6.14}$$

where α_k, $k \in \{1, 2, \cdots, N_t\}$ are the elements of $\boldsymbol{\alpha}$. Due to the fact that the product of a Gaussian random vector and a unitary matrix has statistics identical to the original Gaussian random vector, the elements in $\boldsymbol{\alpha}$ have identical statistics as the elements in $\boldsymbol{h}_1$. The CDF of $\gamma_{R_{MMSE,1}}$ can be derived as

$$F_{\gamma_{R_{MMSE,1}}}(x) = F_Z(x) - \left[\frac{L_1 e^{\frac{-x}{L_1}} x^{N_t - 1}}{L_2^{N_t} \left(\frac{L_1}{L_2} + x\right)^{N_t} \Gamma(N_t)} \times {}_2F_1\left(N_t, N_t - 1; N_t; \frac{x}{\frac{L_1}{L_2} + x}\right) \right] \tag{6.15}$$

where Z is chi-square distributed with $2N_t - 2$ degrees of freedom and ${}_2F_1(a, b; c; z)$ is the Gauss hypergeometric function. A similar expression can be derived for the SINR of BS2 by interchanging the values of L_1 and L_2. The derivation of (6.15) is presented in Appendix 6.A.

6.3.2 SNR/SINR analysis at the MS

We first consider the case when the MS is using selection diversity combining on the received signals in two time slots. The MS selects the signal with the largest SNR or SINR for data detection. The SNR/SINR at the MS after combining can be found as

$$\gamma_{MS,SC} = \text{max.}(\gamma_{SD}, \gamma_{RD}) \tag{6.16}$$

where γ_{SD} is the SINR of the signal received in the first time slot and γ_{RD} is the SNR of the signal received in the second time slot. The SINR γ_{SD} can be found as

$$\gamma_{SD} = \frac{|g_{1,1}|^2}{1 + |g_{2,1}|^2} \tag{6.17}$$

and the CDF and PDF of γ_{SD} are given by

$$F_{\gamma_{SD}}(x) = 1 - \left(\frac{\Upsilon}{x+\Upsilon}\right)\exp\left(\frac{-x}{L_{g1,1}}\right) \tag{6.18a}$$

$$f_{\gamma_{SD}}(x) = \left[\frac{\Upsilon}{(x+\Upsilon)^2} + \frac{1}{L_{g1,1}}\left(\frac{\Upsilon}{x+\Upsilon}\right)\right]\exp\left(\frac{-x}{L_{g1,1}}\right) \tag{6.18b}$$

where $\Upsilon = \frac{L_{g1,1}}{L_{g2,1}}$. The distribution of γ_{RD} depends on the transmit mode used by the RS and we give the CDF of γ_{RD} for each mode.

- If the RS used the ZF mode, $\gamma_{RD,ZF} = \frac{||\boldsymbol{h}_{R1}\boldsymbol{t}_1||^2}{2}$, and it follows a Gamma distribution $\Gamma(k_{ZF}, \theta_{ZF})$ with $k_{ZF} = N_t - 1$ and $\theta_{ZF} = \frac{L_{R1}}{2}$ [9].
- If the RS used the MRT mode, $\gamma_{RD,MRT} = ||\boldsymbol{h}_{R1}||^2$ and the distribution can be found as $\Gamma(k_{MRT}, \theta_{MRT})$ with $k_{MRT} = N_t$ and $\theta_{MRT} = L_{R1}$.
- If the RS used the power save mode, since $N_t - 1$ number of antennas are selected without considering the channel quality, $\gamma_{RD,PS}$ is distributed as $\Gamma(k_{PS}, \theta_{PS})$ with $k_{PS} = N_t - 1$ and $\theta_{PS} = \frac{L_{R1}}{2}$ which is identical to the ZF mode.

Next, we consider the case when the MS uses MMSE combining on the received signals. To perform MMSE combining, the MS requires knowledge of the channel coefficients of the direct links from its BS and the interfering BS. In order to conduct the output SINR analysis, we first write the received signals using vector notations

$$\boldsymbol{y} = \boldsymbol{h}s_1 + \boldsymbol{h}_I s_2 + \boldsymbol{n} \tag{6.19}$$

where $\boldsymbol{h} = \left[||\boldsymbol{h}_{\text{eff}}||^2 \; g_{1,1}\right]^T$, $||\boldsymbol{h}_{\text{eff}}||^2$ is the effective channel from the RS to the MS, $\boldsymbol{h}_I = [0 \; g_{2,1}]^T$ and $\boldsymbol{n} = [n_1 \; n_2]^T$. The received signal vector is multiplied by the weight vector $\boldsymbol{w}_M$, which is computed as

$$\boldsymbol{w}_M = \boldsymbol{R}_M^{-1}\boldsymbol{h}_M \tag{6.20}$$

where $\boldsymbol{h}_M = \left[1 \; g_{1,1}^*\right]^H$ and $\boldsymbol{R}_M = \boldsymbol{h}_I\boldsymbol{h}_I^H + \boldsymbol{I}_2$. The matrix $\boldsymbol{R}_M$ is diagonal and the SINR at the MS can be represented as

$$\gamma_{MS,OC} = \boldsymbol{h}^H\boldsymbol{w}_M = \underbrace{\frac{|g_{1,1}|^2}{1+|g_{2,1}|^2}}_{\gamma_{SD}} + \underbrace{||\boldsymbol{h}_{\text{eff}}||^2}_{\gamma_{RD}}. \tag{6.21}$$

It is cumbersome to derive the CDF of $\gamma_{MS,OC}$ for arbitrary values of N_t and L_{R1}. Therefore, we only consider a special case where the RS uses the power save mode and $L_{g1,1} = L_{R1}/2$. The CDF of $\gamma_{MS,OC}$ can be found as

$$F_{\gamma_{MS,OC}}(x) = F_{\gamma_{RD}}(x) + \frac{L_{g1,1}\exp\left(\frac{-x}{L_{g1,1}}\right) x^{N_t-1}}{L_{g2,1}\Gamma(N_t)\left(\frac{L_{R1}}{2}\right)^{N_t-1}} \left[-\left(\frac{L_{g1,1}}{L_{g2,1}} + x\right)\right]^{-1} {}_2F_1\left(1, N_t-1; N_t; \frac{x}{\Upsilon + x}\right) \quad (6.22)$$

with γ_{RD} distributed as $\Gamma(k_{PS}, \theta_{PS})$. The derivation of (6.22) is similar to (6.15), and hence is omitted.

6.4 Outage Probability Analysis

In this section, we provide an outage probability analysis for the SRS. The outage probability is defined as the probability of the output SINR, γ_{MS}, dropping below a predefined threshold value, γ_{TM}.

6.4.1 Selection combining at the MS

With SC at the MS, the outage probability is given by

$$P_{\text{MS}}^{\text{SC}} = \Pr\left(\text{max.}(\gamma_{SD}, \gamma_{RD}) < \gamma_{TM}\right). \quad (6.23)$$

Since the distribution of γ_{RD} depends on the transmit mode used at the relay, we use the total probability theorem to derive an expression for the system outage probability, namely

$$\begin{aligned} P_{\text{ZF-SC}} = {} & [\Pr(\gamma_{R_1} < \gamma_{TR}) \times \Pr(\gamma_{SD} < \gamma_{TM})] \\ & + [\Pr(\gamma_{R_1} > \gamma_{TR} \,\text{and}\, \gamma_{R_2} > \gamma_{TR}) \Pr\left(\text{max.}(\gamma_{SD}, \gamma_{RD,ZF}) < \gamma_{TM}\right)] \\ & + [\Pr(\gamma_{R_1} > \gamma_{TR} \,\text{and}\, \gamma_{R_2} < \gamma_{TR}) \Pr\left(\text{max.}(\gamma_{SD}, \gamma_{RD}) < \gamma_{TM}\right)]. \end{aligned} \quad (6.24)$$

If the relay uses the power save mode for transmission when it decodes only one BS's signal in the first time slot, the distributions of $\gamma_{RD,ZF}$ and $\gamma_{RD,PS}$ are identical. Therefore, whenever the RS decodes BS1's signal correctly, γ_{RD} follows a

Gamma distribution $\Gamma(k_{ZF}, \theta_{ZF})$. Then the system outage probability for the power save mode can be simplified to

$$P_{\text{ZF-SC}}^{\text{PS}} = [\Pr(\gamma_{R_1} < \gamma_{TR}) \times F_{\gamma_{SD}}(\gamma_{TM})] + \left[\Pr(\gamma_{R_1} > \gamma_{TR}) \times F_{\gamma_{SD}}(\gamma_{TM}) F_{\gamma_{RD,ZF}}(\gamma_{TM})\right]. \quad (6.25)$$

For the case when ZF reception is used at the RS in the first time slot, $\gamma_{R_1} = \gamma_{R_{ZF,1}}$ and

$$\Pr(\gamma_{R_{ZF,1}} < \gamma_{TR}) = 1 - \exp\left(\frac{-\gamma_{TR}}{L_1}\right) \sum_{k=0}^{N_t-2} \frac{\gamma_{TR}^k}{k! L_1^k}. \quad (6.26)$$

An exact closed-form expression for the system outage probability can be derived as

$$\begin{aligned} P_{\text{ZF-SC}}^{\text{PS}} = & \left[\left(1 - \exp\left(\frac{-\gamma_{TR}}{L_1}\right) \sum_{k=0}^{N_t-2} \frac{\gamma_{TR}^k}{k! L_1^k}\right)\left(1 - \left(\frac{\Upsilon}{\gamma_{TM} + \Upsilon}\right) \exp\left(\frac{-\gamma_{TM}}{L_{g1}}\right)\right)\right] \\ & + \left[\left(\exp\left(\frac{-\gamma_{TR}}{L_1}\right) \sum_{k=0}^{N_t-2} \frac{\gamma_{TR}^k}{k! L_1^k}\right)\left(1 - \left(\frac{\Upsilon}{\gamma_{TM} + \Upsilon}\right) \exp\left(\frac{-\gamma_{TM}}{L_{g1}}\right)\right)\right. \\ & \left. \times \left(1 - \exp\left(\frac{-\gamma_{TM}}{\theta_{ZF}}\right) \sum_{k=0}^{N_t-2} \frac{\gamma_{TM}^k}{k! \theta_{ZF}^k}\right)\right]. \quad (6.27) \end{aligned}$$

When MMSE reception is used at the RS, $\Pr(\gamma_{R_1} < \gamma_{TR}) = F_{\gamma_{R_{MMSE,1}}}(\gamma_{TR})$, and the outage probability with the power save mode can be found similarly.

If the RS uses the MRT mode when it successfully decodes only one BS's symbol, the outage probability with SC at the MS can be given as

$$\begin{aligned} P_{\text{ZF-SC}}^{\text{MRT}} = & [\Pr(\gamma_{R_1} < \gamma_{TR}) \times F_{\gamma_{SD}}(\gamma_{TM})] \\ & + \left[\Pr(\gamma_{R_1} > \gamma_{TR} \text{ and } \gamma_{R_2} > \gamma_{TR}) F_{\gamma_{SD}}(\gamma_{TM}) F_{\gamma_{RD,ZF}}(\gamma_{TM})\right] \\ & + \left[\Pr(\gamma_{R_1} > \gamma_{TR} \text{ and} \gamma_{R_2} < \gamma_{TR}) \times F_{\gamma_{SD}}(\gamma_{TM}) F_{\gamma_{RD,MRT}}(\gamma_{TM})\right]. \quad (6.28) \end{aligned}$$

In general, the events $(\gamma_{R_1} > \gamma_{TR})$ and $(\gamma_{R_2} > \gamma_{TR})$ are not independent. This makes deriving an exact closed-form expression for the outage probability intractable for a general case. However, assuming independence between these events, we derive an approximation which closely estimates the precise outage probability obtained using simulations. The approximate system outage probability for the MRT

mode can be found by substituting

$$\Pr(\gamma_{R_1} > \gamma_{TR} \text{ and } \gamma_{R_2} > \gamma_{TR}) = (1 - F_{\gamma_{R_1}}(\gamma_{TR}))(1 - F_{\gamma_{R_2}}(\gamma_{TR})) \quad (6.29a)$$

$$\Pr(\gamma_{R_1} > \gamma_{TR} \text{ and } \gamma_{R_2} < \gamma_{TR}) = (1 - F_{\gamma_{R_1}}(\gamma_{TR}))(F_{\gamma_{R_2}}(\gamma_{TR})) \quad (6.29b)$$

into (6.28).

6.4.2 Optimum combining at the MS

With OC at the MS, the outage probability is given by

$$P_{\text{MS}}^{\text{OC}} = \Pr\left(\gamma_{SD} + \gamma_{RD} < \gamma_{TM}\right). \quad (6.30)$$

Applying the total probability theorem, the outage probability for the power save mode is computed using

$$P_{\text{MMSE-OC}}^{\text{PS}} = \left[\Pr(\gamma_{R_1} < \gamma_{TR}) \times F_{\gamma_{SD}}(\gamma_{TM})\right] + \left[\Pr(\gamma_{R_1} > \gamma_{TR}) \times F_{\gamma_{MS,OC}}(\gamma_{TM})\right]. \quad (6.31)$$

6.4.3 Asymptotic outage probability

The closed-form expressions derived for the outage probability are useful for numerical computations. However, they may not provide direct insights such as diversity gain and array gain of the system. Therefore, in this section, we derive outage probability expressions for the asymptotically high-SNR regime and identify the diversity and array gains of the SRS. For simplicity, We assume $L_2 = \kappa L_1$, $L_{g1,1} = \eta L_1$, $L_{g2,1} = \zeta L_1$, $L_{R1} = \tau L_1$ and let $L_1 \to \infty$. The asymptotic outage probability for the SRS when ZF is used at the relay and SC is used at the destination can be found as

$$P_{\text{ZF-SC}}^{\infty} = \frac{\gamma_{TR}^{N_t-1}}{\Gamma(N_t)\left(1 + \frac{\eta}{\zeta\gamma_{TD}}\right) L_1^{N_t-1}} + \frac{\gamma_{TD}^{N_t-1}}{\Gamma(N_t)\left(1 + \frac{\eta}{\zeta\gamma_{TD}}\right)\left(\frac{\tau L_1}{2}\right)^{N_t-1}} + \mathcal{O}\left(L_1^{-N_t}\right) \quad (6.32)$$

where $\mathcal{O}(L_1^{-N_t})$ denotes the terms where the exponent of L_1 is smaller than $N_t - 1$. The asymptotic outage probability for the PS mode is shown to be exactly the same as (6.32). The proof is given in Appendix 6.B.

The asymptotic outage probability for the SRS when MMSE is used at the relay and SC is used at the destination can be found as

$$P_{\text{MMSE-SC}}^{\infty} = \frac{\gamma_{TR}^{N_t-1}}{\left(1+\frac{\eta}{\zeta\gamma_{TD}}\right)\Gamma(N_t)L_1^{N_t-1}}\left[1-\frac{\frac{1}{\kappa}}{\left(\gamma_{TR}+\frac{1}{\kappa}\right)}\right] + \frac{\gamma_{TD}^{N_t-1}}{\Gamma(N_t)\left(1+\frac{\eta}{\zeta\gamma_{TD}}\right)\left(\frac{\tau L_1}{2}\right)^{N_t-1}} + \mathcal{O}\left(L_1^{-N_t}\right). \quad (6.33)$$

The proof is shown in Appendix 6.B.

The asymptotic outage probability for the SRS when ZF is used at the relay and OC is used at the destination can be found as

$$P_{\text{ZF-OC}}^{\infty} = \frac{\gamma_{TR}^{N_t-1}}{\Gamma(N_t)\left(1+\frac{\eta}{\zeta\gamma_{TD}}\right)L_1^{N_t-1}} + \frac{\gamma_{TD}^{N_t-1}}{\Gamma(N_t)\left(\frac{\tau L_1}{2}\right)^{N_t-1}} - \frac{\eta\gamma_{TD}^{N_t-1}V}{\zeta\Gamma(N_t)\left(\frac{\tau L_1}{2}\right)^{N_t-1}\left(\gamma_{TD}+\frac{\eta}{\zeta}\right)} + \mathcal{O}\left(L_1^{-N_t}\right) \quad (6.34)$$

where

$$V = -\frac{(N_t-1)}{\left(\frac{\gamma_{TD}}{\gamma_{TD}+\frac{\eta}{\zeta}}\right)^{N_t-1}}\left(\log\left(1-\frac{\gamma_{TD}}{\gamma_{TD}+\frac{\eta}{\zeta}}\right)\right).$$

The proof is given in Appendix 6.B.

The asymptotic outage probability for the case when MMSE is used at the relay and OC is used at the destination can be deduced as

$$P_{\text{MMSE-OC}}^{\infty} = \frac{\gamma_{TR}^{N_t-1}}{\left(1+\frac{\eta}{\zeta\gamma_{TD}}\right)\Gamma(N_t)L_1^{N_t-1}}\left[1-\frac{\frac{1}{\kappa}}{\left(\gamma_{TR}+\frac{1}{\kappa}\right)}\right] + \frac{\gamma_{TD}^{N_t-1}}{\Gamma(N_t)\left(\frac{\tau L_1}{2}\right)^{N_t-1}} - \frac{\eta\gamma_{TD}^{N_t-1}V}{\zeta\Gamma(N_t)\left(\frac{\tau L_1}{2}\right)^{N_t-1}\left(\gamma_{TD}+\frac{\eta}{\zeta}\right)} + \mathcal{O}\left(L_1^{-N_t}\right). \quad (6.35)$$

It can be identified from the asymptotic outage probability expressions that the SRS has diversity order of $N_t - 1$.

6.5 Ergodic Rate Analysis

In this section, we provide a closed-form expression for the ergodic rate of the SRS, when SC is used at the MSs. A simple upper bound based on the commonly used Jensen's inequality is derived for the case when OC is used at the MSs. The ergodic rate of a wireless communications system with SNR/SINR γ is given by

$$C = \frac{1}{2}\mathbb{E}_{\gamma}\log_2(1+\gamma) = \frac{1}{2}\int_0^{\infty} \log_2(1+\gamma) f_{\gamma}(\gamma) d\gamma. \tag{6.36}$$

Changing the base of the logarithm to the natural logarithm, and applying integration by parts, one can rewrite (6.36) in terms of the CDF of γ as [14]

$$C = \frac{1}{2}\int_0^{\infty} \frac{1 - F_{\gamma}(x)}{(1+x)} dx. \tag{6.37}$$

The factor $\frac{1}{2}$ comes from the half-duplex operation of the relay.

6.5.1 Selection combining at the MS

Applying the total probability theorem, the ergodic rate for the system when the power save mode is used at the RS can be evaluated from

$$C_{PS,SC} = \left[\Pr(\gamma_{R_1} > \gamma_{TR}) \underbrace{\frac{1}{2}\int_0^{\infty} \frac{1 - F_{\gamma_{SD}}(x) F_{\gamma_{RD,ZF}}(x)}{1+x} dx}_{\mathcal{I}_1(\theta_{ZF}, N_t - 2)} \right] + \left[\Pr(\gamma_{R_1} < \gamma_{TR}) \underbrace{\frac{1}{2}\int_0^{\infty} \frac{1 - F_{\gamma_{SD}}(x)}{1+x} dx}_{\mathcal{I}_2} \right]. \tag{6.38}$$

The solutions for the integrals $\mathcal{I}_1$ and $\mathcal{I}_2$ are provided in Appendix 6.C. Similarly, the approximate ergodic rate with SC when the PS mode is not used at the relay, can be found as

$$\begin{aligned} C_{MRT,SC} &= (1 - F_{\gamma_{R_1}}(\gamma_{TR}))(1 - F_{\gamma_{R_2}}(\gamma_{TR}))\mathcal{I}_1(\theta_{ZF}, N_t - 2) \\ &\quad + (1 - F_{\gamma_{R_1}}(\gamma_{TR}))(F_{\gamma_{R_2}}(\gamma_{TR}))\mathcal{I}_1(\theta_{MRT}, N_t - 1) + (F_{\gamma_{R_1}}(\gamma_{TR}))\mathcal{I}_2. \end{aligned} \tag{6.39}$$

In the high SNR regime, the ergodic rate is given by

$$C^{\infty} \approx \frac{1}{2}\left[\frac{\gamma_{TR}^{N_t-1}\left(-\frac{\frac{\eta}{\zeta}}{1-\frac{\eta}{\zeta}}\log(\frac{\eta}{\zeta})\right)}{\Gamma(N_t)L_1^{N_t-1}} + \log\left(\frac{\tau L_1}{2}\right) + \psi_0(N_t-1)\right] \tag{6.40}$$

where $\psi_0()$ is the psi function [15, 8.360]. The derivation is explained in Appendix 6.D. From (6.40), it can be observed that the ergodic rate grows linearly in the high SNR regime.

6.5.2 Optimum combining at the MS

Due to the complicated form of the CDF of $\gamma_{MS,OC}$, derivation of an exact expression for the ergodic rate when OC is used at the MSs is intractable. Instead, we apply a commonly used upper bound on the ergodic rate based on Jensen's inequality, namely

$$C_{OC} = \frac{1}{2}\mathbb{E}\left[\log_2\left(1+\gamma_{MS,OC}\right)\right] \leq \frac{1}{2}\log_2\left(1+\mathbb{E}[\gamma_{MS,OC}]\right). \tag{6.41a}$$

Since $\gamma_{MS,OC} = \gamma_{SD} + \gamma_{RD}$,

$$\mathbb{E}[\gamma_{MS,OC}] = \mathbb{E}[\gamma_{SD}] + \mathbb{E}[\gamma_{RD}] \tag{6.41b}$$

where

$$\mathbb{E}[\gamma_{SD}] = \Upsilon\exp\left(\frac{\Upsilon}{L_{g1,1}}\right)\boldsymbol{E}_1\left(\frac{\Upsilon}{L_{g1}}\right) \tag{6.41c}$$

and

$$\mathbb{E}[\gamma_{RD}] = \frac{(N_t-1)L_{R1}}{2}. \tag{6.41d}$$

The ergodic rate upper bound for the system with power save mode is computed using

$$C_{PS,OC} \leq [\Pr(\gamma_{R_1} > \gamma_{TR})\log_2\left(1+\mathbb{E}[\gamma_{MS,OC}]\right)] + [\Pr(\gamma_{R_1} < \gamma_{TR})\log_2\left(1+\mathbb{E}[\gamma_{SD}]\right)]. \tag{6.42}$$

6.6 Impact of Finite Rate CSI Feedback

In a frequency division duplex (FDD) system, downlink channel conditions may be significantly different from uplink channel conditions. Therefore, in order to obtain

CSI of the RS-MS links at the RS, the RS must rely on the feedback it receives from the MSs. In this section, we have relaxed the assumption of the availability of perfect CSI of the RS-MS channels at the RS, due to imperfections in the feedback channel. It is assumed that the MSs estimate their own RS-MS channel and feed back the channel direction information (CDI) given by $\boldsymbol{h}_{R1}/||\boldsymbol{h}_{R1}||$ and $\boldsymbol{h}_{R2}/||\boldsymbol{h}_{R2}||$ to the RS. Before sending back, the MSs quantize the CDI using distinct codebooks $\mathcal{C}_{MS1} = \{\boldsymbol{c}_{1,1}, \cdots, \boldsymbol{c}_{1,2^B}\}$ and $\mathcal{C}_{MS2} = \{\boldsymbol{c}_{2,1}, \cdots, \boldsymbol{c}_{2,2^B}\}$. Codebooks consist of 2^B number of N_t-dimensional unit norm vectors, where B is the number of feedback bits used. For simplicity, we assume random vector quantization is used to generate the codebooks [16]. The index of the codeword for the k^{th} MS is selected according to

$$n_k = \underset{1 \leq j \leq 2^B}{\arg\max} |\boldsymbol{h}_{Rk}^H \boldsymbol{c}_{k,j}| \tag{6.43}$$

and the indices are fed back to the RS. The RS compiles the estimate of the multiuser channel as

$$\hat{\boldsymbol{H}} = [\hat{\boldsymbol{h}}_{R1} \hat{\boldsymbol{h}}_{R2}] = [\boldsymbol{c}_{1,n_1} \boldsymbol{c}_{1,n_2}]. \tag{6.44}$$

In the MRT mode, the weight vector is given by $\hat{\boldsymbol{h}}_{Rk}$, while in the ZF mode, the precoding vector $\boldsymbol{v}_k$ for the k^{th} user is found by normalizing the k^{th} column of the pseudo-inverse of $\hat{\boldsymbol{H}}$.

6.6.1 Output SINR analysis

In this section, we present the statistics of the e2e SNR/SINR at MS1 when finite rate feedback is used. The SNR at the MS1 for the second hop reception when the MRT mode is used by the RS can be given as

$$\gamma_{MRT,q} = |\boldsymbol{h}_{R1} \hat{\boldsymbol{h}}_{R1}|^2. \tag{6.45}$$

The exact statistics of $\gamma_{MRT,q}$ are complicated. Therefore, we use a tight approximation proposed in [16],

$$\gamma_{MRT,q} \approx ||\boldsymbol{h}_{R1}||^2 \left(1 - 2^{-\frac{B}{N_t - 1}}\right). \tag{6.46}$$

The approximate distribution of $\gamma_{MRT,q}$ can be found as $\Gamma\left(k_{MRT,q}, \theta_{MRT,q}\right)$ with $k_{MRT,q} = N_t$ and $\theta_{MRT,q} = L_{R1}\left(1 - 2^{-\frac{B}{N_t - 1}}\right)$.

If the RS uses the ZF mode for the second hop transmission, the inter-user interference is not fully eliminated due to the finite rate feedback. The MSs are not aware of this additional interference and treat it as additional noise. The SINR at the MS1 for the second hop reception in the ZF mode can be found as

$$\gamma_{ZF,q} = \frac{\frac{1}{2}|\boldsymbol{h}_{R1}^H \boldsymbol{v}_1|^2}{1 + \frac{1}{2}|\boldsymbol{h}_{R1}\boldsymbol{v}_2|^2}. \tag{6.47}$$

The desired signal term is chi-square distributed with $2N_t - 2$ degrees of freedom [17], while the noise-plus-interference term is assumed to be a zero mean complex Gaussian RV with variance $1 + \sigma_I^2$, where σ_I^2 can be computed for the case when $N_t = 2$ as [16]

$$\begin{aligned}\sigma_I^2 &= \frac{1}{2}\mathbb{E}[|\boldsymbol{h}_{R1}\boldsymbol{v}_2|^2| = \frac{L_{R1}}{2}\mathbb{E}[||\boldsymbol{h}_{R1}||^2]\mathbb{E}\left[\left|\frac{\boldsymbol{h}_{R1}}{||\boldsymbol{h}_{R1}||}\boldsymbol{v}_2\right|^2\right] \\ &= L_{R1}2^B\beta\left(2^B, \frac{N_t}{N_t - 1}\right).\end{aligned} \tag{6.48}$$

For other values of N_t, reference [17] proposed the approximation $\sigma_I^2 \approx 2^{-\frac{B}{N_t-1}}$. Then the SINR $\gamma_{ZF,q}$ is distributed as $\Gamma\left(k_{ZF,q}\theta_{ZF,q}\right)$ with $k_{ZF,q} = N_t - 1$ and $\theta_{ZF,q} = \frac{L_{R1}}{2(1+\sigma_I^2)}$.

6.6.2 Ergodic rate analysis

Following similar steps as employed in Section V-A, the ergodic rate with SC at the MSs can be found as

$$\begin{aligned}C_{SC,q} = (1 - F_{\gamma_{R_1}}(\gamma_{TR}))(1 - F_{\gamma_{R_2}}(\gamma_{TR}))\mathcal{I}_1(\theta_{ZF,q}, N_t - 2) \\ + (1 - F_{\gamma_{R_1}}(\gamma_{TR}))(F_{\gamma_{R_2}}(\gamma_{TR}))\mathcal{I}_1(\theta_{MRT,q}, N_t - 1) \\ + (F_{\gamma_{R_1}}(\gamma_{TR}))\mathcal{I}_2.\end{aligned} \tag{6.49}$$

An upper bound for the ergodic rate when OC is used at the MSs can be found by replacing $\mathbb{E}[\gamma_{RD}]$ in (6.41b) with

$$\mathbb{E}[\gamma_{MRT,q}] = k_{MRT,q}\theta_{MRT,q} \tag{6.50}$$

or

$$\mathbb{E}[\gamma_{ZF,q}] = k_{ZF,q}\theta_{ZF,q} \tag{6.51}$$

accordingly.

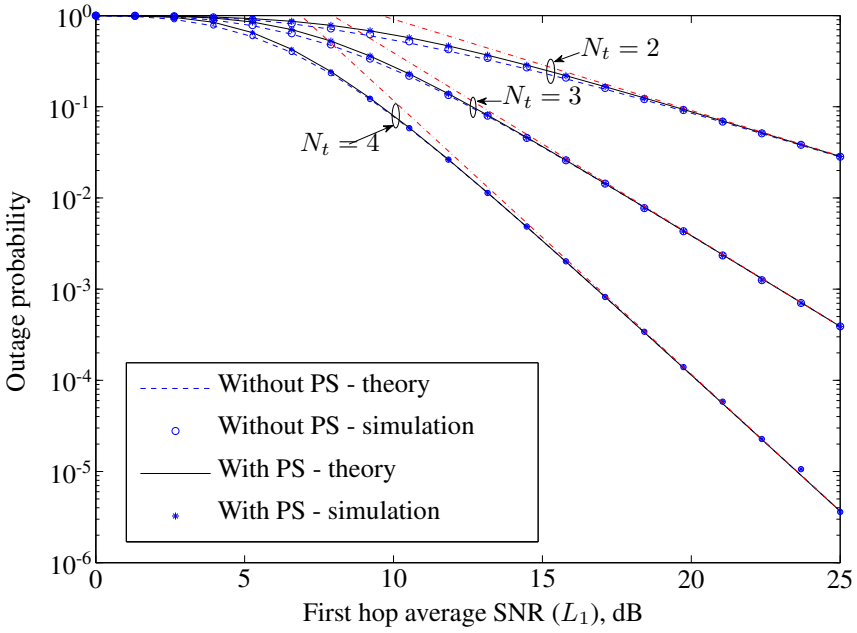

Figure 6.2: The outage probability of the system with ZF at the relay and SC at the destination.

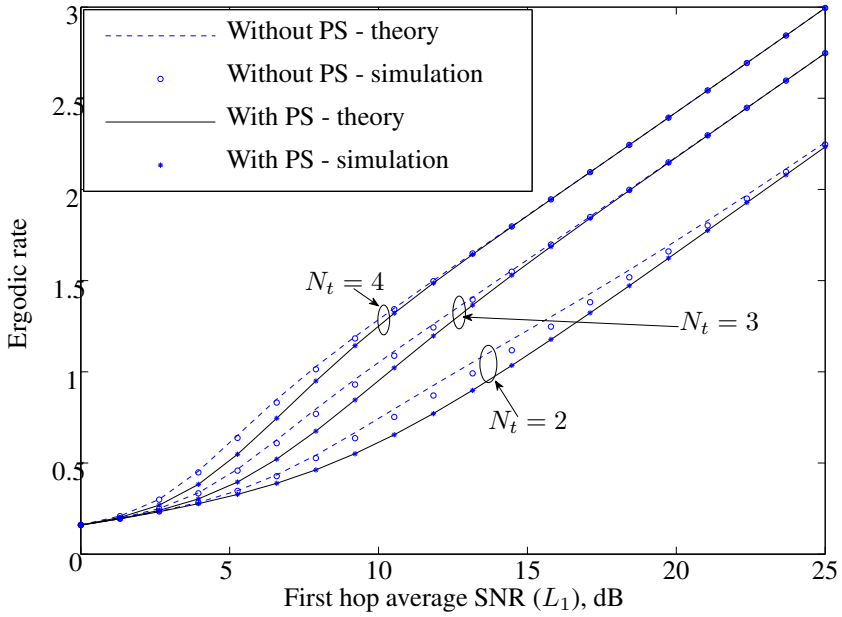

Figure 6.3: The ergodic rate with ZF at the relay and SC at the destination.

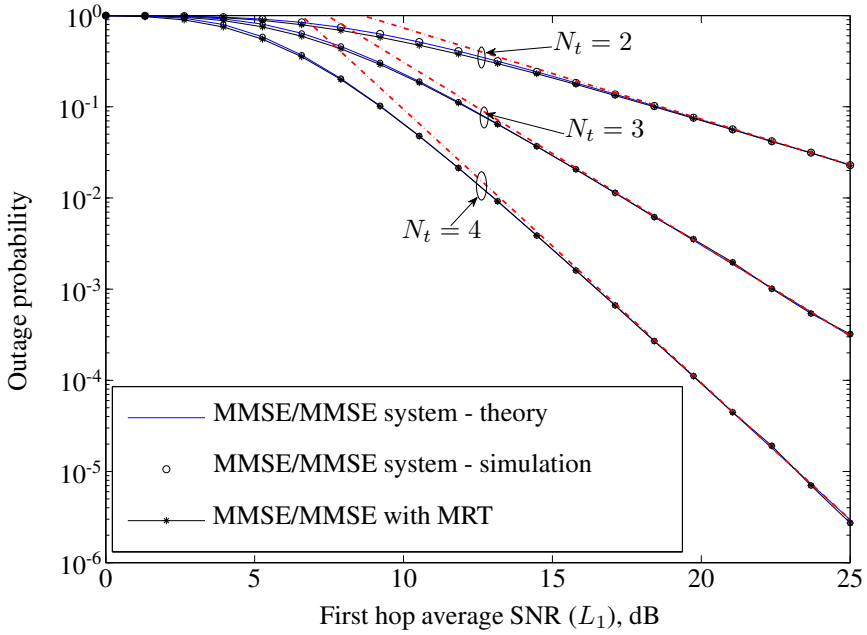

Figure 6.4: The outage probability of the system when MMSE is used at the relay and the destination.

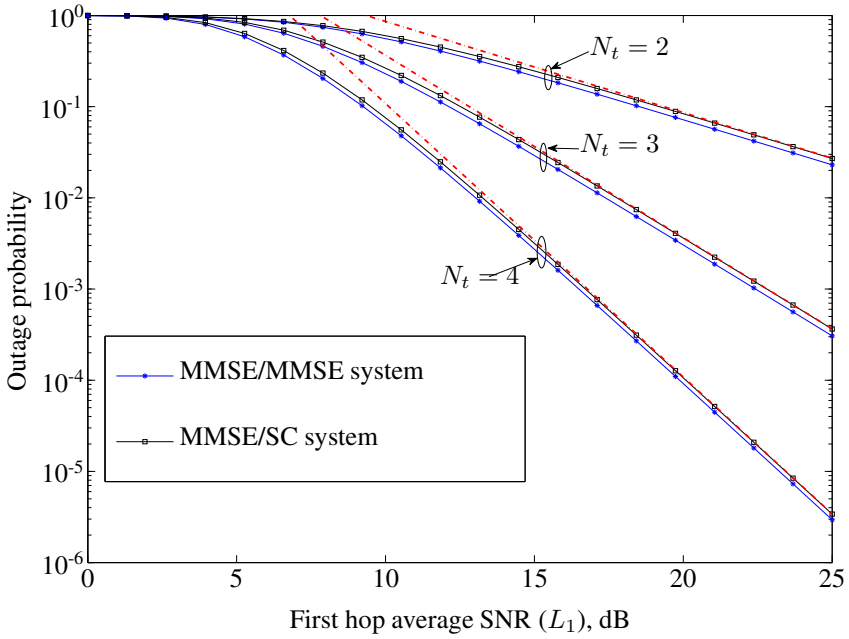

Figure 6.5: Outage probability comparisons for the MMSE/SC system with the MMSE/MMSE system.

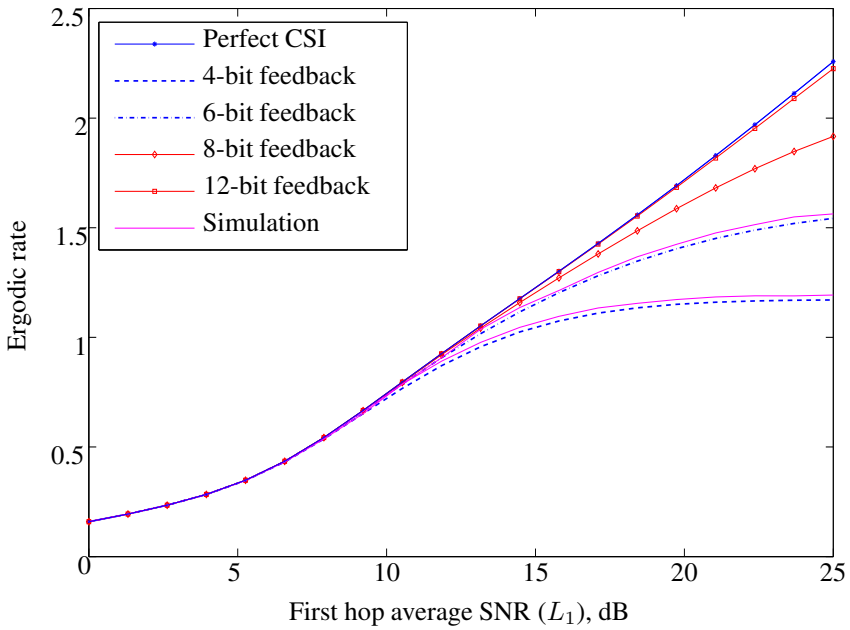

Figure 6.6: The ergodic rate with ZF at the relay and SC at the destination for different codebook sizes.

6.7 Numerical and Simulation Results

In this section, we present some numerical results obtained from the analyses presented in Sections IV and V. It is assumed that the RS is located at the intersection region of the two cells such that it is placed equidistant from the two BSs. Furthermore, we assume that the BSs use identical transmit powers, so $L_1 = L_2$. The system outage probabilities and the ergodic rates are calculated by varying the first hop (BS to RS) link average SNR. The RS to MS link average SNR $L_{R1} = \tau L_1$ and we assume $\tau = 1$ in our numerical results. Also, we set $L_{g1,1} = \frac{L_1}{2}$ and $L_{g2,1} = \frac{L_1}{5}$. The threshold SINR at the relay and the MSs is set to 10 dB.

Fig. 6.2 gives the outage probabilities of MS1 for different values of N_t when ZF reception is used at the RS and the MS uses SC. One can observe excellent agreement between the theoretical and simulation results for the PS mode, while the approximations derived for the system without the PS mode follow the simulation results extremely closely. When the BS to RS link average SNR increases the outage probability approaches the performance of the PS mode, since the common

transmit mode for both systems, the ZF mode, dominates the performance in the high-SNR regime. The asymptotic outage probabilities in the high SNR regime are shown using dotted lines in red color.

Fig. 6.3 shows the ergodic rate in nats per second per bandwidth unit for MS1. The theoretical values are in excellent agreement with the simulation results for the PS mode and the theoretical approximations for the MRT mode follow the simulation results with small discrepancy. Again, we observe that the rate gap between the PS mode and the MRT mode decreases with increasing SNR and with the number of antennas at the RS. This occurs due to the small probability of outage for both users in the first hop.

Fig. 6.4 shows the outage probability of MS1 when MMSE reception is used at both the RS and MS1. The theoretical results are in excellent agreement with the simulation results for the PS mode and can be used as accurate approximations to compute the outage probability with the MRT mode in the high SNR regime. The asymptotic outage probabilities in the high SNR regime are shown using dotted lines in red color.

Fig. 6.5 compares MS1's outage probability for the MMSE/MMSE system with the MMSE/SC system operating in the PS mode. The performance gain obtained by MMSE reception over the SC receiver at the MS decreases as N_t increases. For $N_t = 2$, the gain with MMSE reception at the MS is around 1.5 dB, while the gain drops to a fraction of a dB when $N_t = 4$. The asymptotic outage probabilities for the MMSE/SC system in the high SNR regime are shown using dotted lines in red color.

Fig. 6.6 shows the impact of finite rate feedback on the ergodic rate of MS1 when $N_t = 2$. Performance with different codebook sizes are compared with the case with perfect CSI at the RS. One can observe that 12-bit feedback will achieve ergodic rate performance close to the perfect CSI case. Our analysis tells the design engineer that resources will be wasted by implementing more than 12-bit feedback.

6.8 Conclusion

In this chapter, we presented an analysis of the downlink performance of a two-cell two-user SRS. Exact closed-form expressions were derived for the outage probability and the ergodic rate for any user when operating in the PS mode. Approximate expressions derived for the system without the PS mode can be used to estimate the performance metrics with high accuracy. Finally, we examined the feedback requirements for the RS-MS links and derived approximate expressions for the ergodic rate when finite rate feedback is used for the RS-MS links.

6.A The Derivation of (6.15)

In this appendix, we outline the derivation of (6.15). One has

$$\begin{aligned} F_{\gamma_{R_{MMSE,1}}}(x) &= \Pr\left(\gamma_{R_{MMSE,1}} \leq x\right) = \Pr\left(\frac{|\alpha_1|^2}{1+||\boldsymbol{h}_2||^2} + Z \leq x\right) \\ &= \Pr\left(|\alpha_1|^2 \leq (x-Z)(1+||\boldsymbol{h}_2||^2)\right) \\ &= \int_0^x \int_0^\infty F_{|\alpha_1|^2}\left((x-Z)(1+Y)\right) f_{||\boldsymbol{h}_2||^2}(Y) f_Z(Z) dY dZ. \quad (6.52) \end{aligned}$$

The RV $|\alpha_1|^2$ is exponentially distributed and $||\boldsymbol{h}_2||^2$ is chi-square distributed. Then the double integral in (6.52) is solved using the identities [15, eq. 3.35.3] and [18, 1.2.4.3].

6.B The Derivations of Asymptotic Outage Probability Expressions

In this appendix, we present the derivations of asymptotic outage probability expressions given in (6.32), (6.33) and (6.34). When $L_1 \to \infty$, we apply the Taylor series expansions of the PDFs of $\gamma_{R_{ZF,1}}$, γ_{SD}, $\gamma_{RD,ZF}$ and $\gamma_{RD,MRT}$ and obtain their respective CDFs as

$$F^{\infty}_{\gamma_{R_{ZF,1}}}(x) \approx \frac{x^{N_t-1}}{\Gamma(N_t) L_1^{N_t-1}}, \quad F^{\infty}_{\gamma_{SD}}(x) \approx \frac{\Upsilon}{x+\Upsilon}$$

$$F^{\infty}_{\gamma_{R_{RD,ZF}}}(x) \approx \frac{x^{N_t-1}}{\Gamma(N_t)\left(\frac{L_{R1}}{2}\right)^{N_t-1}},$$
$$F^{\infty}_{\gamma_{RD,MRT}}(x) \approx \frac{x^{N_t}}{\Gamma(N_t+1)L_{R1}^{N_t}}.$$

Then we substitute the respective CDFs in (6.24) and considering only the terms with the largest exponent of L_1, we obtain (6.32). One can observe that substituting the relevant CDFs in (6.25) and considering only the terms with the largest exponent of L_1, the PS mode results in the identical asymptotic outage probability expression as the system without the PS mode.

Using the series representation of the hypergeometric function and the exponential function and considering only the terms with the largest exponent of L_1, the CDF of $\gamma_{R_{MMSE,1}}$ is approximated as

$$F_{\gamma_{R_{MMSE,1}}}(x) \approx \frac{x^{N_t-1}}{\Gamma(N_t)L_1^{N_t-1}}\left[1-\frac{1}{\left(x+\frac{1}{\kappa}\right)\kappa}\right]. \tag{6.53}$$

Then the asymptotic outage probability of the system can be found as (6.33).

When OC is used at the destination, the high SNR CDF of $\gamma_{MS,OC}$ is obtained using the Taylor series expansion for the exponential function and the alternative representation for the hypergeometric function given in [19],

$$F_{\gamma_{MS,OC}}(x) \approx \frac{x^{N_t-1}}{\Gamma(N_t)\left(\frac{\tau L_1}{2}\right)^{N_t-1}} - \frac{\eta x^{N_t-1}V}{\zeta\Gamma(N_t)\left(\frac{\tau L_1}{2}\right)^{N_t-1}\left(x+\frac{\eta}{\zeta}\right)}. \tag{6.54}$$

6.C The Solutions for $\mathcal{I}_1$ and $\mathcal{I}_2$

In this appendix, we present the solutions for the integrals $\mathcal{I}_1$ and $\mathcal{I}_2$, used in (6.38). One has

$$\mathcal{I}_1 = \frac{1}{2}\int_0^{\infty}\left(1-\left[1-\exp\left(\frac{-x}{\theta_{ZF}}\right)\sum_{k=0}^{N_t-2}\frac{x^k}{k!\theta_{ZF}^k}\right]\right.$$
$$\left.\times\left[1-\left(\frac{\Upsilon}{x+\Upsilon}\right)\exp\left(\frac{-x}{L_{g1,1}}\right)\right]\right)\frac{1}{1+x}dx$$

$$\mathcal{I}_1 = \frac{1}{2}\int_0^{\infty} \underbrace{\frac{\exp\left(\frac{-x}{\theta_{ZF}}\right)\sum_{k=0}^{N_t-2}\frac{x^k}{k!\theta_{ZF}^k}}{1+x}}_{\mathcal{J}_1} + \underbrace{\frac{\left(\frac{\Upsilon}{x+\Upsilon}\right)\exp\left(\frac{-x}{L_{g1,1}}\right)}{1+x}}_{\mathcal{J}_2(L_{g1,1})} - \underbrace{\frac{\sum_{k=0}^{N_t-2}\frac{\Upsilon x^k}{k!\theta_{ZF}^k(x+\Upsilon)}\exp\left(-x\left(\frac{1}{L_{g1,1}}+\frac{1}{\theta_{ZF}}\right)\right)}{1+x}}_{\mathcal{J}_3} dx. \tag{6.55}$$

The integrals $\mathcal{J}_1$, $\mathcal{J}_2$ and $\mathcal{J}_3$ can be solved using [14, Lemma 3] and the result can be found as

$$\mathcal{J}_1 = e^{\frac{1}{\theta_{ZF}}}\boldsymbol{E}_1\left(\tfrac{1}{\theta_{ZF}}\right) + \sum_{k=1}^{N_t-2}\tfrac{1}{k!\theta_{ZF}^k}\left[\sum_{n=1}^{k}(n-1)!(-1)^{k-n}\theta_{ZF}^n - (-1)^{k-1}e^{\frac{1}{\theta_{ZF}}}\boldsymbol{E}_1\left(\frac{1}{\theta_{ZF}}\right)\right]$$

$$\mathcal{J}_2(L_{g1,1}) = \Upsilon\left[\frac{e^{\frac{\Upsilon}{L_{g1,1}}}\boldsymbol{E}_1\left(\frac{\Upsilon}{L_{g1,1}}\right)}{1-\Upsilon} + \frac{e^{\frac{1}{L_{g1,1}}}\boldsymbol{E}_1\left(\frac{1}{L_{g1,1}}\right)}{\Upsilon-1}\right]$$

$$\mathcal{J}_3 = \mathcal{J}_2(\mu) + \sum_{n=1}^{N-2}\left[\frac{e^{\mu\Upsilon}}{1-\Upsilon}\left((-\Upsilon)^n\boldsymbol{E}_1(\mu\Upsilon) + \sum_{p=1}^{n}\binom{n}{p}(-\Upsilon)^{n-p}e^{-\mu\Upsilon}\sum_{q=0}^{p-1}\frac{(p-1)!\Upsilon^q}{q!\mu^{p-q}}\right) + \frac{e^{\mu}}{\Upsilon-1}\left((-1)^n\boldsymbol{E}_1(\mu) + \sum_{p=1}^{n}\binom{n}{p}(-1)^{n-p}e^{-\mu}\sum_{q=0}^{p-1}\frac{(p-1)!}{q!\mu^{p-q}}\right)\right]$$

where $\mu = \frac{1}{\theta_{ZF}} + \frac{1}{L_{g1,1}}$ and $\boldsymbol{E}_1(x)$ is the exponential integral function of order 1. Also, one can observe that $\mathcal{I}_2 = \mathcal{J}_2(L_{g1,1})$.

6.D The Derivation of (6.40)

In the following, we present the derivation of (6.40). Substituting the relevant high SNR CDFs in (6.39) and assuming $\max(\gamma_{RD}, \gamma_{SD}) = \gamma_{RD}$ in the high SNR regime, the ergodic rate expression can be given as

$$C^{\infty} \approx \frac{\gamma_{TR}^{N_t-1}}{\Gamma(N_t)L_1^{N_t-1}}\mathcal{I}_2 + \frac{1}{2}\mathcal{J}_1. \tag{6.56}$$

Using the series representation of the $\boldsymbol{E}_1(\cdot)$ given in [20] and the asymptotic expansion of Ei function [21], and using some manipulations, $\mathcal{J}_1$ can be approximated as

$$\mathcal{J}_1 \approx \log\left(\frac{\tau L_1}{2}\right) + \psi_0(N_t - 1). \tag{6.57}$$

Applying the same expansions, $\mathcal{I}_2$ can be approximated as

$$\mathcal{I}_2 = -\frac{\Upsilon}{1-\Upsilon}\log(\Upsilon). \tag{6.58}$$

References

[1] M. K. Karakayali, G. J. Foschini, and R. A. Valenzuela, "Network coordination for spectrally efficient communications in cellular systems," *IEEE Wireless Commun.*, vol. 13, no. 4, pp. 56–61, 2006.

[2] S. W. Peters, A. Y. Panah, K. T. Truong, and R. W. Heath, "Relay architectures for 3GPP LTE-advanced," *EURASIP J. Wirel. Commun. Netw.*, vol. 2009, pp. 1:1–1:14, Mar. 2009.

[3] J.-W. Kwon, K.-H. Park, Y.-C. Ko, and H.-C. Yang, "Cooperative joint precoding in a downlink cellular system with shared relay: Design and performance evaluation," *IEEE Trans. Wireless Commun.*, vol. 11, no. 10, pp. 3462 –3473, Oct. 2012.

[4] Y. Lin and W. Yu, "Fair scheduling and resource allocation for wireless cellular network with shared relays," *IEEE J. Select. Areas Commun.*, vol. 30, no. 8, pp. 1530–1540, Sep. 2012.

[5] J. Kim, J.-Y. Hwang, and Y. Han, "Joint processing in multi-cell coordinated shared relay network," in *proc. 21st IEEE International Symposium on Personal Indoor and Mobile Radio Communications (PIMRC)*, 2010, pp. 702–706.

[6] N. Gresset, "Precoder optimization for user fairness in shared relay channels with interference," in *proc. 22nd IEEE International Symposium on Personal Indoor and Mobile Radio Communications (PIMRC)*, 2011, pp. 1475–1479.

[7] T. Hui, W. Xi-jun, J. Fan, D. Gang, and Z. Jie-Tao, "An inter-cell interference mitigation scheme based on MIMO-relay technique," in *Proc. 71st IEEE Veh. Tech. Conf.*, May 2010.

[8] T. K. Y. Lo, "Maximum ratio transmission," *IEEE Trans. Commun.*, vol. 47, pp. 1458–1461, Oct. 1999.

[9] R. Heath, T. Wu, Y. H. Kwon, and A. Soong, "Multiuser MIMO in distributed antenna systems with out-of-cell interference," *IEEE Trans. Signal Process.*, vol. 59, no. 10, pp. 4885–4899, Oct. 2011.

[10] D. G. Brennan, "Linear diversity combining techniques," *Proc. IEEE*, vol. 91, no. 2, pp. 331–356, 2003.

[11] N. C. Beaulieu, "A novel generalized framework for performance analysis of selection combining diversity," *IEEE Trans. Commun.*, vol. 61, pp. 4196–4205, Oct. 2013.

[12] J. Winters, "Optimum combining in digital mobile radio with cochannel interference," *IEEE J. Select. Areas Commun.*, vol. 2, no. 4, pp. 528–539, 1984.

[13] D. A. Gore, J. Heath, R. W., and A. J. Paulraj, "Transmit selection in spatial multiplexing systems," *IEEE Commun. Lett.*, vol. 6, no. 11, pp. 491–493, Nov. 2002.

[14] J. Zhang, R. W. Heath, M. Kountouris, and J. G. Andrews, "Mode switching for the multi-antenna broadcast channel based on delay and channel quantization," *EURASIP J. Adv. Signal Process*, vol. 2009, pp. 1:1–1:15, Feb. 2009.

[15] I. Gradshteyn and I. Ryzhik, *Table of Integrals, Series, and Products, Seventh Edition*. Academic Press, 2007.

[16] N. Jindal, "MIMO broadcast channels with finite-rate feedback," *IEEE Trans. Inf. Theory*, vol. 52, pp. 5045–5060, Nov. 2006.

[17] J. Zhang, M. Kountouris, J. G. Andrews, and R. W. Heath, "Multi-mode transmission for the MIMO broadcast channel with imperfect channel state information," *IEEE Trans. Commun.*, vol. 59, no. 3, pp. 803–814, 2011.

[18] A. P. Prudnikov, Y. Brychkov, and O. Marichev, *Integrals and Series*. Gorden and Breach Science, 1998, vol. 1.

[19] Wolfram functions site, "Hypergeometric2F1." [Online]. Available: http://functions.wolfram.com/HypergeometricFunctions/Hypergeometric2F1%/03/06/07/02/0004/

[20] Wolfram functions site, "ExpIntegralE." [Online]. Available: http://functions.wolfram.com/GammaBetaErf/ExpIntegralE/03/01/02/0007/

[21] Wolfram functions site, "ExpIntegralEi." [Online]. Available: http://functions.wolfram.com/06.35.06.0001.01

Chapter 7

Average Rate Analysis for Full-Duplex Underlay Device-to-Device Networks

A theoretical framework is presented for the evaluation of sum ergodic rate of a full-duplex underlay device-to-device network, when it shares the uplink resources of a conventional cellular user. The sum-rate of the full-duplex network is compared with a half-duplex network with equivalent radio frequency hardware complexity. Closed-form approximations are derived for the sum ergodic rate of the systems. Furthermore, the sum-rate performances are investigated for the case when a transmit power constraint is imposed on the underlay network to minimize the interference on the cellular network. The analytical results presented can be used as a tool to identify when full-duplex transmissions are viable in underlay device-to-device networks.

7.1 Introduction

Almost all the current wireless communications technologies enable bidirectional communications using frequency division duplexing (FDD) or time division duplexing (TDD). This requires allocating orthogonal time (TDD) or spectral (FDD) resources for transmission (Tx) and reception (Rx). Although this mechanism has proved to be extremely successful, it may not be able to cater for the spectral efficiency requirements of future generation wireless communication technologies.

Therefore, recently there has been a surge of interest on the systems where Tx and Rx is performed using the same time or spectral resources. These systems are commonly known as full-duplex (FD) systems, while conventional TDD and FDD systems are referred to as half-duplex (HD) systems. An inherent challenge of FD system is the interference on Rx by it's own Tx. This is known as self interference (SI). Recent studies [1, 2] have proposed SI cancellation schemes that can achieve 110 dB isolation between the Tx and the Rx. Experimental results of [3] have shown that FD systems are capable of achieving higher spectral efficiencies than HD systems for SI isolation above 74 dB. However, these gains have been observed in point-to-point FD systems with short distance between the nodes. Exploiting this fact, we aim to investigate the applicability of FD technique in device-to-device (D2D) networks, where the communications are generally short range.

In a D2D network, users connect with each other without communicating through the central base station (BS) to improve the overall spectral efficiency of the system, to reduce battery consumption and to reduce the workload of the BS [4, 5]. Recently the idea of underlaying D2D communications has gained interest in cellular networks, where D2D network coexists with a conventional cellular network while maintaining a maximum interference constraint on the cellular network. The results of [6] point out the feasibility of underlay D2D networks in 3rd generation partnership project (3GPP) long term evolution-Advanced (LTE-A) networks.

Surveys [7] indicate that the D2D type communications will become more commonplace in the future. It has been added as a study item in 3GPP and investigated as a feature in possible 5th generation (5G) communications. Several works have proposed efficient communication techniques for D2D networks including resource allocation [8], and power optimization [9]. However, all the previous works on D2D networks, did not consider FD communications for D2D users. It is interesting to combine the concepts of FD and D2D, since it may allow us to harvest the benefits of both technologies to improve the spectral efficiency of wireless communications. For example, latest wireless standards such as LTE-A do not support FD communications. However, introduction of FD communications to underlay D2D users that coexist with other LTE-A users, may result in increased total network throughput

without changing the infrastructure of the network.

In this chapter, we investigate the feasibility of FD communications in underlay D2D networks. We study the sum ergodic rate of an underlay D2D network when D2D users operate in FD mode and compare the performance to a HD underlay D2D network with equivalent total energy and radio frequency (RF) hardware complexity. Furthermore, we compare the performance of both HD and FD D2D networks to a conventional cellular network. Next, we analyze the case when transmit power adaptation is used at the D2D nodes to maintain a maximum interference constraint on the cellular network. Our analytical results can be used to identify when FD networks are advantageous to improve the overall system sum-rate. To the best of authors' knowledge, this is the first work investigating the sum ergodic rate of FD D2D networks.

The remainder of this chapter is organized as follows. In Section 7.2, we present FD, and HD D2D network models. Section 7.3 presents the ergodic rate analysis of each network configuration. Section 7.4 presents numerical results and comparisons while Section 7.5 concludes this chapter. The derivations are presented in appendices.

7.2 System Model

In this Section, we present the network models used for our analytical study. We consider a single circular cell with radius R_c with BS located at the center of the cell. A single cellular user (CU) and a pair of D2D users (D1 and D2) are located inside the cell. The D2D pair is assumed to be operating using the same resources as the uplink of the CU. We assume that the transmitters do not have channel state information (CSI). Two communication modes are considered for the D2D pair.

1. **FD Mode**: In the FD mode, both D2D users transmit and receive at the same time instant using the same frequency band. We assume a 1×1 FD D2D system where each node requires 1 up-converting RF chain for Tx, 1 down-converting RF chain for Rx and 1 up-converting RF chain for SI cancellation. A total transmission period of T seconds is considered. The available power

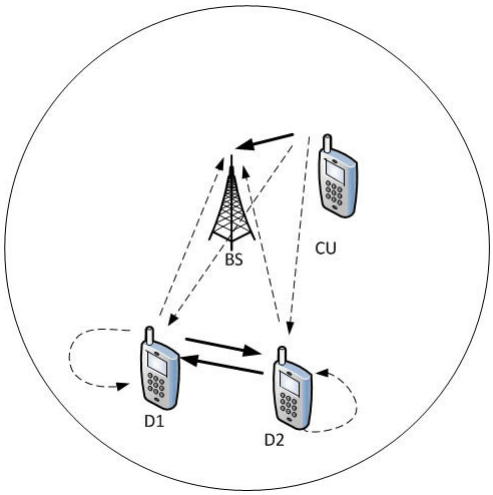

Figure 7.1: Underlay D2D network model, where the solid lines denote the desired signals and the dashed lines denote the interference links.

at D2D nodes is P_d. Therefore, the total energy consumed by the D2D pair in the FD mode is $2P_dT$.

2. **HD Mode**: In the HD mode, each D2D user transmit for $\frac{T}{2}$ time period. In order to make a fair comparison between the FD mode and the HD mode, we assume that both systems have equal RF hardware complexity. Since in the FD mode, a D2D node uses 2 up-converting RF chains and 1 down-converting RF chain, similar to [3, 10], we define an equivalent HD system with two up-converting RF chains for Tx and one down-converting RF chain for Rx. Therefore, the RF equivalent HD system for 1×1 FD pair is a 2×1 multiple-input single-output (MISO) system. In order to keep the total energy consumption of the two modes equal, each antenna transmits with power P_d with unit energy symbols, such that the total energy consumed is $2P_dT$.

In the first stage of this work, we assume that there is no interference coordination between the cellular network and the D2D pair. The channels between all the entities are assumed to be flat Rayleigh faded with average fading power of unity. We assume a log-distance path loss model with reference distance of 10 m. The performance metric we are interested in is the sum ergodic rate of the network. We derive closed-form expressions for the sum ergodic rate for both FD and HD modes. Furthermore, to understand the feasibility of D2D networks over conventional net-

works, we compare both FD and HD D2D systems with a two-way relay network (TWRN), where the BS acts as a relay between the two D2D users to facilitate the data exchange in a spectrally efficient manner.

7.3 Ergodic Rate Analysis

In this Section, we present the sum ergodic rate analysis for each D2D communication mode.

7.3.1 FD mode

The signal received at the BS can be written as

$$y_{BS,\text{FD}} = \sqrt{P_u L_u} h_u s_u + \sum_{k=1}^{2} \sqrt{P_d L_{dk}} h_{dk} s_{dk} + n_1$$

where P_u is the transmit power of CU, L_u is the path loss between the CU and the BS, h_u is the flat fading channel coefficient between the CU and the BS, s_u is the unit energy signal transmitted by the CU, n_1 is the additive white Gaussian noise (AWGN) with variance N_0 at the BS, s_{dk} is the unit energy signal transmitted by the k^{th} D2D user, L_{dk} and h_{dk} are the path loss and the flat fading channel coefficient between the k^{th} D2D user and the BS, respectively. The signal-to-interference-plus-noise ratio (SINR) at the BS can be written as

$$\gamma_{U,\text{FD}} = \frac{P_u L_u |h_u|^2}{\sum_{k=1}^{2} P_d L_{dk} |h_{dk}|^2 + N_0}. \tag{7.1}$$

The path loss coefficients are computed using

$$L(dB) = \begin{cases} 32 + 20\log_{10}(f_c d) & \text{if} d \leq 10 \\ 60 + 10\eta \log_{10}(d/10) & \text{if } d > 10 \end{cases} \tag{7.2}$$

where $f_c = 2.4$ is the carrier frequency in GHz, d is the distance between the nodes and η is the path loss exponent. The received signal at the k^{th} D2D user is given by

$$y_{k,\text{FD}} = \sqrt{P_d L_{12}} h_{kj} s_j + \sqrt{P_u L_{uk}} h_{uk} s_u + I_k + n_{kd}, \;\; k, j \in \{1, 2\}, k \neq j \tag{7.3}$$

where L_{uk}, h_{uk} are the path loss and the fading channel coefficient between the CU and the k^{th} D2D user, L_{12}, and h_{kj} are the path loss and the channel coefficient

between the D2D pair, and n_{kd} is the AWGN with variance $d_{uk}N_0$ at the k^{th} D2D user. The SI I_k at the k^{th} D2D user is modeled as additional Gaussian noise with variance σ_{Ik}^2. The variance σ_{Ik}^2 depends on the SI cancellation technique used at the nodes. According to the experimentally verified SI model given in [3], σ_{Ik}^2 can be computed using

$$\sigma_{Ik}^2(dBm) = P_d(dBm) - L_{SI}(dB) \\ - (\lambda(dB/dBm)(P_d(dBm) - L_{SI}(dB)) + \beta(dB)) \quad (7.4)$$

where L_{SI} is the passive SI cancellation due to antenna isolation, λ and β are coefficients depending on the active cancellation [11]. The SINR at the k^{th} D2D user can be given as

$$\gamma_{k,\text{FD}} = \frac{P_d L_{12}|h_{kj}|^2}{P_u L_{uk}|h_{uk}|^2 + \sigma_{Ik}^2 + N_0}. \quad (7.5)$$

The sum ergodic rate of the system can be computed using

$$R_{FD,D2D} = \overbrace{\mathbb{E}\left[\log_2\left(1+\gamma_{U,\text{FD}}\right)\right]}^{R_{U,\text{FD}}} + \underbrace{\sum_{k=1}^{2}\mathbb{E}\left[\log_2\left(1+\gamma_{k,\text{FD}}\right)\right]}_{R_{D2D,\text{FD}}} \quad (7.6)$$

where $R_{U,\text{FD}}$ and $R_{D2D,\text{FD}}$ are the ergodic rates of the CU and D2D pair, respectively. For our analysis, we assume that the position of the CU is randomly located at a distance r_1 from the BS and the D2D pair is fixed at a distance of r_2 from the BS (see Fig. 7.5). The mean distance between the CU and the k^{th} D2D user can be found using

$$\bar{d}_{uk} = \frac{2\sqrt{A+B}}{\pi}\boldsymbol{K}\left(\sqrt{\frac{2B}{A+B}}\right) \quad (7.7)$$

where $A = r_1^2 + r_2^2$, $B = 2r_1r_2$, and $\boldsymbol{K}(\cdot)$ is the complete elliptic integral of the second kind [12, 8.112]. The derivation of (7.7) is given in Appendix A. To account for the randomness of the CU location, we propose to substitute $\bar{d}_{uk}$ in (7.2), for calculating the values of L_{uk}. This approach is mathematically tractable compared to averaging over the PDF of d_{uk}, and results in extremely good approximations for the ergodic rate. The ergodic rate of the CU, $R_{U,\text{FD}}$, can be computed by solving the integral

$$R_{U,\text{FD}} = \log_2(e)\int_0^\infty \frac{1 - F_{\gamma_{U,\text{FD}}}(x)}{(1+x)}dx \quad (7.8)$$

where $F_{\gamma_{U,\text{FD}}}(x)$ is the cumulative distribution function (CDF) of $\gamma_{U,\text{FD}}$ given by

$$F_{\gamma_{U,\text{FD}}}(x) = 1 - \exp\left(-\frac{x}{\bar{\gamma}_u}\right) \frac{1}{\left(1 + \frac{\bar{\gamma}_b}{\bar{\gamma}_u} x\right)^2} \tag{7.9}$$

where $\bar{\gamma}_u = \frac{P_u L_u}{N_0}$, and $\bar{\gamma}_b = \frac{P_d L_{dk}}{N_0}$. The closed-form solution for (7.8) is given by

$$\begin{aligned} R_{U,\text{FD}} = \log_2(e)\Upsilon^2 \Bigg[& \frac{1}{1-\Upsilon}\left(\frac{1}{\Upsilon} - \frac{1}{\bar{\gamma}_u} e^{\frac{1}{\bar{\gamma}_b}} \boldsymbol{E}_1\left(\frac{1}{\bar{\gamma}_b}\right)\right) \\ & - \frac{1}{(1-\Upsilon)^2} e^{\frac{1}{\bar{\gamma}_b}} \boldsymbol{E}_1\left(\frac{1}{\bar{\gamma}_b}\right) + \frac{1}{(\Upsilon-1)^2} e^{\frac{1}{\bar{\gamma}_u}} \boldsymbol{E}_1\left(\frac{1}{\bar{\gamma}_u}\right) \Bigg] \end{aligned} \tag{7.10}$$

where $\Upsilon = \frac{\bar{\gamma}_u}{\bar{\gamma}_b}$, and $\boldsymbol{E}_1(\cdot)$ is the exponential integral function.

The CDF of $\gamma_{k,\text{FD}}$ is given by

$$F_{\gamma_{k,\text{FD}}}(x) = 1 - \frac{\Phi \exp\left(-\frac{x(1+\bar{I}_k)}{\bar{\gamma}_{k,\text{FD}}}\right)}{(x + \Phi)} \tag{7.11}$$

and the ergodic rate of the k^{th} D2D user can be found as

$$R_{D2D,\text{FD}} = \log_2(e)\Phi \left[\frac{e^{\frac{1+\bar{I}_k}{\bar{\gamma}_{k,\text{ FD}}}} \boldsymbol{E}_1\left(\frac{1+\bar{I}_k}{\bar{\gamma}_{k,\text{FD}}}\right)}{\Phi - 1} + \frac{e^{\frac{1+\bar{I}_k}{\bar{\gamma}_{k,u}}} \boldsymbol{E}_1\left(\frac{1+\bar{I}_k}{\bar{\gamma}_{k,u}}\right)}{1 - \Phi} \right] \tag{7.12}$$

where $\Phi = \frac{\bar{\gamma}_{k,\text{FD}}}{\bar{\gamma}_{k,u}}$, $\bar{\gamma}_{k,\text{FD}} = \frac{P_d L_{12}}{N_0}$, $\bar{\gamma}_{k,u} = \frac{P_u L_{uk}}{N_0}$ and $\bar{I}_k = \frac{\sigma_{Ik}^2}{N_0}$. The derivations of (7.9), (7.8), (7.11) and (7.12) are shown in Appendix B.

7.3.2 HD mode

In the HD mode, the D2D pair forms a 2×1 MISO system. Therefore, during the first $T/2$ period, 1st D2D user transmits using 2 antennas and the other user receives with a single antenna. Since CSI is not available at the transmitter, D2D users transmit using Alamouti space-time code (STC) to achieve transmit diversity. Then, the received signal at the BS in a particular symbol period during the first $\frac{T}{2}$ interval can be written as

$$y_{T/2,\text{HD}} = \sqrt{P_u L_u} h_u s_u + \sum_{k=1}^{2} \sqrt{P_d L_{k,1}} h_{k,1} s_{k,1} + n_1 \tag{7.13}$$

where $s_{k,1}$ is the transmit signal from the k^{th} Tx antenna of the 1st D2D user, $L_{k,1}$ and $h_{k,1}$ are the path loss and the fading channel between the BS and the k^{th} Tx

antenna of the 1st D2D user, respectively. The SINR in the first $T/2$ period is given by

$$\gamma_{T/2,\text{HD}} = \frac{P_u L_u |h_u|^2}{\sum_{k=1}^{2} P_d L_{k,1} |h_{k,1}|^2 + N_0}. \tag{7.14}$$

Since the D2D transmitter uses Alamouti STC, we consider two symbol periods for analysis. The received signal vector at the 2nd D2D user can be given as

$$\mathbf{y}_{2,\text{HD}} = \sqrt{P_d L_{12}} \begin{bmatrix} h_1 & -h_2 \\ h_2^* & -h_1^* \end{bmatrix} \begin{bmatrix} s_{1,1} \\ s_{2,1} \end{bmatrix} + \mathbf{n} + \sqrt{P_u L_{u1}} \mathbf{I}_u$$

where h_1, h_2 are channel gains between the two transmit antennas of the 1st D2D user and the 2nd D2D user, $s_{1,1}$, $s_{2,1}$ are the symbols transmitted by the 1st D2D user, $\mathbf{n}$ is the AWGN vector with covariance matrix $N_0\mathbf{I}$ and $\mathbf{I}_u$ is the interference vector from the CU at the 2nd D2D user. After matched filtering, the SINR per symbol is given by

$$\gamma_{2,\text{HD}} = \frac{P_d L_{12}(|h_1|^2 + |h_2|^2)}{P_u L_{u1} |h_{u1}|^2 + N_0} \tag{7.15}$$

The SINRs at the BS and the 1st D2D user in a particular symbol period during the second $T/2$ interval can be found similarly. One can observe that if $L_{k,1} = L_{k,2}$ $\forall k \in [1, 2]$, the overall SINR at the BS during the time period T in the HD mode has similar form as the SINR in the FD mode. Then, SINR CDFs of the BS are equivalent, and the ergodic rate for the HD mode can be found as (7.8). Following the procedure given in Appendix B, the CDF of the SINR at each D2D user can be found as

$$F_{\gamma_{k,\text{HD}}}(x) = 1 - \exp\left(-\frac{x}{\bar{\gamma}}\right) \left[\frac{\Delta}{x + \Delta} + \frac{x}{\bar{\gamma}_{k,u}(x + \Delta)} + \frac{x\Delta}{(x + \Delta)^2}\right] \tag{7.16}$$

where $\bar{\gamma} = \frac{P_d L_{12}}{N_0}$, and $\Delta = \frac{\bar{\gamma}}{\bar{\gamma}_{k,u}}$. Using the integral identities given in [13], the ergodic rate for each D2D user in the HD mode can be found in closed-form as

$$\begin{aligned} R_{k,\text{HD}} = \frac{\log_2(e)}{2} \Bigg[& \frac{2\Delta e^{\frac{1}{\bar{\gamma}_{k,u}}} \boldsymbol{E}_1\left(\frac{1}{\bar{\gamma}_{k,u}}\right)}{(1 - \Delta)} + \frac{\Delta e^{\frac{1}{\bar{\gamma}}} \boldsymbol{E}_1\left(\frac{1}{\bar{\gamma}}\right)}{(\Delta - 1)} \\ & - \frac{\Delta}{1 - \Delta} - \frac{e^{\frac{1}{\bar{\gamma}}} \boldsymbol{E}_1\left(\frac{1}{\bar{\gamma}}\right)}{\bar{\gamma}_{k,u}(\Delta - 1)} + \frac{\Delta^2 e^{\frac{1}{\bar{\gamma}_{k,u}}} \boldsymbol{E}_1\left(\frac{1}{\bar{\gamma}_{k,u}}\right)}{(1 - \Delta^2)} \\ & - \frac{\Delta e^{\frac{1}{\bar{\gamma}}} \boldsymbol{E}_1\left(\frac{1}{\bar{\gamma}}\right)}{(\Delta - 1)^2} \Bigg]. \end{aligned} \tag{7.17}$$

7.3.3 Comparison with TWRN

In order to understand the gain of underlay D2D deployment, we also compare the sum rate results of FD and HD D2D networks with conventional cellular network. To perform this comparison, we select TWRN as the conventional cellular counterpart of the D2D network, since TWRNs have been identified as a spectrally efficient scheme for data exchange between two nodes with the aid of a central network entity.

In the TWRN model, communication occurs in three time slots. In the first time slot, CU communicates with the BS. In the second time slot, the two users (D1 and D2 in D2D model) send their data to the BS which functions essentially as a relay. The BS applies a gain on the received signal and transmits the amplified signal in the third time slot. The users D1 and D2 subtract their own signal parts from the signal received and use the remainder for data decoding. In order to make comparisons fair, we assume D1 and D2 are equipped with 2 Tx antennas and the BS (relay) is equipped with a single antenna. The users apply maximal ratio transmission (MRT) for data transmission and maximal ratio combining (MRC) for reception. A similar system model was analyzed in [14] for users with correlated antennas. For simplicity, we do not consider the antenna correlation in this chapter. To make sure that the energy consumptions of D2D model and the TWRN model are equal, per antenna transmit power of D1 and D2 is set to $\frac{P_d}{4}$ and the transmit power of the BS is set to P_d thus making the total energy consumed by the network during the two time slots to be equal to $2P_dT$. The sum ergodic rate for the system can be written as

$$R_{sum,TWRN} = \frac{R_{U,TWRN} + 2R_{TWRN}}{3} \tag{7.18}$$

where $R_{U,TWRN}$ is the ergodic rate of the CU and R_{TWRN} is the ergodic rate of the TWRN. The ergodic rate of the CU is given by

$$R_{U,TWRN} = \exp\left(\frac{1}{\bar{\gamma}_u}\right) \boldsymbol{E}_1\left(\frac{1}{\bar{\gamma}_u}\right). \tag{7.19}$$

The ergodic rate of the TWRN can be found using the results presented in [14, Sec. III-C].

7.3.4 Impact of an interference constraint

Next, we analyze the sum rate of the system when a maximum interference constraint is imposed on the D2D network, when the D2D nodes are operating in the FD mode. In this situation, the BS measures the interference it receives from the D2D users and informs them through a control channel to limit their transmit power accordingly. The maximum interference threshold is computed to maintain a minimum quality of service (QoS) guarantee for the CU. Then the transmit power at the D2D users are adjusted according to

$$P_{k,D2D} = \min\left(\frac{I_{th,k}}{L_{dk}|h_{dk}|^2}, P_d\right) \tag{7.20}$$

where $I_{th,k}$ is the maximum interference allowed from the k^{th} D2D user. The SINR at the k^{th} D2D user is given by

$$\gamma_{k,D2D} = \frac{P_{k,D2D}L_{12}|h_{kj}|^2}{P_u L_{uk}|h_{uk}|^2 + \sigma_{Ik} + N_0}. \tag{7.21}$$

In this situation, to compute the statistics of SI, one must require the average transmit power of D2D nodes. The average transmit power $\bar{P}_{k,D2D}$ can be found as

$$\bar{P}_{k,D2D} = \sqrt{\Omega_k P_d}\exp\left(-\frac{\Omega}{2P_d}\right)\mathcal{W}_{-\frac{1}{2},0}\left(\frac{\Omega}{P_d}\right) + P_d\left(1 - \boldsymbol{Q}\left(1, \frac{\Omega}{P_d}\right)\right) \tag{7.22}$$

where $\Omega = \frac{I_{th,k}}{L_{dk}}$, $\mathcal{W}_{a,b}(\cdot)$ is the Whittaker function [12, eq. 9.221.1] and $\boldsymbol{Q}(c,d)$ is the incomplete gamma function [12, eq. 8.350.2]. (The derivation of (7.22) is given in Appendix C.) Then the variance of SI can be computed by replacing P_d with $\bar{P}_{k,D2D}$ in (7.4).

Obtaining an exact expression for the ergodic rate of D2D users appears to be intractable with the SINR expression (7.21). Therefore, we approximate the interference component from the CU by its average value $P_u L_{uk}$ and treat interference as an additional Gaussian noise. With this assumption, the CDF of $\gamma_{k,D2D}$ can be found using [15, eq. (8)], and has the form

$$F_{\gamma_{k,D2D}}(x) = 1 + \exp\left(-\frac{L_{12}\sigma^2 x}{P_d}\right)\left(\frac{\exp\left(-\frac{\alpha L_{12} I_{th,k}}{P_d}\right)}{\frac{\alpha I_{th,k}}{\sigma^2 x} + 1} - 1\right)$$

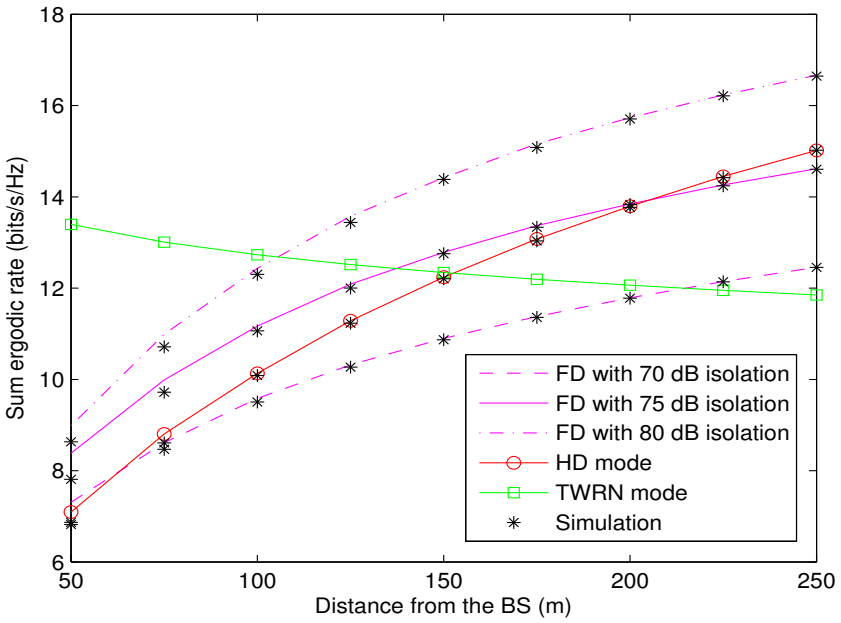

Figure 7.2: The sum ergodic rates of the system as a function of the distance of D2D pair from the BS

where $\sigma^2 = P_u L_{uk} + \sigma_{Ik} + N_0$ and $\alpha = \frac{L_{dk}}{L_{12}}$. Now the ergodic rate can be derived as

$$R_{k,D2D} = \exp\left(\frac{L_{12}\sigma^2}{P_d}\right)\boldsymbol{E}_1\left(\frac{L_{12}\sigma^2}{P_d}\right) - \frac{\exp\left(-\frac{\alpha L_{12} I_{th,k}}{P_d}\right)}{\frac{L_{12}\sigma^2}{P_d}\left(\frac{\alpha I_{th,k}}{\sigma^2} - 1\right)} + \frac{\exp\left(-\frac{\alpha L_{12} I_{th,k}}{P_d}\right)\exp\left(\frac{L_{12}\sigma^2}{P_d}\right)\boldsymbol{E}_1\left(\frac{L_{12}\sigma^2}{P_d}\right)}{\left(\frac{\alpha I_{th,k}}{\sigma^2} - 1\right)} + \frac{\frac{\alpha I_{th,k}}{\sigma^2}\boldsymbol{E}_1\left(\frac{\alpha L_{12} I_{th,k}}{P_d}\right)}{\left(1 - \frac{\alpha I_{th,k}}{\sigma^2}\right)} - \frac{\exp\left(-\frac{\alpha L_{12} I_{th,k}}{P_d}\right)}{\frac{L_{12}\sigma^2}{P_d}\left(1 - \frac{\alpha I_{th,k}}{\sigma^2}\right)} \quad (7.23)$$

For the HD mode, exact analysis becomes intractable with Alamouti STC transmission. Therefore, we propose to approximate the ergodic rate of the D2D users by substituting $\bar{P}_{k,D2D}$ instead of P_d in (7.15).

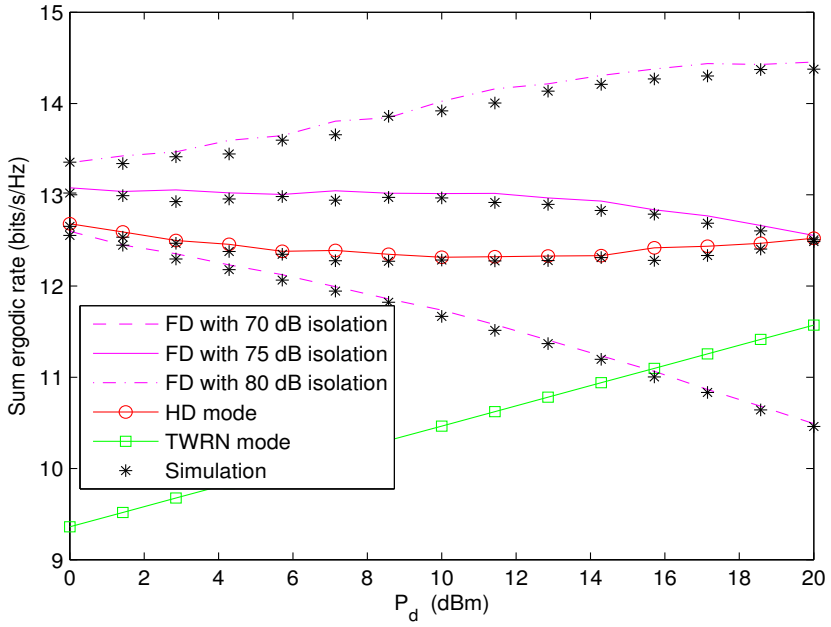

Figure 7.3: The sum ergodic rates of the system as a function of the transmit power of the D2D pair

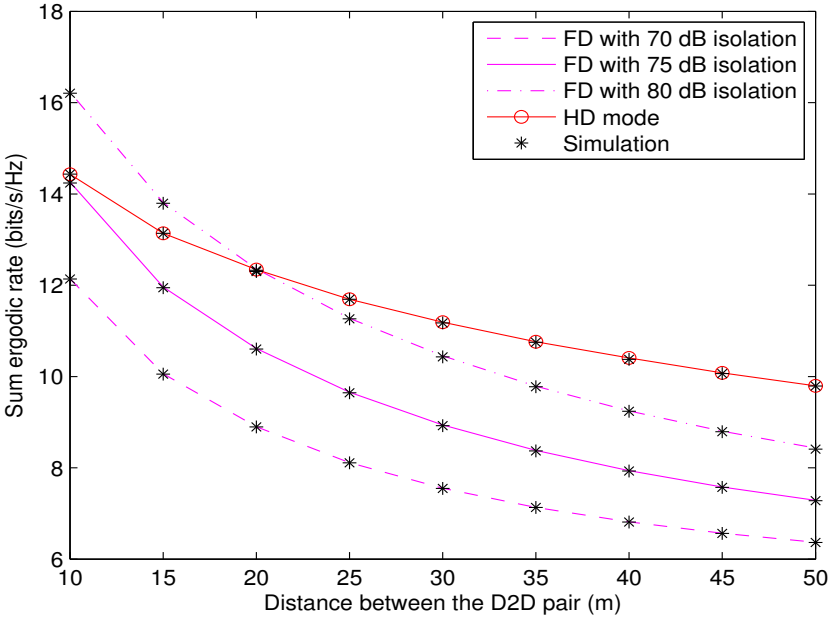

Figure 7.4: The sum ergodic rates of the system as a function of the distance between the D2D pair

7.4 Numerical Results and Discussion

In this Section, we provide some numerical results to verify the analysis conducted in Sec. 7.3. For our numerical results, we assume a circular cell of radius 250 m. The CU location is uniformly distributed at a distance r_1 from the BS. The position of the D2D pair is fixed at a distance r_2 from the BS. Carrier frequency of 2.4 GHz is used for path loss calculations with path loss exponent of 2. The D2D pair is assumed to be located 10 m apart from each other. The transmit power of the CU is set to 24 dBm. Noise variance N_0 is assumed to be -116.4 dBm. In all simulation results, 10000 random CU locations were used with 1000000 independent channel realizations. MATLAB software is used to perform the simulations and to compute the theoretical values of sum ergodic rates.

Fig. 7.2 shows the sum rate performance comparisons for each mode as a function of the distance of the D2D pair from the BS. Transmit power of the D2D users is set to 20 dBm with no maximum interference constraint. The CU is located near the BS at a distance of 75 m. One can observe that the theoretical results are in excellent agreement with the simulation results. It can be observed that the D2D communication is beneficial when the users are closer to the cell edge. The HD mode outperforms FD mode when the self interference cancellation is below 75 dB.

Fig. 7.3 shows the system sum rate comparisons for each mode as a function of the transmit power of D2D pair. The sum rate in the FD mode decreases with increasing transmit power due to the increase in SI. The ergodic rate of the HD mode remains almost constant and outperforms FD mode for SI cancellations below 75 dB. When the SI cancellation capability increases, the sum rate tends to improve with the increasing transmit power.

Fig. 7.4 gives the sum rate performances with the distance between the D2D pair, with $P_d = 20$ dBm. It is clear that the FD mode outperforms the HD mode when the distance between the D2D pair is shorter. As the distance increases, FD with 80 dB SI cancellation results in lower sum rate than the HD mode. The performance of TWRN does not depend on the distance between the nodes, hence not

considered for this comparison.

7.5 Conclusion

A theoretical framework was derived to evaluate the sum ergodic rate of underlay D2D network operating in FD and HD modes. Closed-form expressions were derived for the sum ergodic rates, when the location of the D2D pair is fixed, while the CU is randomly located. The derived expressions can be conveniently evaluated using common mathematical software packages. The theoretical results were verified using extensive Monte-carlo simulations. The new expressions can be used to save computation time in performance evaluation of underlay D2D networks operating in FD and HD modes. Analytical results can be used to identify the performance crossover point between the HD and FD modes.

7.A The Derivation of (7.7)

In this Appendix, we present the derivation of (7.7). The CU is randomly located at a distance r_1 from the BS and the locations of D1 and D2 are fixed. We assume that the angle θ is a uniformly distributed random variable (RV) in the interval $[-\pi, \pi]$. We consider the case when $r_2 > r_1$ where D2D communication is beneficial over conventional system. The results for $r_2 < r_1$ can be found in a similar manner. Applying the cosine law on the triangle, the squared distance can be found as

$$d_{u,k}^2 = r_1^2 + r_2^2 - 2r_1 r_2 \sin(\theta).$$

Applying standard transformation principles, the probability density function (PDF) of $d_{u,k}^2$ can be found as

$$f_{d_{u,k}^2}(y) = \frac{1}{\pi\sqrt{1 - \left(\frac{y-A}{B}\right)^2}}, \quad y \in \{A - B, A + B\}.$$

The mean distance can be computed as

$$\bar{d}_{u,k} = \int_{A-B}^{A+B} \frac{\sqrt{y}}{\pi\sqrt{1 - \left(\frac{y-A}{B}\right)^2}} dy.$$

Applying the variable transformation $\frac{y-A}{B} = \cos(x)$ and solving the resulting integral using [12, eq. 3.670.1], the mean distance between the CU and D1 can be found as in (7.7). Due to the symmetry, the mean distance between CU and D2 is also equal to $\bar{d}_{u,k}$.

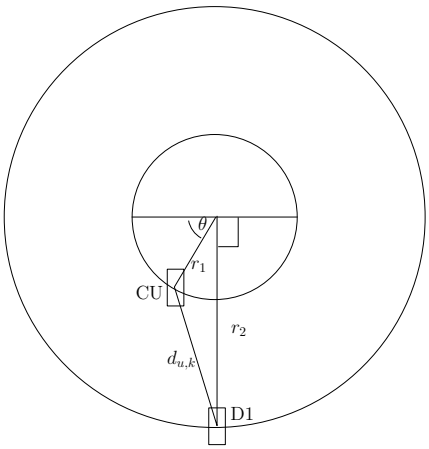

Figure 7.5: The distance between the CU and D1

7.B The Derivations of (7.9), (7.8), (7.11) and (7.12)

In this Appendix, we present the derivations of (7.9), (7.8), (7.11) and (7.12). Assuming $L_{d1} = L_{d2}$, the total interference power at the BS is gamma distributed and the PDF is given by

$$f_{\gamma_I}(x) = \frac{x}{\bar{\gamma}_b} \exp\left(-\frac{x}{\bar{\gamma}_b}\right).$$

The CDF of $\gamma_{U,\text{FD}}$ is found using

$$\begin{aligned} F_{\gamma_{U,\text{FD}}}(x) &= \Pr\left(\frac{P_u L_u |h_u|^2}{\sum_{k=1}^{2} P_d L_{dk} |h_{dk}|^2 + N_0} \leq x\right) \\ &= \int_0^\infty 1 - \exp\left(-\frac{x(y+1)}{\bar{\gamma}_u}\right) f_{\gamma_I}(y) dy \end{aligned} \tag{7.24}$$

and a closed-form solution is found using [12, 3.381.4]. Substituting (7.9) in (7.8) and applying the result in [13, Lemma 3], the ergodic rate is found in closed-form as (7.8). The derivation of (7.11) and (7.12) follow the same method as (7.9) and (7.8), and can be deduced in a straightforward manner.

7.C The Derivation of (7.22)

In this Appendix, we present the derivation of (7.22). The RV $P_{k,D2D}$ is a mixed RV with a continuous and discrete components in the PDF. The RV $X = \frac{\Omega}{|h_{dk}|^2}$ is inverse gamma distributed with PDF

$$f_X(x) = \Omega x^{-2} \text{exp}\left(-\frac{\Omega}{x}\right).$$

Then $\bar{P}_{k,D2D}$ can be computed using

$$\bar{P}_{k,D2D} = \underbrace{\int_0^{P_d} x f_X(x) dx}_{\mathcal{I}_1} + \underbrace{P_d \int_{P_d}^{\infty} f_X(x) dx}_{\mathcal{I}_2}$$

with

$$\mathcal{I}_2 = P_d \left(1 - \boldsymbol{Q}\left(1, \frac{\Omega}{P_d}\right)\right).$$

Using the variable transformation $\frac{\Omega}{x} = t$ and applying the integral identity [12, eq. 3.381.6] the integral $\mathcal{I}_1$ can be solved in closed-form.

References

[1] E. Everett, *Full-Duplex Infrastructure Nodes: Achieving Long Range with Half-duplex Mobiles.* Masters Thesis, Rice University., 2012, available: http://hdl.handle.net/1911/64704.

[2] D. Bharadia, E. McMilin, and S. Katti, "Full duplex radios," in *Proc. ACM 2013 Conference on SIGCOMM*, Hong Kong, China, 2013, pp. 375–386. [Online]. Available: http://doi.acm.org/10.1145/2486001.2486033

[3] M. Duarte, C. Dick, and A. Sabharwal, "Experiment-driven characterization of full-duplex wireless systems," *IEEE Trans. Wireless Commun.*, vol. 11, no. 12, pp. 4296–4307, 2012.

[4] K. Doppler, C. H. Yu, C. B. Ribeiro, and P. Janis, "Mode selection for device-to-device communication underlaying an LTE-Advanced network," in *Proc. IEEE Wireless Communications and Networking Conference (WCNC)*, 2010.

[5] B. Kaufman and B. Aazhang, "Cellular networks with an overlaid device to device network," in *Proc. 42nd Asilomar Conference on Signals, Systems and Computers*, 2008, pp. 1537–1541.

[6] K. Doppler, M. Rinne, C. Wijting, C. B. Ribeiro, and K. Hugl, "Device-to-device communication as an underlay to LTE-Advanced networks," *IEEE Commun. Mag.*, vol. 47, no. 12, pp. 42–49, 2009.

[7] *Cisco report, Cisco Visual Networking Index: Global Mobile Data Traffic Forecast Update, 2012-2017*, 2011.

[8] C.-H. Yu, O. Tirkkonen, K. Doppler, and C. Ribeiro, "Power optimization of device-to-device communication underlaying cellular communication," in

Proc. IEEE International Conference on Communications, 2009. (ICC 09), 2009.

[9] X. Chen, L. Chen, M. Zeng, X. Zhang, and D. Yang, "Downlink resource allocation for device-to-device communication underlaying cellular networks," in *Proc. IEEE 23rd International Symposium on Personal Indoor and Mobile Radio Communications (PIMRC), 2012*, 2012, pp. 232–237.

[10] M. Duarte, A. Sabharwal, V. Aggarwal, R. Jana, K. K. Ramakrishnan, C. W. Rice, and N. K. Shankaranarayanan, "Design and characterization of a full-duplex multi-antenna system for WiFi networks," *IEEE Trans. Veh. Technol.*, 2012, available: http://arxiv.org/abs/1210.1639.

[11] M. Duarte and A. Sabharwal, "Full-duplex wireless communications using off-the-shelf radios: Feasibility and first results," in *Proc. 44th Asilomar Conference on Signals, Systems and Computers*, 2010, pp. 1558–1562.

[12] I. Gradshteyn and I. Ryzhik, *Table of Integrals, Series, and Products, Seventh Edition*. Academic Press, 2007.

[13] J. Zhang, R. W. Heath, M. Kountouris, and J. G. Andrews, "Mode switching for the multi-antenna broadcast channel based on delay and channel quantization," *EURASIP J. Adv. Signal Process*, vol. 2009, pp. 1:1–1:15, Feb. 2009.

[14] N. S. Ferdinand, N. Rajatheva, and M. Latva-aho, "Performance analysis of two-way relay system with antenna correlation," in *Proc. IEEE Global Telecommunications Conference (GLOBECOM)*, Houston, Tx, USA, 2011.

[15] J. Lee, H. Wang, J. G. Andrews, and D. Hong, "Outage probability of cognitive relay networks with interference constraints," *IEEE Trans. Wireless Commun.*, vol. 10, no. 2, pp. 390–395, 2011.

Chapter 8

Concluding Remarks and Future Research Directions

This thesis attempted to advance the theory in wireless communications and obtain valuable system design insights in multiple aspects.

- Chapter 3 presented an outage probability analysis for multiuser relay networks in the presence of CCI. Exact expressions as well as approximations were derived for the outage probabilities of the network configurations assuming interference limited network entities. From the results one can identify that the outage probability is less sensitive to the number of interferers at the destination, while it is mainly dominated by the interference at the relay. Furthermore, the analytical results can be used to identify the maximum tolerable delay for the feedback channel.

- Chapter 4 used a second-order moment matching technique to derive simple approximations for the ergodic rate of limited feedback DASs operating in the presence of out-of-cell interference. The tightness of the approximations was tested using extensive simulations. The results show that even though RVQ based beamforming proved to be effective in conventional MISO systems, it is highly suboptimal for DASs and the results can be used to obtain a worst case performance benchmark.

- Chapter 5 presented a detailed outage probability analysis for relay coordination schemes in two-hop DF relay networks. Closed-form outage probability

expressions were derived for four relay coordination schemes. Simplified outage probability expressions were derived for the high-SNR regime to identify important parameters such as array gain and the diversity order of the system. Furthermore, an approximation technique was proposed to incorporate the impact of user location randomness in outage probability computations. The results were used to come up with some thumb rules useful in designing coordinated relay networks.

- Chapter 6 presented an outage probability and average rate analysis for a shared relay based interference coordination scheme. The results show that by implementing linear transceiver structures at the shared relay node can effectively reduce the ICI levels. Even though the analysis was conducted using single antenna source nodes, the results can be easily extended to a system model with multiple antenna source nodes where source nodes use TAS for first-hop transmission. Furthermore, the impact of CSI quantization on the average rate performance was investigated to identify the necessary codebook sizes to maintain a desirable level of system performance.

- Chapter 7 presented an average rate analysis for an underlay full-duplex D2D network. The analysis compared the average rate performance with conventional half-duplex network with equivalent hardware complexity and energy consumption. The results can be used to identify the SI cancellation requirements required to outperform half-duplex systems. Furthermore, the analytical results can be used to identify the performance cross-over points between FD and HD modes.

The results of this thesis have provided basis for many other research works including [1–5]. Apart from these works, the results of this thesis may be used as a basis for the following future research directions.

- The analytical results in Chapters 3 and 4 are derived assuming a homogenous deterministic interference model. However, future wireless networks will support heterogeneous services in multiple tiers. Therefore, it is im-

portant to revist the problems studied in Chapters 3 and 4 with interference models accounting for heterogeneous user services.

- The analysis in Chapters 5 and 6 assumed that the coordinating cells have similar QoS requirements. However, the heterogeneous nature of the future wireless networks will result in the need to coordinate interference among cells with different types of QoS requirements. For example, one cell may contain users with guaranteed QoS, while the other cell may contain best effort users. It will be interesting to design resource allocation schemes at the relay to cater the demands of users with different QoS levels.

- The results developed in Chapter 7 are still in a preliminary stage, where the performance of a simplified network model is studied. It is important to conduct further theoretical analysis on FD D2D networks with complex network topologies, by computing the achievable data rate and the probability of service outages. It is expected that 5G networks will be ultra-dense and heterogeneous. Several types of networks may co-exist in the same spectrum. Therefore, it is crucial to identify the impact of different types of interference from other networks on FD D2D networks. D2D networks such as vehicular networks will operate in environments where impulsive noise sources and inaccurate CSI estimates are common performance degradation factors. Due to the safety critical nature of D2D applications, designers must make sure that the systems are capable of extremely reliable communications in the presence of these hostile conditions. Therefore, it is important to consider the impacts of impulsive noise and CSI estimation errors in the analysis. Experimentally verified Laplace noise model can be used to model impulsive noise sources in the analysis. Furthermore, the results of these analyses can be used to develop new transceiver structures to enhance the performance of FD D2D systems in the presence of practical imperfections such as interference, CSI estimation errors and impulsive noise.

References

[1] Y. Huang, F. Al-Qahtani, C. Zhong, Q. Wu, J. Wang, and H. Alnuweiri, "Performance analysis of multiuser multiple antenna relaying networks with co-channel interference and feedback delay," *IEEE Trans. Commun.*, vol. 62, no. 1, pp. 59–73, Jan. 2014.

[2] Y. Gu, S. Ikki, and S. Aissa, "Opportunistic cooperative communication in the presence of co-channel interferences and outdated channel information," *IEEE Commun. Lett.*, vol. 17, no. 10, pp. 1948–1951, Oct. 2013.

[3] M. Di Renzo and W. Lu, "End-to-end error probability and diversity analysis of AF-based dual-hop cooperative relaying in a poisson field of interferers at the destination," *IEEE Trans. Wireless Commun.*, vol. 14, no. 1, pp. 15–32, Jan. 2015.

[4] T. Lu, P. Liu, I. Kim, F. Chan, and W. Read, "End-to-end optimum ML detection for DF cooperative diversity networks in the presence of interference," *IEEE Trans. Wireless Commun.*, (Available in IEEE Early Access).

[5] N. Miridakis, M. Matthaiou, and G. Karagiannidis, "Multiuser relaying over mixed RF/FSO links," *IEEE Trans. Commun.*, vol. 62, no. 5, pp. 1634–1645, May 2014.

Bibliography

[1] Cisco, "Cisco visual networking index: Global mobile data traffic forecast update, 2013–2018," 2013.

[2] G. L. Stüber, *Principles of Mobile Communication*. Norwell: Kluwer Academic, 2001.

[3] W. C. Jakes, *Microwave Mobile Communications*. New York: IEEE press, 1994.

[4] E. Telatar, "Capacity of multi-antenna Gaussian channels," *Europ. Trans. Telecommun.*, pp. 585–596, Nov.-Dec. 1999.

[5] J. G. J. Foschini and M. J. Gans, "On limits of wireless communication in a fading environment when using multiple antennas," *Wireless Personal Commun.*, no. 3, pp. 311–355, Mar. 1998.

[6] J. G. J. Foschini, "Layered space-time architecture for wireless communication in a fading environment when using multi-element antennas," *Bell Labs Tech. J.*, pp. 41–59, 1996.

[7] V. Tarokh, H. Jafarkhani, and A. R. Calderbank, "Space-time block codes from orthogonal designs," *IEEE Trans. Inf. Theory*, vol. 45, no. 5, pp. 1456–1467, Jul. 1999.

[8] H. Sampath, P. Stoica, and A. Paulraj, "Generalized linear precoder and decoder design for MIMO channels using the weighted MMSE criterion," *IEEE Trans. Commun.*, vol. 49, no. 12, pp. 2198–2206, 2001.

[9] A. F. Molisch and M. Z. Win, "MIMO systems with antenna selection," *IEEE Microw. Mag.*, vol. 5, no. 1, pp. 46–56, Mar. 2004.

[10] S. Sanayei and A. Nosratinia, "Antenna selection in MIMO systems," *IEEE Commun. Mag.*, vol. 42, no. 10, pp. 68–73, Oct. 2004.

[11] J. N. Laneman, D. N. C. Tse, and G. W. Wornell, "Cooperative diversity in wireless networks: Efficient protocols and outage behavior," *IEEE Trans. Inf. Theory*, vol. 50, no. 12, pp. 3062–3080, 2004.

[12] A. Sendonaris, E. Erkip, and B. Aazhang, "User cooperation diversity - part I: System description," *IEEE Trans. Commun.*, vol. 51, no. 11, pp. 1927–1938, 2003.

[13] A. Sendonaris, E. Erkip, and B. Aazhang, "User cooperation diversity - part II: Implementation aspects and performance analysis," *IEEE Trans. Commun.*, vol. 51, no. 11, pp. 1939–1948, 2003.

[14] K. T. Truong and R. W. Heath, "Joint transmit precoding for the relay interference broadcast channel," *IEEE Trans. Veh. Technol.*, vol. 62, no. 3, pp. 1201–1215, Mar. 2013.

[15] "3GPP TR 36.814. Evolved universal terrestrial radio access (E-UTRA); further advancements for E-UTRA (LTE-Advanced)." [Online]. Available: http://www.3gpp.org/ftp/Specs/html-info/36814.htm.

[16] A. Saleh, A. Rustako, and R. Roman, "Distributed antennas for indoor radio communications," *IEEE Trans. Commun.*, vol. 35, no. 12, pp. 1245 –1251, Dec. 1987.

[17] W. Choi and J. Andrews, "Downlink performance and capacity of distributed antenna systems in a multicell environment," *IEEE Trans. Wireless Commun.*, vol. 6, no. 1, pp. 69–73, Jan. 2007.

[18] S. W. Peters, A. Y. Panah, K. T. Truong, and R. W. Heath, "Relay architectures for 3GPP LTE-advanced," *EURASIP J. Wirel. Commun. Netw.*, vol. 2009, pp. 1:1–1:14, Mar. 2009.

[19] M. K. Karakayali, G. J. Foschini, and R. A. Valenzuela, "Network coordination for spectrally efficient communications in cellular systems," *IEEE Wireless Commun.*, vol. 13, no. 4, pp. 56–61, 2006.

[20] D. Lee, H. Seo, B. Clerckx, E. Hardouin, D. Mazzarese, S. Nagata, and K. Sayana, "Coordinated multipoint transmission and reception in LTE-advanced: deployment scenarios and operational challenges," *IEEE Commun. Mag.*, vol. 50, no. 2, pp. 148–155, Feb. 2012.

[21] S. Rangan, T. S. Rappaport, and E. Erkip, "Millimeter-wave cellular wireless networks: Potentials and challenges," *Proc. IEEE*, vol. 102, no. 3, pp. 366–385, Mar. 2014.

[22] E. Larsson, O. Edfors, F. Tufvesson, and T. Marzetta, "Massive MIMO for next generation wireless systems," *IEEE Commun. Mag.*, vol. 52, no. 2, pp. 186–195, Feb. 2014.

[23] L. Lu, G. Y. Li, A. L. Swindlehurst, A. Ashikhmin, and R. Zhang, "An overview of massive MIMO: Benefits and challenges," *IEEE J. Sel. Topics Signal Process.*, vol. 8, no. 5, pp. 742–758, Oct 2014.

[24] S. Haykin, "Cognitive radio: Brain-empowered wireless communications," *IEEE J. Select. Areas Commun.*, vol. 23, no. 2, pp. 201–220, Feb. 2005.

[25] A. A. Abu-Dayya and N. C. Beaulieu, "Outage probabilities of diversity cellular systems with cochannel interference in Nakagami fading," *IEEE Trans. Veh. Technol.*, vol. 41, no. 4, pp. 343–355, Nov. 1992.

[26] A. A. Abu-Dayya and N. C. Beaulieu, "MDPSK on frequency-selective Ricean channels with diversity and cochannel interference," in *Proc. IEEE Vehicular Technology Conf. (VTC)*, Jun 1994, pp. 996–1000 vol.2.

[27] A. A. Abu-Dayya and N. C. Beaulieu, "Diversity MPSK receivers in cochannel interference," *IEEE Trans. Veh. Technol.*, vol. 48, no. 6, pp. 1959–1965, Nov 1999.

[28] A. A. Abu-Dayya and N. C. Beaulieu, "Diversity $\pi/4$-DQPSK on microcellular interference channels," *IEEE Trans. Commun.*, vol. 44, no. 10, pp. 1289–1297, Oct 1996.

[29] A. A. Abu-Dayya and N. C. Beaulieu, "Outage probabilities in the presence of correlated lognormal interferers," *IEEE Trans. Veh. Technol.*, vol. 43, no. 1, pp. 164–173, Feb 1994.

[30] V. A. Aalo and J. Zhang, "Performance analysis of maximal ratio combining in the presence of multiple equal-power cochannel interferers in a Nakagami fading channel," *IEEE Trans. Veh. Technol.*, vol. 50, no. 2, pp. 497–503, Mar 2001.

[31] K. T. Hemachandra and N. C. Beaulieu, "Outage analysis of opportunistic scheduling in dual-hop multiuser relay networks in the presence of interference," *IEEE Trans. Commun.*, vol. 61, no. 5, pp. 1786–1796, May 2013.

[32] K. T. Hemachandra and N. C. Beaulieu, "A moment matching technique to estimate the achievable ergodic rate for limited feedback distributed antenna systems in the presence of out-of-cell interference," *IEEE Commun. Lett.*, vol. 17, no. 7, pp. 1360–1363, July 2013.

[33] K. T. Hemachandra and N. C. Beaulieu, "Relay coordination schemes for two-hop networks: Two-cell case," *IEEE Trans. Commun.*, 2015, (accepted).

[34] K. T. Hemachandra and N. C. Beaulieu, "Shared relay networks with linear receivers at the relay: Two-cell case," *IEEE Trans. Commun.*, vol. 62, no. 4, pp. 1230–1239, Apr. 2014.

[35] K. T. Hemachandra, N. Rajatheva, and M. Latva-aho, "Sum-rate analysis for full-duplex underlay device-to-device networks," in *IEEE Wireless Commun. and Networking Conf. (WCNC)*, April 2014, pp. 514–519.

[36] E. Beres and R. Adve, "Outage probability of selection cooperation in the low to medium SNR regime," *IEEE Commun. Lett.*, vol. 11, no. 7, pp. 589–597, 2007.

[37] A. Osseiran, F. Boccardi, V. Braun, K. Kusume, P. Marsch, M. Maternia, O. Queseth, M. Schellmann, H. Schotten, H. Taoka, H. Tullberg, M. A. Uusitalo, B. Timus, and M. Fallgren, "Scenarios for 5G mobile and wireless communications: the vision of the METIS project," *IEEE Commun. Mag.*, vol. 52, no. 5, pp. 26–35, May 2014.

[38] A. J. Goldsmith and P. P. Varaiya, "Capacity of fading channels with channel side information," *IEEE Trans. Inf. Theory*, vol. 43, no. 6, pp. 1986–1992, Nov. 1997.

[39] S. Verdu, *Multiuser Detection*, 1st ed. Cambridge University Press, 1998.

[40] V. M. Bogachev and I. G. Kiselev, "Optimal combination of signals in space-diversity reception," *Radiotekhnika*, vol. 35, pp. 32–34, Oct. 1980.

[41] J. Winters, "Optimum combining in digital mobile radio with cochannel interference," *IEEE J. Select. Areas Commun.*, vol. 2, no. 4, pp. 528–539, 1984.

[42] T. K. Y. Lo, "Maximum ratio transmission," *IEEE Trans. Commun.*, vol. 47, pp. 1458–1461, Oct. 1999.

[43] N. Jindal, "MIMO broadcast channels with finite-rate feedback," *IEEE Trans. Inf. Theory*, vol. 52, pp. 5045–5060, Nov. 2006.

[44] N. Jindal, "High SNR analysis of MIMO broadcast channels," in *Proc. 2005 IEEE International Symposium on Information Theory*, Sep. 2005, pp. 2310–2314.

[45] J. Tang and X. Zhang, "Transmit selection diversity with maximal-ratio combining for multicarrier DS-CDMA wireless networks over Nakagami-*m* fading channels," *IEEE J. Select. Areas Commun.*, vol. 24, no. 1, pp. 104–112, Jan. 2006.

[46] W. Santipach and M. L. Honig, "Signature optimization for CDMA with limited feedback," *IEEE Trans. Inf. Theory*, vol. 51, no. 10, pp. 3475–3492, Oct. 2005.

[47] J. Zhang, R. W. Heath, M. Kountouris, and J. G. Andrews, "Mode switching for the multi-antenna broadcast channel based on delay and channel quantization," *EURASIP J. Adv. Signal Process*, vol. 2009, pp. 1:1–1:15, Feb. 2009.

[48] H. A. Suraweera, H. K. Garg, and A. Nallanathan, "Performance analysis of two hop amplify-and-forward systems with interference at the relay," *IEEE Commun. Lett.*, vol. 14, no. 8, Aug. 2010.

[49] S. S. Ikki and S. Aïssa, "Performance analysis of dual-hop relaying systems in the presence of co-channel interference," in *Proc. IEEE Global Telecommunications Conference, GLOBECOM 2010*, Miami, FL.

[50] D. B. da Costa, H. Ding, and J. Ge, "Interference-limited relaying transmissions in dual-hop cooperative networks over Nakagami-*m* fading," *IEEE Commun. Lett.*, vol. 15, pp. 503–505, May 2011.

[51] D. Lee and J. H. Lee, "Outage probability of decode-and-forward opportunistic relaying in a multicell environment," *IEEE Trans. Veh. Technol.*, vol. 60, pp. 1925–1930, May 2011.

[52] C. Zhong, S. Jin, and K.-K. Wong, "Dual-hop systems with noisy relay and interference-limited destination," *IEEE Trans. Commun.*, vol. 58, no. 3, Mar. 2010.

[53] D. Lee and J. H. Lee, "Outage probability for dual-hop relaying systems with multiple interferers over Rayleigh fading channels," *IEEE Trans. Veh. Technol.*, vol. 60, no. 1, Jan. 2011.

[54] D. B. da Costa and M. D. Yacoub, "Outage performance of two hop AF relaying systems with co-channel interferers over Nakagami-*m* fading," *IEEE Commun. Lett.*, vol. 15, pp. 980–982, Sep. 2011.

[55] F. S. Al-Qahtani, T. Q. Duong, C. Zhong, K. A. Qaraqe, and H. Alnuweiri, "Performance analysis of dual-hop AF systems with interference in Nakagami-*m* fading channels," *IEEE Signal Process. Lett.*, vol. 18, pp. 454–457, Aug. 2011.

[56] J. B. Kim and D. Kim, "Comparison of two SNR-based feedback schemes in multiuser dual-hop amplify-and-forward relaying networks," *IEEE Commun. Lett.*, vol. 12, no. 8, pp. 557 –559, Aug. 2008.

[57] N. Yang, M. Elkashlan, and J. Yuan, "Outage probability of multiuser relay networks in Nakagami-*m* fading channels," *IEEE Trans. Veh. Technol.*, vol. 59, no. 5, pp. 2120 –2132, Jun. 2010.

[58] C. K. Sung and I. B. Collings, "Multiuser cooperative multiplexing with interference suppression in wireless relay networks," *IEEE Trans. Wireless Commun.*, vol. 9, no. 8, pp. 2528 –2538, Aug. 2010.

[59] N. Yang, M. Elkashlan, and J. Yuan, "Impact of opportunistic scheduling on cooperative dual-hop relay networks," *IEEE Trans. Commun.*, vol. 59, no. 3, pp. 689 –694, Mar. 2011.

[60] N. Yang, P. L. Yeoh, M. Elkashlan, J. Yuan, and I. B. Collings, "Cascaded TAS/MRC in MIMO multiuser relay networks," *IEEE Trans. Commun.*, vol. 11, no. 10, pp. 3829 –3839, Oct. 2012.

[61] N. Yang, M. Elkashlan, P. Yeoh, and J. Yuan, "Multiuser MIMO relay networks in Nakagami-*m* fading channels," *IEEE Trans. Commun.*, vol. 60, no. 11, pp. 3298–3310, Nov. 2012.

[62] M. Soysa, H. Suraweera, C. Tellambura, and H. Garg, "Multiuser amplify-and-forward relaying with delayed feedback in Nakagami-*m* fading," in *IEEE Wireless Communications and Networking Conference (WCNC), 2011*, Mar. 2011, pp. 1724 –1729.

[63] R. Heath, T. Wu, Y. H. Kwon, and A. Soong, "Multiuser MIMO in distributed antenna systems with out-of-cell interference," *IEEE Trans. Signal Process.*, vol. 59, no. 10, pp. 4885–4899, Oct. 2011.

[64] T. Ahmad, R. Gohary, H. Yanikomeroglu, S. Al-Ahmadi, and G. Boudreau, "Coordinated port selection and beam steering optimization in a multi-cell distributed antenna system using semidefinite relaxation," *IEEE Trans. Wireless Commun.*, vol. 11, no. 5, pp. 1861–1871, 2012.

[65] O. Haliloglu, C. Toker, G. Bulu, and H. Yanikomeroglu, "Radio resource management in a coordinated cellular distributed antenna system by using particle swarm optimization," in *IEEE Veh. Technol. Conf. (VTC - 2013 spring),*, 2013, pp. 1–5.

[66] K. Truong and R. Heath, "Interference alignment for the multiple-antenna amplify-and-forward relay interference channel," in *Signals, Systems and Computers (ASILOMAR), 2011 Conference Record of the Forty Fifth Asilomar Conference on*, 2011, pp. 1288–1292.

[67] K. Truong, P. Sartori, and R. Heath, "Cooperative algorithms for mimo amplify-and-forward relay networks," *IEEE Trans. Signal Process.*, vol. 61, no. 5, pp. 1272–1287, 2013.

[68] K. T. Truong and R. W. Heath, "Relay beamforming using interference pricing for the two-hop interference channel," in *IEEE Global Telecommunications Conference (GLOBECOM 2011),*, 2011, pp. 1–5.

[69] J. Zhang and K. Letaief, "Interference management with relay cooperation in two-hop interference channels," *IEEE Trans. Wireless Commun.*, vol. 1, no. 3, pp. 165–168, 2012.

[70] J.-W. Kwon, K.-H. Park, Y.-C. Ko, and H.-C. Yang, "Cooperative joint precoding in a downlink cellular system with shared relay: Design and performance evaluation," *IEEE Trans. Wireless Commun.*, vol. 11, no. 10, pp. 3462 –3473, Oct. 2012.

[71] T. Hui, W. Xi-jun, J. Fan, D. Gang, and Z. Jie-Tao, "An inter-cell interference mitigation scheme based on MIMO-relay technique," in *Proc. 71st IEEE Veh. Tech. Conf.*, May 2010.

[72] Y. Lin and W. Yu, "Fair scheduling and resource allocation for wireless cellular network with shared relays," *IEEE J. Select. Areas Commun.*, vol. 30, no. 8, pp. 1530–1540, Sep. 2012.

[73] E. Everett, *Full-Duplex Infrastructure Nodes: Achieving Long Range with Half-duplex Mobiles.* Masters Thesis, Rice University., 2012, available: http://hdl.handle.net/1911/64704.

[74] D. Bharadia, E. McMilin, and S. Katti, "Full duplex radios," in *Proc. ACM 2013 Conference on SIGCOMM*, Hong Kong, China, 2013, pp. 375–386. [Online]. Available: http://doi.acm.org/10.1145/2486001.2486033

[75] M. Duarte, C. Dick, and A. Sabharwal, "Experiment-driven characterization of full-duplex wireless systems," *IEEE Trans. Wireless Commun.*, vol. 11, no. 12, pp. 4296–4307, 2012.

[76] D. Bharadia and S. Katti, "Full duplex MIMO radios," in *Proc. 11th USENIX Symposium on Networked Systems Design and Implementation (NSDI 14)*, Seattle, WA, Apr. 2014, pp. 359–372. [Online]. Available: https://www.usenix.org/conference/nsdi14/technical-sessions/bharadia

[77] K. Doppler, M. Rinne, C. Wijting, C. B. Ribeiro, and K. Hugl, "Device-to-device communication as an underlay to LTE-Advanced networks," *IEEE Commun. Mag.*, vol. 47, no. 12, pp. 42–49, 2009.

[78] C.-H. Yu, O. Tirkkonen, K. Doppler, and C. Ribeiro, "Power optimization of device-to-device communication underlaying cellular communication," in *Proc. IEEE International Conference on Communications, 2009. (ICC 09)*, 2009.

[79] X. Chen, L. Chen, M. Zeng, X. Zhang, and D. Yang, "Downlink resource allocation for device-to-device communication underlaying cellular networks,"

in *Proc. IEEE 23rd International Symposium on Personal Indoor and Mobile Radio Communications (PIMRC), 2012*, 2012, pp. 232–237.

[80] S. Ali, N. Rajatheva, and M. Latva-aho, "Full duplex device-to-device communication in cellular networks," in *Proc. 2014 European Conference on Networks and Communications*, Bologna, Italy.

[81] W. Xu, J. Zhang, and P. Zhang, "Outage probability of two-hop fixed-gain relay with interference at the relay and destination," *IEEE Commun. Lett.*, vol. 15, pp. 608–610, Jun. 2011.

[82] H. A. Suraweera, D. S. Michalopoulos, R. Schober, G. K. Karagiannidis, and A. Nallanathan, "Fixed gain amplify-and-forward relaying with co-channel interference," in *Proc. IEEE International Conference on Communications (ICC), 2011*, Jun. 2011.

[83] H. Suraweera, M. Soysa, C. Tellambura, and H. Garg, "Performance analysis of partial relay selection with feedback delay," *IEEE Signal Process. Lett.*, vol. 17, no. 6, pp. 531 –534, Jun. 2010.

[84] D. Michalopoulos, H. Suraweera, G. Karagiannidis, and R. Schober, "Amplify-and-forward relay selection with outdated channel estimates," *IEEE Trans. Commun.*, vol. 60, no. 5, pp. 1278 –1290, May 2012.

[85] H. Suraweera, T. Tsiftsis, G. Karagiannidis, and A. Nallanathan, "Effect of feedback delay on amplify-and-forward relay networks with beamforming," *IEEE Trans. Veh. Technol.*, vol. 60, no. 3, pp. 1265 –1271, Mar. 2011.

[86] M. Soysa, H. Suraweera, C. Tellambura, and H. Garg, "Partial and opportunistic relay selection with outdated channel estimates," *IEEE Trans. Commun.*, vol. 60, no. 3, pp. 840 –850, Mar. 2012.

[87] H. Phan, T. Duong, M. Elkashlan, and H.-J. Zepernick, "Beamforming amplify-and-forward relay networks with feedback delay and interference," *IEEE Signal Process. Lett.*, vol. 19, no. 1, pp. 16 –19, Jan. 2012.

[88] I. Gradshteyn and I. Ryzhik, *Table of Integrals, Series, and Products, Seventh Edition*. Academic Press, 2007.

[89] A. H. Nuttall, "Some integrals involving the q-function," *Naval Underwater Systems Center (NUSC) Technical Report*, Apr. 1972.

[90] W. Roh and A. Paulraj, "Performance of the distributed antenna systems in a multi-cell environment," in *Proc. IEEE Veh. Technol. Conf., 2003. VTC 2003-Spring*, Apr. 2003, pp. 587 – 591.

[91] Y. Liu, J. Liu, H. Chen, L. Zheng, G. Zhang, and W. Guo, "Downlink performance of distributed antenna systems in multicell environment," *IET Communications*, vol. 5, no. 15, pp. 2141 –2148, 2011.

[92] L. Li, G. Li, F. Zhou, and M. Wu, "Downlink performance evaluation of centralized and distributed antenna systems in multicell multiuser spatial multiplexing environment," in *Proc.4th Int. Conf. on Wireless Commun., Networking and Mobile Computing, 2008. WiCOM '08.*, Oct. 2008.

[93] X. Chen, Z. Zhang, and H.-H. Chen, "On distributed antenna systems with limited feedback precoding: Opportunities and challenges," *IEEE Wireless Commun.*, vol. 17, no. 2, pp. 80–88, Apr. 2010.

[94] W. Santipach and M. Honig, "Asymptotic performance of MIMO wireless channels with limited feedback," in *Proc. IEEE Military Communications Conference, 2003. MILCOM '03*, vol. 1, Oct. 2003, pp. 141–146.

[95] N. Zhang, G. Kang, Y. Guo, and X. Gui, "Symbol error rate analysis and antenna selection in limited feedback distributed antenna systems," in *Proc. IEEE Veh. Technol. Conf. Fall (VTC 2010-Fall)*, Sep. 2010.

[96] E. Zeng, S. Zhu, and Z. Zhong, "On the performance of adaptive limited feedback beamforming in distributed MIMO systems," in *Proc. IEEE Global Telecommun. Conf., GLOBECOM 2008.*, Dec. 2008.

[97] C. K. Au-Yeung and D. J. Love, "On the performance of random vector quantization limited feedback beamforming in a MISO system," *IEEE Trans. Wireless Commun.*, vol. 6, no. 2, pp. 458–462, Feb. 2007.

[98] X. W. Cui and Z. M. Feng, "Lower capacity bound for MIMO correlated fading channels with keyhole," *IEEE Commun. Lett.*, vol. 8, no. 8, pp. 500–502, Aug. 2004.

[99] S. Al-Ahmadi and H. Yanikomeroglu, "On the approximation of the generalized-K distribution by a Gamma distribution for modeling composite fading channels," *IEEE Trans. Wireless Commun.*, vol. 9, no. 2, pp. 706 –713, Feb. 2010.

[100] P. Moschopoulos, "The distribution of sum of independent Gamma random variables," *Ann. Inst. Statist. Math.*, vol. 37, pp. 541–544, 1985.

[101] *3rd Generation Partnership Project-Technical Specification Group Radio Access Network-Evolved Universal Terrestrial Radio Access (E-UTRA)-relay architectures for E-UTRA (LTE-Advanced)(release 9)*, vol. 3GPP TR 36.806 V9.0.0, Mar. 2010.

[102] J. Zhang and K. B. Letaief, "Interference management with relay cooperation in two-hop interference channels," *IEEE Wireless Commun. Lett.*, vol. 1, no. 3, pp. 165–168, June 2012.

[103] Y. Shi, J. Zhang, and K. B. Letaief, "Coordinated relay beamforming for amplify-and-forward two-hop interference networks," in *IEEE Global Telecommun. Conf.*, Dec. 2012, pp. 2408–2413.

[104] N. Lee, W. Shin, R. W. Heath, and B. Clerckx, "Interference alignment with limited feedback for two-cell interfering MIMO-MAC," in *International Symposium on Wireless Communication Systems (ISWCS), 2012*, 2012, pp. 566–570.

[105] C.-B. Chae, I. Hwang, R. W. Heath, and V. Tarokh, "Jointly optimized two-cell MIMO systems," in *IEEE GLOBECOM Workshops (GC Wkshps), 2011*, 2011, pp. 421–425.

[106] C. Na, X. Hou, and A. Harada, "Two-cell coordinated transmission scheme based on interference alignment and MU-MIMO beamforming," in *75th IEEE Vehicular Technology Conference (VTC Spring), 2012*, 2012, pp. 1–5.

[107] K. Lee, "Uplink interference alignment for two-cell MIMO interference channels," *IEEE Trans. Veh. Technol.*, vol. 62, no. 4, pp. 1861–1865, 2013.

[108] Y. Fan, J. S. Thompson, A. Adinoyi, and H. Yanikomeroglu, "On the diversity-multiplexing tradeoff for multi-antenna multi-relay channels," in *IEEE International Conference on Communications,*, Jun. 2007, pp. 5252–5257.

[109] A. Adinoyi and H. Yanikomeroglu, "Cooperative relaying in multi-antenna fixed relay networks," *IEEE Trans. Wireless Commun.*, vol. 6, no. 2, pp. 533–544, Feb 2007.

[110] Y. Fan, A. Adinoyi, J. S. Thompson, H. Yanikomeroglu, and H. V. Poor, "A simple distributed antenna processing scheme for cooperative diversity," *IEEE Trans. Commun.*, vol. 57, no. 3, pp. 626–629, Mar. 2009.

[111] A. Talebi and W. A. Krzymień, "Multiple-antenna multiple-relay cooperative communication system with beamforming," in *IEEE Vehicular Technology Conference,*, May 2008, pp. 2350–2354.

[112] A. Talebi and W. A. Krzymień, "Cooperative MIMO multiple-relay system with optimised beamforming and power allocation," *IET Communications*, vol. 4, no. 14, pp. 1677–1686, Sep. 2010.

[113] J. Cui and A. U. H. Sheikh, "Outage probability of cellular radio systems using maximal ratio combining in the presence of multiple interferers," *IEEE Trans. Commun.*, vol. 47, pp. 1121–1124, Aug. 1999.

[114] E. G. Larsson and E. A. Jorswieck, "Competition versus cooperation on the MISO interference channel," *IEEE J. Select. Areas Commun.*, vol. 26, no. 7, pp. 1059–1069, Sep. 2008.

[115] A. Papoulis and U. S. Pillai, *Probability, Random Variables and Stochastic Processes*, 4th ed. New York: McGraw-Hill, 2002.

[116] A. P. Prudnikov, Y. Brychkov, and O. Marichev, *Integrals and Series*. Gorden and Breach Science, 1998, vol. 1.

[117] Wolfram functions site, "Hypergeometric2F1." [Online]. Available: http://functions.wolfram.com/HypergeometricFunctions/Hypergeometric2F1%/03/06/01/0001/

[118] N. Suraweera and N. C. Beaulieu, "Performance analysis of amplify-and-forward relaying with optimum combining in the presence of co-channel interference," in *IEEE Global Communications Conference (GLOBECOM)*, Dec. 2013, pp. 3565–3570.

[119] P. L. Yeoh, M. Elkashlan, and I. B. Collings, "Exact and asymptotic SER of distributed TAS/MRC in MIMO relay networks," *IEEE Trans. Wireless Commun.*, vol. 10, no. 3, pp. 751–756, Mar. 2011.

[120] S. Srinivasa and M. Haenggi, "Distance distributions in finite uniformly random networks: Theory and applications," *IEEE Trans. Veh. Technol.*, vol. 59, no. 2, pp. 940–949, Feb. 2010.

[121] J. Kim, J.-Y. Hwang, and Y. Han, "Joint processing in multi-cell coordinated shared relay network," in *proc. 21st IEEE International Symposium on Personal Indoor and Mobile Radio Communications (PIMRC)*, 2010, pp. 702–706.

[122] N. Gresset, "Precoder optimization for user fairness in shared relay channels with interference," in *proc. 22nd IEEE International Symposium on Personal Indoor and Mobile Radio Communications (PIMRC)*, 2011, pp. 1475–1479.

[123] D. G. Brennan, "Linear diversity combining techniques," *Proc. IEEE*, vol. 91, no. 2, pp. 331–356, 2003.

[124] N. C. Beaulieu, "A novel generalized framework for performance analysis of selection combining diversity," *IEEE Trans. Commun.*, vol. 61, pp. 4196–4205, Oct. 2013.

[125] D. A. Gore, J. Heath, R. W., and A. J. Paulraj, "Transmit selection in spatial multiplexing systems," *IEEE Commun. Lett.*, vol. 6, no. 11, pp. 491–493, Nov. 2002.

[126] J. Zhang, M. Kountouris, J. G. Andrews, and R. W. Heath, "Multi-mode transmission for the MIMO broadcast channel with imperfect channel state information," *IEEE Trans. Commun.*, vol. 59, no. 3, pp. 803–814, 2011.

[127] Wolfram functions site, "Hypergeometric2F1." [Online]. Available: http://functions.wolfram.com/HypergeometricFunctions/Hypergeometric2F1%/03/06/07/02/0004/

[128] Wolfram functions site, "ExpIntegralE." [Online]. Available: http://functions.wolfram.com/GammaBetaErf/ExpIntegralE/03/01/02/0007/

[129] Wolfram functions site, "ExpIntegralEi." [Online]. Available: http://functions.wolfram.com/06.35.06.0001.01

[130] K. Doppler, C. H. Yu, C. B. Ribeiro, and P. Janis, "Mode selection for device-to-device communication underlaying an LTE-Advanced network," in *Proc. IEEE Wireless Communications and Networking Conference (WCNC)*, 2010.

[131] B. Kaufman and B. Aazhang, "Cellular networks with an overlaid device to device network," in *Proc. 42nd Asilomar Conference on Signals, Systems and Computers*, 2008, pp. 1537–1541.

[132] *Cisco report, Cisco Visual Networking Index: Global Mobile Data Traffic Forecast Update, 2012-2017*, 2011.

[133] M. Duarte, A. Sabharwal, V. Aggarwal, R. Jana, K. K. Ramakrishnan, C. W. Rice, and N. K. Shankaranarayanan, "Design and characterization of a full-duplex multi-antenna system for WiFi networks," *IEEE Trans. Veh. Technol.*, 2012, available: http://arxiv.org/abs/1210.1639.

[134] M. Duarte and A. Sabharwal, "Full-duplex wireless communications using off-the-shelf radios: Feasibility and first results," in *Proc. 44th Asilomar Conference on Signals, Systems and Computers*, 2010, pp. 1558–1562.

[135] N. S. Ferdinand, N. Rajatheva, and M. Latva-aho, "Performance analysis of two-way relay system with antenna correlation," in *Proc. IEEE Global Telecommunications Conference (GLOBECOM)*, Houston, Tx, USA, 2011.

[136] J. Lee, H. Wang, J. G. Andrews, and D. Hong, "Outage probability of cognitive relay networks with interference constraints," *IEEE Trans. Wireless Commun.*, vol. 10, no. 2, pp. 390–395, 2011.

[137] Y. Huang, F. Al-Qahtani, C. Zhong, Q. Wu, J. Wang, and H. Alnuweiri, "Performance analysis of multiuser multiple antenna relaying networks with co-channel interference and feedback delay," *IEEE Trans. Commun.*, vol. 62, no. 1, pp. 59–73, Jan. 2014.

[138] Y. Gu, S. Ikki, and S. Aissa, "Opportunistic cooperative communication in the presence of co-channel interferences and outdated channel information," *IEEE Commun. Lett.*, vol. 17, no. 10, pp. 1948–1951, Oct. 2013.

[139] M. Di Renzo and W. Lu, "End-to-end error probability and diversity analysis of AF-based dual-hop cooperative relaying in a poisson field of interferers at the destination," *IEEE Trans. Wireless Commun.*, vol. 14, no. 1, pp. 15–32, Jan. 2015.

[140] T. Lu, P. Liu, I. Kim, F. Chan, and W. Read, "End-to-end optimum ML detection for DF cooperative diversity networks in the presence of interference," *IEEE Trans. Wireless Commun.*, (Available in IEEE Early Access).

[141] N. Miridakis, M. Matthaiou, and G. Karagiannidis, “Multiuser relaying over mixed RF/FSO links,” *IEEE Trans. Commun.*, vol. 62, no. 5, pp. 1634–1645, May 2014.